Phil. Trans. R. Soc. Lond. B **325**, 561–666 (1989) [561]
Printed in Great Britain

THE PACHYPLEUROSAURIDS (REPTILIA: NOTHOSAURIA) FROM THE MIDDLE TRIASSIC OF MONTE SAN GIORGIO (SWITZERLAND) WITH THE DESCRIPTION OF A NEW SPECIES

By P. M. SANDER

Paläontologisches Institut und Museum, Universität Zürich, Künstlergasse 16, *CH*-8006 *Zurich, Switzerland*

(*Communicated by P. H. Greenwood, F.R.S. – Received* 30 *November* 1988)

[Plates 1–4; Pullouts 1 and 2]

CONTENTS

The largest and most diverse collection of Pachypleurosauridae (Nothosauria, Reptilia) comes from Monte San Giorgio, Switzerland. Several hundred complete skeletons were collected from four distinct horizons of bituminous limestones and shales of Anisian–Ladinian boundary to early Ladinian age (Middle Triassic).

Serpianosaurus mirigiolensis comes from the oldest strata, the Grenzbitumenzone Beds. The three younger strata, all in the Lower Meride Limestone, yield three species of *Neusticosaurus*. *Neusticosaurus pusillus* comes from the Cava Inferiore horizon, *Neusticosaurus peyeri*, new species, from the Cava Superiore horizon, and *Neusticosaurus edwardsii*, new combination, from the Alla Cascina horizon. *Neusticosaurus pusillus* is biostratigraphically important because it is one of the rare species reported from both the Germanic and the Alpine Triassic.

Neusticosaurus pusillus and *N. peyeri* are small and very similar in their anatomy. *Neusticosaurus* species are easiest separated by their number of presacral vertebrae. Ornamentation of the bone surface is distinctive for all four pachypleurosaurids. Soft parts are rarely preserved, except for one partial squamation. The biological age of *Neusticosaurus* individuals can be determined by skeletochronology (aging by bone annuli). Small species of *Neusticosaurus* were sexually mature after three to four years and lived for six to nine years.

Taphonomic analysis of the small species indicates attritional mortality and suggests weak bottom currents in the Monte San Giorgio basin during early Ladinian times.

Morphometric comparison of all four pachypleurosaurids indicates that the changing vertebral numbers between species are largely due to a change in number of segments.

All Monte San Giorgio pachypleurosaurids are sexually dimorphic in forelimb

development. Sex *x* has poorly differentiated and relatively short humeri whereas sex *y* has well differentiated and relatively long humeri. The sexes are of about the same size and represented in roughly equal numbers. Identification of gender was not possible.

Good growth series, especially of *Neusticosaurus peyeri*, from embryo to large adult permitted qualitative and quantitative study of ontogeny. The skull grows with negative allometry; the humerus grows isometrically or with positive allometry, depending on sex and species; the femur grows isometrically. The adult size range in *N. peyeri* is considerably larger than in modern reptiles.

The Monte San Giorgio pachypleurosaurids are a monophyletic group. The phylogeny of this group is congruent with the stratigraphic distribution of its members.

1. Introduction

Monte San Giorgio in southern Switzerland (Canton Ticino) is probably the most important locality for marine reptiles of Middle Triassic age in the world. Sixty years of collecting have uncovered a very diverse, largely marine, fauna with ichthyosaurs (four genera), placodonts (two genera), thalattosaurs (three genera), protorosaurs (two genera), rauisuchids (one genus), the enigmatic *Helveticosaurus*, and last but not least, five genera of nothosaurs.

The marine reptile order Nothosauria consists of two major groups, the medium-sized to large nothosaurs *sensu stricto* and the generally small pachypleurosaurs. Both groups are known from Middle to late Triassic sediments of central Europe, southwest, and eastern Asia. The best collection of nothosaurs (three genera of nothosaurs *sensu stricto* and two genera of pachypleurosaurs) is housed at the Palaeontological Institute and Museum of the University of Zurich and comes from the Monte San Giorgio region.

Pachypleurosaurs, including the genera *Serpianosaurus* (Rieppel 1989*a*) and *Neusticosaurus* (Carroll & Gaskill 1985), are by far the most abundant tetrapod fossils at this locality. The preservation of complete, articulated skeletons along with the large sample size allow unusual insights into the biology of an extinct reptile group. The palaeobiology and life history of one of the species, *Neusticosaurus peyeri* n.sp., is now better known than those of many extant reptiles.

The occurrence of pachypleurosaurs in the Middle Triassic sediments of the southern Alps has been known since Cornalia described the first specimens in 1854 as *Pachypleura edwardsii*. *Pachypleura*, however, was preoccupied by a coleopteran (Lydekker 1889) and later changed to *Pachypleurosaurus* independently by Broili (1927) and Nopcsa (1928). Details of the taxonomic history of *Pachypleurosaurus edwardsii* were discussed by Peyer (1932, 1934), Zangerl (1935), Kuhn-Schnyder (1959), Carroll & Gaskill (1985) and Rieppel (1987).

The first pachypleurosaur from the Swiss part of Monte San Giorgio was bought by the Zurich palaeontologist B. Peyer in the village of Meride in 1924. He traced the origin of the specimen (T 3796) and collected additional material. A preliminary description based on 11 specimens was published (Peyer 1932) and the fossils were assigned to *Pachypleurosaurus edwardsii*. Subsequent palaeontological excavations resulted in a large sample (105 specimens) that formed the basis of the first complete morphological description of this animal by Zangerl (1935). His most notable conclusion was that *Pachypleurosaurus edwardsii* showed an enormous variability, far exceeding that of extant reptiles. Zangerl's material originated from eight outcrops from four different stratigraphic horizons in the Monte San Giorgio region in southern Switzerland and northern Italy.

Continuous excavation activity by the University of Zurich until the mid-1970s produced an additional 800 specimens from 6 major and 13 minor localities all in the vicinity of the Monte

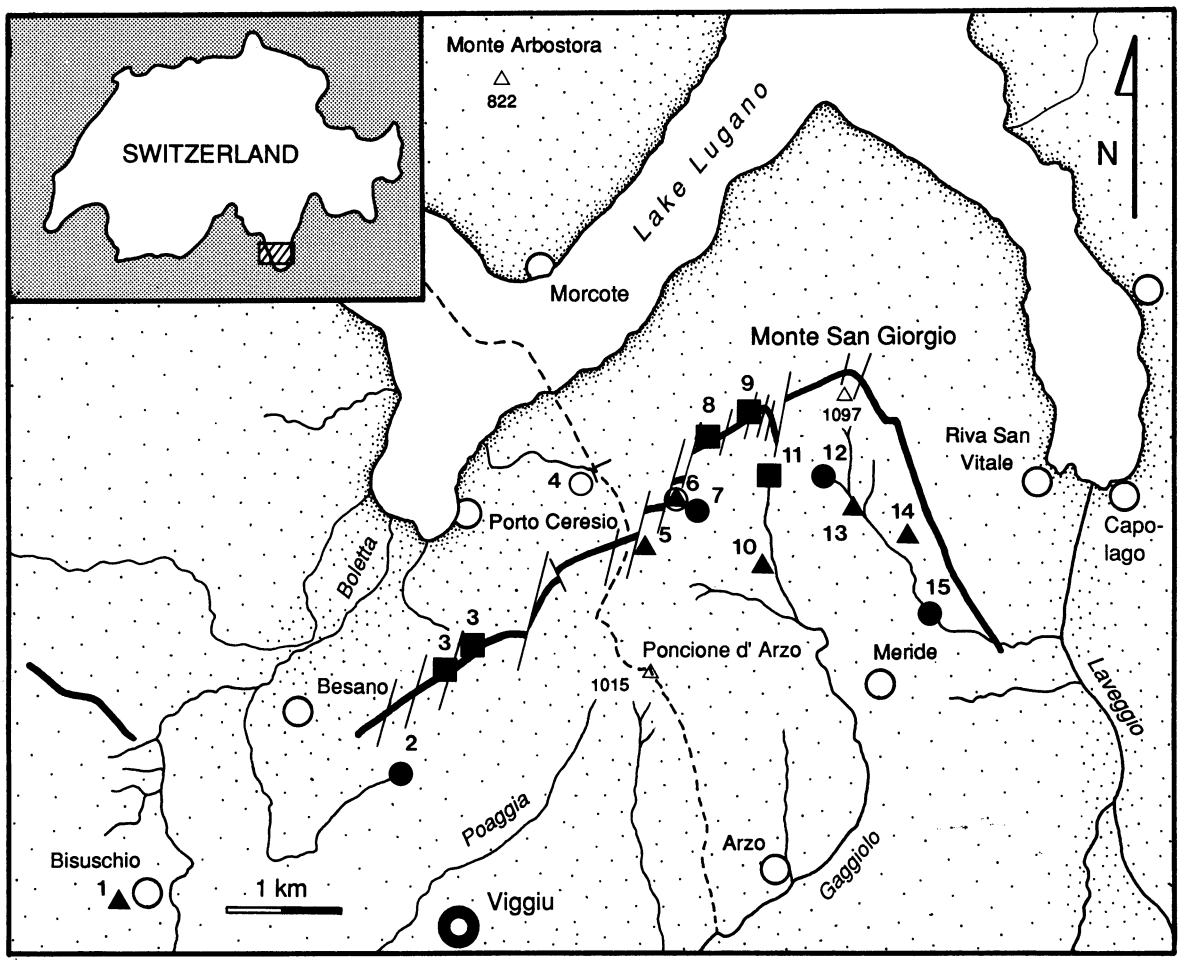

FIGURE 1. Map of the Monte San Giorgio area with localities from which pachypleurosaurids were collected. The numbered symbols mark the localities and indicate their stratigraphic position. Key: (■), Grenzbitumenzone Beds; (▲), Cava Inferiore horizon; (○), Cava Superiore horizon; (●), Alla Cascina horizon. 1, Ronca sopra Bisuchio; 2, Ca' del Frate; 3, Cave di Besano; 4, Ca' del Monte; 5, Acqua Ferruginosa; 6, Acqua del Ghiffo; 7, Road Crocifisso–Serpiano; 8, Cava Tre Fontane; 9, P. 902; 10, lower Val Porina; 11, Val Porina mine; 12, Alla Cascina; 13, Val Serrata (Cava Don Luigi); 14, Cascinello; 15, Val Serrata below cave Bööggia. The heavy black line marks the outcrop of the Grenzbitumenzone Beds (Bernoulli *et al.* 1976; unpublished maps by D. Bernoulli and D. Trümpy). The thin dashed line is the Swiss-Italian border.

San Giorgio (figure 1). In the course of this work it became apparent that at least three different forms were present, differentiated by the phalangeal formula (Kuhn-Schnyder 1959) and skull morphology (Kuhn-Schnyder 1963, 1974). The three forms were presumed to be one small and one large form of *Pachypleurosaurus*, and one form tentatively assigned to *Phygosaurus* (Arthaber 1924).

The large *Pachypleurosaurus* has recently been redescribed by Carroll & Gaskill (1985) as the only member of the species *Pachypleurosaurus edwardsii*. They identified the small pachypleurosaur as *Neusticosaurus*, a genus that was first described from the German Muschelkalk (Seeley 1882). Rieppel (1989*a*) restudied '*Phygosaurus*' and designated a new genus and species for it, *Serpianosaurus mirigiolensis*.

The original purpose of my study was to describe the small Monte San Giorgio pachypleurosaur. As documented below, it was correctly assumed to be synonymous with

Neusticosaurus by Carroll & Gaskill (1985). There are, however, two species that are separated stratigraphically. One is identical to *N. pusillus* known from the German Lettenkeuper Beds (Middle Triassic) and the other is newly described here as *N. peyeri* n.sp. The large sample size of about 800 (340 prepared) specimens for both small *Neusticosaurus* species represents a unique situation among Mesozoic reptiles, and in the course of this study its enormous palaeobiological potential was realized. The two other pachypleurosaurs (Carroll & Gaskill 1985; Rieppel 1989*a*) were included as much as possible in the palaeobiological and phylogenetic analysis to provide a comprehensive picture of the Monte San Giorgio pachypleurosaurs.

A few results that need to be considered to understand this paper are summarized here: firstly, the relative age and stratigraphic distribution of these pachypleurosaurs. *Serpianosaurus* is the oldest followed by *Neusticosaurus pusillus*, *Neusticosaurus peyeri*, and *Pachypleurosaurus edwardsii* (the correct name of which, used hereafter, is *Neusticosaurus edwardsii*, see §15*a*). No stratigraphic overlap exists. The identity of *Neusticosaurus pusillus* from Monte San Giorgio and Germany is established by quantitative arguments. All Monte San Giorgio pachypleurosaurs exhibit a peculiar dimorphism in forelimb morphology and proportions, which is best interpreted as being sex-differences. Identification of males and females was not possible, and the terms 'sex *x*' and 'sex *y*' used here carry no biological meaning.

Abbreviations used for institutions are as follows: PIMUZ, Paläontologisches Institut und Museum der Universität Zürich, Switzerland; BM(NH), British Museum (Natural History), London, U.K.; MCSNM, Museo Civico di Storia Naturale di Milano, Italy; MCL, Museo Civico Lugano, Switzerland; PMM, Palaeontological Museum Meride, Canton Ticino, Switzerland; PMU, Palaeontological Museum, Uppsala, Sweden; SMNS, Staatliches Museum für Naturkunde Stuttgart, West Germany; GPIT, Geologisch-Paläontologisches Institut Tübingen, F.R.G.

2. Methods and materials

Two hundred and twenty-nine prepared specimens of *Neusticosaurus pusillus* and 104 prepared specimens of *Neusticosaurus peyeri* in the collections of the PIMUZ form the basis of this study. Most are preserved dorsoventrally and were prepared from only one side, usually by using a fine steel needle under a binocular microscope. Air abrasive or phosphatic acid treatments were occasionally employed. X-rays were taken of many unprepared specimens. They were used in a few cases to supply additional measurements to broaden the quantitative data-base.

The starting point of my investigation was the origin of the unusual variation in *Neusticosaurus*. A correlation between variation and stratigraphic distribution of the specimens had been previously suspected, but could not be sufficiently documented (Zangerl 1935; Carroll & Gaskill 1985). This failure was apparently due to false locality data and insufficient understanding of regional stratigraphy at Monte San Giorgio. Variation and stratigraphy were successfully correlated, mainly because of the insight that a locality name is not necessarily equal to a stratigraphic horizon; this was an assumption of earlier workers.

Because of the large sample size, a quantitative approach to variation could be employed with the aid of a microcomputer data-base management program. A number of measurements and character states were recorded from prepared specimens that were clearly not *Neusticosaurus edwardsii* or *Serpianosaurus*, as well as from a few specimens of these two species for comparison. At first, only specimens from the same stratigraphic horizon (e.g. Cava Inferiore horizon, *livello*

buono) were compared with one another, and specimens without good stratigraphic data were neglected. This approach left samples from a single stratigraphic horizon with no unusual variation.

Measurements (figure 2) and character states were selected for their taxonomic importance and ease of observation. Roughly in order of importance on the species level, they are: number of vertebrae (figure 3), a standard length, trunk, humerus, femur and skull lengths, and separation or union of the nasals along the skull midline. A second series of measurements concerns the limbs and the tail. The minimal shaft diameter and the distal width of the humerus were measured to quantify the sexual dimorphism of this bone. The lengths of radius, ulna, the third metacarpal, tibia, fibula, and the fourth metatarsal were measured for allometric and sex-difference analyses. The first and last chevron bones, the point at which the size of the neural spine abruptly decreases, the last neural spine, and the last neural arch in the tail were recorded.

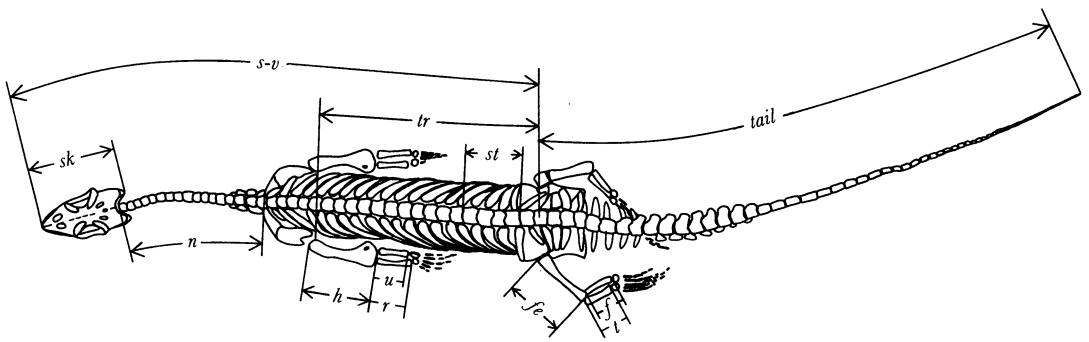

FIGURE 2. Measurements taken of pachypleurosaurid skeletons: *f*, fibula length; *fe*, femur length; *h*, humerus length; *n*, neck length; *r*, radius length; *sk*, skull length; *st*, standard length; *s–v*, snout–vent length; *t*, tibia length; *tail*, tail length; *tr*, trunk length; *u*, ulna length.

Five vertebral counts were recorded: (i) cervical (figure 3*c*), (ii) dorsal (figure 3*d*), (iii) presacral (figure 3*a*, *b*), (iv) sacral, and (v) caudal (figure 3*e*). The presacral count is the most accurate, because the loss of the rib articulation with the centrum (the theoretical border between cervical and dorsal column) is difficult to discern because of the dorsal or ventral position of the skeletons. The first vertebra in contact with the shoulder girdle was chosen as the 'working definition' for the first dorsal vertebra. It seems to coincide closely with the actual first dorsal, as can be seen in PIMUZ T 3728 (all specimen numbers starting with 'T' refer to PIMUZ specimens). Shifting of the shoulder girdle during decay or compaction does not seem to have introduced much error into cervical or dorsal counts. This is supported by the observation that the ranges of the cervical and dorsal counts are not appreciably greater than the range of the presacral count (figure 3).

The orthometric linear unit (OLU) of Romer & Price (1940) is usually used for interspecific size comparisons. Although the OLU itself is not applicable in ontogeny (Currie 1978), some derivative of it could be suitable for ontogenetic size comparisons as demonstrated by Currie & Carroll (1984) with the eusochian *Thadeosaurus*. However, one of the basic assumptions of the OLU concept, namely that vertebral size reflects strain on the vertebral column (and thereby indicates body mass), is not valid in pachypleurosaurids. Many pachypleurosaurids, particularly the small ones, show pronounced pachyostosis. which increases the transverse

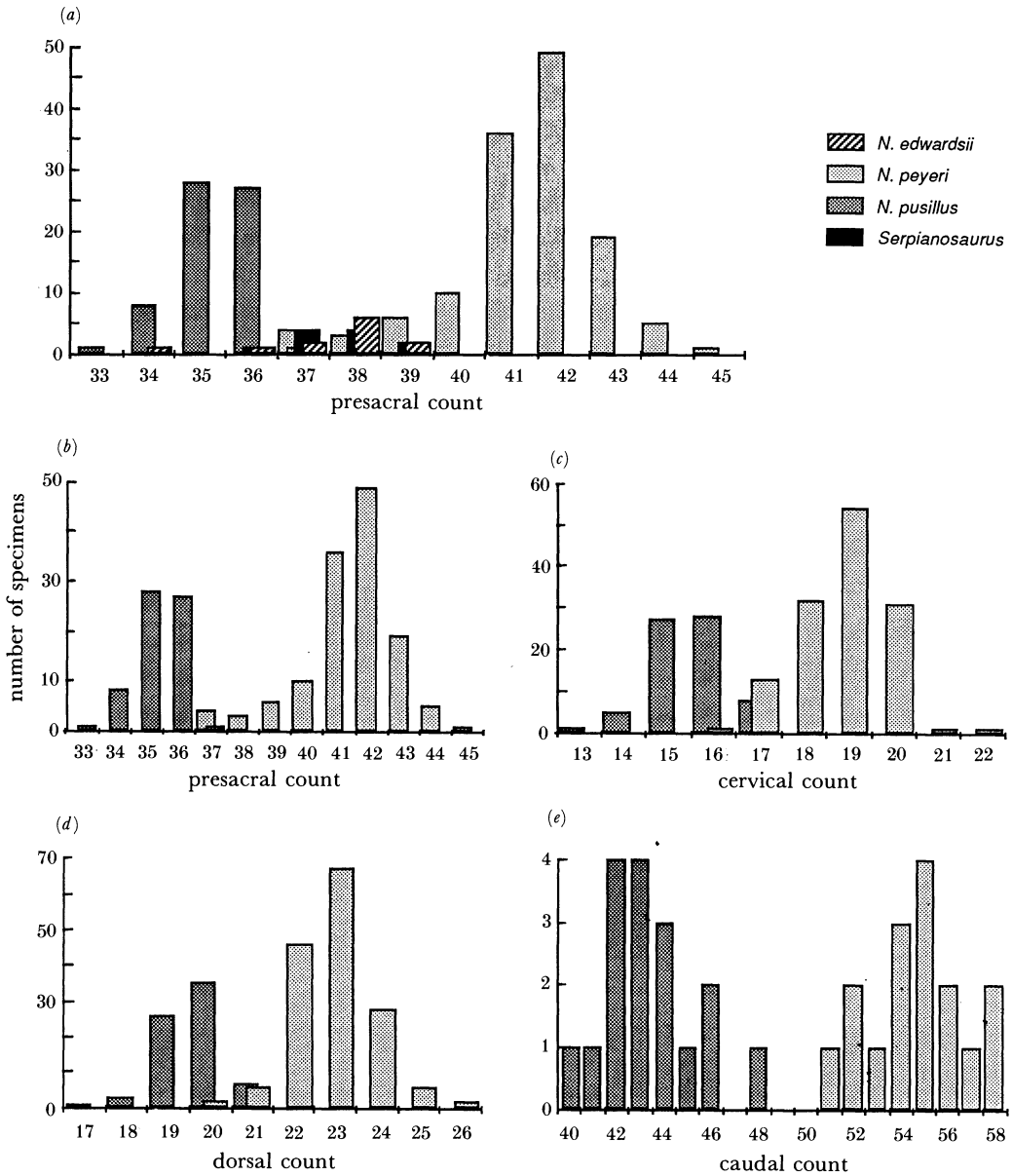

FIGURE 3. Comparison of vertebral counts of Monte San Giorgio pachypleurosaurids: (*a*) presacral counts of all four taxa; (*b–e*) presacral, cervical, dorsal, and caudal counts of the two small species of *Neusticosaurus*. Note clear separation of the two species in all counts.

width (r) of a vertebral centrum independently of body mass. It is also unclear if this basic assumption of the OLU concept is valid for aquatic reptiles.

In their study of *Thadeosaurus*, Currie & Carroll (1984) were unable to measure r for different reasons, but instead used the length of a dorsal centrum (x), because it showed a simple relation to r throughout ontogeny. This does not hold true for *Neusticosaurus* because juveniles show wider and shorter centra than adults. Thus the $x:r$ ratio changes ontogenetically in this genus. No independent measure of body size could be found, but vertebral dimensions are generally rather accurate measurements of absolute body size (Romer & Price 1940; Currie 1978, 1981). The best choice for a standard length appeared to be the length of the four posterior dorsal

centra. A limitation of this standard length is that its use is restricted to intraspecific comparison, particularly between specimens with identical presacral counts. It can serve in combination with various other length measurements as an indirect measure of the number of presacral vertebrae. Ratios of various measurements to standard length can be successfully used to distinguish species.

Trunk length is here defined as the distance between glenoid and acetabulum. It is useful for size comparisons between species with different vertebral counts. Trunk length was measured from the proximal posterior corner of the humerus to the proximal posterior corner of the femur (figure 2). If the column was slightly bent, the arithmetic mean of the values for each side was taken. A taut string was extended along the midline of the few, strongly bent specimens from the mid-point between the proximal posterior corners of the humeri to the mid-point between the proximal posterior corners of the femora.

The ratio of trunk length:standard length, termed standard length correction factor (F; table 8), indicates the number of presacral vertebrae. It can also be used to compensate for different vertebral counts when using standard length for interspecific size comparison. The value F does not change during ontogeny.

Size classes were designated for *Neusticosaurus peyeri* (figure 4*c*), which shows the most complete growth series. Increments of 2 mm standard length were arbitrarily chosen for this species beginning at 2 mm. Class A includes specimens from 2 to 3.9 mm standard length, class B ranges from 4 to 5.9 mm standard length, and so on. Classes for the trunk length were calculated by using F.

Size classes for *N. pusillus* were based on those for *N. peyeri*. Increments were calculated by

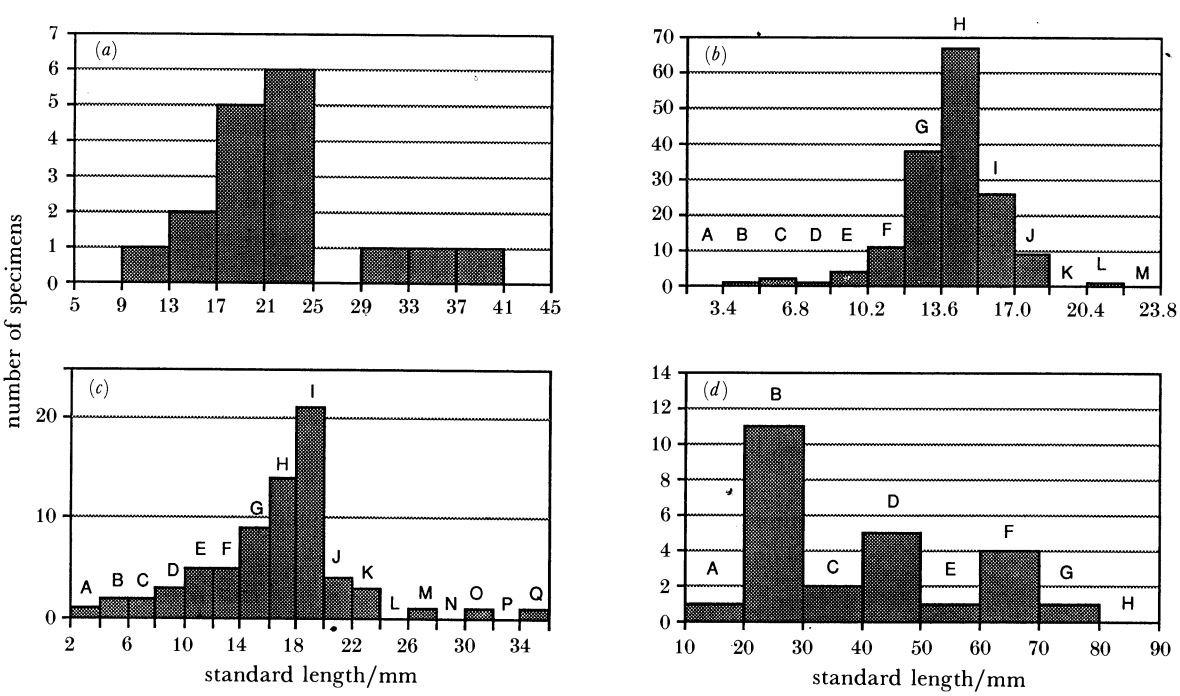

FIGURE 4. Size classes and standard length distributions of Monte San Giorgio pachypleurosaurids. (*a*) *Serpianosaurus mirigiolensis*, data from Rieppel (1989), no size classes were designated; (*b*) *Neusticosaurus pusillus*, a large size range is present but the small and large sizes are underrepresented; (*c*) *Neusticosaurus peyeri*, this is the best sample with many small individuals; (*d*) *Neusticosaurus edwardsii*, a good size range, but very small specimens are absent.

using *F* of *N. pusillus* with the underlying assumption that trunk length is the same in both species, and only the number of segments (equivalent to vertebrae) has changed. The validity of this assumption is demonstrated in §11. The class increments for *N. pusillus* are 1.7 mm, beginning at 1.7 mm (figure 4*b*).

The size classes of *N. edwardsii* were also designated arbitrarily because the vertebral centra of this species are relatively elongated compared to the small *Neusticosaurus* (see §11). Class increments for *N. edwardsii* are 10 mm, beginning at 10 mm (figure 4*d*). The sample of *Serpianosaurus* was arbitrarily subdivided into size classes of 4 mm standard length beginning at 9 mm (figure 4*a*). Specimens of *N. edwardsii* and *Serpianosaurus* vary greatly in size, but small juveniles are lacking; this may partially be because of the relatively small sample sizes for these species.

Neck length was measured from the anterior margin of the shoulder girdle to the occipital condyle (figure 2); the length of the tail was measured from its tip to the mid-point between the anterior proximal corners of the femora; snout–vent length was taken from this mid-point to the lower jaw symphysis or to the tip of the rostrum; overall length is the distance between the tip of the snout and the end of the tail.

The quality of the length measurements varies. The most accurate are the values for the long bones (humerus, femur, radius, ulna, tibia fibula, third metacarpal and fourth metatarsal). The measurements indicate the distances between the proximal and distal articular surfaces (figure 2).

Skull length was initially measured along the skull midline from the premaxillary or lower jaw symphysis to the occipital condyle. However, it was too difficult to measure owing to poor exposure of the occipital condyle resulting from crushing of the skull. Consequently, the length of one lower jaw ramus was substituted as the standard measurement for skull length (figure 2).

Various ratios of the measurements were calculated (tables 4, 5 and 9). Humerus:standard length, femur:standard length, humerus:femur, and skull:standard length are the basic ratios. Ratios with the trunk length were calculated, if one of the basic ratios could not be obtained, to be used as a control.

3. Stratigraphy of pachypleurosaur horizons

Detailed knowledge of the regional and local stratigraphy of the Ladinian (Middle Triassic) rocks of Monte San Giorgio was the key to understanding diversity and evolution of the pachypleurosaurs. General overviews of the geology of the Monte San Giorgio region are contained in Bernoulli (1964) and Rieber & Sorbini (1983). The tetrapod-bearing strata of the Ladinian carbonates at Monte San Giorgio begin with the Grenbitumenzone Beds followed by the San Giorgio Dolomite, which is overlain by the Meride Limestones. No adequate geological map of Monte San Giorgio exists, and the last lithostratigraphic work on this sequence was done by Wirz (1945). Wirz measured a complete lithologic section but failed to indicate the exact stratigraphic position of the vertebrate localities excavated by the University of Zurich since 1924.

To ascertain the exact geographical and stratigraphic location of all pachypleurosaur localities, field work was done. Ten sections were measured to clarify the stratigraphy and to correlate the fossil localities (Sandler 1989). Four tetrapod-bearing horizons can be identified

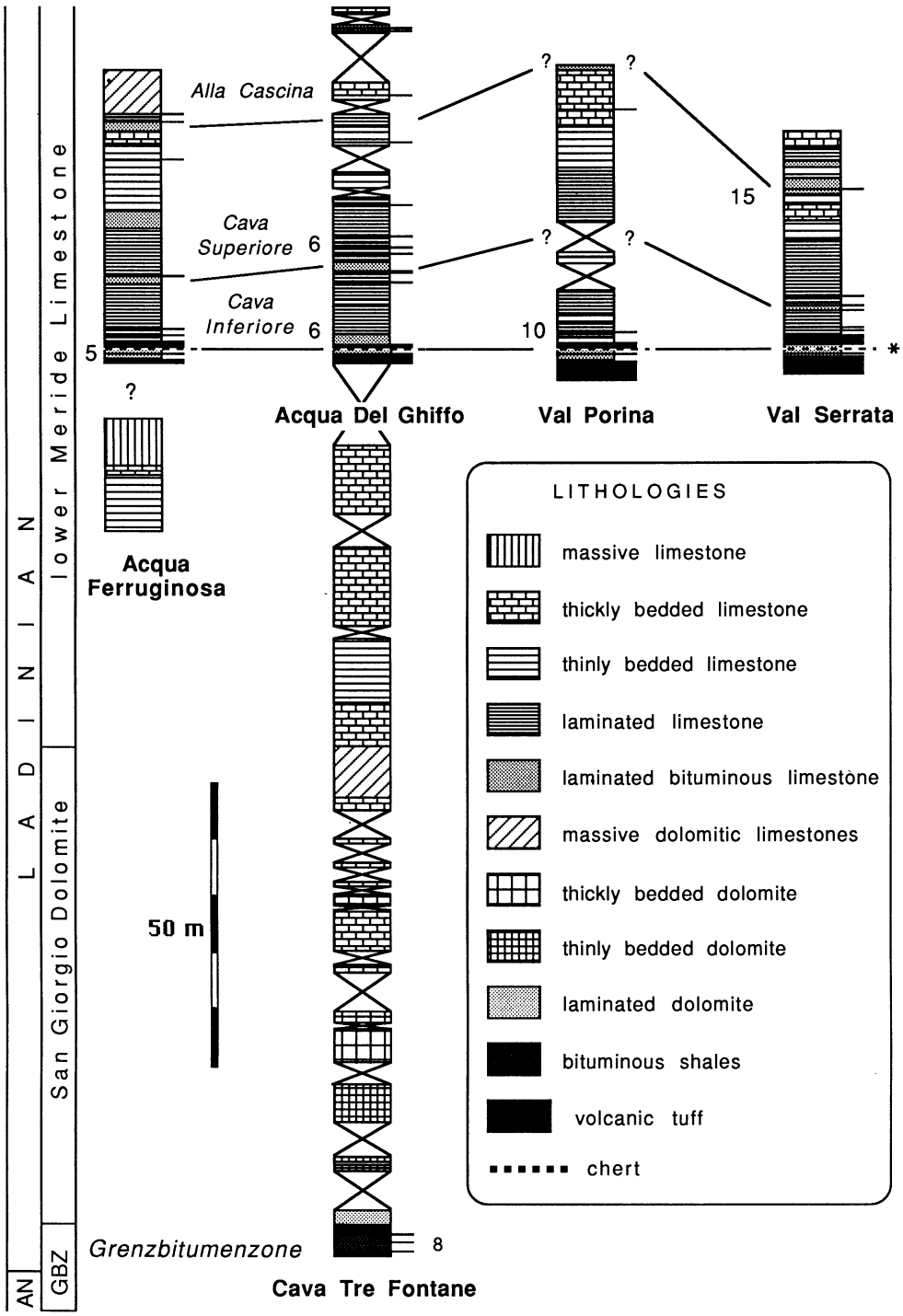

FIGURE 5. Stratigraphy and correlation of the four pachypleurosaur-bearing horizons (Grenzbitumenzone, Cava Inferiore, Cava Superiore, and Alla Cascina) of the Anisian and Ladinian carbonate sediments of Monte San Giorgio illustrated by four representative lithologic sections. The numbers to the left of the sections correspond to the locality numbers in figure 1. Only the section from Cava Tre Fontane to Acqua del Ghiffo spans the entire profile, all the others begin with the Cava Inferior horizon. The chert (*scherzi*) of the Cava Inferiore horizon was used as datum. The asterisk marks position of the detailed section in figure 6.

in the lower part of the Ladinian carbonates. From oldest to youngest, they are the Grenzbitumenzone Beds, the Cava Inferiore horizon, the Cava Superiore horizon, and the Alla Cascina horizon (figure 5). Except for the Grenzbitumenszone Beds, these are all informal miners' or collectors' names. The horizons usually contain pachypleurosaurs at more than one bed. These beds also bear informal collectors' names.

The Grenzbitumenzone Beds are relatively well understood because of the work of Müller (1969), Zorn (1971) and Rieber (1973*a*, *b*, 1975). They consist of 16 m of interbedded dolomites, bituminous shales, and a few thin ash-fall tuffs (Müller *et al.* 1964; figure 5). About 190 beds were distinguished (Rieber 1973*b*) but the first pachypleurosaurs (*Serpianosaurus mirigiolensis*) are not encountered below bed 139. About 180 m of massive or bedded carbonates (San Giorgio Dolomite and Lower Meride Limestone) separate the Cava Inferiore horizon from the Grenzbitumenzone Beds (figure 5). The Cava Inferiore horizon, averaging about 1.2 m in thickness, is underlain by massive ash-fall tuffs. Depending on locality, between one and eleven beds with *Neusticosaurus pusillus* were recognized in the Cava Inferiore horizon (figure 6).

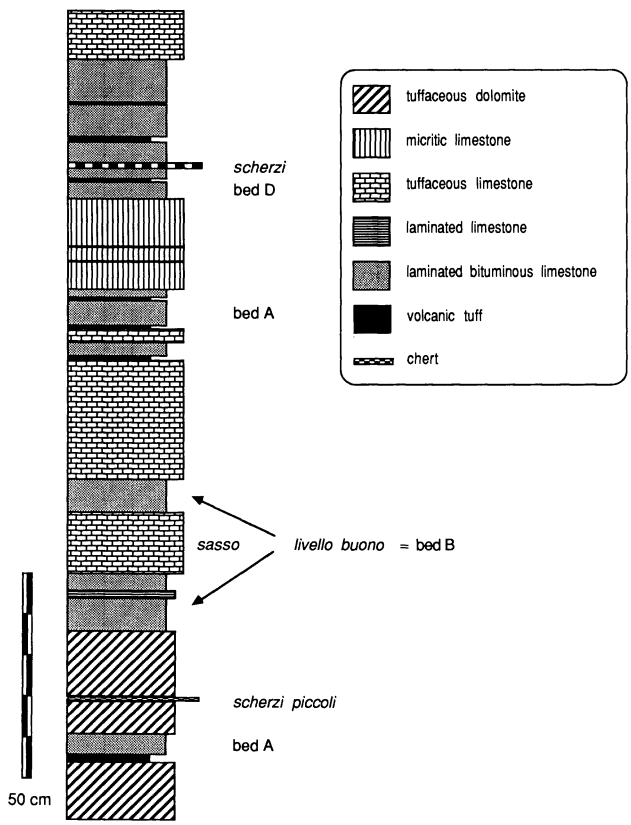

FIGURE 6. Lithologic section of Cava Inferiore horizon, detail of section 'Val Serrata' in figure 5. It contains four beds with *Neusticosaurus pusillus*, designated oldest to youngest as beds A–D. Other bed names are those used by the excavators. Note scale.

The fossiliferous beds are bituminous, finely laminated limestones. Only 6–10 m of thinly bedded and laminated carbonates lie between the Cava Inferiore horizon and the Cava Superiore horizon.

Eight beds of the Cava Superiore horizon have exclusively contained *Neusticosaurus peyeri* and

exhibit the same lithology as those of the Cava Inferiore horizon. The Cava Superiore horizon averages about 4 m in thickness. The 20–30 m of section between the Cava Superiore and the Alla Cascina horizons consists of thinly bedded or laminated carbonates. Disarticulated pachypleurosaur remains are occasionally found in the upper 10 m. It is unclear how many fossiliferous beds are present in the 2 m thick Alla Cascina horizon, but all of them have yielded only *Neusticosaurus edwardsii*. This horizon is the stratigraphically highest occurrence of pachypleurosaurids but not of tetrapods at the Monte San Giorgio. About 380 m higher, in the 'Kalkschieferzone' (Upper Ladinian), a single, small specimen of *Lariosaurus* was found in 1971. It was described as a new species, *L. lavizzarii*, by Kuhn-Schnyder (1987) but recognized by Tschanz (1989) as juvenile *Lariosaurus balsami*.

A fifth bed with pachypleurosaurids, located along the road between Crocifisso and Serpiano (above Acqua del Ghiffo), was mentioned by Zangerl (1935). As a result of recent fieldwork, it could be correlated to the Alla Cascina horizon. All species are strictly stratigraphically separated, no range overlap exists. None of the claims to the contrary cited by earlier workers (Peyer 1932, 1934; Zangerl 1935; Carroll & Gaskill 1985) could be verified. Either the identification of the specimens or the locality information turned out to be wrong.

Table 1 lists the localities at which the four horizons crop out. The PIMUZ collections include pachypleurosaurs from 19 different localities, 13 of which are located in the Swiss region of Monte San Giorgio. Only 14 of the old quarries could be located in 1986 (figure 1). The stratigraphic position of the other localities was inferred from their fossil content. Most of the localities produced vertebrates from only one bed, but at a few sites up to three horizons crop out. This confused earlier workers because specimens from the same locality were assumed to have come from the same bed. More confusion was introduced by abbreviated locality names. For example, specimens with the label 'Val Porina' came from the Grenzbitumenzone Beds of the Val Porina Mine (locality 11 in figure 1) or from the Cava Inferiore horizon cropping out in a small ravine in the lower Val Porina (locality 10 in figure 1).

Pachypleurosaurs were collected from the Grenzbitumenzone Beds at four sites (numbers in parentheses refer to the localities shown in figure 1): The Cava Tre Fontane Mine (8)

TABLE 1. CORRELATION BETWEEN FOSSILIFEROUS HORIZON, PACHYPLEUROSAUR TAXON AND LOCALITY

age	stratigraphy		pachypleurosaurid	localities
Ladinian	Meride limestone	Alla Cascina beds	*Neusticosaurus edwardsii*	Alla Cascina, Val Serrata (P. 5), Val Serrata (Bööggia), Road Crocifisso-Serpiano, Pra dei Spiriti, Ca' del Frate
		Cava Superiore beds	*Neusticosaurus peyeri*	Acqua del Ghiffo, Ca' del Monte
		Cava Inferiore beds	*Neusticosaurus pusillus*	Cascinello, Val Serrata (Cavo Don Luigi), lower Val Porina, Acqua del Ghiffo, Acqua Ferruginosa
	San Giorgio Dolomite			Ronco sopra Bisuschio, Vallone Bochetta, Val Piodissa
		Grenzbitumenzone	*Serpianosaurus mirigiolensis*	Cava Tre Fontane, Val Porina Mine, P. 902 Excavation, Cave di Besano
Anisian	Anisian Dolomite			

(coordinates: 716325/085475); the palaeontological excavation at P.902, sometimes called 'Mirigioli' (9) (coordinates: 716515/085525); the Val Porina Mine (11) (coordinates: 716115/085392) and The Cave di Besano Mines, Italy (3) (approximate coordinates: 713725/083450). The Cava Inferiore horizon produced useful results at eight localities, all excavations: Cascinello (14) (coordinates: 717650/084647); Val Serrata (Cava Don Luigi) (13) (coordinates: 717240/084915); lower Val Porina (10) (coordinates: 716580/084937); Acqua del Ghiffo (6) (coordinates: 715842/084902); Acqua Ferruginosa (5) (coordinates: 715500/084510); Ronco sopra Bisuschio, Italy (1) (approximate coordinates: 711900/081350); Vallone Bocchetta, Italy, and Val Piodissa, Italy. Only two localities, Acqua del Ghiffo (6) and Ca' del Monte, Valle dei Puncit, Italy (4) (approximate coordinates: 714850/085125), have yielded good fossils from the Cava Superiore horizon. Acqua del Ghiffo was a mining attempt turned palaeontological excavation. Pachypleurosaurs were collected from the Alla Cascina horizon at six localities: Alla Cascina, the type locality (12) (coordinates: 717015/085027); Val Serrata (P.5), Val Serrata below cave Bööggia (15) (coordinates: 717664/084325); Road Crocifisso–Serpiano (above Acqua del Ghiffo) (7) (coordinates: 715902/084892); Pra dei Spiriti (Italy), Ca' del Frate (near Viggiu, sometimes described as 'near Besano'), Italy (2) (approximate coordinates: 713400/082625). This last locality is important because the first pachypleurosaur, the type specimen of *Neusticosaurus edwardsii*, was found here (Carroll & Gaskill 1985).

It is difficult to evaluate the absolute ages of the pachypleurosaur horizons. The oldest, the Grenzbitumenzone Beds, spans the Anisian–Ladinian boundary (Rieber 1973*a*, *b*), whereas all the others are early to Middle Ladinian. Radiometric dating of some tuffs from the Grenzbitumenzone Beds and the Cava Inferiore horizon (Hellman & Lippolt 1981) produced absolute ages of around 230 Ma. Because the margins of error of the two ages overlap, they do not indicate how much time is represented in the 180 m of San Giorgio Dolomite and Lower Meride Limestone below the Cava Inferiore horizon. Considering the lithologies of massive carbonates (fast deposition) and bituminous laminated limestones (slow deposition), one can assume that a few million years are involved. However, because the sedimentology of the Ladinian carbonates remains virtually unstudied (Rieber & Sorbini 1983), time estimates must remain guesswork. The next youngest stratigraphic datum is a late Ladinian palynoflora (Scheuring 1978) from the 'Kalkschieferzone' of Frauenfelder (1916). It indicates that the Meride Limestones do not reach into the Carnian.

4. *Neusticosaurus pusillus* from Monte San Giorgio

(*a*) *Comparison with the German* Neusticosaurus pusillus

Carroll & Gaskill (1985) referred the small pachypleurosaurs from Monte San Giorgio to the genus *Neusticosaurus*, which was first described from the German Middle Triassic. They were reluctant to assign the Alpine material to the type species *N. pusillus* because the German material is so poorly preserved. Little needs to be said about the morphology of the German specimens as they were adequately described by Seeley (1882), and Carroll & Gaskill (1985). My own studies of the type specimen and referred material at Stuttgart and Tübingen lead me to agree with the description and conclusions of Carroll & Gaskill (1985). Although the German and the Alpine *Neusticosaurus* species show no anatomical differences, their preservation is too different to support synonymy on morphological grounds. This problem may be solved

with a morphometric approach, and this section will demonstrate that one species of the small Alpine pachypleurosaurs can indeed be referred to *Neusticosaurus pusillus*.

This identification has important biostratigraphic implications. A long-standing problem in European Triassic stratigraphy has been the correlation between the Germanic Triassic and the Alpine Triassic because their lithologies are very different and because few fossils are found in common. *Neusticosaurus pusillus* is one of the few fossils and the only fossil vertebrate that can be found in both regions. This is especially significant because *Neusticosaurus pusillus* is a very short-lived species at Monte San Giorgio (see §§3 and 15*c*). Its disappearance can be pinpointed to the interval between the Cava Inferiore horizon and the Cava Superiore horizon, both of early Ladinian age. The German Lettenkeuper Beds are considered to be early to Middle Ladinian in age (Brinkmann 1986). *Neusticosaurus pusillus* thus corroborates this correlation between the Alpine and the Germanic Triassic.

Quantitative analysis

The holotype of *Neusticosaurus pusillus* (BM(NH) R 53) comes from the Lower Keuper Hoheneck-Dolomite at Hoheneck near Ludwigsburg, southwest Germany. From this and another quarry nearby, additional material was collected and deposited at the Staatliches Museum für Naturkunde at Stuttgart and at the Geologisch-Paläontologisches Institut at Tübingen (see referred material). Although up to 12 skeletons commonly occur on one slab, most of them are incomplete, and sometimes only the vertebral column remains. Preservation is much worse than at Monte San Giorgio but the fossils are less crushed, and long bone measurements are easily and accurately done.

Twenty-five German *Neusticosaurus* specimens were measured and compared with the Monte San Giorgio pachypleurosaurs. The great similarity between this sample and the Monte San Giorgio sample is evident in table 2. The Monte San Giorgio sample that was used for this analysis consists exclusively of adults of both sexes (sex *x* and sex *y*, sexual dimorphism is discussed below); the German sample contains one juvenile by Monte San Giorgio standards (SMNS 9748a). Sex *y* is strongly underrepresented in the German sample with only two specimens (SMNS 7381-1 and BM(NH) R 53, the type) and one of indeterminate sex (SMNS 53932-7).

The number of dorsal vertebrae in the German and the Alpine *Neusticosaurus pusillus* is virtually identical. This character is of great systematic value because it varies little within species but serves well to separate species (figure 3). The (adult) size range and its mean (table 2) are also very close in both samples. Two unusually large specimens (SMNS 8297 and BM(NH) R 53, the type) in the German sample fall into the uppermost part of the size range of the Monte San Giorgio sample. This, and the rarity of sex *y* in the German sample could reflect taphonomic bias and habitat bias and differences between populations, or both. Although these two samples are widely separated palaeogeographically, they are remarkably similar. This similarity is enhanced if a scarcely younger population of the same species from Monte San Giorgio and the sample of the closely related, slightly younger *Neusticosaurus peyeri* are entered into the comparison.

Most proportions are not statistically different for the two samples except where sexual dimorphism is involved (table 3). The Monte San Giorgio sample differs from the German sample in both sexes only in one out of ten counts. The radius:ulna ratio may have a large margin of error because it was available in only five specimens of the German sample. In

TABLE 2. COMPARISON OF THE MONTE SAN GIORGIO SAMPLE AND THE GERMAN SAMPLE OF *NEUSTICOSAURUS PUSILLUS*

(Sexes are not separated except where a clear sexual dimorphism is apparent in the Monte San Giorgio sample. All measurements are in mm.)

	Germany		Monte San Giorgio		
	range	mean	range	sex *y*	mean
number of trunk vertebrae	23–24	23.4	22–24	—	23.0
trunk length	55–93.6	68.3	50–81	—	66.1
ratios					
skull:standard	1.70–2.00		1.64–2.20		
trunk:standard	4.21–5.44		3.91–5.46		
humerus:standard	0.89–1.25		0.95–1.20 (1.50)		
radius: standard	0.48–0.68		0.50–0.75 (0.65)		
femur:standard	0.91–1.50		0.97–1.40		
fibula:standard	0.54–0.92		0.56–0.72		
skull:trunk	0.33–0.41		0.31–0.58		
humerus:trunk	0.18–0.24		0.20–0.25 (0.33)		
femur:trunk	0.20–0.29		0.22–0.25 (0.30)		
humerus:femur	0.87–1.03		0.88–1.00 (1.15)		
humerus:radius	1.73–1.80		1.70–1.95		
radius:ulna	1.17–1.26		1.10–1.24		
femur:humerus	0.97–1.18		1.00–1.14 (0.87)		
femur:fibula	1.69–2.26		1.75–2.26		
fibula:tibia	1.03–1.20		1.01–1.16		

TABLE 3. IDENTITY OF SELECTED PROPORTIONS OF *NEUSTICOSAURUS PUSILLUS* FROM TABLE 2

(Test for significance at $p = 0.2$; ×, not rejected; +, rejected. Italic indicates proportions that are sexually dimorphic in the Monte San Giorgio sample.)

	Germany	Monte San Giorgio			
		sex *x*		sex *y*	
ratio	mean	mean	sign	mean	sign
trunk:standard	4.80	4.60	×	4.65	×
skull:standard	1.83	1.96	×	1.97	×
humerus:standard	1.08	1.06	×	1.31	+
femur:standard	1.20	1.12	+	1.20	×
radius:standard	0.61	0.59	×	0.69	+
fibula:standard	0.67	0.61	+	0.65	×
humerus:femur	0.94	0.94	×	1.07	+
radius:ulna	1.21	1.12	+	1.16	+
fibula:tibia	1.13	1.11	×	1.08	+

addition, the radius and ulna are often poorly preserved. Sex *x* of the Monte San Giorgio sample differs from the German sample only in femur:standard, radius:standard, and radius:ulna ratios (table 3). Sex *y* differs from the German sample in five counts, three of which (humerus:standard, radius:standard and humerus:femur ratios) are clearly related to sex differences, because the German sample consists largely of sex *x*.

Because the vertebral count (table 2), the size range (table 2), and all of the important ratios (i.e. trunk:standard, skull:standard, humerus:standard and humerus:femur) show no significant differences (except for sex differences, table 3), the German and the Alpine sample are considered to represent the same species, *Neusticosaurus pusillus*.

(b) Systematic palaeontology

Class: Reptilia Linnaeus, 1758
Order: Sauropterygia Owen, 1860
Suborder: Nothosauria Zittel, 1889
Family: Pachypleurosauridae Nopcsa, 1928
Genus: *Neusticosaurus* Seeley, 1882

Synonymy.

1854 *Pachypleura* – E. Cornalia, *Giorn. I. R. Ist. Lombard.* ser. 2, **6**, p. 5.
1881 *Simosaurus* – O. Fraas, *Jh. Ver. vaterl. Naturk. Württ.* **37**, p. 321 ff.
1882 *Neusticosaurus* – H. G. Seeley, *Q. Jl geol. Soc. Lond.* **38**, p. 350 ff.
1889 *Neusticosaurus* (*Pachypleura*) – R. Lydekker, *Catalogue of fossil Amphibia and Reptilia in the British Museum* (*Nat. Hist.*), part 2, p. 285.
1927 *Pachypleurosaurus* – F. Broili, *Sber. bayer. Akad. Wiss., math.-nat. Abt* **1927**, p. 220.
1928 *Pachypleurosaurus* – F. v. Nopcsa, *Geol. Hung.* ser. paleo. **1**, p. 20.

Diagnosis. Small to large pachypleurosaurid with very small head. Orbits large with well-developed sclerotic rings. Small, conical thecodont teeth with longitudinal striations; 17–25 teeth in upper jaw, 25–28 in lower jaw. Upper temporal openings small, postorbitals sometimes participating. Ectopterygoids absent.

There are 15–20 cervical vertebrae, 19–24 dorsal vertebrae, resulting in a presacral count of 34–44 vertebrae; 3 or 4 sacral vertebrae, and 40–60 tail vertebrae; 22–28 gastralia, consisting of three elements each. Anterior cervical ribs with distinct anterior processes. Ribs and other bones pachyostotic in the smaller members of the genus; 8–13 caudal ribs, 25–35 haemapophyses.

Scapula with large ventral part and narrow, rounded blade. Humerus slightly shorter to almost twice as long as femur. Humerus length and shape sexually dimorphic. Sex *x* have humeri with slightly expanded distal ends and poorly developed muscle attachment surfaces. Sex *y* have humeri with greatly expanded distal ends and constricted shafts. Humeri of sex *y* usually longer than those of sex *x*; two or three elements in carpus. Well developed entepicondylar foramen. Primitive reptilian or slightly reduced phalangeal count in hand.

Femur the size of humerus or reduced to half its length. Femur slender with expanded proximal end. Only two elements in carpus. Primitive reptilian or slightly reduced phalangeal count in foot.

Type species. Neusticosaurus pusillus Seeley, 1882, p. 350.

Other species. Neusticosaurus edwardsii (Cornalia) n.comb. and *Neusticosaurus peyeri* n.sp.

Age. Middle Triassic, Ladinian.

Occurrence. Southern Alps of Switzerland (Meride Limestone of Monte San Giorgio) and Italy (Besano, Perledo, Campione); Southwestern Germany (Hoheneck Dolomite of Hoheneck and Eglosheim, both near Stuttgart).

Neusticosaurus pusillus (Fraas, 1881); Seeley, 1882

Synonymy.

1881 *Simosaurus pusillus* – O. Fraas, *Jh. Ver. vaterl. Naturk. Württ.* **37**, p. 321.
1882 *Neusticosaurus pusillus* (Fraas) – H. G. Seeley, *Q. Jl geol. Soc. Lond.* **38**, p. 350.

1889 *Neusticosaurus pusillus* (Fraas) – R. Lydekker, *Catalogue of fossil Amphibia and Reptilia in the British Museum (Nat. Hist.)*, part 2, p. 285.
1896 *Neusticosaurus (Pachypleura) pusillus* – E. Fraas, *Festgabe des Königl. Nat.-Cabinets Stuttgart zur 42. Jahresversammlung der Dt. geol. Ges.*, p. 13.
1896 *Neusticosaurus pygmaeus* nov.sp. – E. Fraas, *Festgabe des Königl. Nat.-Cabinets Stuttgart zur* 42. *Jahresversammlung der Dt. geol. Ges.*, p. 13.
1924 *Neusticosaurus pusillus* – G. v. Arthaber, *Acta Zool.* **5**, p. 446.
1924 *Neusticosaurus pygmaeus* – G. v. Arthaber, *Acta Zool.* **5**, p. 449.
1927 *Neusticosaurus pusillus* – F. Broili, *Sber. bayer. Akad. Wiss., math.-nat. Abt* **1927**, p. 214.
1927 *Neusticosaurus pygmaeus* – F. Broili, *Sber. bayer. Akad. Wiss., math.-nat. Abt* **1927**, p. 214.
1928 *Pachypleurosaurus* – F. v. Nopcsa, *Geol. Hung.* ser. paleo. **1**, p. 20.
1928 *Pachypleurosaurus edwardsi* Cornalia – B. Peyer, *Acta Soc. Helv. Sci. Nat.* 109th. Sess., **1928**, p. 219.
1928 *Neusticosaurus pusillus* – M. Schmidt, *Die Lebewelt unserer Trias*, Öhringen, Hohenlohe'sche Buchhandlung, p. 406.
1928 *Neusticosaurus pygmaeus* – M. Schmidt, *Die Lebewelt unserer Trias*, Öhringen, Hohenlohe'sche Buchhandlung, p. 407.
1932 *Pachypleurosaurus edwardsii* Cornalia spec. (in part) – B. Peyer, *Abh. Schw. Pal. Ges.* **52**, p. 3.
1935 *Pachypleurosaurus edwardsi* Cornalia sp. (in part) – R. Zangerl, *Abh. Schw. Pal. Ges.* **56**, p. 1.
1941 *Pachypleurosaurus Edwardsii* (Cornalia) – V. Vialli, *Riv. Sci. Nat.* '*Natura*' **32**, p. 34.
1950 *Neusticosaurus pygmaeus* – G. Wagner, *Einführung in die Erd- und Landschaftsgeschichte*, Öhringen, Hohenlohe'sche Buchhandlung, p. 448, pl. 170.
1956 *Pachypleurosaurus* (in part) – F. v. Huene, *Paläontologie und Phylogenie der niederen Tetrapoden*, Jena, VEB Gustav Fischer, p. 383.
1956 *Neusticosaurus pusillus* – F. v. Huene, *Paläontologie und Phylogenie der niederen Tetrapoden*, Jena, VEB Gustav Fischer, p. 384.
1956 *Neusticosaurus pygmaeus* – F. v. Huene, *Paläontologie und Phylogenie der niederen Tetrapoden*, Jena, VEB Gustav Fischer, p. 384.
1958 *Neusticosaurus* – C. C. Young, *Vertebr. Palasiat.* **2**, pp. 76, 80.
1958 *Pachypleurosaurus* (in part) – C. C. Young, *Vertebr. Palasiat.* **2**, p. 75.
1959 *Pachypleurosaurus edwardsi* (Cornalia) (in part) – E. Kuhn-Schnyder, *Eclog. geol. Helv.* **52**, p. 650.
1963 *Pachypleurosaurus edwardsi* (in part) – E. Kuhn-Schnyder, *Arch. Sto. Tic.* **16**, p. 825.
1964 *Pachypleurosaurus edwardsi* (Cornalia 1854) (in part) – E. Kuhn-Schnyder, *Geol. Rdsch.* **53**, p. 403.
1967 *Pachypleurosaurus edwardsi* (Cornalia) (in part) – G. Pinna, *Natura, Milano* **58**, p. 188.
1974 *Pachypleurosaurus edwardsi* (Cornalia) (in part) – E. Kuhn-Schnyder, *Neujahrsblatt, Naturf. Ges. Zürich* **176**, p. 65.
1976 *Pachypleurosaurus* cf. *staubi* Kuhn-Schnyder – N. J. Mateer, *Bull. geol. Inst. Univ. Upsala, N.S.* **6**, p. 107.
1984 *Neusticosaurus* (in part) – R. L. Carroll, *3rd Symposium Mesozoic Terrestrial Ecosystems Short Papers*, Tübingen, Attempto Verlag, p. 43.
1985 *Neusticosaurus* sp. (in part) – R. L. Carroll & P. Gaskill, *Phil. Trans. R. Soc. Lond.* B **309**, p. 354.
1987 *Neusticosaurus* (in part) – S. Schmidt, *Neues Jb. geol. Paläont. Abh.* **173**, p. 341, p. 344.

Diagnosis. Small *Neusticosaurus*, rarely up to 520 mm overall length and 105 mm trunk length, but usually not more than 400 mm overall length and 85 mm trunk length. Average trunk length 66 mm, at sexual maturity 55 mm. Skull table narrow with parallel margins, orbits relatively small. Relatively large, oval upper temporal openings; 17 tooth alveoli in upper jaw, 25 in lower jaw.

There are 18–20 cervical vertebrae and 22–24 dorsal vertebrae resulting in 41–43 presacral vertebrae; 3–4 sacral vertebrae and 54–58 caudals. No atlas ribs. Anterior and posterior process of anterior cervical ribs of equal size. Posterior cervical, dorsal, and sacral vertebrae and ribs strongly pachyostotic; 10–12 caudal ribs, up to 23 haemapophyses. Low neural spines throughout the entire column.

Anterior margin of shoulder girdle normal to body axis, narrow and straight clavicles with short posterior processes. Interclavicle small, without posterior process. Scapular blade long and thin, posteromedial corner of scapula and anteromedial corner of coracoid with indentations for the coracoid foramen. Relatively large pectoral window.

Humerus sexually dimorphic. Sex *x* humerus:femur ratio $\leqslant 1$ and humerus strongly pachyostotic. Sex *y* humerus:femur ratio $\geqslant 1$. Two elements in carpus. Phalangeal formula of hand 2–3–4–4/5–3.

Thyroid fenestra large, obturator foramen always slit-like. Femur with oval cross section, triangular at proximal end. Two elements in tarsus, astragalus clearly wider than calcaneum, phalangeal formula of foot 2–3–4–4/5–3.

Age. Middle Triassic, early to Middle Ladinian.

Horizon and localities. Known from the Cava Inferiore horizon (figure 5, table 1) of the Lower Meride Limestone from the following localities (figure 1): Acqua del Ghiffo, Acqua Ferruginosa, Cascinello, lower Val Porina, Val Serrata, and Val Serrata (Cava Don Luigi) in the Monte San Giorgio area of southern Switzerland; Besano, Ronco sopra Bisuschio, and Val Piodissa in northern Italy; and from the Hoheneck Dolomite of the Lettenkeuper Beds, from the following localities: Hoheneck and Eglosheim, Baden-Württemberg, Southwest Germany.

Holotype. BM(NH) R 53, Hoheneck Dolomite (Lettenkeuper Beds), from a quarry at Hoheneck near Ludwigsburg, Baden-Württemberg, Germany, probably collected in 1880, and purchased by the BM(NH) in June 1881 from J. Hoser of Stuttgart.

Referred material. PIMUZ: T 3387, T 3388, T 3390, T 3392, T 3405, T 3409, T 3416, T 3418, T 3419, T 3421, T 3424, T 3426, T 3429, T 3432, T 3434, T 3442, T 3451, T 3468, T 3478, T 3481, T 3483, T 3484, T 3509, T 3513–T 3519, T 3525–T 3530, T 3532–T 3534, T 3535a, T 3535b, T 3536, T 3538, T 3540, T 3541, T 3544, T 3545, T 3547a, T 3547b, T 3548a–T 3548e, T3551, T 3553a, T 3553b, T 3555, T 3556, T 3558–T 3573a, T 3575b–T 3580, T 3585, T 3590, T 3591, T 3593–T 3600a, T 3600b–T 3606, T 3610–T 3614, T 3616–T 3618, T 3620–T 3636a, T 3636b–T 3645, T 3649a–T 3649c, T 3650a, T 3650b, T 3651–T 3654, T 3657–T 3658a, T 3658b–T 3661, T 3664, T 3670–T 3673, T 3703, T 3714, T 3717, T 3720, T 3721, T 3725, T 3737–T 3740, T 3741a–T 3741e, T 3743, T 3745–T 3748, T 3750, T 3751, T 3756, T 3757, T 3761, T 3763, T 3765, T 3767, T 3777, T 3779–T 3782, T 3784–T 3786, T 3790, T 3792–T 3796, T 3798, T 3802a–T 3802d, T 3803a–T 3803d, T 3805, T 3852, T 3905, T 3907, T 3909, T 3912, T 3934, T 3936, T 3937, T 3938a–T 3938h, T 4289, T 4293, T 4296, T 4300. Most of these are largely complete skeletons. The specimen numbers ending in a small letter indicate several skeletons on one slab.

BM(NH): R 54 (Seeley 1882), R 5720, R 5727–R 5738, all of these are largely complete skeletons; MCL, some uncatalogued specimens; PMM, a few uncatalogued specimens; MCSNM, 3, 4, 5, all of these are complete skeletons (Vialli 1941; Pinna 1967); PMU, R 441, skeleton without tail (Mateer 1976); R 442, skeleton without skull and anterior part of the neck (Mateer 1976).

SMNS, 7831, slab with 12 partial skeletons (Wagner 1950); 7382, two incomplete skeletons; 8279, large skeleton; 9142 partial skeleton; 9748, partial skeleton (E. Fraas 1896); 9748a, partial skeleton (E. Fraas 1896); 53929, slab with several incomplete skeletons; 53930, posterior trunk with proximal femora, poorly preserved; 53931, incomplete skeleton, poorly preserved; 53932, slab with three complete skeletons and nine partial skeletons; GPIT, 17968, slab with four partial skeletons; five uncatalogued slabs with one to five partial skeletons.

Taxonomic notes. Neusticosaurus pusillus was first described as *Simosaurus pusillus* by O. Fraas in 1881. Soon afterwards, the type and one additional specimen were purchased by the British Museum (Natural History) and redescribed by Seeley in 1882. Seeley pointed out that the animal in question differed greatly from *Simosaurus* by having large suborbital vacuities not found in any other nothosaur. This was a misinterpretation of poorly preserved material (Carroll & Gaskill 1985) but nevertheless it led Seeley on the right track. He erected the genus *Neusticosaurus* for this animal apparently without knowing about *Pachypleura edwardsii* (now *Neusticosaurus edwardsii*), which was described in 1854 by Cornalia, from Besano in northern Italy.

A few years later, Lydekker (1889) noted the great similarity between the two genera and stated that the differences between them were not sufficient to warrant generic separation. Noting that *Pachypleura* was preoccupied by a coelopteran, he tentatively proposed *Pachypleura* to be synonymous with *Neusticosaurus* and wrote *Neusticosaurus* (*Pachypleura*) Curioni. Although Lydekker gave the correct journal citation to *Pachypleura*, he erroneously cited Curioni and not Cornalia as the author. The synonymy of the genera *Neusticosaurus* and *Pachypleura* was further supported by Zittel (1887–1890). Deecke (1886) also believed that both genera were closely related. In 1896, E. Fraas described an additional species of *Neusticosaurus*, *N. pygmaeus*, which is distinguished only by its small size. In the same publication, he described additional material of *Neusticosaurus pusillus* and appeared to support the synonymy of *Neusticosaurus* and *Pachypleura* by writing *Neusticosaurus* (*Pachypleura*) *pusillus*.

The pendulum swung back with Arthaber (1924), who separated the two genera again. From then on, until this work, they were treated separately. In 1927, Broili suggested *Pachypleurosaurus* for the preoccupied *Pachypleura*. He discussed this form and the two species of *Neusticosaurus* in conjunction with the description of a new sauropterygian, *Rhäticonia rothpletzii*. Nopcsa arrived independently at *Pachypleurosaurus* for *Pachypleura* in 1928 (Nopcsa 1928). M. Schmidt (1928) designated small and large *N. pusillus* specimens as *N. pygmaeus* and *N. pusillus*, respectively.

In 1924, B. Peyer of Zurich acquired the first tetrapod fossil from the Lower Meride Limestone, the torso of a *Neusticosaurus pusillus* (T 3796). He assigned this fossil to *Pachypleurosaurus edwardsii* Cornalia (Peyer 1928). He described 11 more pachypleurosaurids from Monte San Giorgio as *P. edwardsii* in 1932, consisting of one *N. pusillus* (T 3400), eight *N. peyeri* (T 3393–T 3399, T 3403), and two *Serpianosaurus mirigiolensis* (T 3401, T 3402) specimens.

In 1934, Peyer changed the spelling of *Pachypleurosaurus edwardsii* from *P. edwardsii* to

P. edwardsi, reluctantly dropping the second '*i*' in '*edwardsii*'. He followed Nopcsa who, in 1928, dropped the second '*i*' according to a change in the *International code of zoological nomenclature* in 1927. Nopcsa's spelling change was not warranted because the original spelling was correct (Article 32 of the *International code of zoological nomenclature*). As I accept Cornalia's original spelling, '*edwardsii*' is used in this paper.

A sample of 105 specimens was monographically described by Zangerl (1935) as *Pachypleurosaurus edwardsi*. However, it contained specimens of *Serpianosaurus mirigiolensis* (Rieppel 1989*a*), *Neusticosaurus pusillus*, *N. peyeri*, and *N. edwardsii*. Not surprisingly, Zangerl noted a great variability in his sample.

In 1941, Vialli described three small skeletons as *Pachypleurosaurus edwardsi*, from Besano (Italy) that clearly belong to *N. pusillus*. A slab with small *Neusticosaurus pusillus* from Eglosheim was figured by Wagner in 1950 as *N. pygmaeus*. Huene (1956) instituted the family Pachypleurosauridae and figured the skull of a *N. pusillus* from the Alpine Triassic. He also briefly mentioned the German *Neusticosaurus*. When Young described *Keichousaurus hui* (Young 1958), he used *Neusticosaurus* and *Pachypleurosaurus* in the sense of Zangerl (1935) for comparison. Kuhn-Schnyder (1959, 1963, 1964) described some additional material of all three *Neusticosaurus* species under the name *Pachypleurosaurus edwardsi*, but expressed the opinion that this species could probably be subdivided into at least two species based on phalangeal counts and bone configuration of the rostrum. The same view was reiterated in a 1974 paper (Kuhn-Schnyder 1974). The three specimens described by Vialli in 1941 were figured together with the type of *Neusticosaurus edwardsii* by Pinna in 1967.

A new species of *Pachypleurosaurus*, *P. staubi*, was erected by Kuhn-Schnyder (1959) for a pachypleurosaurid torso with limbs from Stulseralp (Grisons, Switzerland). Two pachypleurosaurid specimens from the Calcare di Meride from Vallone Caves near Lake Lugano, northern Italy were carefully described and well illustrated by Mateer (1976). He tentatively assigned his specimens to *P. staubi* but failed to give the reasons for doing so. The specimens are, however, identical to *Neusticosaurus pusillus* and are referred here to this species. They probably come from the exact same beds (Cava Inferiore horizon) as the PIMUZ specimens of *N. pusillus*.

Carroll (1984) suggested that the small pachypleurosaurids in Zangerl's sample pertained to the genus *Neusticosaurus*. This view was elaborated by Carroll & Gaskill in 1985 and is supported by this study. As the three youngest pachypleurosaurids from Monte San Giorgio are congeneric (see §15*a*), all are assigned to the genus *Neusticosaurus* Seeley (1882*a*), the name with priority over *Pachypleurosaurus* Broili (1927).

(*c*) *Description*

Two hundred and twenty-nine prepared specimens of *Neusticosaurus pusillus* are in the PIMUZ collections, most of which are complete, articulated skeletons with skull, e.g. T 3934 (figure 7*a*; figure 24*a*, plate 1). *Neusticosaurus pusillus* comes exclusively from the Cava Inferiore horizon. It is generally somewhat smaller than *Neusticosaurus peyeri*. The standard length of the adults ranges from 10.8 to 17.0 mm and the trunk length from 50 to 82 mm. Juveniles are uncommon.

Skull

The description of the skull is based on a selection of the best specimens: T 3442, T 3597 (figure 8*a*), T 3617, T 3661 (figure 8*b*), and T 3751 (prepared by air abrasive; figure 8*c*) that

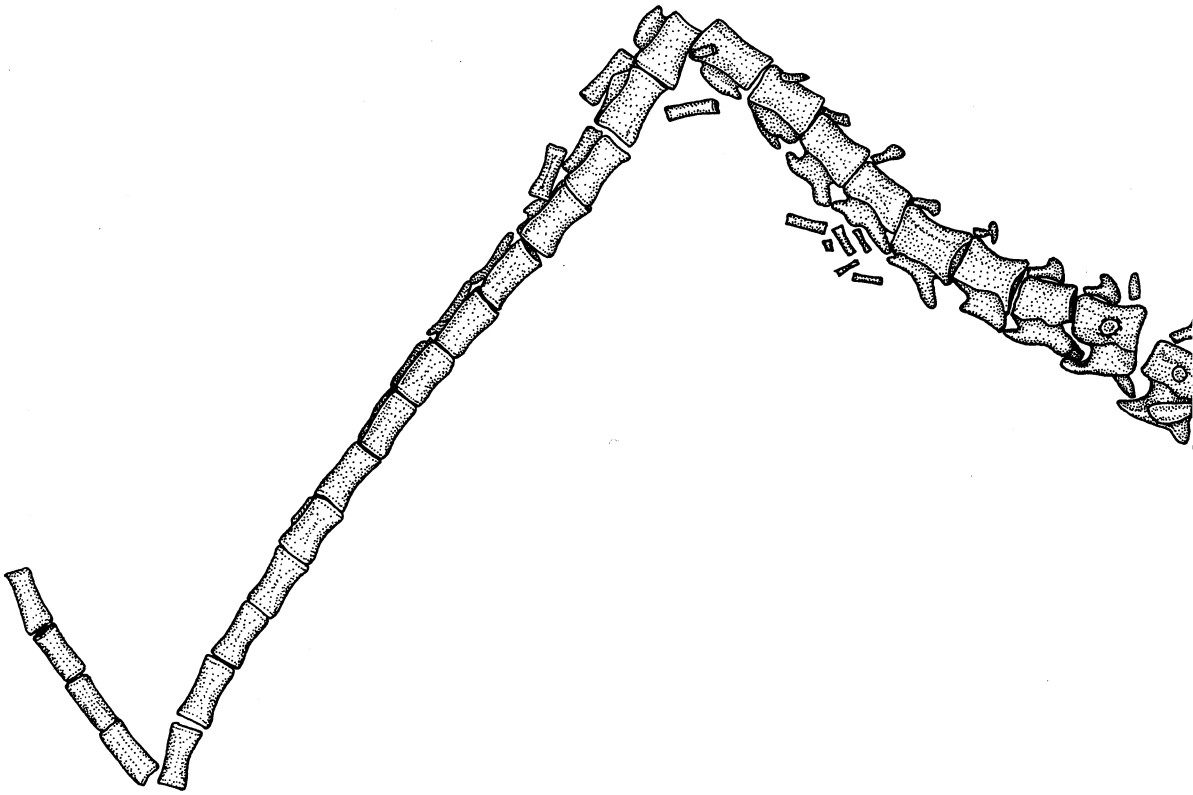

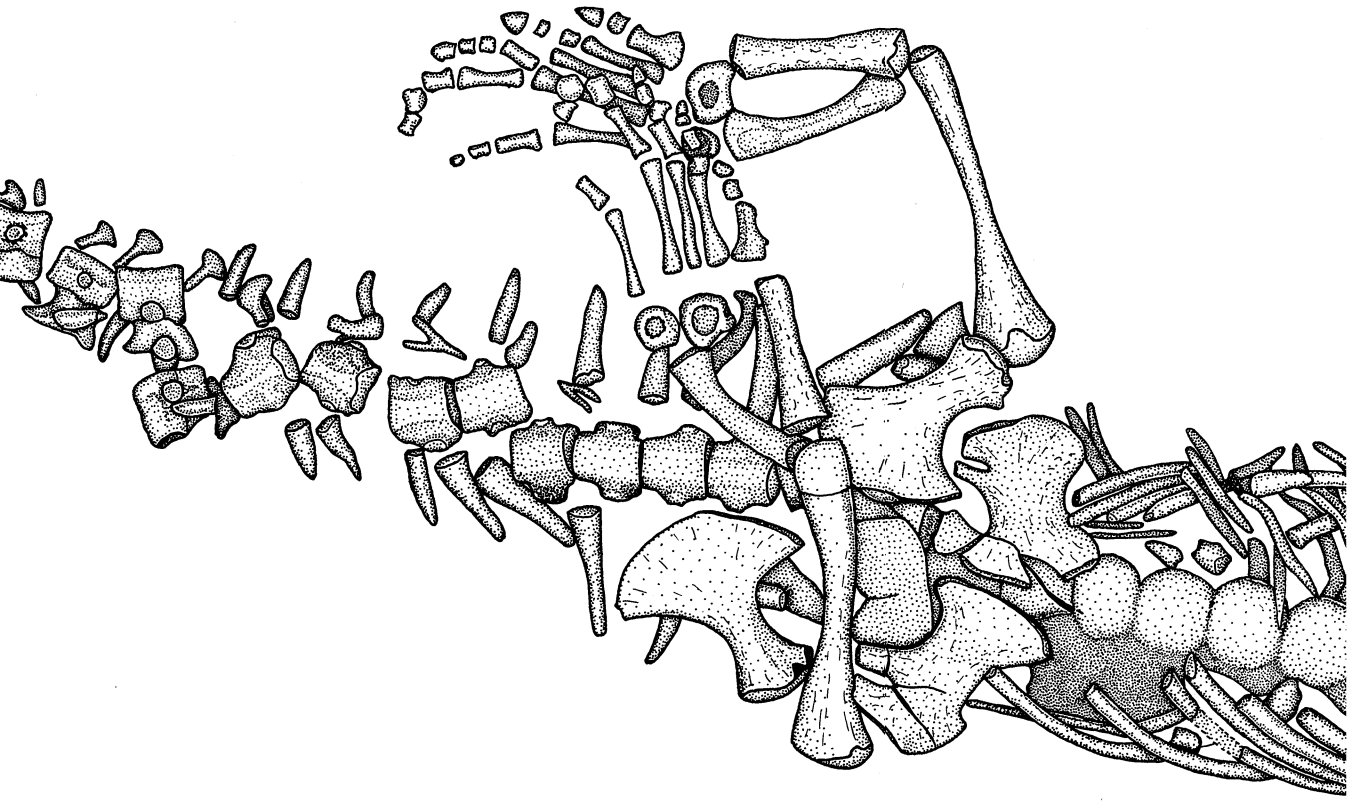

FIGURE 7*a*. Large adult specimen (T 3934) of *Neustico*

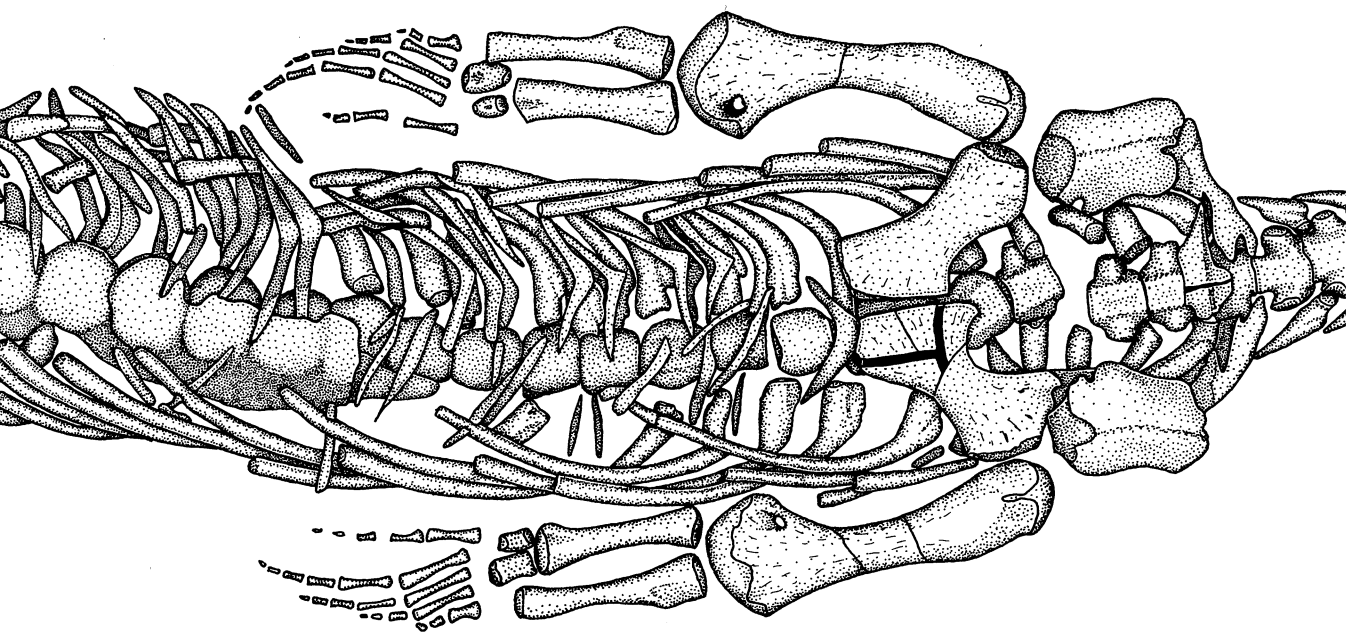

of *Neusticosaurus pusillus* from Monte San Giorgio; ventral view.

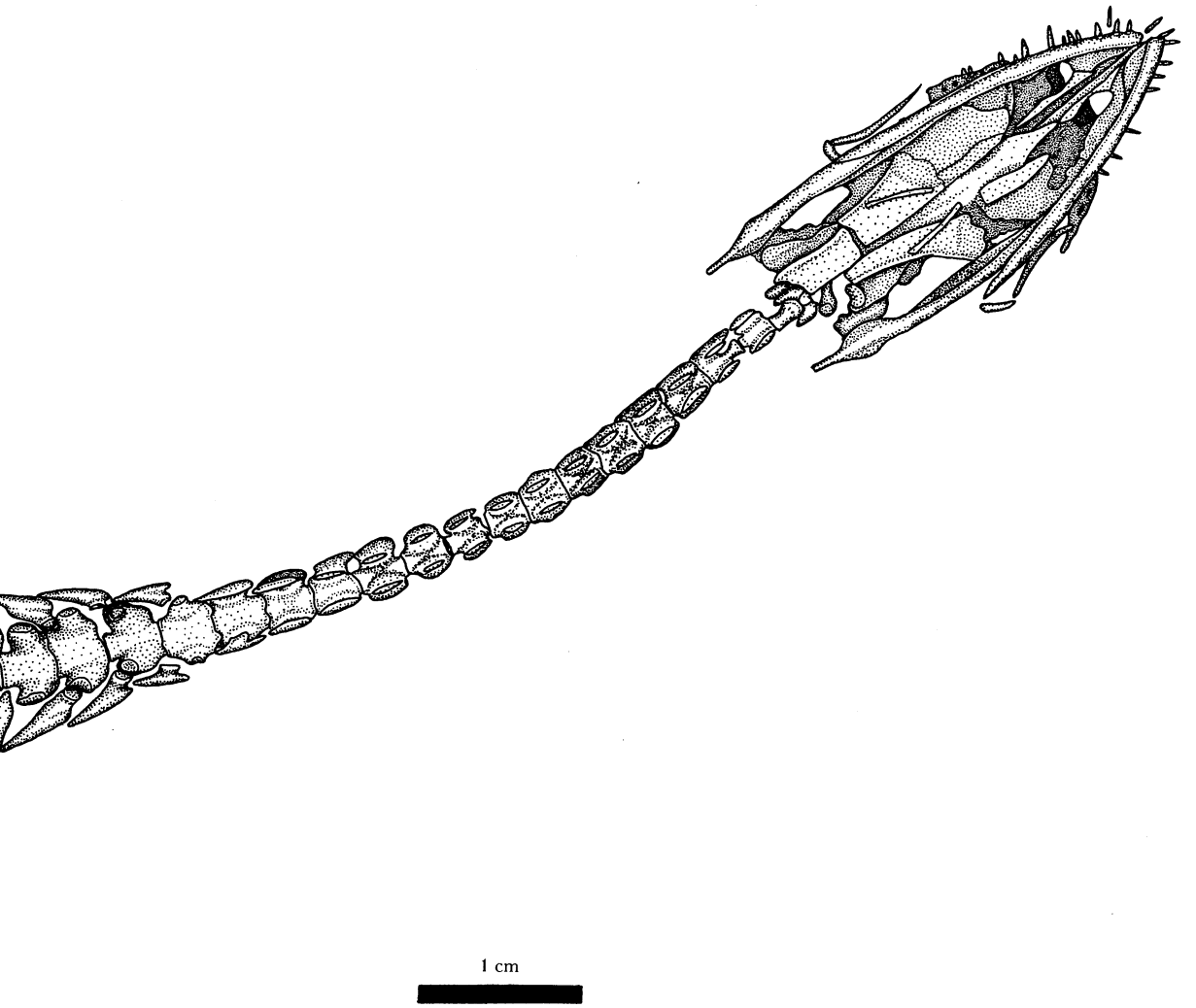

1 cm

(*Facing p.* 580)

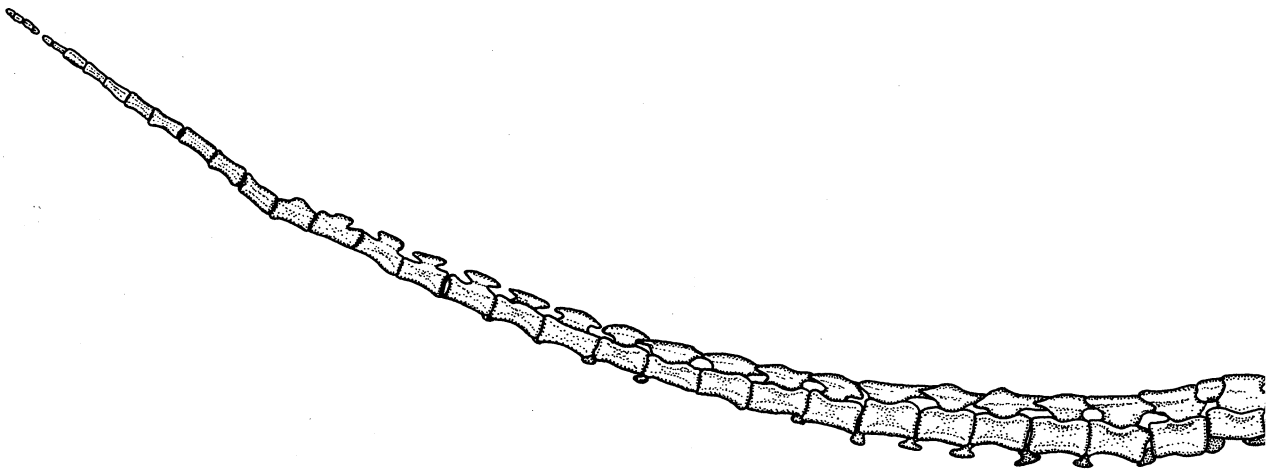

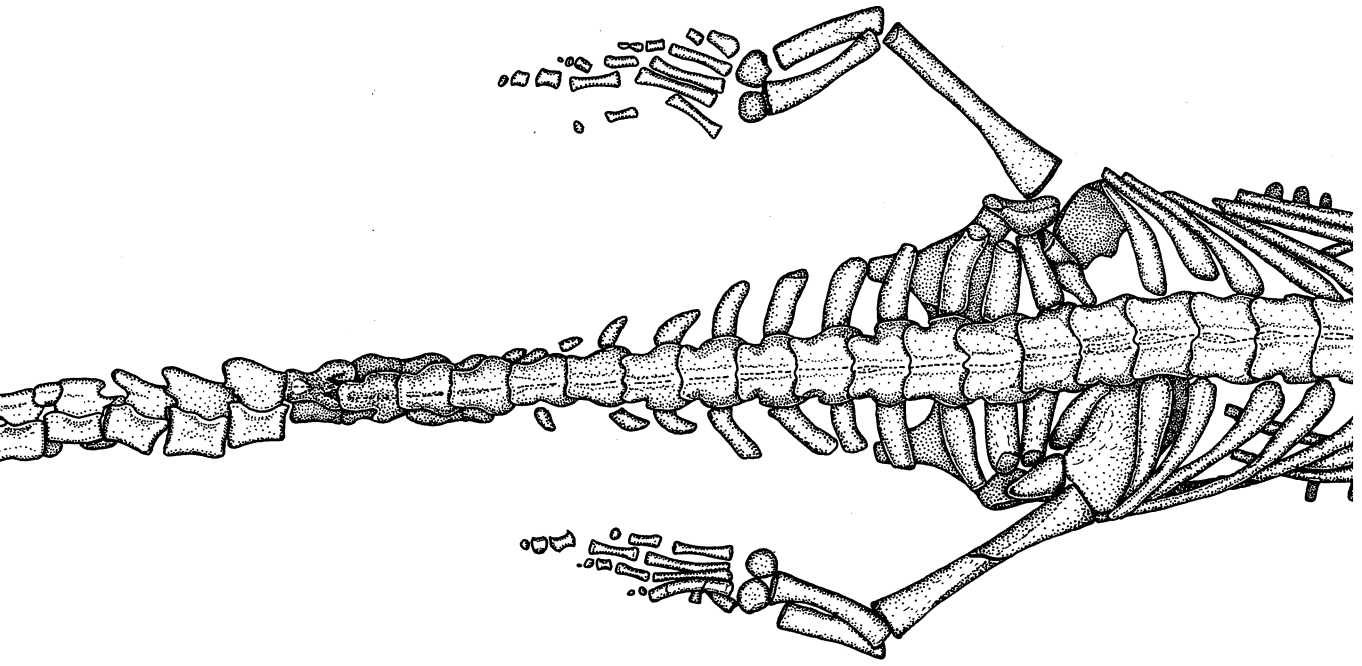

FIGURE 7*b*. The type specimen of *Neusticosaurus peyeri* (T 3615); c

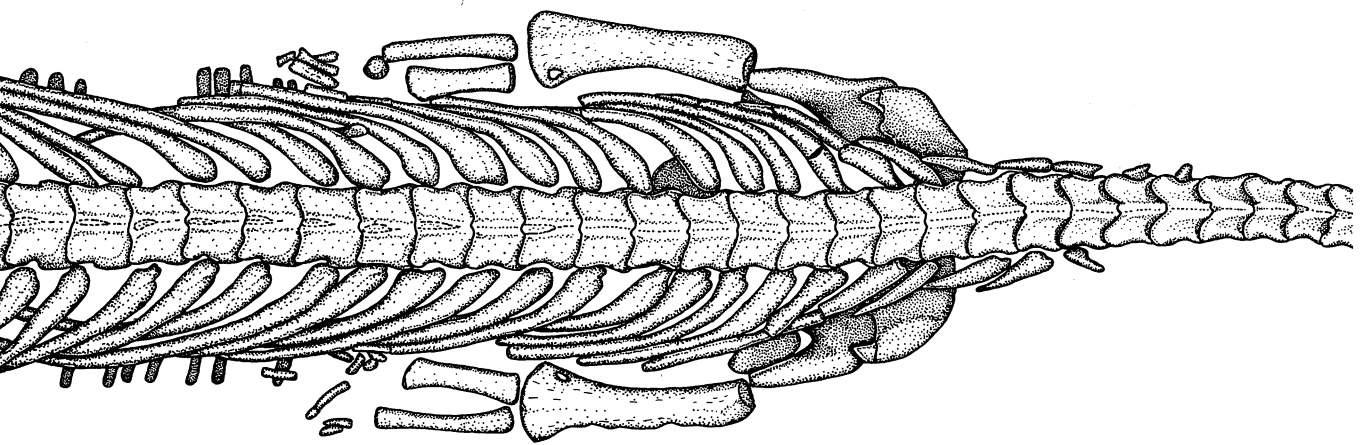

1 cm

(T 3615); dorsal view.

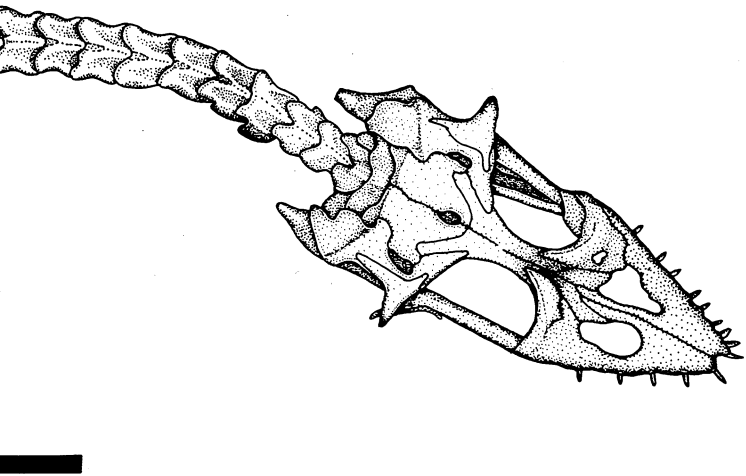

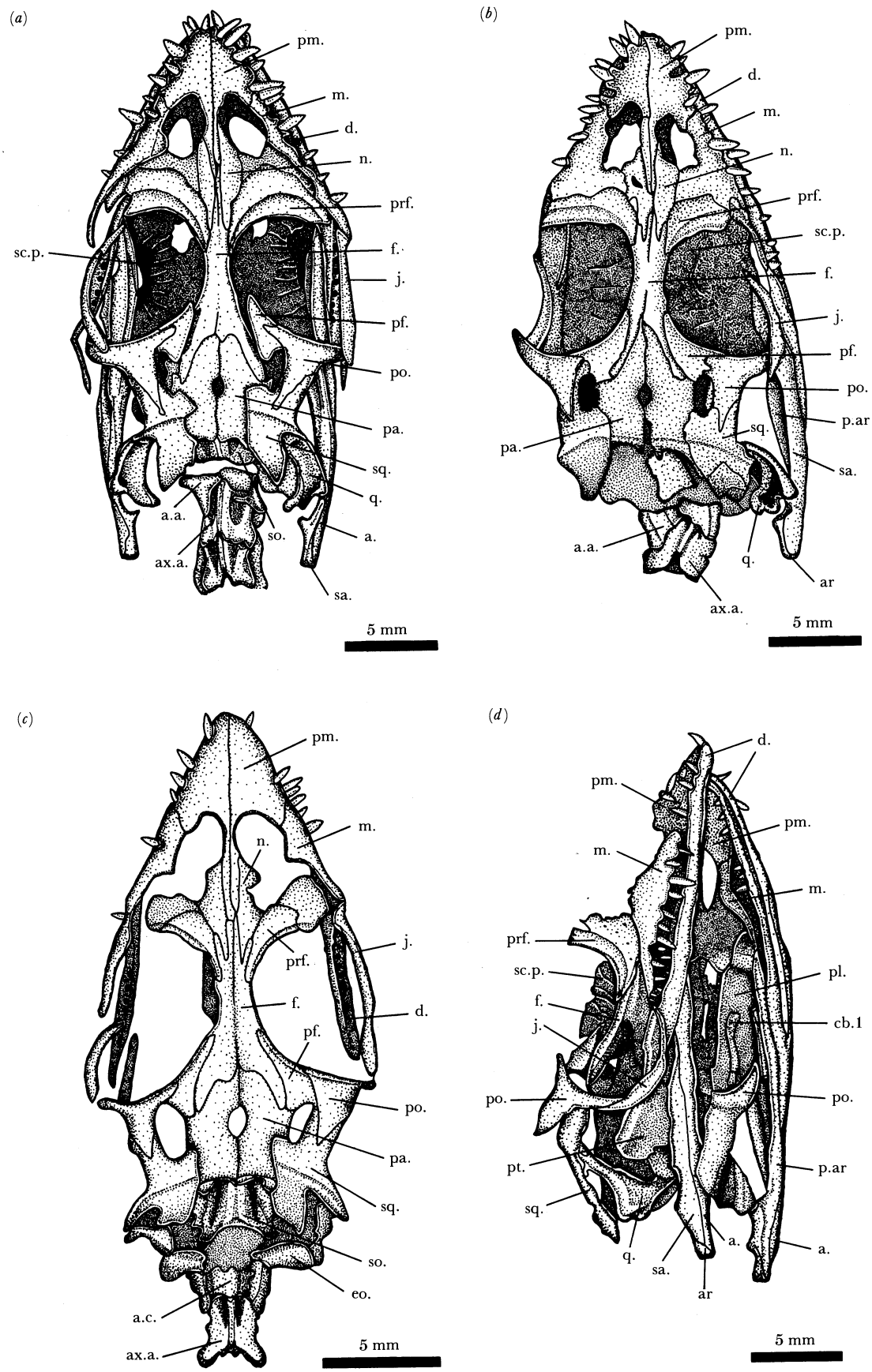

FIGURE 8. *Neusticosaurus pusillus* (*a–c*) the skull in dorsal view. (*a*) T 3597, (*b*) T 3661, (*c*) T 3751. These specimens clearly illustrate the variation observed in the anterior extent of the frontals and posterior extent of the premaxillae. The nasals touch each other in (*b*), only the right frontal and premaxilla make contact in (*a*), and both frontals and premaxillae touch in (*c*). (*d*) A latero-ventral view of the skull (T 3599). Note the articulation of the jugal with the postorbital. Abbreviations used in figures follow text.

are all exposed in dorsal view; T 3599 (figure 8*d*), exposed in a lateroventral view; T 3574, T 3576 (figure 9*b*), T 3585 (figure 10*a*), T 3624 (figure 9*c*), and T 3948 (figure 9*a*), all ventrally exposed. Specimen T 3624 is partially disarticulated. Specimens T 3530 (figure 12*a*), T 3573 (figure 12*b*), T 3658*b* (figure 12*c*), and T 3576 were the main sources of information about

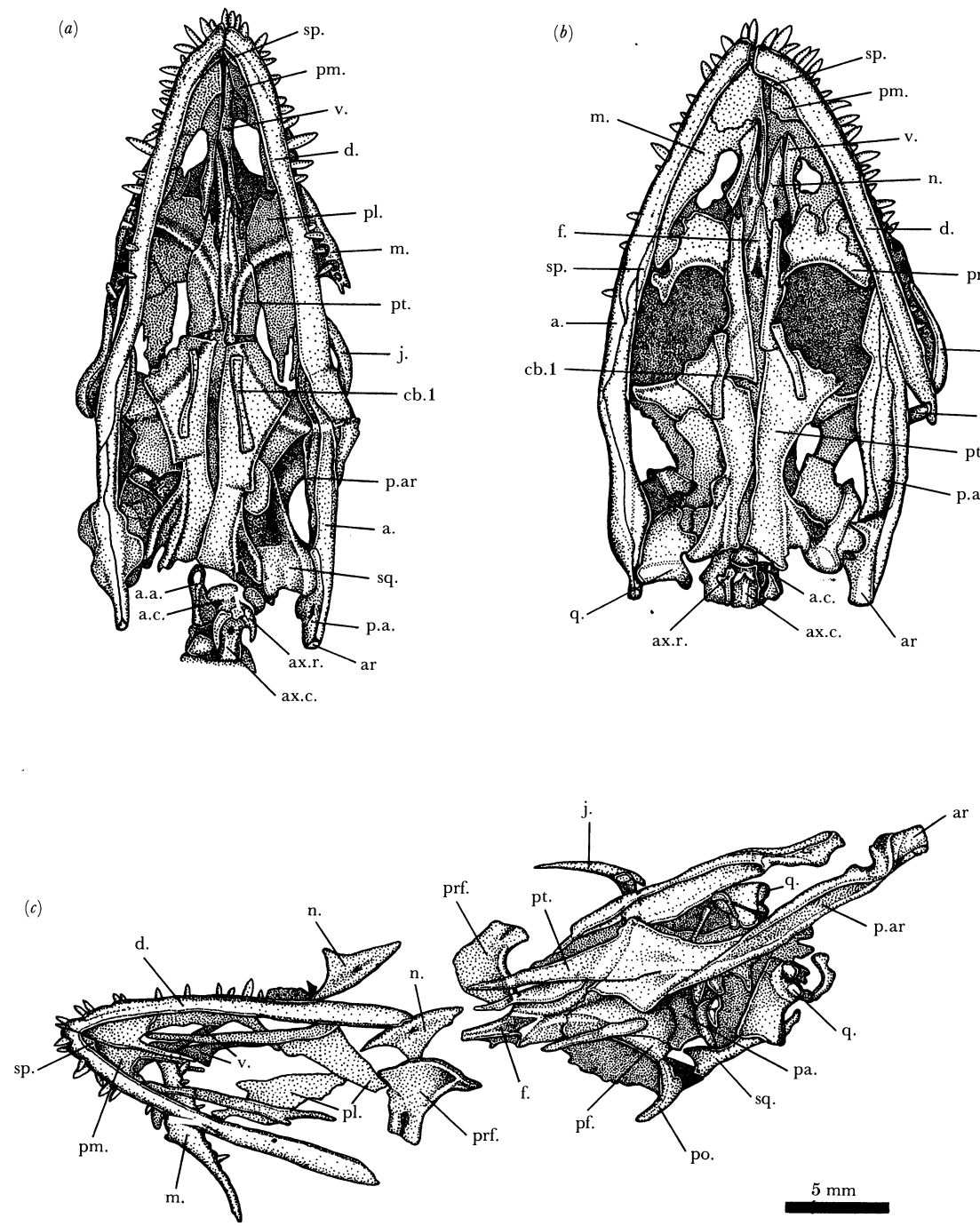

FIGURE 9. Skulls of *Neusticosaurus pusillus* in ventral view. (*a*) T 3948, (*b*) T 3576. The width of this specimen was greatly increased by compaction. Note the well preserved right lower jaw; (*c*) T 3624; this specimen was disarticulated before compaction. Note the articulated dentaries indicating the original width of the lower jaw, and the shape of the nasals with the central foramina.

lower jaw anatomy and its reconstruction (figure 13). Because all specimens are crushed dorsoventrally and no specimens in true lateral view are known, no direct information about height of the skull could be obtained. The reconstructions (figure 11) are necessarily composites, but the dorsal view is mainly based on T 3751 (figure 8*c*), the ventral view owes a great deal to T 3624 (figure 9*c*). The specimens are all of roughly the same size and can be considered as adults.

In general, the skull structure and proportions are similar to the other pachypleurosaurids (other species of *Neusticosaurus* (Carroll & Gaskill 1985), *Serpianosaurus* (Rieppel 1989*a*), *Anarosaurus* (Dames 1890), *Dactylosaurus* (Gürich 1884; Nopcsa 1928; Suess & Carroll 1985)), but are most similar to *Neusticosaurus peyeri*. The most striking features of the skull are its very low width, without an expanded skull table and generally poor ossification. The skull reaches close to maximum width at the anterior end of the orbits (figure 11*a*, *b*). From there on, the margins of the skull table are essentially parallel, in contrast to those of *N. edwardsii* (Carroll & Gaskill 1985) and *N. peyeri*, both of which show a broad skull table resulting in a somewhat wedge-shaped skull (figures 17 and 19). The orbits are relatively smaller and farther forward than in the two other forms.

The premaxillae form the snout and laterally reach back almost halfway to the anterior margin of the orbit. They are never fused. The region anterior to the nares often show some irregularly spaced small foramina, probably for the medial ethmoidal nerves and the subnarial branches of maxillary arteries (Oelrich 1956). Ventrally, the premaxillae extend medial shelves that make contact at the front but become separated farther back by the vomers. After participating in the anterior margin of the internal nares, the medial shelf makes contact with the maxillary shelf. The premaxilla has five alveoli, often found with all teeth in place but sometimes with only two. The teeth are all of about the same size (1.5 mm long) and show longitudinal striations.

The premaxillae send median processes back towards the anterior processes of the frontals. In dorsal view, a complete gradation can be seen from both premaxillary processes touching the anterior processes of the frontals (T 3751; figure 8*c*) to only one process touching the frontals (T 3597; figure 8*a*) to a complete separation of the premaxillae and the frontals by the nasals that meet at the skull midline (T 3661; figure 8*b*). This condition could also be described as 'united nasals'. Because of this complete gradation, the nasals separated – nasals united criterion, as advocated by Kuhn-Schnyder (1963, 1974), cannot be used for taxonomic purposes. In ventral view (figure 9*b*), it can be seen that the nasals always touch at the midline. The apparent separation or union of the nasals in dorsal view is only a function of the degree of posterior ossification of the posterior premaxillary processes and the anterior ossification of the anterior frontal processes. However, it should be noted that a complete dorsal union of the nasals is rare. The degree of nasal contact shows no correlation with size of the individual specimens.

The nasal is always a slender bone and never extends laterally around the anterior margin of the prefrontal contrary to the condition in *N. edwardsii* (Carroll & Gaskill 1985). The external nasal opening is not as elongate as in *N. edwardsii*; its length is about 30% of the antorbital length. The anterior margin is formed by the premaxilla and the lateral margin by the maxilla, the medial margin by the nasal. In some cases, the prefrontal seems to contribute to its posterior margin, but it is often difficult to delineate the medial part of the suture between maxilla and prefrontal because the prefrontal is invariably cracked owing to the heavy

preorbital ridge. The posterior ends of the nasal and prefrontal are usually separated by a lateroanterior process of the frontal that results in a characteristic trident shape of the anterior end of both frontals.

The prefrontal makes up the entire anterior margin of the orbit. This bone is labelled as lacrimal in earlier descriptions of pachypleurosaurids by Zangerl (1935), Kuhn-Schnyder (1941), and Mateer (1976), following a tradition established by Peyer (1932) who stated that his denotion 'lacrimal' is synonymous with Nopcsa's (1928) 'prefrontal'. A separate lacrimal is clearly absent (T 3599; figure 8*d*) in contrast to *Neusticosaurus edwardsii* in which Carroll & Gaskill (1985) were unable to decide whether this bone was present or not. The ventral margin of the orbit is made up by a slender jugal. The anterior end of this bone is wedged in between prefrontal and maxilla whereas the posterior end articulates with the postorbital. The maxilla reaches from its contact with the premaxilla as far back as the anterior end of the ventral margin of the orbit. As noted above, it reaches up the side of the snout to varying degrees. Ventrally the maxilla extends a narrow shelf in the plane of the palate making up the lateral margin of the internal nares and supporting the anterior lateral edge of the palatine. The maxilla bears about 12 alveoli for the thecodont teeth, but only six to nine teeth appear to have been functional at any one time.

Although the dentition appears essentially isodontal, the anterior maxillary teeth are some of the largest in the entire jaw and bear a resemblance to caniniform teeth (figure 8*a*, *b*, *d*). The teeth have a somewhat semicircular cross section with a flattened lateral side with longitudinal striations and a convex medial side with longitudinal ridges but no keels. The ridges and striations mark off the crown. The teeth are pointed and recurved towards the tip. In adult specimens they are up to 2 mm long but usually not more than 1.5 mm. They protrude well over the margin of the jaws (even when compaction is taken into account) and the anterior teeth interlock. This isodont dentition is typical for piscivorous reptiles adapted to catching and holding slippery fish and cephalopods.

The frontals are fairly massive bones separating the orbits. They show varying degrees of fusion. Complete separation could only be observed in juveniles (figure 33). They possess posterolateral processes that embrace the anterior margin of parietals. Posterior to the frontal, the margin of the orbit continues into the postfrontal that fits with a notch into the frontal. Postfrontal and postorbital bones both contribute about half each to the posterior margin of the orbit. Sclerotic plates are visible in many orbits (figure 8*a*, *b*) and in one case, half a sclerotic ring fell out of the orbit before fossilization (figure 10*c*). The number of sclerotic plates is hard to determine, but it was probably between 14 and 20.

The postorbital reaches deep into the postfrontal with a medial process, but it is nevertheless excluded from the upper temporal opening in many specimens. A lateral process of the postorbital reaches far down the side of the skull to articulate with the posterior end of the jugal, and a third, posterior process reaches deep dorsally into the squamosal, but is ventrally much less prominent (figures 9*c* and 10*a*).

The parietals form the medial part of the skull table and enclose the fairly large pineal foramen. Its centre is located two-fifths of the way back from the anterior margin of the parietals. The parietal reaches deep into the frontal and makes up the medial margin of the upper temporal opening. The upper temporal opening is rather small and oval, and measures less than 30% of the orbit length. The anterior margin of the upper temporal opening is made up by the postfrontal, and its lateral margin, by the squamosal.

The squamosal forms the lateral part and margin of the skull table and is anteriorly separated from the parietal by the upper temporal opening. Both bones are divided by an oblique crest, for the insertion of the neck musculature, which delineates the posterior margin of the skull table. The squamosal has a large lobe, extending down the posterior wall of the skull, which is medially joined by a much narrower and somewhat shorter process from the parietal.

The supraoccipital is suspended between (but not suturally connected to) the posteroventral processes of the parietals by means of the exoccipitals that, in turn, articulate with the posterior lobes of the squamosals. Thus the skull must have possessed post-temporal foramina. Because of flattening of the specimens, no three-dimensional reconstruction of the posterior view of the skull was possible.

The basioccipital is well exposed ventrally in many specimens, but dorsally in only one specimen (T 3442; figure 10*b*). The occipital condyle, and the exoccipitals only participate laterally. The dorsal surface of the basciocciptal shows a conspicuous ridge along the midline of the bone that does not reach the condyle (figure 10*b*). This same ridge was observed in an eosuchian by Evans (1980). It probably represents an ossification of the parachordals above the notochord (De Beer 1937).

The squamosal articulates with the quadrate and quadratojugal via a lateral process, which separates the latter two on the surface for about a third of their length. The quadrate is the posterior corner post of the skull. Its anterior surface is almost completely covered by the quadratojugal. The posteromedial margin of the quadrate shows a deep crescent-shaped embayment and a well-developed posterior process behind the articular surface with the lower jaw. Both features probably supported a large tympanum. Identification of a stapes like that figured by Carroll & Gaskill (1985, fig. 13*g*) could not be confirmed but must be assumed if a tympanum was present. The presence of a large tympanum implies that pachypleurosaurids were not deep divers, a point discussed in greater detail by Carroll & Gaskill (1985) and Rieppel (1989*a*).

No lower temporal bar is present as in all other nothosaurs. A lower temporal 'embayment' is formed with the anterior margin made up by postorbital and jugal, dorsal margin by the squamosal, and posterior margin by the quadratojugal.

The palate (figures 9 and 10*a*) is made up by the medial shelves of premaxillae and maxillae, by the vomers, palatines, and pterygoids that form most of its posterior half. The vomers make up the inner and anterior margins of the internal nares, the palatines the posterior margin. The palatal (medial) shelves of maxillae and premaxillae are responsible for the remainder of the margin of the internal nares. The internal nares are of about the same size as the external nares but moved slightly caudally (figure 11*b*). The pterygoid sends out a medial anterior process that makes contact with the vomer, but does not participate in the margin of the internal nares.

Laterally to this process, the palatine extends to the side of the skull. It seems to have closed the palate completely but was certainly very thin. The palatine was draped over the bones of the roof of the skull during diagenetic compaction so that the orbits are well delineated in a ventral view. A notable exception is T 3624 (figure 9*c*); this specimen is conveniently disarticulated so as to show the shape of the palatine well. The palatine makes up the posterior margin of the internal nares as described above. In the usual state of disarticulation, the vomer and anterior pterygoid process are separated along the skull midline exposing the nasal in ventral view. It has a characteristic foramen in the centre (figure 9*b*, *c*) that probably carried

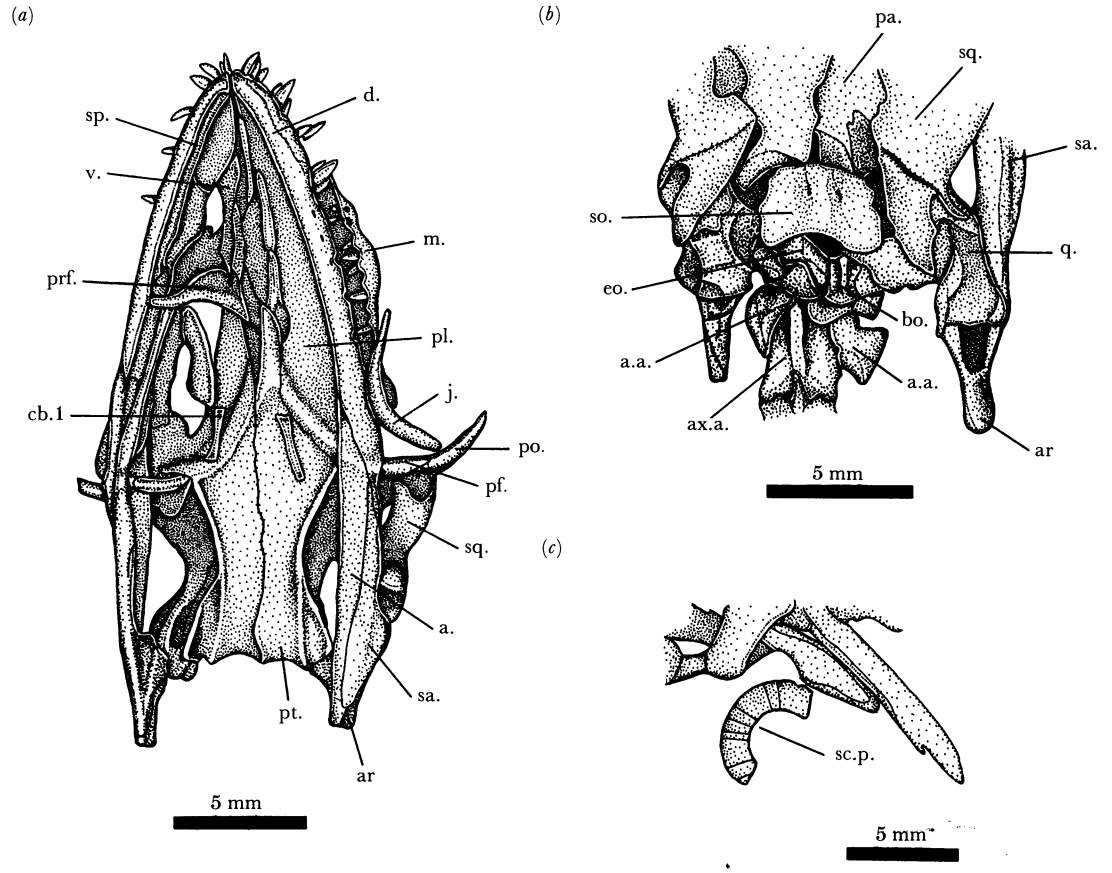

FIGURE 10. *Neusticosaurus pusillus*: (*a*) skull in ventral view (T 3585). Note the articulation of the left squamosal with the postorbital and postfrontal: (*b*) occipital region in dorsal view (T 3442). Note the median ridge on the basioccipital and the paired atlas arch; (*c*) part of a sclerotic ring with lower jaw fragments (T 3577).

the cutaneous branch of the lateral ethmoidal nerve and venous tributaries to the orbital sinus (Oelrich 1956).

The lateral extension of the pterygoid is here called an ectopterygoid process as the ectopterygoid seems not to be ossified separately, in contrast to *N. edwardsii* (Carroll & Gaskill 1985). No definite epipterygoid could be identified. In the region of the basis of the ectopterygoid process, there is usually a rod-shaped bone with somewhat thickened ends that is a part of the hyoid apparatus, specifically, the first ceratobranchial. In adults, the pterygoids are in contact over their entire length along the ventral midline of the skull, but not in the juveniles, where a deep indentation reaches as far back as the anterior margin of the upper temporal opening.

The posterolateral margin of the pterygoid is thickened and bent downwards to form the transverse flange as opposed to *N. edwardsii* (Carroll & Gaskill 1985). The transverse flange is the anterior margin of the subtemporal fossa. Nothing can be said about the braincase, except for the most caudal region, because it is completely covered by the pterygoids and appears to have been poorly ossified.

The lower jaw (figure 12), as reconstructed (figure 13), closely corresponds to the primitive condition in reptiles. The most noteworthy feature is that the tooth row of the dentary (25 alveoli) reaches considerably farther back than that of the maxilla (12 alveoli) and premaxilla

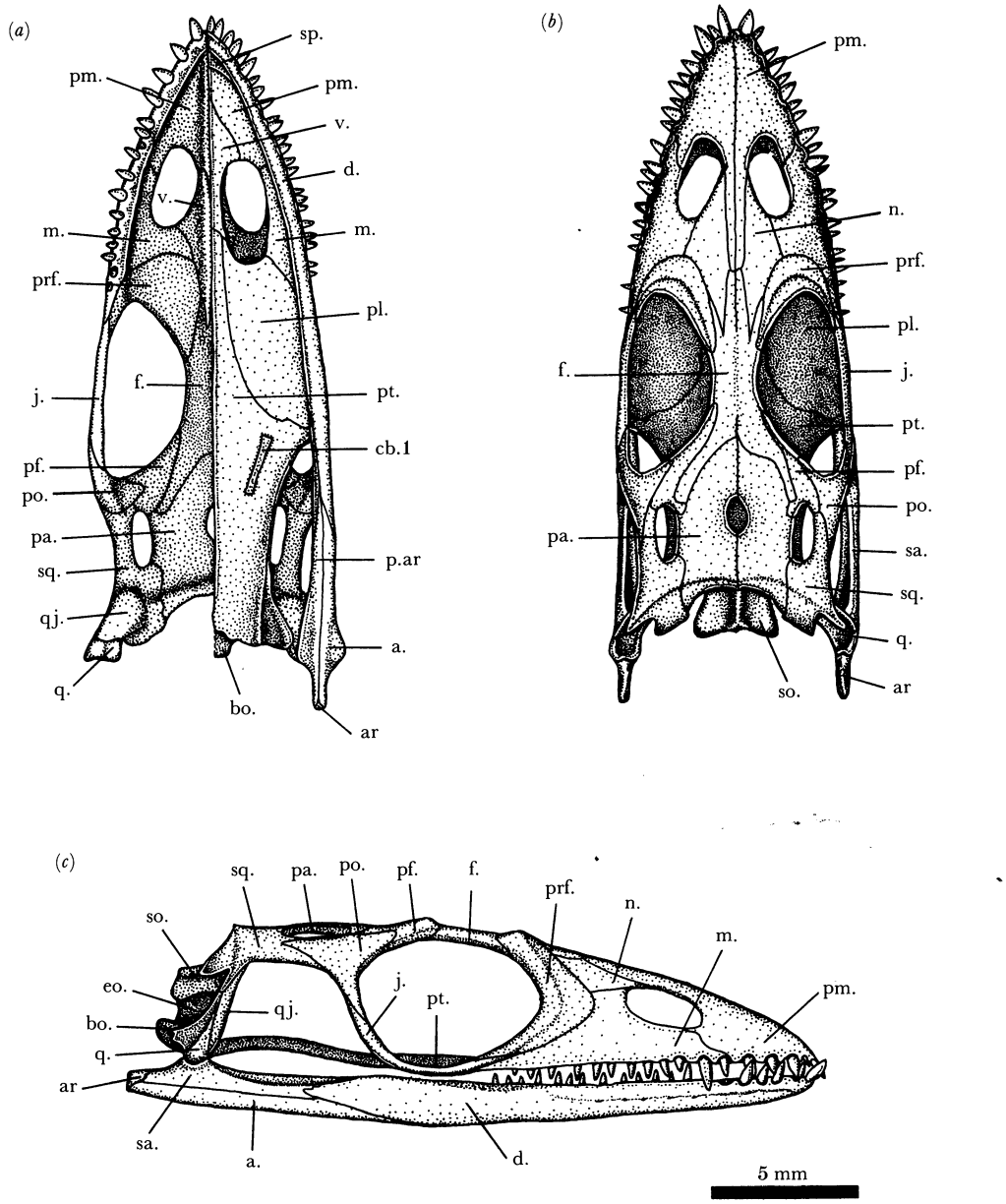

FIGURE 11. Reconstructions of the skull of *Neusticosaurus pusillus*, based mainly on specimens in figures 8*a–d*, 9*a–c*, 10*a*, *b*, and 12*a–c*: (*a*) ventral view, mainly based on specimens in figures 9, 10*a* and 12*b*. The right lower jaw and the right half of the palate are omitted to expose the skull roof from ventral; (*b*) dorsal view, mainly based on T 3751 (figure 8*c*). Note narrow skull table and large upper temporal openings; (*c*) lateral view. The braincase is unknown. Note large second maxillary tooth.

(5 alveoli). Only 13–19 of the 25 alveoli are usually occupied by functional teeth. The posterior teeth of the lower jaw had no counterparts in the upper jaw and were possibly not functional. This discrepancy in tooth row length may be best explained by the way *Neusticosaurus* fed. The prey, small fish, squid, or other soft-bodied invertebrates, was caught and held with the anterior, interlocking fang-like teeth and swallowed whole. No other buccal processing occurred. The teeth therefore had only a grasping and holding function and did not necessarily need a counterpart.

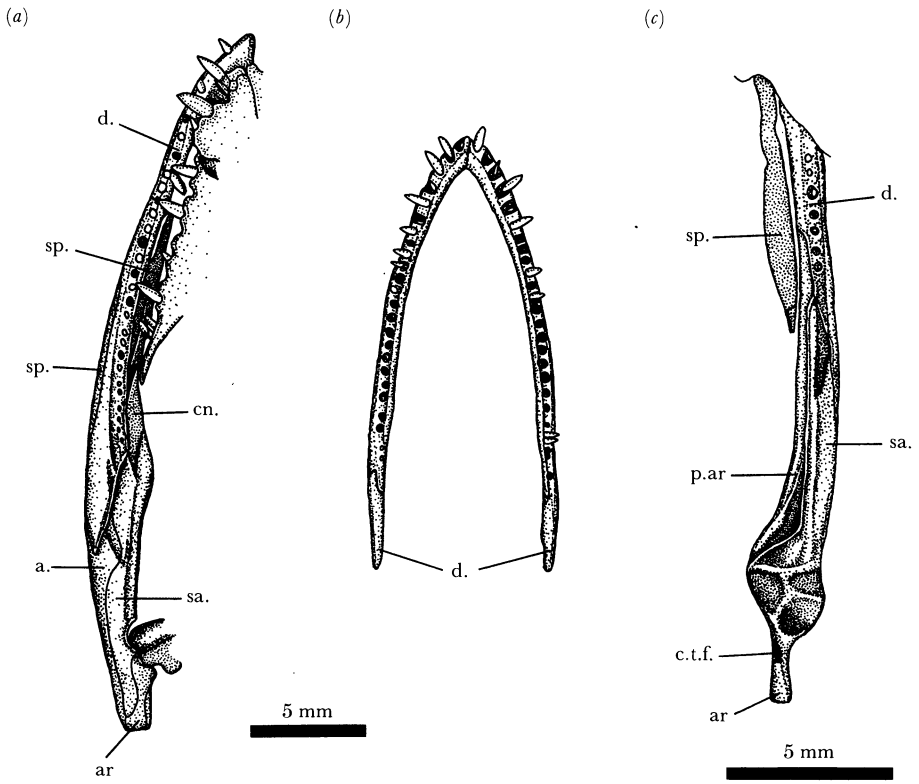

FIGURE 12. *Neusticosaurus pusillus*: (*a*) T 3530, left lower jaw from dorsolateral; (*b*) dorsal view of articulated dentaries (T 3573) that separated from the rest of the skull before compaction, thus indicating the original width of the lower jaw. The teeth were omitted for clarity; (*c*) T 3658b, posterior half of right lower jaw in dorsal view. Note the two articular facets for the quadrate and the deep posterior pit.

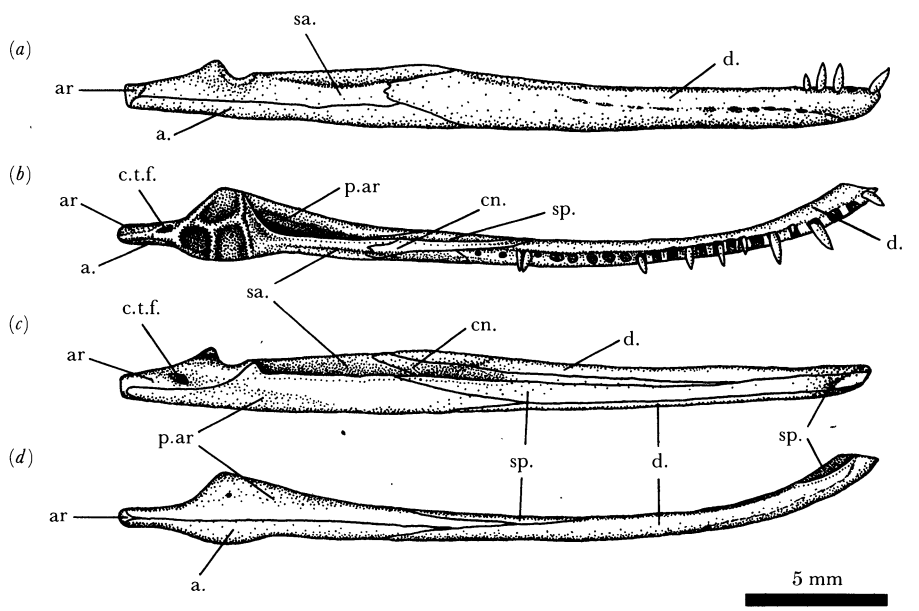

FIGURE 13. Reconstruction of the lower jaw of *Neusticosaurus pusillus*: (*a*) lateral view, mainly based on T 3599; (*b*) dorsal view, based mainly on specimens in figure 12; (*c*) medial view, based mainly on specimens in figures 9*a–c* and 10*a*; (*d*) ventral view, based mainly on T 3576 (figure 9*b*).

These tooth counts are somewhat lower than those in *N. edwardsii* (Carroll & Gaskill 1985), which also shows a higher percentage of functional teeth. The lower jaw usually remains attached to the skull. The symphysis is well-developed, and it often survives disarticulation of the lower jaw. The two dentaries are commonly found still connected to one another whereas the posterior bones of the jaws are disarticulated or lost (figures 9*c* and 12*b*). The same seems to hold true for the other species of *Neusticosaurus*, but not for *Serpianosaurus* where the lower jaw rami are commonly disarticulated at the symphysis and lie laterally to otherwise articulated skulls (Rieppel 1989*a*). These articulated dentaries of *Neusticosaurus pusillus* were very important for the reconstruction of skull shape because they indicate the original width of the skull. During diagenetic compaction of articulated skulls, the symphysis is usually broken, and the jaw rami are spread apart, thereby increasing the apparent width of the skull.

The dentary covers about two-thirds of the outside of the lower jaw, bearing a longitudinal groove running all the way from the back of the tooth row to the symphysis. This groove occasionally widens into mental foramina for the cutaneous branch of the terminals of the inferior alveolar nerve (Oelrich 1956) and blood vessels supplying the teeth.

In lateral view, the posterior part of the lower jaw (figures 12*a* and 13*a*) is made up dorsally by the surangular and ventrally by the angular. A retroarticular process is well developed, consisting mainly of the articular, but supported by surangular, angular and prearticular. In lingual view (figures 8*d*, 10*a* and 13*c*), a very slender coronoid (but virtually no coronoid process) can be seen that parallels the splenial for two-thirds of its length. The splenial makes up most of the inner wall of the lower jaw and also enters the symphysis that is apparent in ventral view in most specimens (figures 9 and 10*a*).

The articular surface of the lower jaw with the quadrate consists of two fairly shallow pits side-by-side, separated by a low ridge (figures 12*c* and 13*b*). Behind them, a somewhat deeper pit probably served to accommodate the posterior process of the quadrate when the jaw was opening. Ventromedially from the articular surface, a well developed foramen (figures 9*a* and 13*c*) pierces the articular, most likely the chorda tympani foramen. In front of the articular surface lies a well developed adductor fossa (figures 12*c* and 13*b*).

Axial skeleton

Of all the pachypleurosaurids from the Monte San Giorgio Middle Triassic, *Neusticosaurus pusillus* has the highest count of presacral vertebrae (figure 3): 18–20 cervical and 22–24 dorsal vertebrae, resulting in a presacral count of 41–43. There are 3 or 4 sacrals, the same as in *N. edwardsii* and *N. peyeri*, but 51–58 caudals, considerably more than in the two other taxa. The many cervicals of *N. pusillus* appear to be tightly packed because the neck is relatively not much longer than in the other forms.

The atlas–axis complex is especially well exposed ventrally in a recently prepared specimen, T 3948 (figure 14*a*). Other ventral views are shown in figure 9*a*, *b*. Dorsal views appear in figures 8*a–c* and 10*b*. The atlas centrum is almost as long as the axis centrum but is shaped very differently. Its anterior articular surface is a somewhat spherical structure. Behind it, the centrum is constricted laterally; in ventral view it disappears under the axis intercentrum and the axis ribs. No atlas intercentrum is present despite the suggestive anterior bevelling of the atlas centrum. No atlas ribs were found, unlike in *N. peyeri* and *N. edwardsi*. The atlas arch is split along the midline, thus lacking a neural spine. Each half has the shape of a triangle with the posterior corner consisting of the postzygapophyses.

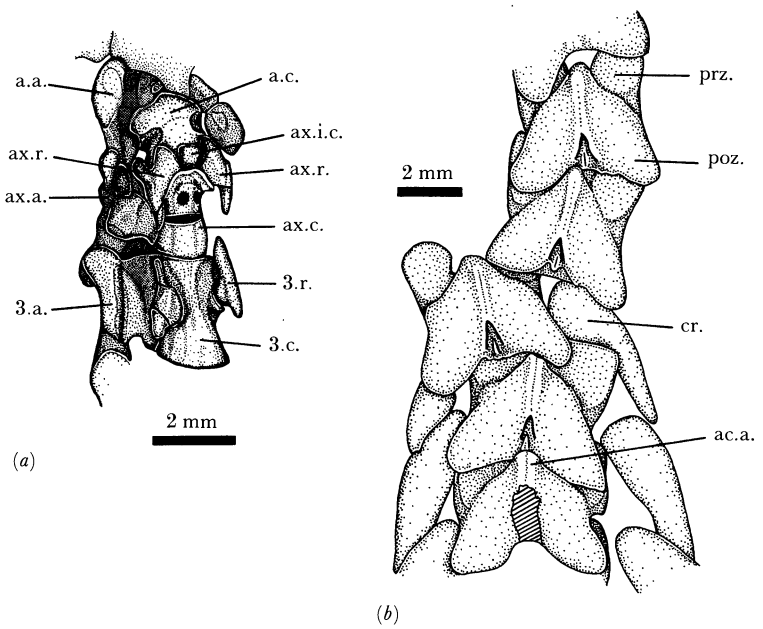

FIGURE 14. *Neusticosaurus pusillus*: (*a*) the atlas–axis complex of T 3948 in ventral view. Note the lack of atlas ribs, the axis intercentrum, and the large foramina in the axis centrum; (*b*) the posterior cervical vertebrae (14–19) of T 3602 in dorsal view. Note the accessory articulations at the base of the neural spines.

The posterior part of the axis centrum (figure 14*a*) has the same morphology as the following vertebrae, but its anterior ventral margin shows a peculiar shelf for the ventral articulation of the heads of the axis ribs (figure 9*b*). These cover up the contact between the atlas and axis centrum. The ribs do not meet ventrally, however, because they are separated by a small trapezoid intercentrum. Right behind the shelf, just laterally to the centrum midline, are two well-defined deep foramina of unknown function. They are probably not identical to the common foramina subcentralia (Hoffstetter & Gasc 1969) because they are too large and occur only in the axis. The dorsal head of the axis ribs is much smaller than the ventral one, and it is not clear where it articulates. The posterior processes of these ribs extend only two-thirds of the way back along the axis centrum, and the anterior processes are even shorter.

The description of the cervical dorsal column is mainly based on T 3518, T 3602 (figure 14*b*), T 3604, and T 3936, the description of the ventral, cervical column is mainly based on T 3556, T 3574, T 3852, and T 3934 (figure 7*a*). The cervical centra are clearly longer than they are wide. The anterior and posterior articular surfaces appear expanded. The articular facets (parapophyses) are in the middle of the centrum and increase in size caudally. They are somewhat raised and enclose a canal in between them and the two rib heads. A curved groove marks off the lower parapophysis ventrally (figures 7*a* and 14*a*).

The neural arch of the axis has relatively the largest and highest spine of the entire cervical column, reaching far forward over the atlas centrum and between the two halves of the atlas arch (figures 8*a*, *b* and 10*b*). The height and prominence of the neural spines decreases caudally and the arches swell increasingly. In dorsal view, the posterior part of the neural spines commonly display a depressed, drop-shaped, rugose area of unfinished bone. In the posterior neck region, a small spike intrudes into the drop shape (T 3602; figure 14*b*). It looks as though it might belong to the succeeding arch, whereas, in fact, it does not.

The postzygapophyses of the anterior cervicals are prominent and enclose an angle of about 20° with the horizontal. This angle decreases gradually to 0° in the trunk vertebrae, suggesting that the neck was probably more flexible anteriorly than posteriorly. However, the angle of the zygapophyses is not readily measured in any kind of vertebra because of their diminutive size.

An additional, but weak, articulation (figure 14*b*) is present between the posterior cervical vertebrae, as in *Neusticosaurus peyeri*, and as described in *N. edwardsii* by Carroll & Gaskill (1985). It consists of a shallow pit at the posterior base of the neural spine into which the rounded tip of the next neural arch fits. This articulation also occurs in the trunk vertebrae (T 3567) but, additionally, a triangular shelf of the more anterior vertebra extends below the tip of the neural spine of the next vertebra, so that the trunk vertebrae interlock fairly well. This process–pit articulation is also seen in the anterior caudals (T 3598, T 3936, T 3604).

The cervical centra gradually increase in size but do not change considerably in proportion. More caudally sited cervical vertebra, 14–16, gradually assume the shape of the trunk centra, which are not much longer than they are wide (i.e. barrel-shaped). The ribs of cervicals 3 to about 13 are all of the same shape: they are double-headed with both heads articulating with the centrum. They have posterior and somewhat longer anterior processes. The latter extends forward, well over the preceding centrum, because the rib articulations are located in the anterior half of the centrum. The posterior processes of the ribs increase in length whereas the anterior process is reduced and lost in the first trunk rib. This first trunk rib looks like the other trunk ribs, only shorter. It is single-headed and articulates only with the neural arch (T 3852, T 3574).

The description of the dorsal column in dorsal view is mainly based on T 3518, T 3602 (figure 14*b*), T 3604, and T 3936, whereas the description of the dorsal column in ventral view was mainly based on T 3556, T 3574, and T 3852.

The neural arches of the dorsal vertebrae are almost rectangular in outline and somewhat wider than they are long. Their outline is that of a squat chevron. The neural arches increase very slightly in size caudally. The neural spine is long and low, and its back half is usually unfinished bone. It is not higher than the lateral part of the arch but is marked off by deep grooves at either side. The zygapophyses seem to be flat and to lie in one plane, facilitating some lateral flexion but allowing no dorso-ventral flexion of the trunk column.

The rib articulations for the single-headed dorsal ribs are on the sides of the arches, somewhat anterior to the middle. They are merely rugose, high-elongate areas and not distinct transverse processes. All but the last few dorsal ribs have the same shape. The first few ribs gradually increase in size, but from posterior to the shoulder girdle to the last three ribs, their length remains constant. The rib size increases greatly immediately after the articular surface, sometimes more than three-quarters of the vertebral length. After the first fifth of their length, the ribs decrease in diameter. All except the last three show a blunt tip of unfinished bone, probably for articulation with a cartilaginous sternum. The last two (T 3604, T 3936) or three dorsal ribs (T 3518, T 3602) decrease rapidly in length and have pointed finished ends, the very last sometimes shows a distal surface for articulation with the sacrum.

Only the centra are visible in ventral view of the dorsal column. They are not as wide as the arches and are cylindrical to barrel-shaped with two shallow ventral grooves or merely a somewhat flattened ventral side. The centra are either shallowly amphicoelus or platycoelus. They clearly show the characteristic surface pattern of many thick postcranial

pachypleurosaurid bones (see §7, figure 25*d*, plate 2). It consists of fine, wavy grooves parallel to the bone long axis. The grooves meet rarely and do not run the entire length of the bone. This pattern resembles finger-print lines, although with more discontinuities.

As usual with the pachypleurosaurids, the number of sacral vertebrae is difficult to count. Three pairs of well-defined sacral ribs and vertebrae are present, but commonly a fourth pair, either anterior or posterior to this trio also shows an articulation with the ilium. An intermediate condition with only one rib of a fourth pair articulating with the ilium (T 3604, T 3658a, T 3937) is occasionally observed. The sacral neural arches and centra have essentially the same shape and size as the trunk centra, except that the outline of the arch can be almost rectangular (T 3602, T 3604, T 3936). The rib articulation is enlarged to a circle and starts to incorporate the centrum from the second sacral on (T 3672).

The sacral ribs (figure 16*b*) are sturdy, straight rods with a circular proximal articulation and a somewhat dorsoventrally flattened distal articulation. The three sacral ribs proper converge onto one point laterally to the second rib, which is the strongest. The first and the third ribs taper somewhat. The ilium is so narrow that the three ribs have difficulty articulating with it. An additional rib often manages to squeeze onto the ilium (figure 16*b*, T 3618).

The first caudal vertebra is defined as the one with the first free pair of ribs. In dorsal view, it can easily be recognized by its markedly smaller neural arch (T 3605). The proportions of the caudals change gradually together with a continuous decrease in size to a very elongate centrum (more than twice as long as it is wide). The last five to six caudals, although rapidly decreasing in size, assume more equal proportions again. These last few vertebrae are rarely preserved and are found in only seven specimens (T 3451, T 3530, T 3605, T 3639, T 3658a, T 3672, and T 3714). The very last caudal has no distal articular surface and is shaped somewhat like a terminal phalanx with a rounded tip.

The first 10–12 caudal vertebrae bear ribs, the first few of which commonly show an unfinished end. They were either finished in cartilage, or some ligaments ran across them to strengthen the base of the tail. From the first to the eighth or tenth cervical, the neural arch participates decreasingly in rib articulation. The last few ribs only articulate with the centrum. If pachyostosis is not too pronounced, these articulations are raised to form transverse processes. The transverse processes usually do not continue beyond the last caudal rib, but in some specimens one or two ribless transverse processes are present.

The neural arches gradually lose their swollen appearance, and the neural spines become more prominent. However, after the seventh or eighth caudal, the size of the neural spine starts to decrease. It decreases not so much in height as in anteroposterior width, so that the last few spines are just thin rods at the posterior end of the neural arches. Sometimes the medial part of the neural spine is reduced first, forming a gradation from a full spine to a forked spine to a posterior spine to no spine. The spine is lost between the 14th and 16th caudals, only a spineless neural arch persists. The arch is lost very far back, between the 39th and 46th caudal. The articulation between the neural arches via the zygapophyses is lost earlier, between the 29th and 36th caudals.

The first haemapophysis usually occurs between the third and fourth caudal. These chevron bones continue up to the 24th–27th caudals. They always have two articulations (i.e. a paired base) that unite ventrally into a blade-shaped expansion that shrinks in accordance with the neural spines. The neural spines and haemapophyses expand the proximal tail dorsoventrally to produce a laterally compressed tail, an adaptation for efficient swimming by lateral

undulation of the body (anguiliform swimming). In this species, however, it is developed to a lesser extent than in all the other pachypleurosaurids, which show higher neural spines and larger haemapophyses and a more abrupt caudal decrease in size of both elements.

A well-developed gastral apparatus with 26–28 gastralia is present. There are two gastral ribs per vertebra, consisting of one central element and two lateral elements each. Actual counts in specimens T 3387, T 3553a, T 3556, T 3566, T 3580, T 3585, T 3639, T 3670, T 3672, T 3714, T 3717, T 3737, T 3852, and T 3934 (figure 7*a*) ranged from 21 to 28 gastralia, but numbers below 25 may be because of loss during preparation as no correlation could be found with any other character or character state, such as the sex of the individuals. The central elements of the last two gastralia seems to consist of two parts owing to poor ossification along the midline. The angle enclosed by the central element increases caudally from 110° to 160°, similar to the situation in *N. peyeri*.

Variation in vertebral number. Because the pachypleurosaurs were thought to exhibit an extraordinary variability in the number of vertebrae (Zangerl 1935; Carroll 1984; Carroll & Gaskill 1985), this problem will be discussed briefly here. It has already been shown that each species actually shows small variability.

Most of the variability in vertebral count was the product of lumping the four species of pachypleurosaurs into one (Zangerl 1935). However, other phenomena contributed to the apparent variability as well. One was the differences between populations of a single species. This can be documented in the sample of *Neusticosaurus pusillus* from the locality Val Serrata (Cava Don Luigi) (see §15*c*). The Cava Inferiore horizon contains four pachypleurosaur beds at this locality (figure 6). A population of *N. pusillus* with a distinctly different presacral count, 37–39 instead of the usual 40–42, was collected from the two upper horizons. The two populations show no other significant differences.

The second explanation for the apparent variability in vertebral counts is that variability varies with the region of the column. Cervical and presacral counts, for example, show little variability. But, in *Neusticosaurus peyeri*, a number of quantitative observations regarding the tail show a decreasing variability towards its base. The number of eight caudal ribs and the decrease of the height of the neural spines at caudal vertebrae 11 and 12 are remarkably constant. The disappearance of the neural arch is spread out over a much wider range, as is the position of the last chevron. The determination of the latter is especially hindered by inadequate preservation. It therefore seems that observations in the distal tail region show more variability because it was much more affected by ontogenetic differences. The largest specimen with a complete tail (T 3393), for example, exhibits the highest count of caudal vertebrae (48), whereas the smallest juvenile (T 3705) shows only 26.

Appendicular skeleton

Pectoral girdle. Description of the pectoral girdle of *Neusticosaurus pusillus* was based mainly on the following specimens: T 3579, T 3603, T 3616, T 3618 (figure 15*b*), T 3636a, T 3637 (figure 15*a*), T 3656b, T 3670, T 3740, T 3782, T 3934 (figure 7*a*), and T 4289. Most of these are exposed in ventral view, because dorsal views are of little interest because of the poor development of the dorsal parts of the shoulder girdle in pachypleurosaurs.

The three most obvious differences between the shoulder girdles of *N. pusillus* and *N. peyeri* are the shape of anterior margin, the shape and relative size of the clavicles, and the relative size of the pectoral fenestra, which is the large central unossified area of the shoulder girdle. The

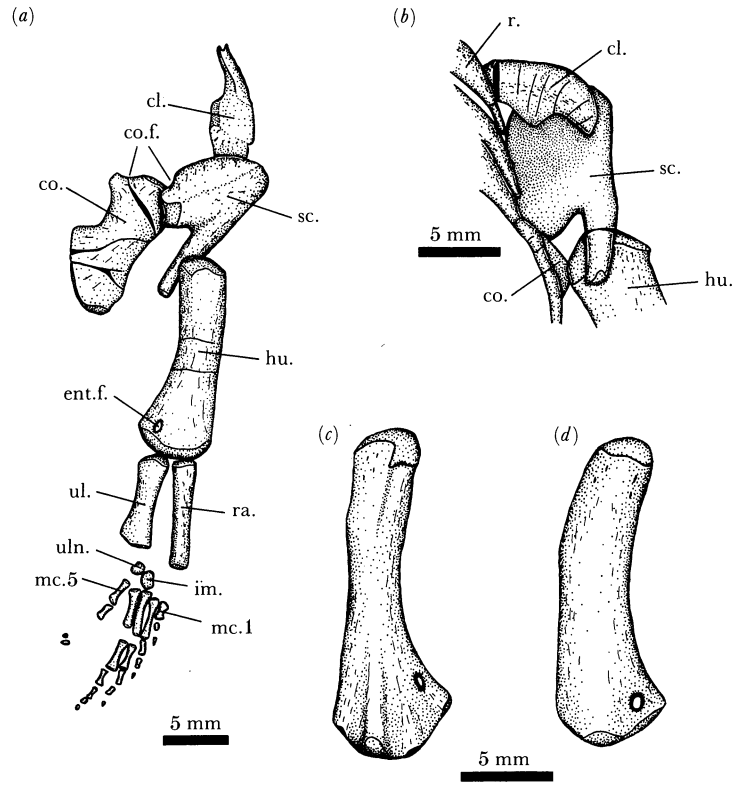

FIGURE 15. *Neusticosaurus pusillus*: (*a*) the right shoulder girdle and forelimb of T 3637 (sex *x*) in ventral view. The shoulder girdle elements are slightly disarticulated and the interclavicle is missing. Note indentations for coracoid foramen. The shape of the humerus is typical for sex *x*; (*b*) right clavicle and scapula of T 3618 in dorsal view. The clavicle has very short posterior processes and the area of overlap with the scapula is small; (*c*) T 4289, a typical left humerus of sex *y* in dorsal view. Note the expanded distal end, the narrow shaft, and the proximal position of the entepicondylar foramen; (*d*) T 3661, a typical left humerus of sex *x* in dorsal view. Note the unconstricted shaft and the poorly differentiated distal end; (*c*) and (*d*) share the same scale.

first two characters especially serve to distinguish the two species. The pectoral fenestra is relatively larger in *N. pusillus*.

The anterior outline of the pectoral girdle of *N. pusillus* (figure 7*a*) is almost straight, and the front half of the girdle can be inscribed into a rectangle. The anterior margins of the clavicles are oriented almost perpendicular to the long axis of the animal, and the scapula almost completely overlaps the clavicular blade ventrally (figure 15*a*). In dorsal view, the stem of the clavicle extends almost to the lateral edge of the scapula but has a poorly developed posterior process (figure 15*b*). The stem is comparatively narrow and not much wider than the blade. Its posterior margin also runs roughly perpendicular to the long axis of the animal, usually with a single weak cranial indentation. The blade appears to be thicker than the stem, a very different condition from that in *N. edwardsii* where the blade is wide and flat (Carroll & Gaskill 1985).

The interclavicle is sunk into the median part of the posteroventral margin of the clavicular blades, producing the even anteroventral surface of the shoulder girdle. The interclavicle of articulated specimens is almost invariably broken along the midline where it was draped over the first trunk centra by compaction. No disarticulated interclavicle was found. The interclavicle appears to be much wider than long and has tapered ends, again in contrast to

N. edwardsii (Carroll & Gaskill 1985). The anterior margin is essentially straight and the posterior margin shows little inclination toward a posterior process. The overall shape of the bone is a very low, bilateral triangle with the long side forward.

The scapula consists of a flat ventral portion and a narrow blade. The ventral surface is divided by a low ridge or keel that probably separated the ventral and lateral portions of the pectoral musculature. The anterior margin of the scapula underlies the clavicle and tapers into a thin edge. The medial margin is slightly convex and thins into an unfinished edge. A shallow to moderately developed indentation for the coracoid foramen can be found near its posterior end. This indentation is not developed in *N. peyeri*.

The anterior surface of the glenoid fossa is formed by the lateral part of the thickened posterior margin of the scapula. Its medial part articulates with the coracoid. The lateral margin of the scapula is straight to slightly concave. The scapular blade arises from its centre as a subcircular rod extending upwards at an angle of about 45°. It extends back, over the glenoid fossa, thereby limiting the dorsal excursion of the humerus.

The scapulae of the two small species of *Neusticosaurus* appear to be very similar in overall shape and cannot be distinguished from one another as disarticulated specimens because of overlapping variation. However, in *N. pusillus* the blade appears to be relatively thinner and longer. It is more steeply inclined and arises further caudally from the main part of the scapula.

The coracoid is an essentially flat, waisted bone. The posterolateral and the anteromedial margins are concave, the latter to a greater degree. Only the posterolateral margin was not rimmed with cartilage. The anterolateral margin can be divided into three parts: (i) the thickened posterior surface of the glenoid fossa, (ii) the articular surface with the scapula and (iii) the indentation for the coracoid foramen, which is consistently formed by an anteromedial process of the coracoid. The coracoid surface of the glenoid fossa faces laterally to anterolaterally. The thickened medial margin of the coracoid is the symphysial margin with its counterpart. The angle of the symphysis is unclear but appears to have been almost 180° as evidenced by the cross section of the coracoid of T 3782 (figure 25*l*). The posterior margin consists of thickened, unfinished bone. It probably served for the attachment of a cartilaginous sternum.

The overall shape of the coracoid is very similar in both small species of *Neusticosaurus*. The coracoidal symphysis is decidedly longer in *N. pusillus* because the anteromedial and especially the posteromedial corners of the bones are not rounded off. The posterolateral margin of the coracoid is less curved in *N. pusillus* than in *N. peyeri*. This curvature is greater in *N. edwardsii*.

Scapula and coracoid show more morphological detail in *N. pusillus* than in *N. peyeri*; this could be because of less pachyostosis in the shoulder girdle of *Neusticosaurus pusillus*.

Forelimb. Description of the forelimb of *Neusticosaurus pusillus* was mainly based on the following specimens: T 3530 (sex *x*), T 3579 (sex *y*), T 3603 (sex *x*), T 3620 (sex *y*), T 3637 (sex *x*; figure 15*a*), T 3661 (sex *x*; figure 15*d*), T 3670 (sex *x*), T 3740 (sex *x*), T 3744 (sex *x*), T 3934 (sex *y*; figure 7*a*; figure 24*a*), and T 4289 (sex *y*; figure 15*c*).

In general, the humerus of *N. pusillus* seems to be more pachyostotic than that of *N. peyeri*, and the shoulder girdle less so.

Sexual dimorphism is clearly evident in the forelimbs of both species of *Neusticosaurus*, expressed morphologically as well as in the proportions (tables 4, 9). This phenomenon is treated in greater detail in §12. The humerus of sex *y* is usually about 30% longer relative to standard length (range 1.2–1.5) than that of sex *x* (range 0.95–1.2). The same dimorphism can

TABLE 4. FORELIMB PROPORTIONS IN ADULTS

(Distal width of humerus, d.; metacarpal, mc.; minimal diameter of humerus, m.d.; proximal width of humerus, p.)

	Neusticosaurus pusillus		*Neusticosaurus peyeri*	
ratio	sex *x*	sex *y*	sex *x*	sex *y*
humerus:trunk length	0.20–0.26[a]	0.24–0.33[a]	0.20–0.26[a]	0.28–0.33[a]
humerus:standard	0.95–1.2[a]	1.2–1.5[a]	0.75–1.00[a]	1.05–1.25[a]
radius:standard	0.5–0.65[a]	0.65–0.75[a]	0.44–0.53[a]	0.49–0.71[a]
third mc.:standard	0.23–0.29[b]	0.26–0.3[b]	0.19–0.21[b]	0.19–0.23[b]
humerus:femur	0.88–1.0[a]	1.0–1.15[a]	0.9–1.1[a]	1.1–1.3[a]
humerus:radius	1.7–1.95	1.75–1.95	1.6–1.9	1.7–1.9
humerus:third mc.	3.8–4.6[a]	4.4–5.1[a]	3.7–4.7[a]	4.7–5.8[a]
radius:ulna	1.1–1.16	1.11–1.24	1.11–1.23	1.12–1.24
humerus:d.	2.7–3.2	2.5–3.1	3.2–3.8[a]	2.8–3.4[a]
d.:p.	1.4–1.7	1.5–2.0	1.3–1.8	1.4–2.1
d.:m.d.	1.16–1.91[a]	1.48–2.43[a]	1.23–1.95[a]	1.89–3.0[a]

[a] Indicates sexual dimorphism.
[b] Indicates differences between species.

be observed for the length of the femur relative to standard length (sex x = 1.04–1.24, sex y = 1.1–1.40). In sex x, the humerus:femur length ratio is 0.88–1.0 (table 4). In sex y, it is 1.0–1.15 (table 4). The qualitative and the quantitative criteria are good enough by themselves for a valid definition of sex.

The distal ends of sex x humeri show almost no morphological features except for the entepicondylar foramen, which is located only slightly more than its own length proximal to the distal articular surface. The distal articular surface of unfinished bone is restricted to the distal end of the humerus. It is convex dorsoventrally as well as lateromedially. The shaft of the bone is subcircular in cross section (figure 25*i*, *l*). The shaft is slightly bent caudally and shows no differentiation. A small lobe of the articular surface reaches back onto the posteroventral surface of the proximal end.

In sex y, the distal end shows a clear separation of the articular surface into a small posterior and much larger anterior part. These two parts are separated by a shallow embayment creating a posterodistal process. This is the best feature to separate the sexes immediately if the specimens are exposed in dorsal view (figure 15*c*). This process probably served as the insertion point for the flexor muscles of the forearm. The ectepicondylar ridge flanked by two grooves is well developed. Its distal end shows a dorsal extension of the articular surface. A supinator ridge is separated from the ectepicondylar ridge by a deep ectepicondylar groove.

In ventral view (figure 7*a*), the distal end of the bone appears almost flat with slightly raised margins. All specimens of sex y show a distinct break in the anterior outline of the humerus, about a quarter of its length from the proximal end. Rugosities are sometimes developed here. These probably served for insertion of the subcoracoscapularis muscle. In some specimens (T 3529, T 3533), a deep, elongate recess is present next to this muscle attachment point. The entepicondylar foramen is located considerably farther proximally in sex y than in sex x. The shaft is round to oval in cross section in sex y as well (figure 25*j*).

On the proximal end, a well defined lobe of the articular surface reaches back onto the posteroventral surface of the bone. In large (old) individuals (T 3533, T 3934 (figure 7*a*)), it

becomes exceedingly narrow and elongate. The well differentiated humerus of sex *y* probably reflects a well developed forearm musculature.

Qualitative morphological observations can be quantified (table 8) to a certain degree by looking at the distal width of the humerus relative to its length, proximal width, and minimal shaft thickness. The last criterion seems to yield the best results (figure 30*b*), but is not sufficient for sexing in this taxon. In the other pachypleurosaurids from Monte San Giorgio it could be employed successfully to quantify the shape dimorphism of the humerus. The ranges for the two sexes overlap considerably in all ratios. The poor morphometric separation of the two sexes is best explained by stronger pachyostosis of the humerus of this species than in other pachypleurosaurids because strong pachyostosis increases shaft diameter in sex *y*. The distal width:minimal shaft diameter for sex *x* is 1.16–1.91, and for sex *y* 1.48–2.43 (figure 30*a*; table 8). The length:distal width ratio for sex *x* is 2.7–3.2, and for sex *y* 2.5–3.1. The distal width:proximal width ratio for sex *x* is 1.4–1.7, and for sex *y* 1.5–2.0.

The morphology of ulna and radius is very similar to *Neusticosaurus edwardsii* (Carroll & Gaskill 1985), and not much new information was acquired. Some interesting insights may be gathered from quantitative data (table 4), however.

The ulna is the shorter, but thicker and wider, bone. Its shaft is slightly constricted. The anterior margin is rounded whereas the posterior margin is flattened into a sharp edge. The radius reaches distally well beyond the ulna. It is much more slender with a wider proximal than distal end. Its shaft is not evenly constricted but the proximal fourth appears to be thickened. Some radii show a deep groove on their anterior margin (sex *y*: T 3623, T 3579; sex *x*: T 3703).

The same sexual dimorphism seen in the humerus can be observed in the radius. In sex *y*, the most obvious feature is a strong anterior trochanter about a quarter of the length distally from the proximal end. The ulna of sex *y* also generally appears to be more differentiated, i.e. with more rugosities and wider articular surfaces together with a stronger constriction of the shaft, and a sharper posterior keel. Radius and ulna in sex *x* are definitely more pachyostotic in addition to showing a lack of morphological differentiation.

Radius and ulna appear to be more slender in *Neusticosaurus peyeri* than in *N. pusillus*, but no differences in morphology could be observed. Their relative length compared with the humerus is about the same for both species and both sexes, ranging from 1.6 to 1.9 (table 4). This is about the same value as observed for *N. edwardsii* by Carroll & Gaskill (1985).

No significant relative length difference of the radius compared to the humerus can be observed in the two sexes. However, some radii are relatively longer than the ulnae in sex *y* (range of radius:ulna ratio is 1.11–1.24; table 4) compared with sex *x* (range of radius:ulna ratio is 1.10–1.16; table 4). These values are about the same for both small species of *Neusticosaurus*. A clear sexual dimorphism is again evident for the length ratio of the humerus to third metacarpal. In sex *x*, this ratio ranges from 3.8 to 4.6, and in sex *y* from 4.4 to 5.1 (tables 4, 9).

Looking at the relative length of forelimb elements to body length (represented by standard length) (table 4), only a weak dimorphism can be observed for the third metacarpal:standard length ratio (sex *x*: 0.23–0.29, sex *y*: 0.26–0.3; table 4). Dimorphism is well developed, however, for the humerus:standard length ratio (sex *x*: 0.95–1.2, sex *y*: 1.2–1.5; figure 32*b*; table 4) and the radius to standard length ratio (sex *x*: 0.5–0.65 and sex *y*: 0.65–0.75; table 4). These are opposite to the relations observed for the humerus:radius ratio (weak dimorphism)

and the humerus:third metacarpal ratio (strong dimorphism). This leads to the conclusion that the size of the hand is about the same in both sexes and that most of the dimorphism is expressed in the proximal elements of the forelimb.

In both small species of *Neusticosaurus*, only two ossified elements are present in the carpus, an elongate to round intermedium, and a roundish and smaller ulnare. The existence of the third element in the carpus of *Neusticosaurus* sp. illustrated by Carroll & Gaskill (1985, fig. 5*h*) could not be verified. In *Neusticosaurus edwardsii*, the third element described by Carroll & Gaskill (1985) could be recognized without problems.

The occurrence of round versus elongate intermedia could not be correlated with any sex differences or individual age. A complete gradation from round (i.e. isometric) to elongate (twice as long as wide) specimens can be noted, but elongate shapes appear to be more common. The ulnare always has a depressed centre that may be enhanced by compaction. The intermedium shows less of a depression or none at all.

The metacarpals show the pattern characteristic for the manus of all pachypleurosaurids. The first metacarpal is much shorter than the others but much stouter with an expanded proximal articulation. Metacarpal 5 is next in length followed by metacarpal 2. A gradation exists from specimens with metacarpal 3 longer than metacarpal 4, to specimens with metacarpal 3 and 4 of equal length, to those with metacarpal 4 longer than metacarpal 3. All three cases are equally common and again, no correlation to individual age or sex could be found. The length of the third metacarpal relative to the humerus is in the same range as for *N. edwardsii*, but it is slightly shorter in sex *y* of this species than in sex *y* of *N. peyeri* (table 8).

The phalangeal formula of the manus of *Neusticosaurus pusillus* is 2–3–4–4/5–3, which is essentially the primitive reptilian count. This count is greater than those in *N. peyeri* or *N. edwardsii*. This high phalangeal count results in the slender and gracile appearance of the hand (figures 7*a*, 15*a*). As in *N. edwardsii* and *N. peyeri*, the digits increase in length from 1 to 4, the fourth being the longest, the fifth ranging in length between the second and third. All unguals have a blunt tip.

Pelvic girdle. Pelvic girdles of *Neusticosaurus pusillus* are usually much less crushed than those of *N. peyeri*, and many good examples could be studied. Description of the pelvic girdle of *N. pusillus* is based mainly on T 3573 (figure 27*b*, plate 4), T 3576 (figure 16*a*), T 3579, T 3585, T 3612 (figure 16*d*), T 3618 (figure 16*b*), T 3629, T 3639, T 3658b and T 3934 (figure 7*a*), most of which are ventrally exposed.

The ilium (figures 16*b*, *d*) is roughly triangular in lateral view with an elongated tip, the iliac blade. The lateral side is concave and the medial side is convex dorsoventrally as well as anteroposteriorly. It shows no articular surfaces for the sacral ribs. The iliac blade is either pointed or ends in a thickened anteroposterior ridge. In ventral view (figure 16*d*), the ilium is roughly oval and covered by two articular facets. The larger, posterior facet has a deep lateral indentation. The two lateral lobes thus make up supra-acetabular buttresses, contrary to Carroll & Gaskill's (1985) observation about *N. edwardsii*. Medial to these acetabular lobes are the larger facets for articulation with the pubis and ischium. The acetabular facets clearly limit the dorsal excursion of the femur but also give it support when rotated under the body. The articulation of the ilium with the other pelvic elements is best preserved in T 3618 (figure 16*b*).

The pubis is a flat, roughly rectangular element with convex medial and lateral margins, and concave anterior and posterior margins. The anterior margin and, particularly, the posterior margin are more concave in this species than in *N. peyeri*. All specimens show the obturator

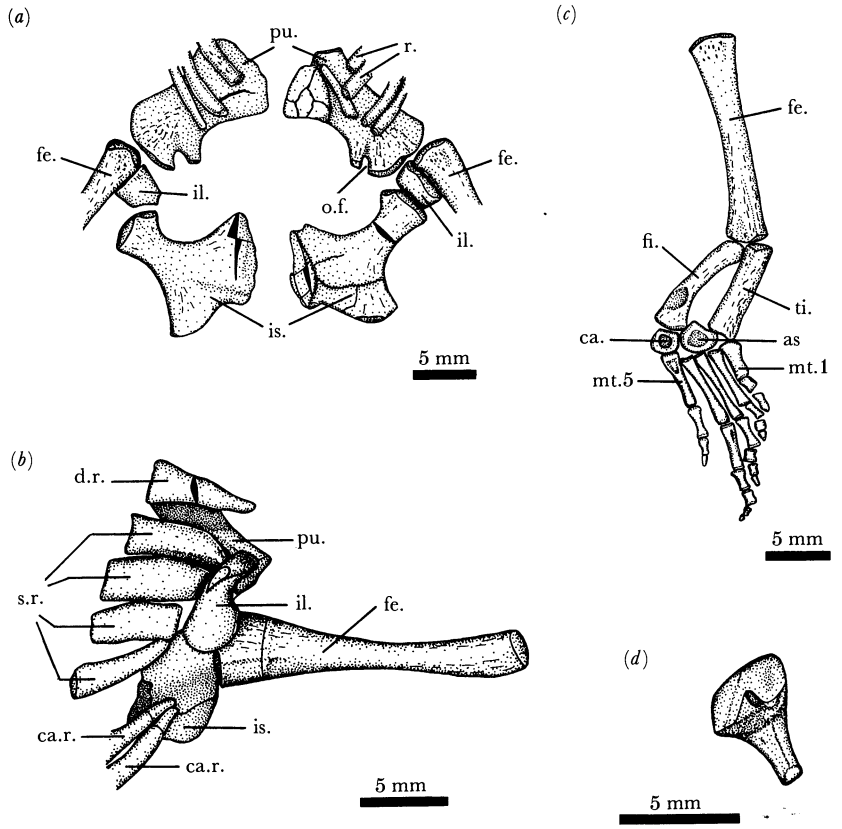

FIGURE 16. *Neusticosaurus pusillus*: (*a*) pelvic girdle of T 3576 in ventral view. The obturator foramen is more like a notch, and the ischia are greatly waisted; (*b*) the right sacral region and femur of T 3618 in dorsal view. Four sacral ribs crowd onto the small ilium; (*c*) the left hind limb of T 3576 in ventral view. Note the maximal phalangeal count; (*d*) the left ilium of T 3612 in ventrolateral view showing the articular facets for pubis and ischium.

foramen developed as a wide, open slit at the posterior margin of the pubis, just distal to the acetabulum. This is the same condition as in *N. edwardsii*.

The ischium (figures 16*a* and 27*b*) of this species is more symmetrical than that of *N. peyeri*, and is more slender than that of *N. peyeri* or *N. edwardsii*. It has an expanded, flat medial part, a narrow waist and a somewhat wider and thickened lateral 'head' for articulation with the other pelvic bones. The medial margin of the ischium is equally divided into two straight to slightly convex portions. The posterior pubic margin and the anterior ischial margin enclose an oval thyroid fenestrum that is larger in this species than in *N. peyeri* or *N. edwardsii*.

Hindlimbs. Description of the hindlimb of *Neusticosaurus pusillus* is based mainly on T 3530, T 3551, T 3558, T 3576 (figure 16*c*), T 3601, T 3602, T 3616, T 3618 (figure 16*b*), T 3629, T 3740, T 3852, T 3934 (figure 7*a*), and T 3937. The proportions and morphology of the hind- limb elements show no sexual dimorphism (table 5). Only in the relative length of the femur do the two sexes differ (table 5).

One of the greatest osteological differences between *Neusticosaurus edwardsii* and the small *Neusticosaurus* is the shape of the femur. The proximal end of the femur appears to be triangular to drop-shaped in cross section. The point of the 'drop' is the posterior margin of the femur ('trochanter major' of Carroll & Gaskill 1985). The femora are usually preserved

TABLE 5. HIND LIMB PROPORTIONS IN ADULTS

(Metatarsal, mt.)

	Neusticosaurus pusillus		*Neusticosaurus peyeri*	
	sex *x*	sex *y*	sex *x*	sex *y*
femur:trunk	0.22–0.26[a]	0.24–0.30[a]	0.21–0.25	0.21–0.25
femur:humerus	1.0–1.14[a]	0.87–1.0[a]	0.9–1.1[a]	0.77–0.9[a]
femur:standard	1.04–1.24[ab]	1.11–1.4[ab]	0.79–0.98[b]	0.78–1.06[b]
fibula:standard	0.56–0.67[b]	0.57–0.72[b]	0.49–0.57[b]	0.47–0.59[b]
fourth mt.:standard	0.39–0.48[b]	0.37–0.49[b]	0.33–0.39[b]	0.31–0.4[b]
femur:fibula	1.76–1.95	1.75–2.04	1.59–1.78	1.61–1.89
femur:fibia	1.9–2.17	1.84–2.14	1.77–2.01	1.83–2.07
femur:fourth mt.	2.47–2.79	2.61–2.93	2.24–2.64	2.33–2.86
fibula:tibia	1.05–1.16	1.01–1.13	1.08–1.16	1.08–1.17
fibula:fourth mt.	1.33–1.53	1.37–1.57	1.36–1.5	1.4–1.67

[a] Indicates sexual dimorphism.
[b] Indicates differences between species.

dorsoventrally, that is, the plane bisecting the drop-shaped head cross section is parallel to the bedding plane. It is not clear, however, if this was the position of the femur in life. A slight protuberance on the anteroventral margin about one-sixth of the way down the length of the shaft can be seen in many specimens. This is probably the proximal anterior branch of the ventral ridge system (i.e. internal trochanter) proposed by Romer (1956). The cross section of the shaft is oval because of slight dorsoventral flattening. In large specimens, the proximal end is expanded because of relative growth of the trochanter major. The expanded head lends the shaft a very slender appearance. In smaller, presumably younger, individuals, the shaft appears to be less slender because the proximal end shows about the same degree of expansion as the distal end because of the smaller trochanter major.

The distal end of the femur is somewhat flattened, reaching a maximum width of about 150% of shaft diameter. The angle between the flat dorsal surface of the proximal end and its distal counterpart is about 60°, and the distal end is rotated forward. The distal end shows a weak ventral intertrochanteric fossa and the proximal end even weaker ventral and dorsal fossae. The proximal ventral intertrochanteric fossa typically exhibits some tuberosities.

Both articular surfaces of the femur are well defined and convex. The proximal articular surface extends a triangular lobe onto the anteroventral margin of the femur. The distal articular surface is oriented distally only, excluding the possibility of ventral articulation of the lower hind limb. In life, the rotation of the distal articulation of the femur brought about a backward orientation of the lower hind limb that probably served as an efficient lateral steering surface.

The tibia and fibula (figure 16*c*) closely resemble their counterparts in *N. edwardsii* (Carroll & Gaskill 1985) but are not quite as stocky. The fibula is also less curved. The tibia is the shorter (fibula:tibia ratio is about 1.1; table 5) but also the thicker and stronger of the two bones. Its proximal end is slightly more expanded than the distal end. The fibula has a strongly concave medial edge that tapers in blade-like fashion. In most instances, the distal end of this bone is clearly more expanded than the proximal, and shows distinct articular surfaces for the astragalus and calcaneum. The anterior margin of the fibula ranges from almost straight to somewhat convex.

Only two elements, the astragalus and the calcaneum (figure 16*c*), are ossified in the tarsus. The calcaneum is usually round but may show a facet for articulation with the tibia. Its entire perimeter is unfinished bone. The centre is commonly depressed, sometimes accentuated by crushing. The somewhat larger astragalus is very similar in morphology except for a crescent-shaped embayment of the proximal margin between areas of articulation with tibia and fibula. This margin is finished bone. No obvious perforating foramen is present, but some astragali show a few small foramina in the centre (e.g. T 3618, T 3612, T 3551). The astragalus is usually wider than it is long, resulting in an oval, or in large specimens, an almost triangular outline. No differences are visible between the ventral and dorsal aspects of both bones.

No distal tarsals are present but in articulated feet (figure 7*a*), there is a space between the calcaneum and astragalus and the metatarsals, probably marking the approximate size of cartilaginous distal carpals.

Except for the first one, all metatarsals look very similar, with expanded proximal and distal ends that sometimes overlap laterally (figure 16*c*). The first metatarsal is very stout and thick, with an expanded proximal end that flares out laterally into a sharp edge. The fourth metatarsal and digit are invariably the longest. The first, second and sometimes the third terminal phalanges are triangular with a pointed tip. These phalanges possibly bore horny claws. The fourth and fifth terminal phalanges are rounded. In one specimen (T 3629), the lateral part of the third terminal phalanx bears a little point whereas the medial part is rounded, illustrating the transition from a triangular to a rounded phalanx in the same specimen. A modification of the same pattern can be observed in the terminal phalanges of *N. edwardsii*, in which the terminal phalanges 1–3 are elongate but bluntly tipped whereas the terminal phalanges 4 and 5 are rounded (Carroll & Gaskill 1985, fig. 20*g*).

The fifth phalanx of the fourth digit is not always ossified and, if present, is always disproportionally small, whereas the fourth phalanx is usually not much smaller than the preceding one. Specimens with five phalanges in digit four are T 3528, T 3576 (figure 16*c*), T 3598, T 3620, T 3636 a, T 3670, T 3671, T 3740, T 4289. Accordingly, the phalangeal formula of the pes for this species can be given as 2–3–4–4/5–3.

5. *Neusticosaurus peyeri* new species

(*a*) *Systematic palaeontology*

Synonymy.

1928 *Pachypleurosaurus edwardsi* Cornalia (in part) – B. Peyer, *Acta. Soc. Helv. Sci. Nat.* 109th Sess., **1928**, p. 219.

1932 *Pachypleurosaurus edwardsii* Cornalia spec. (in part) – B. Peyer, *Abh. Schw. Pal. Ges.* **52**, p. 3.

1935 *Pachypleurosaurus edwardsi* Cornalia sp. (in part) – R. Zangerl, *Abh. Schw. Pal. Ges.* **56**, p. 1.

1958 *Pachypleurosaurus* (in part) – C. C. Young, *Vert. Palasiatica* **2**, p. 75.

1959 *Pachypleurosaurus edwardsi* (Cornalia) (in part) – E. Kuhn-Schnyder, *Eclog. geol. Helv.* **52**, p. 650.

1963 *Pachypleurosaurus edwardsi* (in part) – E. Kuhn-Schnyder, *Arch. Sto. Tic.*, **16**, p. 825.

1964 *Pachypleurosaurus edwardsi* (Cornalia 1854) (in part) – E. Kuhn-Schnyder, *Geol. Rdsch.* **53**, p. 403.

1974 *Pachypleurosaurus edwardsi* (Cornalia) (in part) – E. Kuhn-Schnyder, *Neujahrsblatt, Naturf. Ges. Zürich* **176**, p. 65.

1984 *Neusticosaurus* (in part) – R. L. Carroll, *3rd Symposium Mesozoic Terrestrial Ecosystems Short Papers*, Tübingen, Attempto Verlag, p. 43.

1985 *Neusticosaurus* sp. (in part) – R. L. Carroll and P. Gaskill, *Phil. Trans. R. Soc. Lond.* B **309**, p. 354.

1987 *Neusticosaurus* (in part) – S. Schmidt, *Neues Jb. geol. Paläont. Abh.* **173**, p. 341.

Diagnosis. Small *Neusticosaurus*, up to 550 mm long overall with 130 mm trunk length, but usually not more than 450 mm overall length and 90 mm trunk length. Sex *x* grows larger than sex *y*. Average trunk length is 69 mm, at sexual maturity 55 mm.

Skull distinctly wedge-shaped with wide skull table arching out over lower jaw. Orbits large, upper temporal openings small and slit-like to key hole-shaped. Skull well ossified; 18 tooth alveoli in upper jaw, 24 tooth alveoli in lower jaw.

There are 15–16 cervical vertebrae and 19–20 dorsal vertebrae resulting in 35–36 presacral vertebrae; 3–4 sacral and 42–48 caudal vertebrae. Neural spines moderately high from posterior dorsal column to the 11th or 12th caudal. No accessory articulations in dorsal vertebral column. Atlas ribs present, anterior and posterior process of anterior cervical ribs of equal size. Posterior cervical, dorsal, sacral ribs pachyostotic; 8 caudal ribs, about 21 haemapophyses and 22 gastral ribs.

Anterior margin of shoulder girdle rounded. Clavicle with large blade and long posterior process. Interclavicle small. Scapular blade short. No indentations for coracoid foramen. Pectoral fenestra relatively small.

Humerus strongly sexually dimorphic. Humerus:femur ratio of sex *x* about 1.0. Humerus:femur ratio of sex *y* 1.3. Humerus slender, not pachyostotic. Two elements in carpus. Phalangeal formula of hand reduced to 1–2–3–3–2.

Thyroid fenestra large, obturator foramen sometimes slit-like, sometimes closed off. Femur proximally expanded with triangular cross section. Cross section of shaft oval. Two elements in tarsus. Astragalus clearly wider than calcaneum. Phalangeal formula of foot primitive with 2–3–4–4/5–3.

Age. Middle Triassic, early to Middle Ladinian, younger than *Neusticosaurus pusillus*, older than *Neusticosaurus edwardsii*.

Horizon and localities. Known from the Cava Superiore horizon, Lower Meride Limestone from the following localities: Acqua del Ghiffo, Monte San Giorgio, southern Swiss Alps, and Ca' del Monte, Monte San Giorgio, southern Italian Alps.

Derivatio nominis. The species is named after the late Bernhard Peyer, who discovered and established Monte San Giorgio as the most important Middle Triassic marine vertebrate locality.

Holotype. PIMUZ T 3615, Monte San Giorgio, Acqua del Ghiffo, Lower Meride Limestone, Cava Superiore horizon, *Livello* 2 *sopra* (upper part of second bed), collected 5 October 1928. A complete skeleton of a subadult prepared by air abrasive (figure 7*b*; figure 24*b*).

Referred specimens. PIMUZ T 3386, T 3389, T 3393–T 3397, T 3398a, T 3398b, T 3399, T 3403, T 3404, T 3408, T 3410–T 3414, T 3420, T 3423, T 3431, T 3433, T 3441, T 3443–T 3446, T 3449, T 3461–T 3465, T 3467, T 3469, T 3471, T 3472, T 3474–T 3477, T 3479, T 3482, T 3497, T 3510, T 3511, T 3523, T 3524, T 3531, T 3534, T 3537, T 3539, T 3542, T 3543, T 3546, T 3557, T 3581–T 3584, T 3586–T 3589, T 3592, T 3607, T 3609, T 3662, T 3663, T 3665, T 3688, T 3704, T 3705, T 3710, T 3712, T 3713, T 3715, T 3716, T 3722,

T 3726, T 3728, T 3734, T 3744, T 3752–T 3755, T 3762, T 3764, T 3768, T 3770, T 3787–T 3789, T 3799, T 3801, T 3902, T 3924, T 3932, T 4290–T 4292, T 4294, T 4295, T 4299.

Taxonomic notes. The first eight specimens of *Neusticosaurus peyeri* as well as one *N. pusillus* and two *Serpianosaurus mirigiolensis* (Rieppel 1989*a*) specimens were described in 1932 by Peyer as *Pachypleurosaurus edwardsii*. An additional 32 specimens of this species were described by Zangerl (1935) in his monograph on the Monte San Giorgio pachypleurosaurids as *Pachypleurosaurus edwardsi*. Three other species (*Serpianosaurus mirigiolensis*, *N. edwardsii*, and *N. pusillus*) were included under the same name. From then on, *Pachypleurosaurus edwardsi* contained these four species (see, for example, Young 1958, or Kuhn-Schnyder 1959, 1963, 1974). It was not until much later that they were successfully separated. Carroll (1984) recognized that the small pachypleurosaurids were, in fact, *Neusticosaurus*, a genus first described from the German Middle Triassic (O. Fraas 1881; Seeley 1882). Carroll & Gaskill (1985) gave a more detailed account but believed that only one species existed that differed slightly from the German *N. pusillus*. This difference is partially explained by the fact that their (Carroll & Gaskill 1985) *Neusticosaurus* sp. contained in part *N. pusillus* but also the new species *N. peyeri*.

(*b*) *Description*

All specimens of this species come from the Cava Superiore horizon, largely from one locality, Acqua del Ghiffo. The standard length of *Neusticosaurus peyeri* ranges from 4.6 mm (T 3705) to 34.1 mm (T 3445), specimens under 10 mm are considered juveniles. The type (T 3615, figures 7*b* and 24*b*) is a subadult. Juveniles are fairly common and provide material for detailed study of allometric change during ontogeny (see §13). In comparison with *Neusticosaurus pusillus*, this species shows an increased height of the neural arches of the posterior dorsal vertebrae. This is immediately obvious because in many specimens, the back half of the vertebral column is preserved in lateral view. The phenomenon is better developed in *N. edwardsii*, which has even higher neural spines. This description is based on slightly over 100 prepared specimens of *Neusticosaurus peyeri* in the PIMUZ collection that are mostly complete articulated skeletons with skull. Supplementary data were gathered from X-rays of unprepared material.

(i) *Skull*

The best skulls were selected for the description of cranial anatomy: T 3386, T 3462 (figure 17*b*), T 3582 (figure 17*a*), and T 3607 that are all exposed in dorsal view; T 3789, exposed in a lateroventral view; T 3403 (figure 18*a*), T 3479, 3510 (figure 18*b*), T 3585, and T 3666 (figure 18*c*), all ventrally exposed. Specimen T 3666 is partially disarticulated. Specimen T 3534 provided information about tooth morphology. The reconstructions (figure 19) are necessarily composites, but the dorsal view is based mainly on T 3582 (figure 17*a*) and the ventral view on T 3403 (figure 18*a*). Except for T 3789 (juvenile), T 3403 (subadult) and T 3386 (very large), all these specimens are of about the same size and can be considered as adult. Ontogenetic change in the skull will be discussed in §13. The preservation is about the same as in *Neusticosaurus pusillus*, but with a smaller amount of crushing. Because of the hardness of the Cava Superiore rock, the quality of preparation is generally poorer than in *N. pusillus*.

The skull of *Neusticosaurus peyeri* is so similar to that of *N. pusillus* that only the differences between the two will be discussed. The major difference is the much wider skull table, resulting in a distinctly wedge-shaped skull. In this respect *N. peyeri* assumes a great similarity to

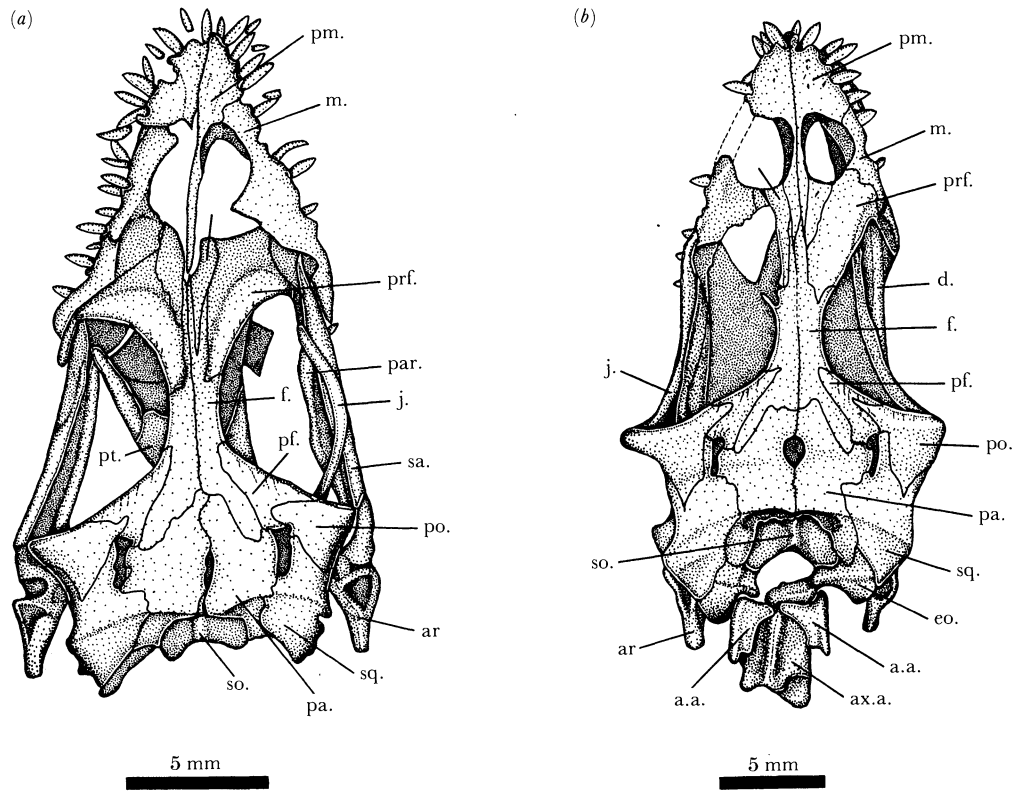

FIGURE 17. The skull of *Neusticosaurus peyeri* in dorsal view. Note the wide but short skull table, the large orbits, and the small, slit-like upper temporal openings; (*a*) T 3582, (*b*) T 3462.

N. edwardsii (Carroll & Gaskill 1985). The functional implications of this wide skull table were discussed by Carroll & Gaskill (1985).

The orbits of *Neusticosaurus peyeri* (figures 17 and 19*a*, *b*) are somewhat larger than in *N. pusillus*. Accordingly, the postorbital region is relatively shorter, but the snout is of the same relative length. The upper temporal opening has an elongate, slit-like form with a widened anterior end resembling a keyhole in shape (figures 17 and 19*a*, *b*). Sometimes it is almost closed. Its length averages about 8% of the skull length.

The pattern of the dermal bones in the skull roof is the same as in *N. pusillus* except that the posterior process of the premaxillae and the anterior processes of the frontals almost always separate the nasals superficially. The bones in the skull roof appear to be more massive and more firmly joined than in *N. pusillus*. The greatest thickness of the ridge of the prefrontal lies directly at the anterior margin of the orbit. The bones of the anterior and posterior margin of the orbit show grooves parallel to the body axis that might be a product of the thickening of the bone. The premaxilla has 5 or 6 alveoli with a maximum of 5 teeth in place. The maxilla possesses 10–12 alveoli with 4–9 functional teeth. These are about the same numbers as for *N. pusillus* but there is more variability.

In ventral view, the skulls of the two small species of *Neusticosaurus* are not significantly different. In adults of *Neusticosaurus peyeri*, the palate seems to have been closed. In the subadult specimen T 4303 (figure 18*a*), however, the anterior processes of the pterygoids do not meet at the skull midline, and their outer margins do not touch the palatines. No separate

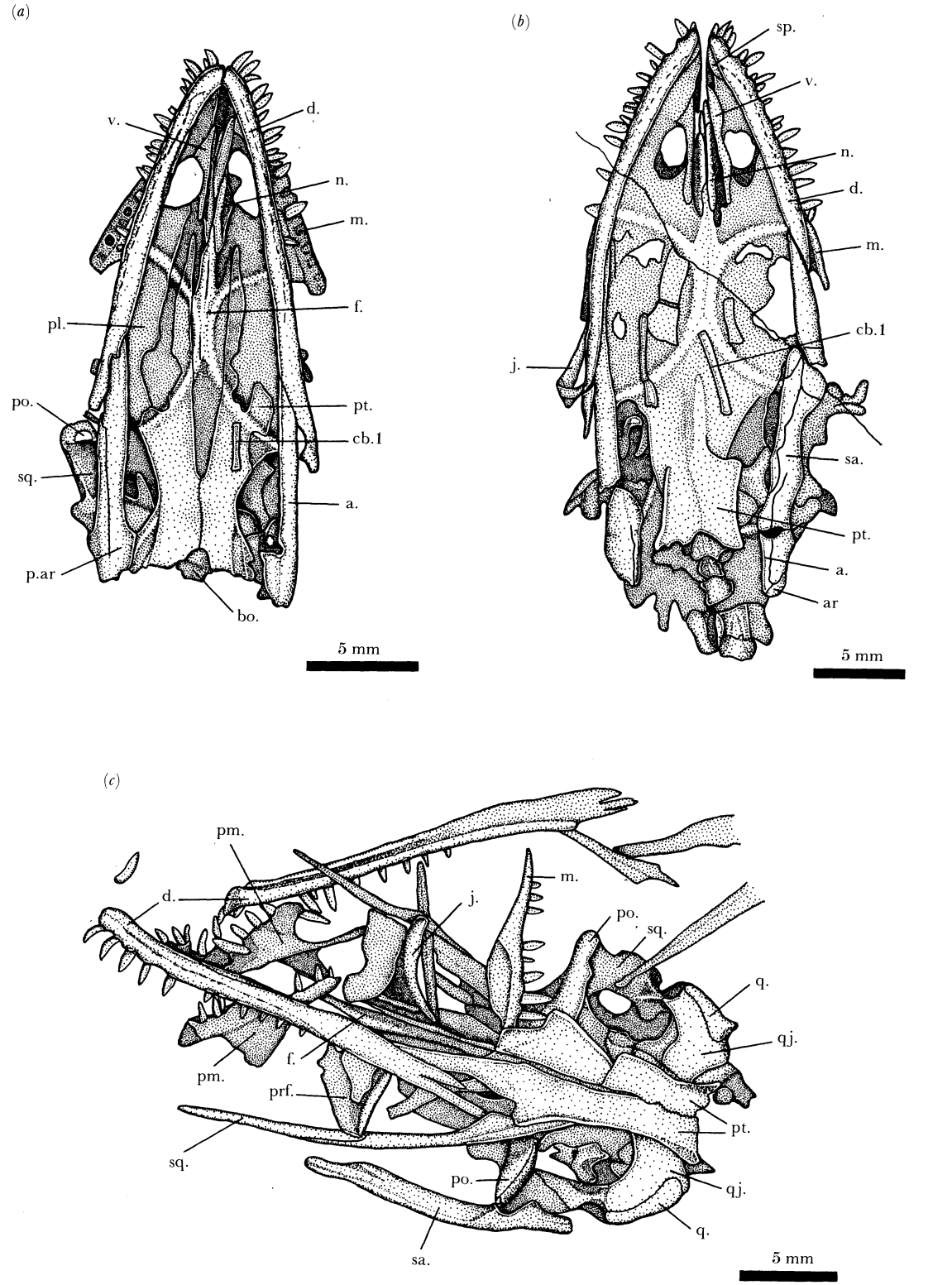

FIGURE 18. The skull of *Neusticosaurus peyeri* in ventral view: (*a*) T 3403, (*b*) T 3510. Note the union of the nasals at the skull midline in (*a*) and (*b*); (*c*) T 3666, showing parts of the skull roof in ventral view and the suture between quadrate and quadratojugal.

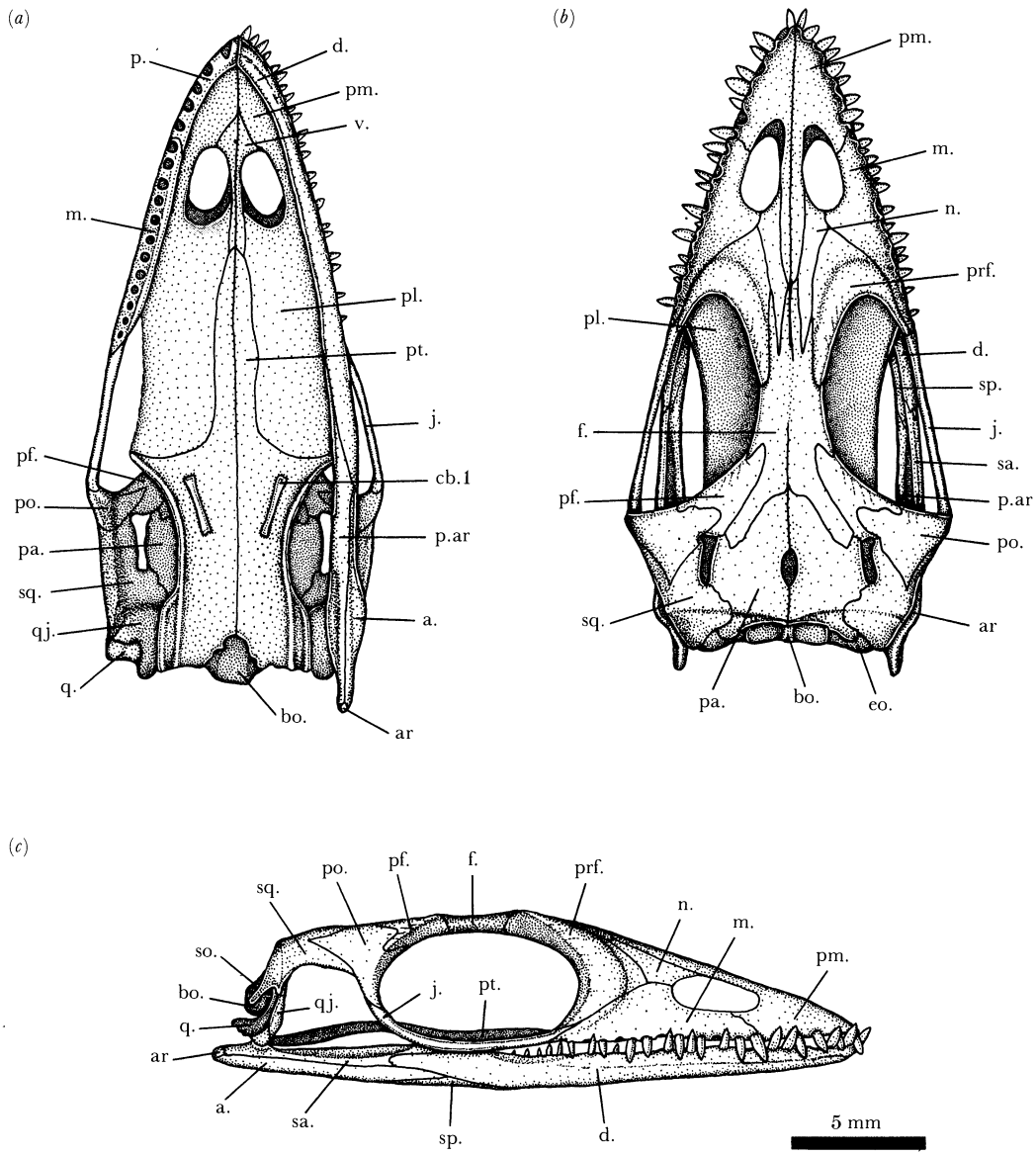

FIGURE 19. Reconstructions of the skull of *Neusticosaurus peyeri*, based mainly on specimens in figures 17*a*, *b* and 18*a–c*: (*a*) ventral view, the right lower jaw is omitted to expose the skull roof ventrally; (*b*) dorsal view. The palate was constricted to expose the lower jaws. Note the wedge shape of the skull due to the wide skull table; (*c*) lateral view. The braincase is unknown.

ectopterygoid could be distinguished in *N. peyeri* either. No additional information about the braincase could be obtained from this species.

The construction of the lower jaw (figure 19) is the same as in *N. pusillus*. The dentary bears a slightly lower number of alveoli (about 24) and has the same low count of teeth in place (10–17). The entire dentition is therefore very similar to *N. pusillus*, except that the teeth are somewhat larger.

(ii) *Axial skeleton*

Quantitative data for the vertebral column of this species were derived from a total of 80 specimens, 65 of which exhibit a complete precaudal vertebral column. The vertebral column of *Neusticosaurus peyeri* consists of 15 or 16 cervical vertebrae (figure 3*c*) and 19 or 20 dorsal vertebrae (figure 3*d*) resulting in a total of 35 or 36 presacrals (figure 3*b*).

Three to four sacral vertebrae are present. Only a few specimens (T 3393, T 3396, T 3461, T 3542, T 3615, T 3688, T 3744, T 3754, T 3755) permit a clear identification of the sacrals. Three well defined sacral ribs are usually seen, but a fourth commonly shows a distal articular surface too. It is sometimes the first and sometimes the last of the series.

The tail is the only part of the vertebral column that shows a great deal of variation in the vertebral count. A sample of 21 seemingly complete adult tails showed a range of 40–48 caudal vertebrae with a weak maximum at 41–43 (figure 3*e*). The number of caudals is distinctly lower than in *N. pusillus*.

In ventral view, the atlas of *Neusticosaurus peyeri* (figure 20*a*) has a small rounded centrum, of which only the front half is visible when articulated. It has a semispherical surface for articulation with the occipital condyle. No atlas intercentrum was observed. The atlas arch (T 3462, figure 17*b*; T 3801) is split in the middle and bears no neural spine. A pair of short double-headed atlas ribs (T 3403, figure 20*a*) is present that shows hints of anterior processes.

The posterior half of the axis centrum (T 3403, figure 20*a*; T 3467, figure 17*b*) has the same morphology as the other cervical centra except its anterior half forms a triangular shelf around which the ventral heads of the axis ribs are draped. The ribs are prevented from making contact with each other by a small intercentrum, the only one in the entire vertebral column except for the chevron bones of the tail. Two large foramina, sometimes unequal in size, could be observed at the posterior margin of the shelf. They are probably not identical to the common foramina subcentralia (Hoffstetter & Gasc 1969) because they are too large and occur only in the axis. In dorsal view, the axis ribs do not differ a great deal from the ribs of the following vertebrae, with a short anterior and a longer posterior process. The axis spine, however, is, relatively, the largest and highest of the entire cervical column, reaching far forward over the atlas arch.

The description of the cervical column in dorsal view is based mainly on T 3615 (figures 7*b* and 24*b*) and T 3801, whereas the description of the cervical column in ventral view is based mainly on T 3431, T 3665, T 3467, and T 3403. Behind the axis, the cervical vertebrae increase gradually in size to reach the size of the trunk vertebrae. The shape of their arches remains constant but the arches become increasingly swollen in appearance. The same can be observed in the vertebral centra. Whereas the first cervical vertebrae show concave sides (the articular surface appears to be expanded) and longitudinal grooves around the ventral margin of the parapophyses, the posterior centra assume the swollen appearance of the trunk vertebrae. The cervical ribs are all double headed. The third (figure 20*b*) and fourth rib each have a larger anterior process whereas all the following ribs have anterior and posterior processes of about the same size. This condition persists to the 13th vertebra, but in ribs 14–16, the posterior process quickly reaches the length of the trunk ribs whereas the anterior process and the ventral head are reduced.

The planes of the zygapophyses are angled at about 20° in the anterior cervicals and are almost planar in the posterior cervicals. Judging from the carcass positions (figure 26, plate 3),

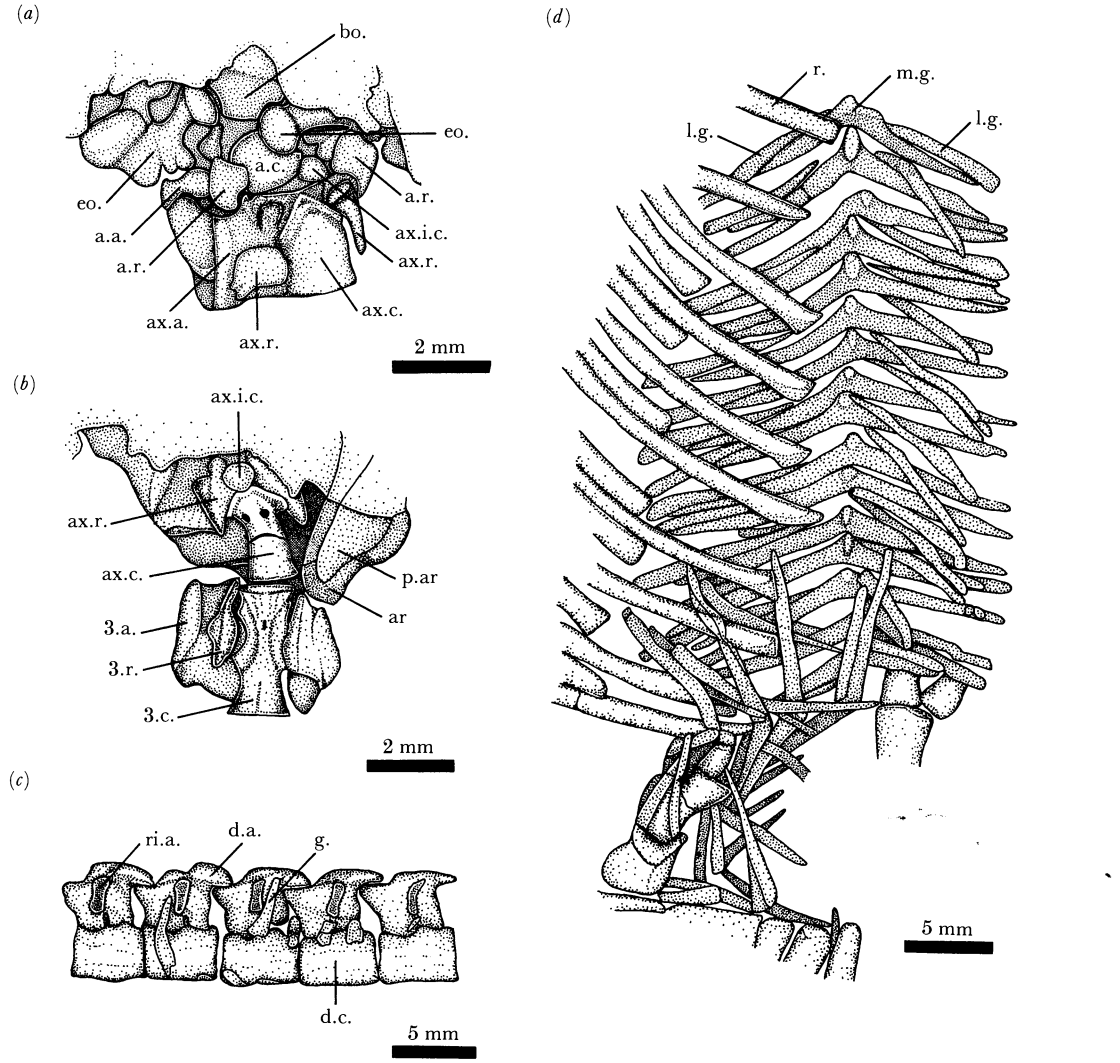

FIGURE 20. *Neusticosaurus peyeri*: (*a*) the occipital region of T 3403 in ventral view. Note the peculiar, round articulations of the exoccipitals and the presence of atlas ribs; (*b*) the axis and third cervical of T 3467 in ventral view with articulated axis ribs and axis intercentrum. Note the shape of the third rib with its large anterior process; (*c*) middle dorsal vertebrae of T 3728. The articular facets for the ribs are restricted to the neural arches. Note the distinct neurocentral suture and the low neural spines; (*d*) the exceptionally well preserved gastralia of T 3396 in dorsal view.

the neck was very flexible laterally, especially in its anterior part. A suture between the arch and the centrum is always present but no separation of arch and centrum has been observed.

The relative height of the cervical neural spines decreases backwards owing to the swelling of the arches. This decrease in spine height leads to a torsion of the neck during fossilization. The anterior cervicals are partially laterally positioned, whereas the posterior cervicals are preserved dorsoventrally. The atlas is separated from the skull. The first five to eight spines are completely ossified whereas the posterior tip of the others shows a drop-shaped surface of cartilage attachment. An accessory articulation is present between the cervical neural arches consisting of a short process at the anterior base of the neural spine in the more posterior vertebra and a shallow depression at the posterior base of the neural spine of the anterior vertebra. This articulation is almost identically developed in *Neusticosaurus pusillus* (figure 14*b*).

The description of the trunk column in dorsal view is based mainly on T 3615 (figure 7*b*), T 3801, T 3471, and T 3386; that of the trunk column in ventral view is based mainly on T 3471; and that of the trunk column in lateral view is based mainly on T 3728 (figure 20*c*) and T 3396 (figure 27*a*). The number of trunk vertebrae is usually 19 or 20, but occasionally 21 (figure 3*d*). In dorsal view, the shape of the neural arches is roughly square, grading in the posterior vertebrae into a squat chevron shape. This indicates an increase in the amount of lateral flexion possible between successive vertebrae, the anterior trunk region being the stiffest part of the entire vertebral column. The neural arches are generally swollen and lack transverse processes. The rib articular surface (figure 20*c*) is kidney-shaped to elliptical. The neurocentral suture is well defined but postmortem separation of arch and centrum is rare. The zygapophyses are broad and flat with horizontal articular surfaces. The neural spines are low and unfinished in small specimens. In adults, the termination of unfinished bone extends over the posterior half of the spine in the anterior vertebrae and over the entire length of the spine in the posterior vertebrae. All the spines are usually finished bone in larger specimens, but remain low with a sharp crest in the anterior region. They do not form the accessory intervertebral articulation that was described for *N. pusillus* (this study) and *N. edwardsii* (Carroll & Gaskill 1985).

Some larger specimens show a partially tilted trunk column that is caused by high neural arches or neural spines in the posterior trunk region. This observation is also useful to distinguish easily between *N. peyeri* and *N. pusillus*. Articulated specimens of the latter never display a lateral view of the trunk column. In ventral view, the centra are drum- to barrel-shaped with a shallow groove along the midline.

The trunk ribs are single-headed and somewhat thickened at the proximal end with an unfinished distal end (figure 20*d*) probably for attachment of the sternal cartilage. The trunk ribs increase slightly in length posteriorly, attaining their greatest length in the middle of the trunk and shortening caudally. The last two to three trunk ribs decrease in length abruptly, changing from a somewhat shorter trunk rib with a finished distal end to a straight, pointed rod.

The number of sacral vertebrae ranges from three to four, but most specimens exhibit an intermediate condition, i.e. three sacral ribs on one side and four on the other. When four sacral ribs are present, the first or the last sacral rib nearly tapers to a point but does have a very small distal articular surface. The three other sacral ribs are short, sturdy rods that are thicker than dorsal ribs, converging on one point of articulation with the ilium. The anterior and posterior sacral ribs are the only ribs that are commonly dislocated. The sacrum seems to have been reinforced by some sort of tough tissue that shrank after death and pulled the posterior and anterior sacral ribs towards the central rib. The proximal articular surface for the sacral ribs increases considerably in size and assumes a roughly circular outline, thereby intersecting the neurocentral suture. The shape of the sacral neural arches is essentially the same as in the last presacral vertebrae.

The description of the caudal vertebral column is based mainly on T 3386, T 3431, T 3615 (figure 7*b*), and T 3728. As noted above, the count of caudal vertebrae ranges between 40 and 48 (figure 3*e*). Most tails are preserved laterally, or at least the last three-quarters. The neural spines of the first 10–12 tail vertebrae are relatively high, and the best developed of the entire column. They, and the large chevrons, produced a tail with a high profile suited for swimming by lateral undulation. Accessory articulations are also found in this part of the tail. The

characteristic swelling of the trunk vertebrae is reduced in the first four tail vertebrae, and the rib articulation migrates across the neurocentral suture from the arch to the centrum. Thus the transverse process arises only from the centrum from the fifth caudal on. The number of eight caudal ribs seems very constant. The major reason of variation in this count is the incorrect recognition of the last sacral vertebra and of the last caudal rib that is often just a tiny nubbin of bone barely set off from the transverse process. A strong morphological change in the tail vertebrae can be observed at around the 11th or 12th caudals. The height of the neural spines decreases markedly over two or three vertebrae, sometimes passing through a two-pronged intermediate and grading into a low, long spine (T 3615, figure 7*b*). The centrum becomes much more slender and loses its transverse processes.

Towards the tip of the tail, the slenderness of the centra increases gradually until the last caudals are more than twice as long as they are wide. The neural arches increase in length accordingly but are lost somewhat abruptly between the 29th and the 36th caudal. The very last caudals sometimes show signs of poor ossification (e.g. a hole in the centre). The last caudal has no distal articular surface and somewhat resembles a blunt terminal phalanx.

The first chevron bone usually appears between the third and the fourth caudal. It consists of the two descending rods terminating in a single, laterally flattened blade. Bimodality in the position of the first chevron, which may aid in sex determination in reptiles (Romer 1956), could not be detected; individuals with the first chevron appearing more caudally would have been females (Romer 1956, p. 267). The general shape of the chevrons does not change but they decrease in size in accordance with the vertebrae and disappear eventually, somewhere between the 21st and 30th vertebrae, most commonly between the 23rd and 25th.

A well preserved gastral skeleton can be seen in T 3396 (figures 20*d* and 27*a*) that is an extraordinary specimen because it is the only adult pachypleurosaurid skeleton from Monte San Giorgio in lateral view. The gastralia have fallen off and are seen in dorsal view. T 3396 exhibits a minimum of 20 gastralia consisting of a central and two lateral elements. The central element bears a ridge along the midline that is drawn out into a short anterior process. The lateral elements lie in front of the central element and almost reach the anterior process, whereas the central element almost reaches the distal ends of the lateral elements. Counts from other specimens (T 3787, T 3932, T 4290) indicate that about 22–24 gastralia were present. This is clearly less than in *Neusticosaurus pusillus* but is in accordance with the lower number of trunk vertebrae in *N. peyeri*. The gastral apparatus begins immediately behind the shoulder girdle and ends in front of the pelvic girdle. Two gastralia are counted per vertebra. The angle enclosed by the central gastral element increases little caudally, from 120° to 150°, in contrast to *N. edwardsii* (Carroll & Gaskill 1985). Pachyostotic thickening of the gastralia is not pronounced.

Appendicular skeleton

Pectoral girdle. Description of the pectoral girdle of *Neusticosaurus peyeri* is based mainly on the following specimens: T 3403 (figure 35*e*), T 3431, T 3444, T 3471, T 3497, T 3615 (figure 7*b*; figure 24*b*), T 3663 (figure 21*a*), T 3665, T 3710 (figure 21*e*), and T 3801.

The three most obvious differences in the shoulder girdle between *Neusticosaurus pusillus* and *N. peyeri* are the shape of the anterior margin, the shape and relative size of the clavicles, and the relative size of the pectoral fenestrae. The first two characters serve especially well to

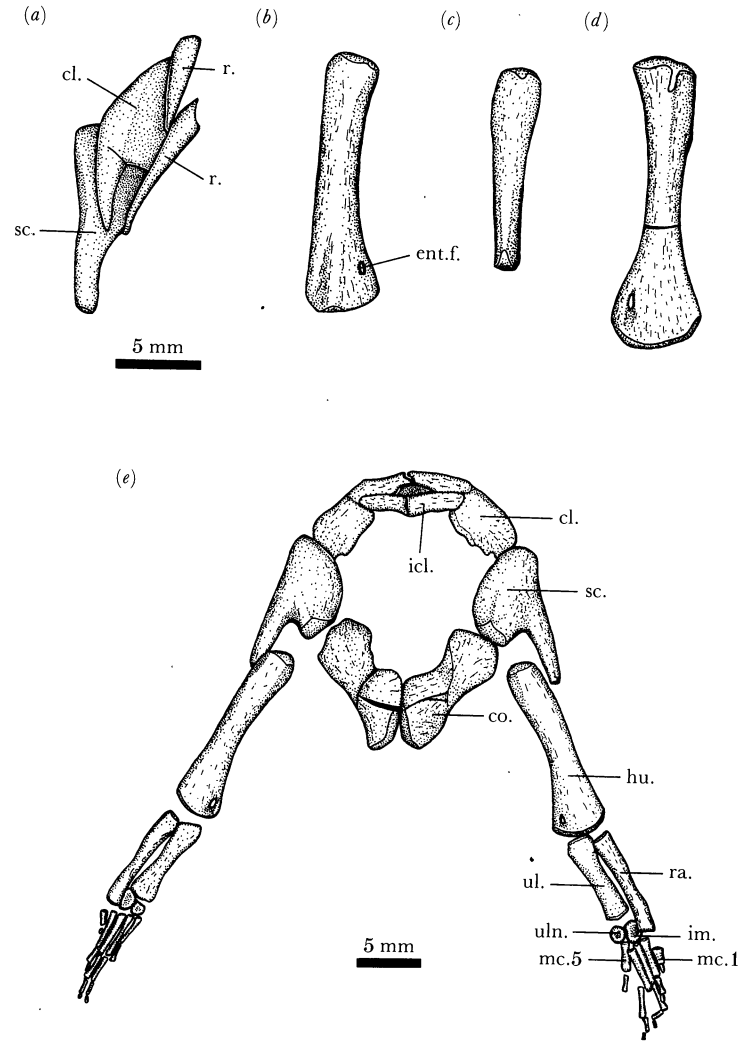

FIGURE 21. *Neusticosaurus peyeri*: (*a*) right clavicle and scapula of T 3663 in dorsal view. Compare to figure 15*b* and note the long posterior process of the clavicle and the large area of overlap with the scapula; (*b*) left humerus of sex *x* (T 3726) in dorsal view. Note the poorly differentiated distal end; (*c*) right humerus of sex *x* (T 3665) in anterior view; (*d*) left humerus of sex *y* (T 3431) in ventral view. Note the expanded distal end, the narrow shaft, and the well differentiated proximal end; (*e*) complete shoulder girdle and forelimbs of T 3710 (sex *x*) in ventral view. Note the rounded anterior margin of the shoulder girdle. The interclavicle lacks a posterior process. The scapulae have a relatively large ascending process and lack a clear indentation for the coracoid foramen. (Note that (*a*)–(*d*) share the same scale bar.)

distinguish between the two species. The pectoral fenestra is generally larger in *N. pusillus* than in *N. peyeri*.

The anterior margin of the pectoral girdle of *N. peyeri* (figure 21*e*) has a very rounded appearance; and the clavicles meet at a point almost one vertebral length cranially to the anterior margin of the scapulae. The clavicles are relatively large in *N. peyeri*, accounting for about one-quarter of the entire length of the pectoral girdle. The anterior margin of the clavicle describes a curve with a central break from its articulation with the scapula to the meeting point with the other clavicle. The break sets the blade off from the stem. A distinct break between the stem and the blade exists at the posterior margin as well. The clavicular blade tapers towards a narrow symphysis with its counterpart. In dorsal view (figure 21*a*), a

well-developed posterior process reaches back, in some cases, well beyond the anterior half of the ventral portion of the scapula.

The interclavicle is sunken into the posteroventral margins of the clavicles, similar to the situation in *N. pusillus*, but it seems to be exposed dorsally to a much greater extent, actually covering the medial parts of the posterodorsal margin of the clavicles. In some specimens (T 3471, T 3497), the posterior process of the interclavicle is developed to a somewhat greater extent than in *N. pusillus*. However, in other, usually smaller specimens (T 3403, T 3710), it is practically non-existent. Thus some interclavicles of *Neusticosaurus peyeri* are clearly triangular whereas others are bar-shaped. No correlation between clavicle shape and sex could be found.

The scapula consists of a flat ventral portion and a narrow blade. The ventral surface is divided into two facets by a low ridge that probably separated the ventral and lateral portions of the pectoral musculature. The anterior margin of the scapula underlies the clavicle and tapers into a thin edge. The medial margin is slightly convex and thins into an unfinished edge. An indentation for the coracoid foramen is almost never present but its position may be indicated by a straight stretch in the posterior part of the medial margin.

The thickened lateral part of the posteroventral margin of the scapula forms the anterior surface of the glenoid fossa. Its medial part articulates with the coracoid. The lateral margin of the scapula is straight to slightly concave. The scapular blade arises from its middle part as a subcircular rod extending upward at an angle of about 45°. It extends back over the glenoid fossa, thereby limiting the dorsal excursion of the humerus.

The scapulae of the two small species of *Neusticosaurus* appear to be very similar in overall shape and could not be identified to species in disarticulated specimens because of their overlapping ranges of variation. However, the blade in *Neusticosaurus peyeri* appears to be relatively thicker and shorter. It is less inclined caudally and arises more cranially.

The overall shape of the coracoid is again very similar in both species. It is an essentially flat, waisted bone. The posterolateral and anteromedial margins are concave, the latter to a greater degree. Only the former was not rimmed with cartilage. The posterolateral margin of the coracoid is more convex in *N. peyeri* than in *N pusillus*. The anterolateral margin can be divided into three parts: (i) the thickened coracoid surface of the glenoid fossa, (ii) the articular surface with the scapula, and (iii) the area of the coracoid foramen. The indentation for the coracoid foramen is inconsistently developed in *N. peyeri*. Its development seems to be age dependent. Some specimens show none at all whereas others show a well-developed anteromedial process. The coracoid surface of the glenoid fossa faces laterally to anterolaterally.

The thickened medial margin of the coracoid is the symphysial margin. The coracoid symphysis is decidedly shorter in *Neusticosaurus peyeri* than in *N. pusillus* because the anteromedial and especially the posteromedial corners of the coracoids are well-rounded. Cartilage apparently filled the gap between the coracoids. The posterior margin of the coracoid is unfinished, thickened bone. It probably served for the attachment of a cartilaginous sternum.

Scapula and coracoid generally appear to be affected more by pachyostosis in *Neusticosaurus peyeri* than in *N. pusillus*.

Forelimb. Description of the forelimb of *Neusticosaurus peyeri* is based mainly on the following specimens: T 3393 (sex *y*; figure 23*a*), T 3403 (sex *y*; figure 35*e*), T 3431 (sex *y*; figure 21*d*), T 3444 (juvenile), T 3445 (sex *x*), T 3523 (sex *y*), T 3589 (sex *x*), T 3615 (sex *x*; figure 7*b*), T 3665 (sex *x*; figure 21*c*), T 3710 (sex *x*; figure 21*e*), T 3726 (sex *x*; figure 21*b*) and T 3755 (sex *x*).

In general, pachyostosis seems to have affected the humerus of *N. pusillus* more than that of

N. peyeri, the reverse of pachyostosis in the shoulder girdle. A clear sexual dimorphism is also evident in *Neusticosaurus peyeri*. It is expressed morphologically as well as in the proportions. The relative size differences of the humeri are very pronounced in this species (tables 4, 9; figures 30*c*, 31*c* and 32*c*).

The humerus of sex *y* is usually about 25% longer relative to the standard length (range is 0.75–1.0) than the humerus of sex *x* (range is 1.05–1.25; tables 4, 9). No dimorphism can be observed for femur length relative to standard length (range of sex *x* is 0.79–0.98, range of sex *y* is 0.78–1.06). Thus the humerus length dimorphism is better expressed relative to the femur length than relative to the standard length. The femur is more often preserved and more easily measured than the standard length (see §2). In sex *x* the humerus:femur ratio is 0.9–1.1, whereas it is 1.1–1.3 in sex *y*. Individuals can be sexed either by qualitative or quantitative criteria.

Morphological differences between sexes are most clearly expressed in the humerus (figures 21*b*, *d*, *e* and 23*a*). In general, it has a rounded proximal end and a dorsoventrally flattened distal end. These characteristics are the only ones that the humeri of the two sexes have in common. The humerus of sex *x* shows almost no morphological differentiation, and pachyostotic swelling seems to have obliterated almost all concave elements. The humerus of sex *y* is generally well differentiated, suggesting a well developed musculature.

Almost no differentiation of the distal end of the humerus of sex *x* is recognizable, only a well-developed entepicondylar foramen and a low ectepicondylar ridge with an angular crest. The distal articular surface of unfinished bone is restricted to the distal end of the humerus and is fairly flat dorsoventrally and convex lateromedially. The bone is slightly arched caudally. A rugose area for the attachment of the deltoid muscle (deltoid crest) is seen dorsally on the proximal end. Ventrally, a somewhat better developed ridge can be interpreted as the pectoral crest.

In sex *y*, the distal end shows an almost complete separation of the convex articular surface into a small posterior and a much larger anterior part. The small posterior part probably served as an insertion point for the flexor muscles of the forearm. The ectepicondylar ridge flanked by grooves is much better developed than in sex *x*. Its distal end has a dorsal extension of the articular surface. A supinator ridge is separated off from the ectepicondylar ridge by a deep ectepicondylar groove.

In ventral view, the distal end of the bone appears almost flat with slightly raised edges. All specimens of sex *y* show a break in the anterior outline of the humerus about one-quarter distally. Sometimes rugosities are developed here. These probably served for insertion of the subcoracoscapularis muscle. In one specimen (T 3403), a deep elongate recess is present next to this muscle attachment. The entepicondylar foramen is located considerably more proximally in sex *y* than in sex *x*. The shaft has a rounded cross section in both sexes (figure 25*k*).

Qualitative morphological observations can be quantified by examination of the distal width of the humerus relative to its length, proximal width, and minimal shaft diameter (table 9; figure 30*c*). The first and especially the last criterion seems to yield the best results. The ranges for the two sexes overlap only slightly in the distal width:minimal shaft diameter ratio (table 9; figure 30*c*). It is 1.23–1.95 in sex *x*, and 1.89–3.0 in sex *y*. The length:distal width ratio in sex *x* is 3.2–3.8, and in sex *y*, 2.8–3.4; the distal width:proximal width ratio in sex *x* is 1.3–1.8 and in sex *y*, 1.4–2.1. These values are very close to those of *Neusticosaurus pusillus*.

The morphology of radius and ulna is very similar to *N. edwardsii* and not much new detail

can be reported here. Some interesting insights can be gathered from quantitative data (table 4), however. No significant difference in length of the radius relative to the humerus can be observed in the two sexes. No dimorphism is evident in the length of the radius relative to the ulna, in contrast to the situation in *Neusticosaurus pusillus*. A clear sexual dimorphism is evident for the humerus:third metacarpal ratio. In sex *x*, this ratio ranges from 3.7 to 4.7, and in sex *y* from 4.7 to 5.8.

A look at the length of the forelimb elements relative to body length (table 4) reveals only a weak dimorphism in the third metacarpal:standard length ratio (sex *x* = 0.19–021, sex *y* = 0.19–0.23). Dimorphism is well developed in the humerus:standard length ratio (sex *x* = 0.75–1.05, sex *y* = 1.04–1.25) and the radius:standard length ratio (sex *x* = 0.44–0.53, sex *y* = 0.49–0.71). These are the inverse relations as observed for the humerus:radius ratio (weak dimorphism) and the humerus:third metacarpal ratio (strong dimorphism; table 4). In conclusion, the size of the hand is about the same in both sexes, and most of the sexual dimorphism is expressed in the proximal elements of the forelimb.

Only two ossified elements are present in the carpus, an elongate (exception T 3431) intermedium, and a roundish and smaller ulnare. The ulnare is always depressed in the centre. This depression may be enhanced by compaction. The intermedium shows a lesser depression or none at all.

The metacarpals show the pattern characteristic for the manus of all pachypleurosaurids. The first metacarpal is much shorter than the others but much stouter with an expanded proximal articulation. Metacarpal 5 is next in length and then metacarpal 2. In *Neusticosaurus peyeri*, metacarpal 3 is either longer than metacarpal 4 or of the same length and is only rarely shorter. Again, no correlation to individual age or sex could be found. This phylogenetic trend of elongation of the third metacarpal from *N. pusillus* to *N. peyeri* is compatible with the fact that metacarpal 3 is always the longest in *N. edwardsii* (Carroll & Gaskill 1985). The length of the third metacarpal relative to all other limb bones of *Neusticosaurus peyeri* is within the range of *N. edwardsii*. It is slightly greater in sex *y* of this species than in sex *y* of *N. pusillus* (table 9).

The phalangeal formula for the manus of *Neusticosaurus peyeri* is 1–2–3–3–2, which is a clear reduction compared to *N. pusillus* and *N. edwardsii*. This reduction of the phalangeal count seems to be accompanied by a reduction in length of the fingers as well. The missing phalanges are not compensated for by a length increase of the others. This results in a less slender appearance of the manus than in *N. pusillus*. As in *N. edwardsii* and *N. pusillus*, the digits increase in length from one to four, the fourth being the longest and the fifth ranging in length between the first and second. The unguals have a blunt tip and are not commonly preserved.

Pelvic girdle. Description of the pelvic girdle of *Neusticosaurus peyeri* is based mainly on T 3413, T 3431 (figure 22*b*), T 3474 (figure 22*a*), T 3523, T 3534, T 3665, T 3722 and T 3744, all of which are ventrally exposed. Unfortunately the pelvic bones are usually deformed by crushing, and no disarticulated specimens exist.

The ilium of *Neusticosaurus peyeri* (figure 22*a*) is so similar to that of *N. pusillus* that it needs no further description. The pubis (figure 22*a*, *b*) is a roughly rectangular, flat element with convex medial and lateral margins and concave anterior and posterior margins. Its anterior margin and, particularly, its posterior margin, is much less concave than in *N. pusillus*. Some variation can be seen in the development of the obturator foramen at the posterior margin of the pubis, just distal to the acetabulum. Some specimens have a completely closed obturator

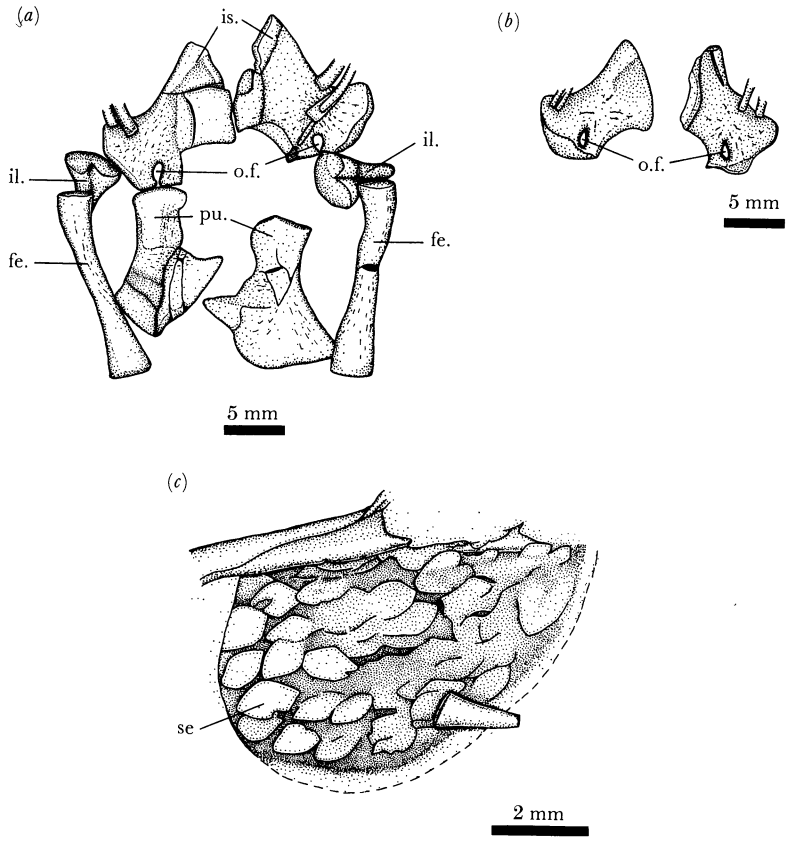

FIGURE 22. *Neusticosaurus peyeri*: (*a*) the pelvic girdle of T 3474 in ventral view. The ischia are clearly less waisted than in *Neusticosaurus pusillus* (figure 16*a*); (*b*) the pubes of T 3431 in ventral view. The obturator foramina are closed in this specimen; (*c*) ventral view of the right orbit of T 3410 showing phosphatized, rhomboidal scales.

foramen (figure 22*b*), some an almost closed one (figure 22*a*), and others only a slit-like foramen. This is different from the condition in *Neusticosaurus pusillus* (figure 16*a*) and *N. edwardsii* both of which always have slit-like obturator foramina.

The ischium of *Neusticosaurus peyeri* is more asymmetrical than that of *N. pusillus* and is more slender than that of *N. edwardsii*. It has a flat, expanded medial part, a fairly narrow waist, and a somewhat wider and thickened lateral 'head' for articulation with the other pelvic bones. The medial margin of the ischium is divided equally into two straight to slightly concave parts. The reduced convexness of the posterior pubic margin and the anterior ischial margin result in a smaller thyroid fenestra than in *Neusticosaurus pusillus*.

Hindlimbs. Description of the hindlimb of *Neusticosaurus peyeri* is based mainly on T 3386, T 3393 (figure 23*b*), T 3394, T 3396 (figure 23*c*), T 3403 (figure 35*e*), T 3471, T 3474 (figure 22*a*), T 3523, T 3534, T 3582, T 3615 (figure 7*b*), T 3710, T 3744, T 3755, T 3801, and T 3902. No qualitative or quantitative (table 5) sexual dimorphism could be observed in any part of the hindlimb.

The overall appearance of the femur of *Neusticosaurus peyeri* (figures 22*a* and 23*b*) is very similar to that of *N. pusillus* (figure 16*b*, *c*). The main differences are less morphological differentiation and the greater flattening of the distal end of the femur. No internal trochanter is developed. The surface is generally smoother and shows fewer concave elements (fossae); the

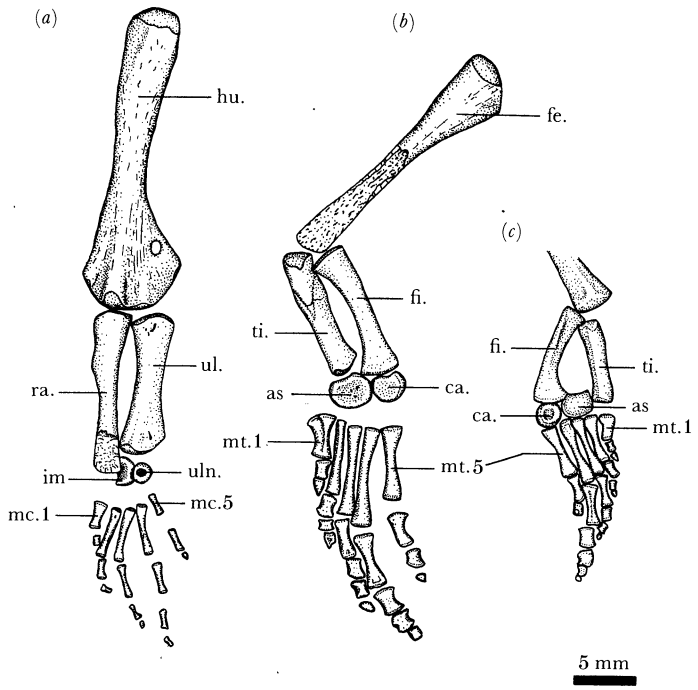

FIGURE 23. *Neusticosaurus peyeri*: (*a*, *b*) left forelimb and hindlimb of T 3393 (sex *y*) in dorsal view. Note the relative size of humerus and femur, also the shape of the unguals of the foot; (*c*) the left lower hindlimb of T 3396 in ventral view displaying the maximal phalangeal count.

articular surfaces are flat in their central parts and not convex. The proximal end appears to be wider in this species than in *N. pusillus* because of greater development of the trochanter major.

Tibia, fibula, and the tarsus of *Neusticosaurus peyeri* (figure 23*b*, *c*) have virtually the same morphology and the same proportions (table 5) as those of *N. pusillus* (figure 16*c*) described above.

With the exception of the first, all metatarsals are very similar with expanded proximal and distal ends that sometimes overlap (figure 23*b*, *c*). The first metatarsal is very stout and thick with an expanded proximal end. The fourth metatarsal and the fourth digit are invariably the longest. The first, second and sometimes the third terminal phalanges are triangular with a pointed tip. However, they are not always as sharply pointed as in *Neusticosaurus pusillus*. The fourth and fifth terminal phalanges are round.

The fifth phalanx of the fourth digit is rarely ossified and always disproportionally small if present, whereas the fourth phalanx is usually not much smaller than the preceding one. Specimens with five phalanges in digit four are T 3396 (figure 23*c*) and T 3801. Accordingly the phalangeal formula of the pes for this species can be given as 2–3–4–4/5–3, the same as for *N. pusillus*, but different from *N. edwardsii*, which exhibits a phalangeal count of 1–2–3/4–4/5–3 (Carroll & Gaskill 1985).

6. *Neusticosaurus edwardsii* (Cornalia) new combination

(*a*) *Systematic palaeontology*

Synonymy.

1854 *Pachypleura Edwardsii* – E. Cornalia, *Giorn. I. R. Ist. Lombard.*, ser. 2, **6**, p. 5.
1863 *Pachypleura Edwardsii* Cornalia – G. Curioni, *Mem. R. Ist. Lombard.*, ser. 2, **3**, pl. 7, fig. 2.
1886 *Pachypleura Edwardsi* Cornalia – W. Deecke, *Z. dtsch. geol. Ges.* **38**, p. 171.
1889 *Neusticosaurus* (*Pachypleura*) *edwardsii* – R. Lydekker, *Catalogue of fossil Amphibia and Reptilia in the British Museum* (*Nat. Hist.*), part 2, p. 285.
1898 *Pachypleura edwardsii* – G. A. Boulenger, *Trans. zool. Soc. London* **14**, p. 7.
1924 *Pachypleura Edwardsii* Cornalia – G. v. Arthaber, *Acta Zool.* **5**, p. 491.
1927 *Pachypleurosaurus* – F. Broili, *Sber. bayer. Akad. Wiss., math.-nat. Abt* **1927**, p. 220.
1928 *Pachypleurosaurus edwardsi* – F. v. Nopcsa, *Geol. Hung.* ser. paleo. **1**, p. 20.
1935 *Pachypleurosaurus edwardsi* Cornalia sp. (in part) – R. Zangerl, *Abh. Schw. Pal. Ges.* **56**, p. 1.
1956 *Pachypleurosaurus* (in part) – F. v. Huene, *Paläontologie und Phylogenie der niederen Tetrapoden*, Jena, VEB Gustav Fischer, p. 383.
1959 *Pachypleurosaurus edwardsi* (Cornalia) (in part) – E. Kuhn-Schnyder, *Eclog. geol. Helv.* **52**, p. 650.
1963 *Pachypleurosaurus edwardsi* (in part) – E. Kuhn-Schnyder, *Arch. Sto. Tic.* **16**, p. 825.
1964 *Pachypleurosaurus edwardsi* (Cornalia 1854) (in part) – E. Kuhn-Schnyder, *Geol. Rdsch.* **53**, p. 403.
1967 *Pachypleurosaurus edwardsi* (Cornalia) (in part) – G. Pinna, *Natura, Milano* **58**, p. 188.
1974 *Pachypleurosaurus edwardsi* (Cornalia) (in part) – E. Kuhn-Schnyder, *Neujahrsblatt, Naturf. Ges. Zürich* **176**, p. 65.
1984 *Pachypleurosaurus* – R. L. Carroll, *3rd Symposium Mesozoic Terrestrial Ecosystems Short Papers*, Tübingen, Attempto Verlag, p. 43.
1985 *Pachypleurosaurus edwardsi* – R. L. Carroll & P. Gaskill, *Phil. Trans. R. Soc. Lond.* B **309**, p. 355.
1987 *Pachypleurosaurus* – S. Schmidt, *Neues Jb. Geol. Paläont. Abh.* **173**, p. 341, p. 343.

Diagnosis. Largest of all pachypleurosaurids. Differs from *N. pusillus* and *N. peyeri* in that it has a relatively small head (skull:trunk ratio is 0.23–0.27), its greater number of teeth (about 30 in upper jaws and 28 in lower jaws), its high neural spines in the posterior trunk and anterior tail region, the presence of three carpals, its relatively short femur (humerus:femur ratio is 1.3–1.8), and its reduced phalangeal count in the foot (1–2–3–4–3).

Age. Middle Triassic, early to Middle Ladinian, younger than *Neusticosaurus pusillus* and *Neusticosaurus peyeri.*

Horizon and localities. Known from the Alla Cascina horizon (figure 5, table 1) of the Lower Meride Limestone from the following localities: Alla Cascina (figure 1), Val Serrata (P. 5), Val Serrata below cave Bööggia (figure 1), and the road Crocifisso–Serpiano above Acqua del Ghiffo (figure 1) in the Monte San Giorgio area of southern Switzerland; Ca' del Frate (near Viggiu, sometimes described as 'near Besano', figure 1) and Pra dei Spiriti in the adjoining parts of northern Italy.

Holotype. Complete skeleton of a juvenile in the Museo Civico di Storia Naturale in Milano (uncatalogued), collected from Ca' del Frate.

Referred specimens. PIMUZ: T 2466, T 2810, T 2811, T 3407, T 3425, T 3427, T 3428, T 3430, T 3435–T 3440, T 3447, T 3450, T 3452–T 3455, T 3458–T 3460, T 3702, T 3708, T 3711, T 3719, T 3732, T 3733, T 3735, T 3736, T 3749, T 3758, T 3759, T 3766, T 3769, T 3775, T 3776, T 3778, T 3797, T 3806, T 3910, T 3935, T 4015 and T 4055. Most of these are largely complete skeletons.

Taxonomic notes. The nomenclature of this species has been reviewed by many workers, most importantly Peyer (1943), Carroll & Gaskill (1985) and Rieppel (1987). See also the taxonomic notes on the two other species of *Neusticosaurus* in this work.

(*b*) *Description*

This species was recently described in an excellent monograph by Carroll & Gaskill (1985) making further description unnecessary.

7. Ornamentation of pachypleurosaur bone

Strong surface sculpturing is common in the membrane bones of various lower tetrapods like labyrinthodont amphibians or crocodiles. Endochondral bone, on the other hand, almost always has a smooth and sculptureless surface. It was therefore surprising to discover that the endochrondral bones of all Monte San Giorgio pachypleurosaurs, especially those of the small *Neusticosaurus*, exhibit a distinct surface ornamentation. This peculiar pattern, observed best under the scanning electron microscope (SEM) (figure 25*a–f*), consists of fine, intertwining grooves, somewhat resembling the skin-ridge pattern of a human hand. This 'finger print ornamentation' appears to be unique to the genera *Neusticosaurus* and *Serpianosaurus*. It is clearly absent in *Dactylosaurus* (uncatalogued specimens, SMNS and GPIT) and was not described in *Anarosaurus* (Dames 1890) or *Keichousaurus* (Young 1958).

The grooves of the 'finger print' cover the bone surface densely and are not more than a few millimeters long and 0.2 mm wide. The ornamentation is best observed in pachyostotic bones like those of the shoulder girdle and the pelvic girdle, the humerus and femur (figure 25*a–c*), and the trunk vertebrae (figure 25*d–f*). Small bones such as the ribs and distal limb elements are 'decorated' the same way. The only bones lacking the ornamentation are the skull bones. The size but not the number of the grooves is independent of the size of the bone and the individual.

The exact configuration and intensity of the ornamentation is bone-specific and species-specific. Long bones like the humerus show many parallel lines in an anastomosing pattern (figure 25*a*) oriented along the long axis of the bone, whereas in less elongated bones such as a vertebral centrum (figure 25*d*), the lines are shorter and less regular.

The ornamentation of *Neusticosaurus pusillus* bone is characterized by well defined grooves persisting over long distances. They are relatively wide and shallow (figure 25*c*). Bone of *Neusticosaurus edwardsii* (figure 25*e*,*f*) shows an ornamentation resembling the skin of an orange. The groove pattern is more irregular (figure 25*e*), and the individual groove is narrower and deeper (figure 25*f*). *Neusticosaurus peyeri* and *Serpianosaurus mirigiolensis* bones are ornamented like those of *Neusticosaurus pusillus* but with finer and deeper grooves. Two lines of evidence indicate that the ornamentation is not the result of some peculiar preservation at Monte San Giorgio but was a feature of the living animal. First, a histological section of the humerus of a *Neusticosaurus pusillus* (figure 25*i*) clearly shows cross sections of the grooves and

ridges on the surface of the growth rings. Thus the animal had this type of bone ornamentation throughout its life. The second argument lies in the fact that the ornamentation is clearly visible in specimens of *Neusticosaurus pusillus* from Germany that were deposited and fossilized under considerably different conditions (O. Fraas 1881).

Interestingly, all Monte San Giorgio pachypleurosaurs exhibit some pachyostosis, and the animal with the best-developed ornamentation, *Neusticosaurus pusillus*, shows the greatest pachyostosis. Nevertheless, the origin and significance of the pattern must remain unclear at present. Further histological studies may shed some light on this peculiarity of *Neusticosaurus* bone. The correlation with pachyostosis is certainly noteworthy.

8. Skeletochronology in *Neusticosaurus pusillus* and *Neusticosaurus peyeri*

Skeletochronology, i.e. aging by growth rings (annuli) in bone, is well established in ectotherms. Castanet (1987) discusses the method and its limitations and reviews studies about living reptiles. Largely through the efforts of Castanet and coworkers, it is now established that skeletochronology works well in all groups of modern reptiles. This method is often able to provide data not otherwise available, for example for long-lived animals such as turtles (Castanet & Cheylan 1979) or rare animals such as *Sphenodon* (Castanet *et al.* 1988). Except for direct observation of individuals throughout their lifetime, skeletochronology is the most accurate method of age determination in ectotherms (Castanet 1987). Aging by growth rings of bone has been demonstrated in fishes (Peabody 1961) and in amphibians (Peabody 1961; Castanet 1987).

Because direct observation is not possible in fossils, skeletochronology is the only method by which the individual age of fossil ectotherms can be determined. Surprisingly few workers have attempted to use skeletochronology in fossils, probably because of the common lack of growth series and sufficient sample sizes. Work on fossils was pioneered by Peabody (1961) who studied growth rings in Permian reptiles and amphibians and used them as a palaeoclimatological tool. Voorhies (1969) observed annual rings in Pliocene catfish vertebrae. The only fossil reptile group that has received a large amount of palaeohistological attention are the dinosaurs (De Buffrenil *et al.* 1986; De Ricqles 1980, 1983; Reid 1981, 1987). Although growth rings are occasionally found in this group and allow aging (Reid 1981; De Ricqles 1983), they are not particularly common. This and other facts led Reid (1987) to argue for a distinctive dinosaurian physiology unlike that of either ectotherms or homeotherms.

Various expressions of growth rings and, consequently, various methods of study are possible. In fish, annuli are commonly visible on the surface of scales or vertebrae (Voorhies 1969). Histological sections, i.e. petrographic thin sections of bone are the standard preparation for fossil reptiles. However, in the case of *Neusticosaurus* I relied mainly on polished sections (figure 25*g–l*), which have the advantage of showing more colour differentiation than thin sections.

Another important point is the selection of the right bone because annuli may be developed in only a few bones of a skeleton (Peabody 1961; Castanet 1987). This was not a problem in *Neusticosaurus*, however. Zangerl (1935, figs 40 and 41) already figured cross sections of ribs with growth rings but was not aware of their identity or significance. Cursory examination of some broken humeri in my sample revealed well developed growth rings in all cases. Annuli

were also observed in the femur, vertebral centra, and ribs. In *Neusticosaurus*, they appear to be present in most bones (figure 25*l*), but in some (e.g. coracoid), the inner annuli were destroyed by bone remodelling. In most cases, the humerus shaft showed very little remodelling (figure 25*g–l*), and only in a few cases did the innermost annulus appear to have been lost.

A crucial question in growth ring aging is whether the 'annuli' really represent annual cycles. A seasonal climate would seem to be a basic condition for the formation of annuli (Peabody 1961), and skeletochronology in reptiles of known age and life history (e.g. Castanet 1978) supports this assumption. However, there are many examples of annuli development in non-seasonal climates that appear to be the result of endogenous cycling linked to reproduction (Peabody 1961; Auffenberg 1980; Castanet 1987). No well-developed, non-annual growth rings have been described in modern reptiles, and Castanet (1987) concludes that in rare instances two annuli per year may be deposited, but never a single annulus every two years. Thus the growth rings in *Neusticosaurus* are most likely to be annual, their count indicating the individual age of the specimen.

Growth series of nine humeri of *Neusticosaurus pusillus* and five humeri of *N. peyeri* as well as one specimen of *N. edwardsii* (T 3455) were sectioned and polished across the central portion of the shaft (figure 25*g–l*). A few thin sections were made but they were no great improvement over polished sections as far as the counting of annuli is concerned. Standard length of the *N. pusillus* specimens ranged from 12.2 mm (class G) to 18.6 mm (class J) and that of the *N. peyeri* specimens from 7 mm (Class C) to 22.2 mm (class K) (table 6). The sample of *N. pusillus* contains mainly medium-sized to large adults, whereas the sample of *N. peyeri* represents a larger size range, from juveniles to large adults. The age of these selected specimens (table 6) was used to estimate the age of the size classes and describe the life history of the two small *Neusticosaurus* in absolute time.

Growth during the first and second years was very rapid. Adulthood was reached during the third or fourth year of life when the animal had grown to size class F. Average-sized adults were from four to six years old and did not grow much older. The rough correlation between size and age indicates that growth continued during adulthood. The largest specimen in each sample is also the oldest. The sexes seem to have grown at the same pace, which is not surprising as they are of the same size. *N. pusillus* did not live much longer than six years, evidenced by

Description of plates 1 and 2

Figure 24. A well-preserved specimen (*a*) (T 3934, sex *y*) of *Neusticosaurus pusillus* in ventral view, (magn. ×0.81); (*b*) the type specimen (T 3615, sex *x*) of *Neusticosaurus peyeri*, new species, in dorsal view, (magn. ×1.15).

Figure 25. Photographs from SEM of the bone surface in *Neusticosaurus* (*a–f*); (*a*) ventral surface of the shaft of the left humerus of a *Neusticosaurus pusillus* (T 3567). Note the finger print-like pattern, (magn. ×13.5); (*b*) close-up of (*a*), (magn. ×33.8); (*c*) close-up of (*b*), (magn. ×135); (*d*) ventral surface of a dorsal vertebra of T 3567, (magn. ×13.5); (*e*) ventral surface of a dorsal vertebra in *Neusticosaurus edwardsii* (T 3455). Note the orange peel-appearance of the bone surface, (magn. ×33.8); (*f*) lateral surface of a dorsal vertebra of a *Neusticosaurus edwardsii* (T 3455), (magn. ×135); (*g–k*) photomicrographs of polished sections of *Neusticosaurus* humerus shafts; (*g*) T 3704, a juvenile (class C) *Neusticosaurus peyeri*. No annuli are visible, (magn. ×28.3); (*h*) T 3432, a juvenile (class D) *Neusticosaurus peyeri*. Two annuli are visible, (magn. ×100); (*i*) T 4297, a small adult (Class G) of sex *x* of *Neusticosaurus pusillus*. Three annuli are visible, (magn. ×20.7); (*j*) T 3786, an average-sized adult (class H) of sex *y* in *Neusticosaurus pusillus*. Four to five annuli are visible, (magn. ×14.1); (*k*) T 3768, a small adult (class F) *Neusticosaurus peyeri*. Five annuli are visible, (magn. ×20.8); (*l*) T 3782, an average-sized adult (class G) *Neusticosaurus pusillus* of sex *x*. Polished section of left coracoid, anterior dorsal vertebra, some ribs, and the shaft of the left humerus. All bones show annuli. Only the coracoid shows strong internal bone remodelling. Four annuli can be counted in the humerus, (magn. ×9).

FIGURE 24. For description see opposite.

(*Facing p.* 620)

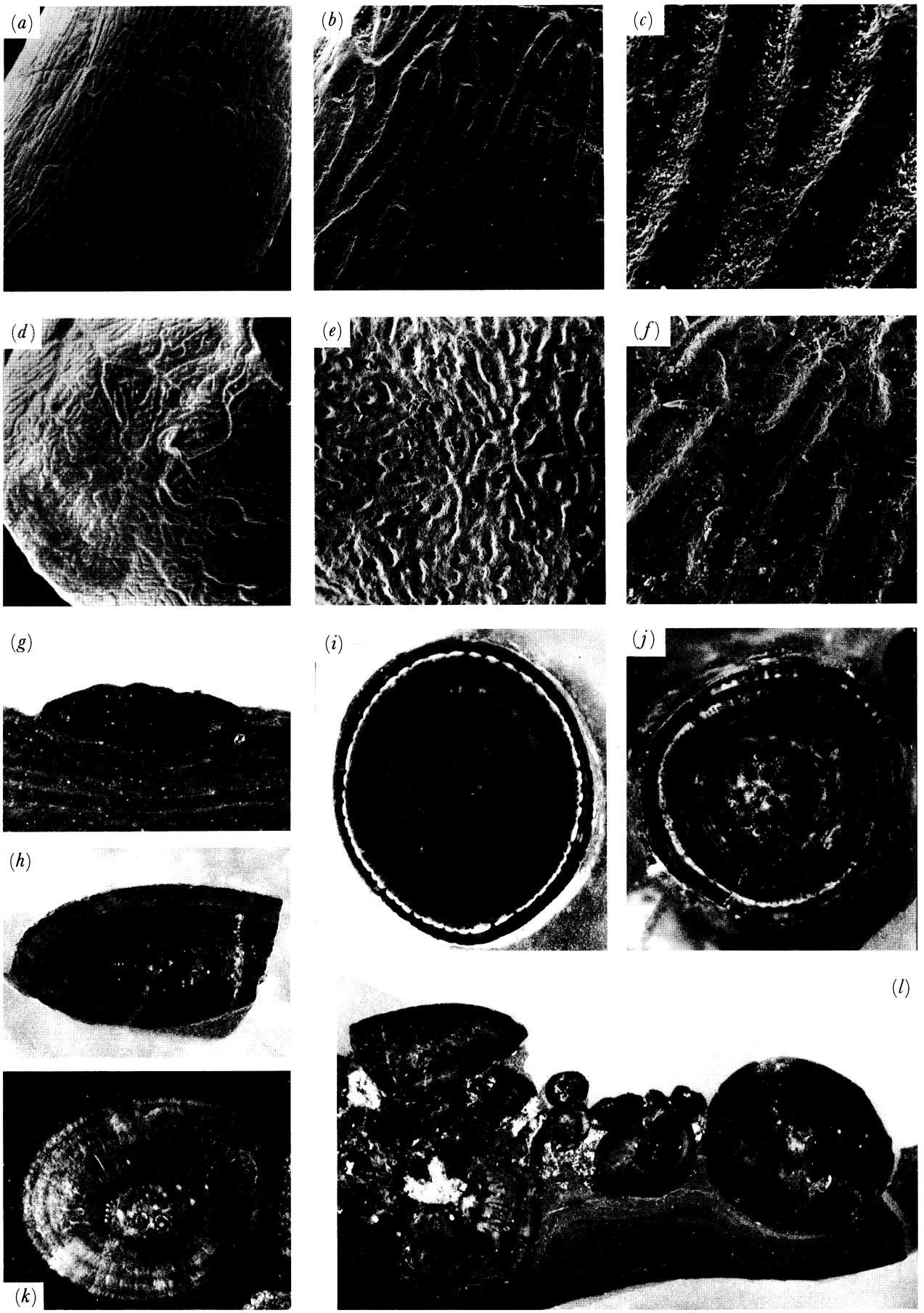

FIGURE 25. For description see page 620.

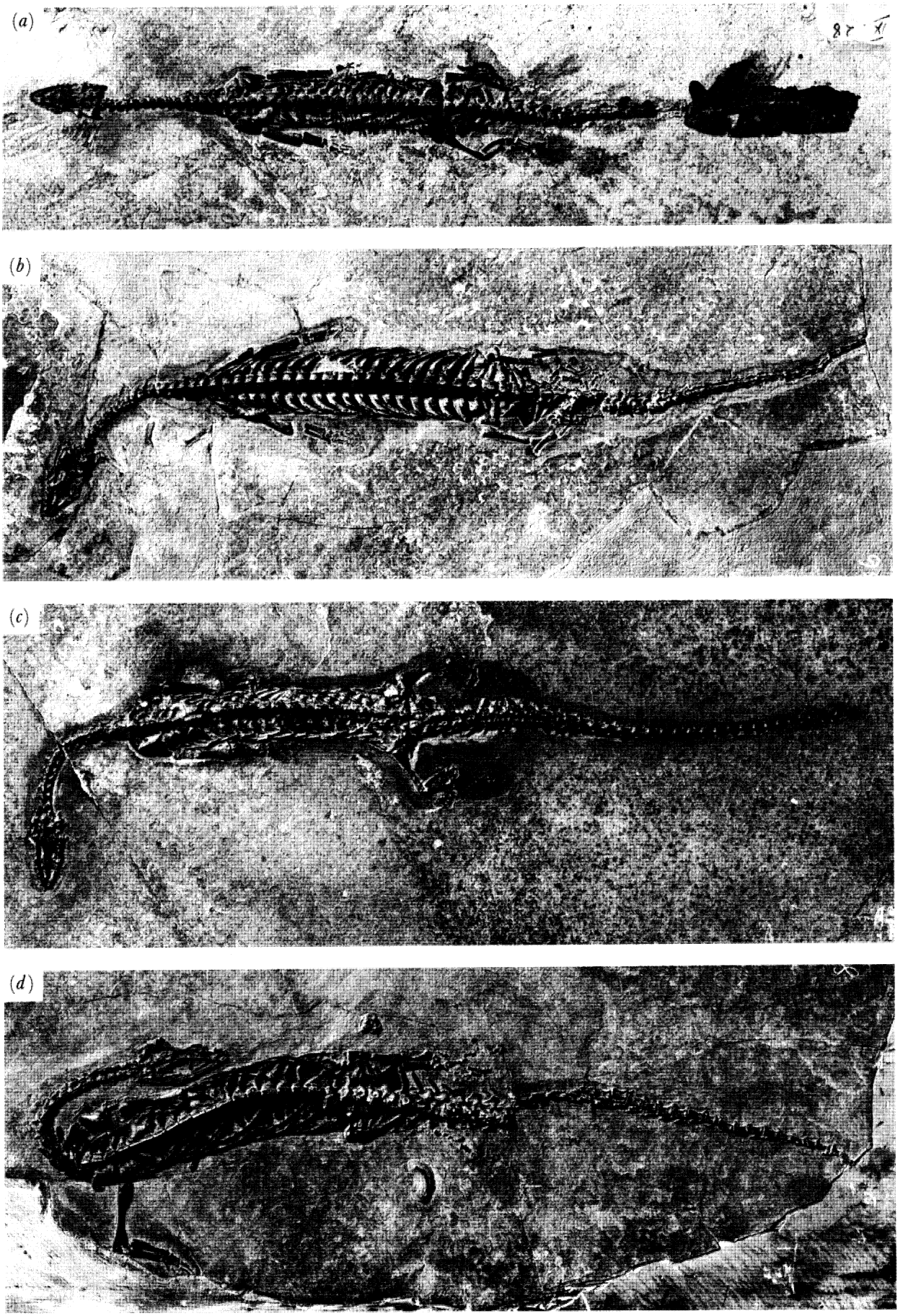

FIGURE 26. For description see page 621.

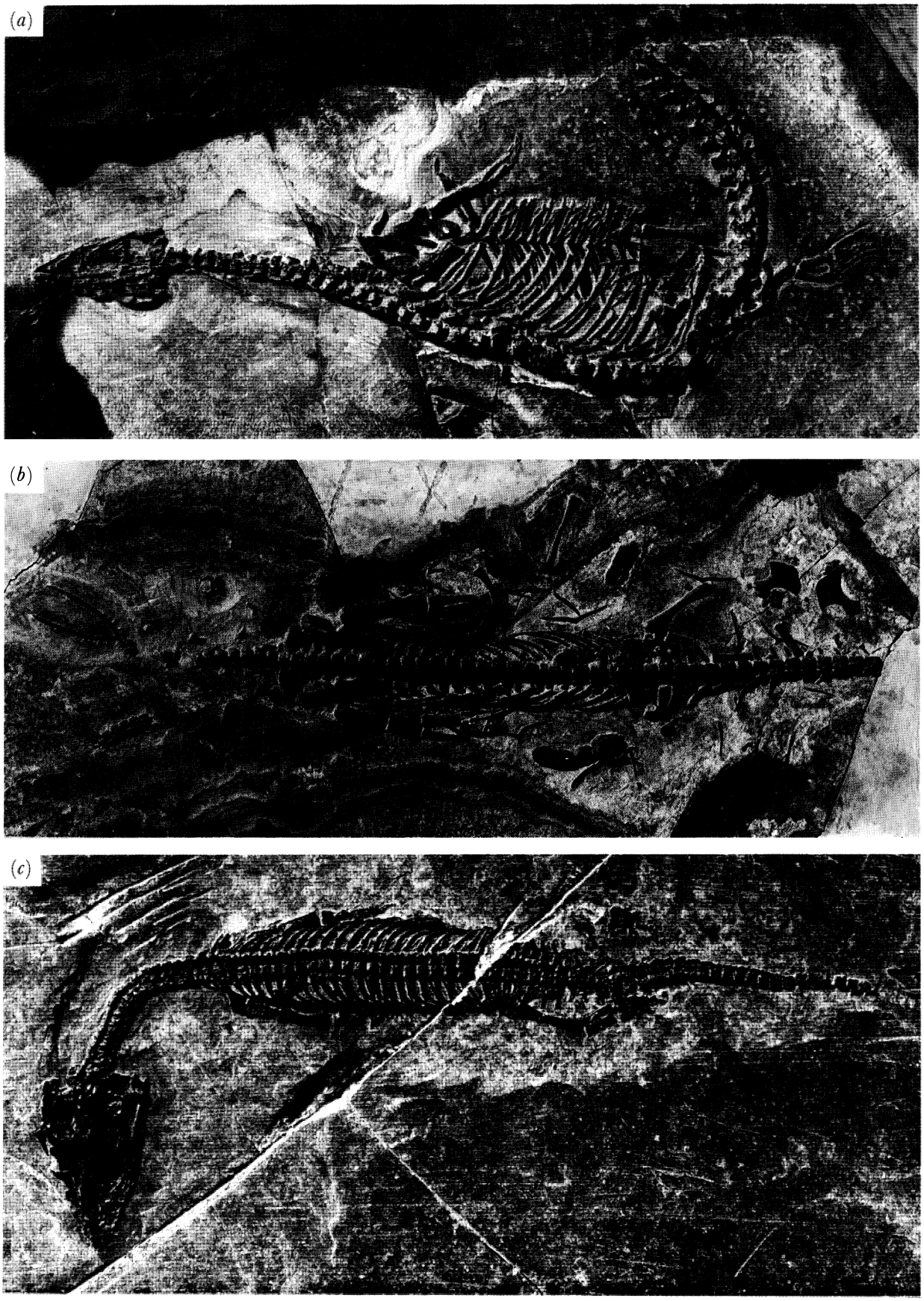

FIGURE 27. For description see opposite.

TABLE 6. CORRELATION BETWEEN STANDARD LENGTH AND NUMBER OF ANNULI

(Annuli were observed in cross sections of humerus shafts; *j*, juvenile.)

specimen	sex	size class	standard length/mm	annuli
Neusticosaurus pusillus				
T 4297	*x*	G	12.2	3
T 3554	*y*	G	12.5	2–3
T 3519	*y*	H	13.8	4
T 3786	*y*	H	14.1	4–5
T 3516	*y*	H	14.2	3–4
T 3782	*x*	H	14.7	4
T 3532	*y*	I	16.5	3–4
T 3566	*y*	I	16.8	3
T 3484	*x*	J	18.6	5
Neusticosaurus peyeri				
T 3704	*j*	C	7.0	0–1
T 3432	*j*	D	9.8	2
T 3768	*x*	F	13.0	5
T 3482	*x*	G	15.4	4
T 3420	?	K	22.2	5+

the maximum of five annuli in T 3484 (class J), one of the largest *N. pusillus* in the PIMUZ collection (figure 4*b*).

The maximum age of *N. peyeri* is more difficult to establish, mainly because none of the few very large specimens could be sectioned but also because of the smaller sample. However, an age of eight or nine years appears likely, which was observed in T 3455, a *Neusticosaurus edwardsii* of about the same size as the largest *N. peyeri*.

Apart from furnishing absolute data on the growth curves for *Neusticosaurus*, annuli can be a powerful palaeoclimatological tool, as pointed out by Peabody (1961) and Voorhies (1969). Sedimentological data (Zorn 1971) and the palaeogeographic position near the palaeoequator suggest a warm, tropical climate with little seasonal variation for Monte San Giorgio during the Middle Triassic. The well-developed annuli of *Neusticosaurus* are remarkable in this light and would seem to argue for a seasonal climate. However, the histology of other taxa would have to be investigated to differentiate between seasonally-induced annuli and endogenously controlled annuli. If many unrelated taxa at Monte San Giorgio were to show annuli, as observed by Peabody (1961) for the early Permian Fort Sill vertebrates, such an observation would be strong evidence for a seasonal climate at Monte San Giorgio during Middle Triassic times.

DESCRIPTION OF PLATES 3 AND 4

FIGURE 26. Vertebral column poses in the small *Neusticosaurus* species illustrated by *Neusticosaurus peyeri*; (*a*) T 3479 (sex *x*), pose A. Note the totally straight vertebral column, (magn. ×0.54); (*b*) T 3524 (sex *x*), pose B. Note the slightly bent neck, (magn. ×0.56); (*c*) T 3431 (sex *y*), pose C. The neck has a right-angle bend while the tail is straight, (magn. ×0.72); (*d*) T 3474 (sex *y*), pose D. The neck is strongly recurved. Note extended right forelimb, (magn. ×0.68).

FIGURE 27. T 3396 (sex *y*) (*a*), the only adult *Neusticosaurus* (*N. peyeri*) preserved in lateral view. Note the well exposed gastralia (see figure 20*d*), (magn. ×0.96); (*b*) a disarticulated *Neusticosaurus pusillus* (T 3573, sex *y*) in ventral view. Some skeletal elements were transported by current action. Note that the dentary symphysis survived the skull disarticulation (see figure 12*b*). Disarticulation proceeded from the distal to the proximal regions of the body, (magn. ×0.92); (*c*) the smallest (class B) *Neusticosaurus pusillus* (T 3409) in dorsal view. The skull is preserved dorsolaterally. For discussion of morphological details see text, (magn. ×2.6).

9. Soft-part preservation

Despite the excellent preservation of whole skeletons in bituminous shales and limestones at Monte San Giorgio, soft parts are rarely preserved. In *Neusticosaurus*, however, four kinds of organic remains were observed. *Serpianosaurus* shows no remains of organic tissue.

The most interesting occurrences are well preserved scales on the ventral side of the head of T 3410 (figure 22*c*). This specimen, a *Neusticosaurus peyeri* of sex *y*, provides rare information about the integument in fossil reptiles. Only in dinosaurs are skin impressions commonly preserved (Lull & Wright 1942; Gilmore 1946; Colbert 1983). The *Neusticosaurus* scales are probably the only fossilized integument in a nothosaur. There appears to be only one other reference to a fossilized sauropterygian (plesiosaur) skin (Rusconi 1948).

The *Neusticosaurus* scales were already noted by Zangerl (1935) and were re-prepared for this study. They are preserved as bluish, translucent apatite (M. Wuttke, personal communication). The long axis of the scale is oriented parallel to the long axis of the animal. The scales are of about equal size, up to 1.4 mm long, and rhombic with rounded corners (figure 22*c*). Towards the neck they lose clarity and grade into an amorphous mass of the bluish apatite covering the first few neck vertebrae. This type of rhombic squamation is similar to that seen in many recent lizards and snakes (Bellairs 1970, p. 284). However, the scales are not imbricated as in some modern forms, contrary to the statement of Zangerl (1935, p. 46). Only a few overlap, due to postmortem deformation.

It is unclear how the unossified, keratinous scales were replaced by apatite. Favourable conditions in this single specimen must have been responsible for their preservation as several other specimens from the same bed and locality (Acqua del Ghiffo, Cava Superiore horizon, *livello 6*) show nothing like it, nor do any others of the hundreds of *Neusticosaurus* specimens from Monte San Giorgio.

Another instance of soft-part preservation is occasionally observed in the tail region. In several specimens (*Neusticosaurus pusillus*: T 3639 and T 3852; *N. peyeri*: T 3411, T 3469, T 3561, and T 3710, *N. edwardsii*: T 3407, T 3428, T 3458, T 3460, and T 3759), a black line of organic matter parallels the ventral side of the tail. Sometimes the haemal arches appear to be embedded in the black mass and appear to have been separated from the tail in conjunction with it. In one specimen (T 3445), this black line even continues beyond the last preserved caudal vertebra (about the 18th) that appears to be truncated unnaturally. The black line probably represents remains of the integument, the ligaments, and the subvertebral arteries. Investigation by using SEM (M. Wuttke, personal communication) of material from these specimens showed that the 'soft parts' are actually fossilized bacterial mats that replaced the original tissue. This type of soft part preservation was first described by Wuttke (1983) from the Eocene vertebrate locality of Messel (West Germany) but has also been reported for early Permian amphibians (Willems & Wuttke 1987) and Jurassic ichthyosaurs (Martill 1987).

A black, sometimes shiny, amorphous matter encrusts the vertebrae in the abdominal region of several specimens (*Neusticosaurus pusillus*: T 3481, T 3510, T 3529, T 3530, T 3551, T 3553 b, T 3559, T 3574, T 3575 b, T 3586, T 3600 a, T 3611, T 3620, T 3623, T 3627, T 3750, T 3785, T 3852, T 3934, and T 3937; *N. peyeri*: T 3511, T 3561, and T 3712; *N. edwardsii*: T 3452 and T 3759). This black matter, which also consists of bacterial mats (M. Wuttke, personal communication), appears to be enclosed in the rib cage. The material is probably the remains of some kind of 'stomach content', possibly actual food matter or remains of the

digestive tract. Two angular quartz grains of 3 mm and 2.5 mm diameter, respectively, are enclosed in the black matter in two specimens of *Neusticosaurus pusillus* (T 3551 and T 3620). A gastral rib is draped over the grain in T 3551 indicating that the grain was most likely present during the life of the animal. These small rocks could have been ingested accidentally or could have been swallowed on purpose. Accidental ingestion appears less likely because the 'stomach stones' were observed in only two out of hundreds of specimens. Stomach stones are commonly observed in plesiosaurs and the eosuchian *Hovasaurus* however, and apparently functioned as buoyancy regulators (Currie 1981; Darby & Ojakangas 1980; Taylor 1981).

Several specimens (*Neusticosaurus peyeri*: T 3408, T 3411, T 3412, T 3431, T 3461, T 3464, T 3511, T 3705, T 3932, and T 4290; *N. pusillus*: T 3409, T 3571, and T 3661) with well-preserved skulls show a black matter inside the orbit, covering the sclerotic plates. This material could well represent remains of the sclera, which was the toughest part of the eyeball. The eye was the largest mass of soft tissue in the skull of the large-eyed *Neusticosaurus* and may have influenced the microenvironment during decay favourably for the preservation of the sclera. The black material is most prominent in juveniles and small adults where it is also visible in palatal view, staining the central part of the pterigoid (T 4303).

10. Taphonomy of *Neusticosaurus pusillus* and *Neusticosaurus peyeri*

Little is known about the depositional environment of the Cava Inferiore horizon and the Cava Superiore horizon (Rieber & Sorbini 1983). Wirz (1945) studied the stratigraphy and not the sedimentology. My field work was also directed at the stratigraphy. A rigorous sedimentological investigation of these beds is necessary but beyond the scope of this study.

The fossiliferous rocks are finely laminated, bituminous micrites devoid of macroinvertebrate fossils, except one very well-preserved regular sea urchin, *Miocidaris hescheleri* (with many articulated spines!) (Jeannet 1933). About 60 couplets of bituminous layers alternating with micritic layers can be found per 1 cm of rock thickness. Wirz (1945) believed the cyclicity to be of diagenetic origin. According to Wirz (1945), the sediments were deposited in deep, quiet water under fully marine conditions. The lamination (indicating complete absence of benthos) and the high organic content of the micrite argue for deposition under anoxic conditions and below the wave base.

The faunas of the Cava Inferiore horizon and Cava Superiore horizon (table 7) are much less diverse than the Grenzbitumenzone fauna (Kuhn-Schnyder 1974). This may be partly due to less collecting, but probably reflects a truly depauperate fauna at Cava Inferiore and Cava Superiore times. Pachypleurosaurids far outnumber any other fossils in these horizons, and in every good bed several skeletons per square meter could be recovered. Accordingly, only small excavations (never more than 30 m^2 in extent) were necessary to produce the great quantity

Table 7. Fauna of the two middle pachypleurosaur horizons

Cava Inferiore horizon	Cava Superiore horizon
—	*Miocidaris hescheleri*
Luganoia	small ganoids
Habroichthys	—
Saurichthys macrocephalus	—
Neusticosaurus pusillus	*Neusticosaurus peyeri*
Ceresiosaurus calcagnii	*Ceresiosaurus calcagnii*

of small *Neusticosaurus* now in the collection of the PIMUZ. Larger animals such as *Ceresiosaurus calcagnii* (Peyer 1931) were less abundantly found (about one *Ceresiosaurus* per 100 *Neusticosaurus*) because they had a much smaller chance of discovery in small quarries. Although small ganoids are found in both horizons, *Saurichthys macrocephalus* was only found in the Cava Inferiore horizon (Rieppel 1985). *Ceresiosaurus* is the most pelagic of all Monte San Giorgio nothosaurs, whereas *Saurichthys* is more reef-oriented (Rieppel 1985).

The most important taphonomic observation about the Monte San Giorgio pachypleurosaurs is the great completeness of the skeletons. All skeletons investigated are virtually complete (but not necessarily articulated), and all exceptions are artefacts of collecting. The tip of the tail, for example, was too inconspicuous to be commonly noticed and was not recovered by the collectors. Most skeletons are articulated as well, but various stages and types of disarticulation can be discerned. One hundred and sixty specimens of adult *Neusticosaurus pusillus* and 71 specimens of adult *Neusticosaurus peyeri* were studied for this taphonomic investigation.

The absence of orientational data for practically all specimens of the small *Neusticosaurus* species hampered taphonomic analysis. The great majority of all fossils was collected before 1942 from small excavations. No record of the orientation was taken or is known, nor is the original top of the specimens known. Because of the lack of orientational data, taphonomic observations were mainly restricted to the specimens themselves, i.e. the carcass position and patterns of disarticulation.

(*a*) *Carcass position*

No differences in preservation are observed between dorsal and ventral sides of the skeletons. The fossils were prepared from the side with less matrix cover. This side was determined by chance when the rock was split open during collecting. Fossils prepared dorsally are about as common in the PIMUZ collection as fossils prepared ventrally. This suggests that there was no preferred depositional orientation, and skeletons with their belly up were about as common in the rock as those with their belly down.

All 231 specimens are preserved in a dorsoventral position with a single exception, T 3396 (figure 27*a*), a *Neusticosaurus peyeri*. Study of carcass position is therefore restricted to observations of the pose of the vertebral column and position of the limbs. The great majority show a 'relaxed' pose with a straight or slightly bent dorsal column, forelimbs closely appressed to the body, and hindlimbs in a half-extended backward pointing pose. This pose is typical for relaxed and floating modern aquatic reptiles with body proportions similar to *Neusticosaurus* such as crocodiles (see Weigelt 1927; Zangerl 1935; Manter 1940), green iguanas (*Iguana iguana*) (see Carroll & Gaskill 1985), marine iguanas (see Bartholomew *et al.* 1976), or for lizards killed with chloroform (see Zangerl 1935). It is also typical of 'Wasserleichen' (see Weigelt 1927; Sander 1987) that are carcasses drifting for some time after death.

Orientation of the vertebral column appears to be largely independent of limb position and is thus discussed separately. Seven types of vertebral column poses could be distinguished. Poses A–D (figure 26) all show a straight or slightly bent tail and dorsal column. They are distinguished from each other by the degree of neck curvature. The skull is always in line with the anterior part of the neck. In pose A (figure 26*a*), the neck is straight, so that the entire vertebral column forms a straight line. Pose B (figure 26*b*) shows some bending of the neck ranging from about 20° to 70° to the long axis of the body. Pose C (figures 26*c*, 27*c*) is very characteristic for *Neusticosaurus*. The anterior half of the neck is oriented at approximately right

angles to the posterior half and the dorsal column. Most of this 90° bend takes place over only a few of the central cervical vertebrae and attests to the great mobility of the neck in contrast to the rigidity of the trunk. The final step in the curving of the neck is pose D (figure 26*d*) in which the neck is clearly bent by more than 90°. In extreme cases, it is recurved to the trunk with the skull touching the trunk. Pose E (figure 27*b*) is found in specimens that are strongly disarticulated. All elements are present but scattered about. Rare specimens with a contorted or disrupted vertebral column are assigned to pose F, whereas pose G are specimens in lateral view (figure 27*a*).

A continuous increase in neck curvature from straight (pose A) to recurved (pose D) is seen in the sample of *Neusticosaurus pusillus* (figure 28). The most common poses are pose B (62 specimens, a good example is T 3672) and pose C (45 specimens, a good example is T 3671), whereas poses A (15 specimens, a good example is T 3481) and D (26 specimens, a good example is T 3639) are much rarer (figure 28). Thirteen specimens are disarticulated to a degree at which it is impossible to determine their original pose (pose E, a good example is T 3573; figure 27*b*), and an additional 13 show some disarticulation.

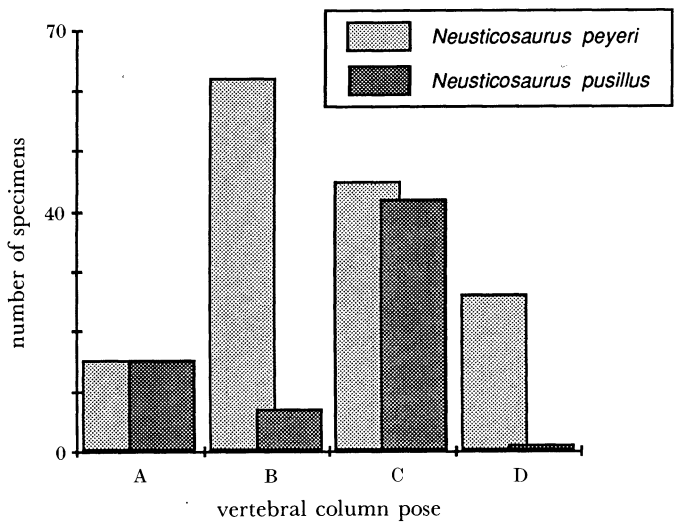

FIGURE 28. Taphonomy of *Neusticosaurus pusillus* and *Neusticosaurus peyeri*. Histogram of vertebral column poses in *Neusticosaurus peyeri* and *Neusticosaurus pusillus*. For illustration of the poses, see figure 26.

In *Neusticosaurus peyeri*, pose C (right angle neck) and pose A (entirely straight column) dominate the sample with 42 and 15 specimens respectively (figure 28). A good example of pose C is T 3431 (figure 26*c*), and a good example of pose A is T 3479 (figure 26*a*). Pose B (seven specimens, a good example is T 3524; figure 26*b*) and pose D (one specimen, T 3474; figure 26*d*) are much less common. It is difficult to explain why the entirely straight column or the neck with a 90° curvature are so prominent in this sample. The right angle curvature was already observed by Deecke (1886) who explained it as an effect of gravity, that 'the head had fallen to one side due to its own weight' (translation from German). This, of course, is not a very satisfactory explanation, especially for subaqueous deposition.

The pelvic and pectoral girdle elements are usually disarticulated from each other but remain in their position relative to each other. The same can be observed in the gastral ribs (figures 7*a* and 20*d*).

A closer look at limb positions (figure 29*a*) indicates the overwhelming abundance of the closely appressed forelimb and 'relaxed' hind limb. A census of 147 *Neusticosaurus pusillus* yielded 88 specimens with both forelimbs closely appressed (figures 7*a* and 24*a*) called pose J (figure 29*a*). Next in abundance is pose K (figure 29*a*) with 40 specimens. In this pose, one forelimb is closely appressed and the other spread away at an angle of less than 45° to the long axis of the body (e.g. T 3781). A correlation exists between pose K and a slightly bent trunk. The spreading forelimb lies on the convex side of the trunk. Only 19 specimens have both forelimbs spread away from the body, but never by more than 45° (e.g. T 3603). This is termed pose L (figure 29*a*).

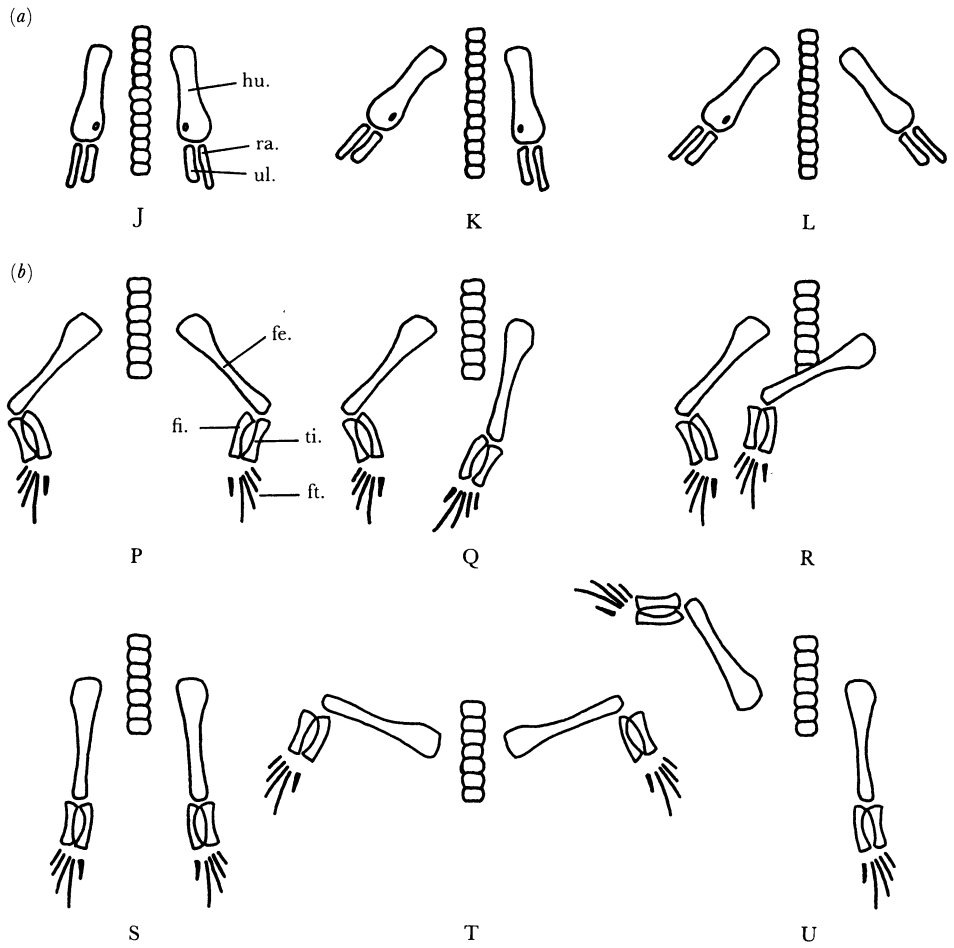

FIGURE 29. Taphonomy of *Neusticosaurus pusillus* and *Neusticosaurus peyeri*; (*a*) the three forelimb poses in dorsoventrally preserved specimens; (*b*) the six hindlimb poses in dorsoventrally preserved specimens.

The census of 64 *Neusticosaurus peyeri* yielded much the same picture: 46 specimens in pose J (figures 7*b*, 24*b*, and 26*c*), nine in pose K (figure 26*a*), eight in pose L (figures 21*c* and 26*b*), and one specimen (figure 26*d*) with one forelimb at a right angle to the body and the other closely appressed. This pose could be a function of the extreme neck curvature (pose F) of the specimen; the most extreme example of this pose in this sample.

The hands in both small *Neusticosaurus* species are rarely complete (figure 7*b*). This is partially because of their close appression to the body. The hand bones were disrupted and

broken during compaction. Additionally, these very delicate bones were very vulnerable to decay and disarticulation. In many cases, all of the fingers are closely appressed to each other; this also leads to increased disruption and breakage during compaction (figure 21*c*).

The position of the hindlimbs (figure 29*b*) is not as similar in the two small *Neusticosaurus* species. Of the 129 *Neusticosaurus pusillus* with sufficiently preserved hind limbs, 44 showed the 'relaxed crocodile' position termed pose P. It is a symmetrical pose with both femora oriented posteriorly at an angle of about 45°, a roughly right-angle bend in the knee joint (so that tibia and fibula point inward at about 45°), and another bend in the ankle joint (so that the foot points outward and backward (figure 29*b*)). Two increasingly asymmetrical varieties (poses Q and R) are assumed by 24 and 30 specimens, respectively. In pose Q (figure 29*b*), one leg is moved toward the spine, with the foot or tibia and fibula resting ventrally on the anterior tail region (e.g. T 3553 b). In pose R (figure 29*b*), the femur is rotated under the vertebral column whereas the lower limb is similar to pose Q (e.g. T 3934, figures 7*a* and 24*a*). The fourth common pose (pose S, figure 29*b*) in *N. pusillus* is with both hindlimbs extended and pointing backwards. Twenty-seven specimens show it (e.g. T 3936). The first of two rare poses is pose T (figure 29*b*). The femora point symmetrically forward at an angle of about 70°, and the lower limb points backward and outward (two specimens, T 3348, T 3597). Pose U (figure 29*b*) is characterized by one hindlimb pointing forward and the other pointing backward (one specimen, T 3604).

In *Neusticosaurus peyeri*, there are 20 specimens in pose P (figures 7*b* and 24*b*), 16 in pose Q (e.g. T 3393), and only three in pose R (e.g. T 3592); seven specimens in pose S (figure 26*b*, *d*), two with pose T (e.g. T 3449), and one (T 3497) in pose U. An additional pose is exhibited by T 3467 where both femora extend at right angles away from the body; the lower limbs are pointing backwards and both feet point in one direction. The feet of both *Neusticosaurus* are usually well-articulated (figures 16*c* and 23*b*, *c*) and only the distal parts are affected by disruptions. It is unclear, if the feet were webbed, as suggested by Zangerl (1935). However, this is likely considering all the other aquatic adaptations of *Neusticosaurus* (Carroll & Gaskill 1985).

The completeness and pose of the tail were studied in 108 specimens of *Neusticosaurus pusillus*. Only 39 tails (36%) were complete or had only minor disruptions such as a dislocated vertebra or two. Twenty-nine of the tails were straight (e.g. T 3582), and ten were bent (e.g. T 3641). The great majority (72 specimens) showed some disruption or partial disarticulation. Most commonly, the tail is broken up into several straight segments (figures 7*a* and 24*a*). Sometimes a short segment is strangely contorted into a knot-like structure (e.g. T 3660). Rarely is the tail bent back on itself (e.g. T 3535 b). A special type of break can sometimes be observed in the region where the height of the neural spines decreases abruptly. The anterior part of the tail lies on one side whereas the posterior part lies on the other (e.g. T 3639). Six specimens have lost considerable parts of the tail (e.g. T 3387).

The tails of *Neusticosaurus peyeri* show a much higher degree of completeness; out of 43, 28 (65%) are complete, and out of those, 23 are straight (figure 26*a*, *c*). Eleven show some disruptions and four are incomplete, i.e. some vertebrae are missing (e.g. T 3712). Two specimens have tails that bend back on themselves (e.g. T 3716), and four have a break where the neural spines decrease in height (figure 26*d*). 'Knotting' was observed in two specimens (T 3431, T 3412). The various stages of disarticulation can all be combined into a decay series: complete tails, tails with one break, tails with several breaks, the loss of several elements and, finally, complete disarticulation into discrete vertebrae and haemal arches.

The percentage of disarticulated skeletons (figure 27*b*) is about the same in both species, 16% in *N. pusillus* and 18% in *N. peyeri*. Thus in comparison, the higher percentage (74% in *N. pusillus* versus 35% in *N. peyeri*) of disrupted or disarticulated tails in *N. pusillus* is remarkable. Possible explanations include the larger number of tail vertebrae in *N. pusillus*, or an intrinsically weaker tail in this species.

No differences in carcass position could be observed between adults and juveniles (figure 34*b*, *c*) except for the more common ventrolateral position of the skull in small juveniles (figure 27*c*). They apparently had a higher and narrower skull that could achieve a stable lateral position more readily than adult skulls. The embryo of *N. peyeri* (Sander 1988) is exceptional because it lies entirely on its side.

(*b*) *Interpretation of carcass position*

One mechanism to explain the observed carcass positions is weak bottom currents. Current influence can be documented in the strongly disarticulated skeletons (figure 27*b*). After the carcass sank to the bottom, it was oriented normal to weak oscillatory currents as is the standard behaviour of unanchored elongate objects (Ziegler 1980). The trunk soon became anchored, and the rolling of the carcass ceased. The neck was able to swing freely above the bottom, possibly because of its greater buoyancy, which may be attributable to the large eyeballs. The head would have then been reoriented parallel to current direction by the transverse oscillatory currents. The tail appears to have been less affected because it was better anchored and offered less resistance to currents, but in most cases it also drifted in the direction of the head. The vertebral column was arched slightly and one forelimb spread away from the body by the pull of head and tail. This type of palaeocurrent system was postulated by Weigelt (1927, p. 150) for the type specimen of *Lariosaurus curioni* that has a *Bauplan* very similar to *Neusticosaurus* and was deposited in similar sediments.

Other effects of transverse currents can be seen in many specimens, especially in those of *N. pusillus*. These current indicators commonly agree with the head position. The clearest examples are disruption and drifting of tail and skull parts and the asymmetrical relaxed pose (poses Q and R) of the hindlimbs. Orientation of several specimens on a slab also supports the hypothesis of oscillatory currents. Even though the individuals did not all die at the same time, they still show roughly the same orientation. Especially good examples are the slabs with two specimens (T 3553, T 3600, T 3636, T 3658, T 3650), but also T 3548 (three specimens) and T 3742 (five specimens, four of which are subparallel). A dominant current system may have been stable over some time. All this must remain speculation, however, in the absence of absolute directional data.

(*c*) *Taphonomic scenario*

Paramount to understanding the taphonomy of the small *Neusticosaurus* species from Monte San Giorgio is the question of autochthony of the fossils. It appears likely from their sheer number and great completeness that the animals actually lived in the coastal surface waters and were not washed in from any other environment. This raises the question of the causes of death. Mass accumulations tend to suggest a catastrophic death event. However, close examination of slabs with several specimens (T 3548a–c, T 3649a–c, T 3741a–e, T 3802a–d, T 3938 a–h and one *Ceresiosaurus calcagnii*) shows that the individuals lie on different laminae and were therefore not embedded at exactly the same time. It is more likely that, as in the

Grenzbitumenzone Beds (Rieber 1973*a*, 1975; Rieber & Sorbini 1983), the fossil accumulation is the result of low sedimentation rates and attritional mortality (continuous death for various reasons in a population) with additional concentration by compaction. The wide size range from embryo or juvenile to old specimens of both species (figures 4*b*, *c*) is additional evidence for attritional mortality (Voorhies 1969).

The much higher number of juveniles in the sample of *Neusticosaurus peyeri* than in that of *N. pusillus* is remarkable. Possible explanations are differences in ecological preference between the juveniles of both species, or closer proximity of the juvenile habitat to the area of deposition during Cava Superiore time.

The immediate reasons of death must remain unclear. It may have been disease or old age, and death most likely occurred in the habitat, which was the surface waters. After death, the carcass soon sank to the bottom of the sea as do most vertebrate carcasses (Weigelt 1927; Wuttke 1983). Sinking of *Neusticosaurus* after death is supported by the fact that jaw or limb element loss, typical for prolonged drifting of carcasses (Schäfer 1972), was not observed in any specimen. After the initial sinking to the bottom, a carcass has the tendency to become buoyant again because of the development of decay gases in the body cavity (Weigelt 1927; Wasmund 1935; Wuttke 1983). Rising to the surface can be inhibited if water pressure exceeds gas pressure in the abdominal cavity (Wuttke 1983) or if the carcass becomes anchored. In the case of Monte San Giorgio, sufficient water depth kept the *Neusticosaurus* carcasses 'grounded' on the sea floor. This is indicated by the observation that the abdominal cavity is intact in all specimens in contrast to the situation commonly observed in the Liassic Holzmaden ichthyosaurs (Hoffmann 1958). In most vertebrate corpses, bacterial degradation of the body cavity contents produces enough gas pressure to rupture the body wall (Weigelt 1927; Schäfer 1972). In the case of *Neusticosaurus*, water pressure was high enough to exceed the pressure of the decay gases in the abdominal cavity, preventing rupture of the body wall. *Ceresiosaurus* specimens from both horizons have intact rib cages as well, in contrast to many animals of similar size (e.g. *Mixosaurus*) from the Grenzbitumenzone Beds, suggesting a greater water depth at Cava Inferiore and Cava Superiore times. The sturdy nothosaur rib cage may also have helped to prevent the body wall rupturing.

After settling on the seafloor, microbial decay continued and eventually led to disruption of the carcass. As Wuttke's (1983) experimental work on anurans has shown, complete disarticulation of the skeleton is the end result of uninterrupted microbial decay. A certain degree of scattering of the bones is solely due to decay processes without any current-induced dispersal. This observation can be safely extrapolated to *Neusticosaurus* that probably had a body mass similar to a large frog. The pattern of bone scattering (figure 27*b*) in most disarticulated skeletons of *Neusticosaurus* is suggestive of some current influence, however. The light skull elements especially, indicate some current transport (T 3523, T 3542, T 3577). Contrary to Wuttke's (1983) observations on *Rana*, disarticulation in *Neusticosaurus* proceeded from the distal to the proximal parts of the body (figure 27*c*).

At Monte San Giorgio, microbial decay appears to have been incomplete in most specimens and ended before any significant disarticulation occurred. The reason for this is not clear; bottom-water chemistry possibly became toxic, even to bacteria. Continuing sedimentation incorporated the skeletons into the fossil record. The sediment and the fossils were greatly compacted during diagenesis, which led to collapse and crushing of the skull and lateral orientation of the posterior trunk column in *Neusticosaurus peyeri* individuals.

11. Morphometric comparison

The major skeletal elements of the Monte San Giorgio pachypleurosaurs were compared quantitatively to differentiate morphometrically and not only morphologically between the four species. Length of the skull, tail, humerus and femur relative to trunk length, length of the neck relative to snout–vent length, and absolute trunk and standard length were compared (table 9). Probably the most interesting comparison is that between trunk length, standard length and the number of presacral vertebrae (table 8).

Cursory examination of the two small *Neusticosaurus* suggested that both show roughly the same proportions within the axial skeleton and relative to the limb elements. Because of the large interspecific variability of the number of presacrals within the Monte San Giorgio pachypleurosaurs, and the great differences in the number of presacrals between *N. pusillus* (42 presacrals) and *N. peyeri* (36 presacrals), it was very interesting to see if the change in vertebral numbers was caused by elongation or shortening of the vertebral column or if only the number of segments, i.e. the number of vertebrae, had changed.

To decide between these two alternatives, in each species the standard length correction factor F (the mean of all trunk:standard length values) was divided by the number of presacral vertebrae. If the resulting quotients, S (table 8), were the same for taxa differing in vertebral numbers, this would strongly suggest a change of the number of trunk segments without a change in relative trunk length.

Table 8. Comparison of trunk length of Monte San Giorgio pachypleurosaurs

	F	number of presacrals	S[a]
Serpianosaurus mirigiolensis	4.426	36	0.123
		37	0.120
		38	0.116
Neusticosaurus pusillus	4.624	41	0.113
		42	0.110
		43	0.107
Neusticosaurus peyeri	3.931	35	0.112
		36	0.109
Neusticosaurus edwardsii	4.255	36	0.118
		37	0.115

[a] $S = F/\text{number of presacrals}$.

The values of S fall within the same range for both small species of *Neusticosaurus* (table 8), which supports the hypothesis of differing number of segments at constant relative trunk length. In *Neusticosaurus edwardsii* the value of S (table 8) is higher than in *N. peyeri* for the same number of vertebrae, indicating that trunk length has increased relative to standard length by elongation of the individual vertebrae and not by an increase in their number. S-values for *Serpianosaurus* are even higher than those for *Neusticosaurus edwardsii*. Thus the vertebrae of *Serpianosaurus* are the relatively longest of all four species.

Relative skull size (table 9) shows the greatest variation of all proportions. *Serpianosaurus* has the largest skull, a fact that is immediately obvious by looking at the specimens. The skulls of the small *Neusticosaurus* are somewhat smaller than that of *Serpianosaurus*. They are of exactly the same absolute and relative size in the two species. The smallest skull by far is encountered in the adult *N. edwardsii*, as already noted by Carroll & Gaskill (1985). This is most likely the result of strong negative allometric growth of the skull of this animal (see §13).

TABLE 9. SEXUAL DIMORPHISM AND PROPORTIONS IN THE MONTE SAN GIORGIO PACHYPLEUROSAURIDS

(For the ratio, the mean and the range (in parentheses) are given.)

	sex	mean trunk length/mm	mean standard length/mm	skull : trunk	snout–vent : neck	tail : trunk	humerus distal width : minimal diameter	humerus : trunk
Serpianosaurus mirigiolensis	*x*	86.0	18.3	0.52 (0.43–0.56)[a]	3.6 (3.2–4.2)[a]	2.5 (2.2–2.7)[a]	1.6 (1.5–1.7)	0.24 (0.21–0.29)
	y	107.0	25.2	—	—	—	2.2 (1.8–2.8)	0.30 (0.23–0.36)
Neusticosaurus pusillus	*x*	66.8	14.5	0.42 (0.34–0.53)[a]	3.5 (3.3–3.7)	2.2 (1.8–2.6)	1.5 (1.2–1.9)	0.23 (0.20–0.26)
	y	65.6	14.1	—	3.5 (3.2–3.9)	2.3 (1.9–2.5)	2.0 (1.5–2.4)	0.28 (0.24–0.33)
Neusticosaurus peyeri	*x*	70.1	18.3	0.42 (0.32–0.56)[a]	3.4 (3.0–3.8)	2.2 (1.9–2.5)	1.6 (1.2–1.9)	0.22 (0.20–0.26)
	y	68.1	17.2	—	3.4 (2.9–3.8)	2.3 (2.0–2.6)	2.4 (1.9–3.0)	0.29 (0.28–0.33)
Neusticosaurus edwardsii	*x*	245.0	56.3	0.25 (0.23–0.27)[a]	3.4 (3.0–3.7)[a]	2.2 (2.1–2.3)[a]	2.0 (1.7–2.3)	0.28 (0.24–0.29)
	y	222.0	54.8	—	—	—	3.2 (3.1–3.5)	0.31 (0.27–0.35)

	sex	humerus : standard	humerus : femur	humerus : radius	humerus : third metacarpal	radius : standard	femur : trunk	femur : standard
Serpianosaurus mirigiolensis	*x*	1.09 (1.00–1.13)	0.95 (0.75–1.04)	1.65 (1.56–1.80)	4.1 (3.8–4.6)	0.65 (0.63–0.68)	0.25 (0.23–0.27)	1.14 (10.9–1.17)
	y	1.21 (1.14–1.48)	1.10 (0.98–1.24)	1.83 (1.60–2.12)	4.5 (3.8–5.0)	0.66 (0.60–0.67)	0.27 (0.21–0.32)	1.13 (0.98–1.32)
Neusticosaurus pusillus	*x*	1.08 (0.95–1.20)	0.94 (0.88–1.00)	1.83 (1.70–1.95)	4.2 (3.2–4.6)	0.59 (0.50–0.65)	0.24 (0.22–0.26)	1.15 (0.97–1.24)
	y	1.28 (1.20–1.50)	1.05 (1.00–1.15)	1.84 (1.75–1.95)	4.6 (4.4–5.1)	0.70 (0.65–0.75)	0.27 (0.24–0.30)	1.23 (1.11–1.40)
Neusticosaurus peyeri	*x*	0.86 (0.75–1.00)	0.96 (0.90–1.10)	1.76 (1.60–1.90)	4.1 (3.7–4.7)	0.49 (0.44–0.53)	0.23 (0.21–0.25)	0.90 (0.79–0.98)
	y	1.10 (1.05–1.25)	1.16 (1.10–1.30)	1.79 (1.70–1.90)	5.0 (4.7–5.0)	0.61 (0.49–0.71)	0.24 (0.21–0.25)	0.94 (0.78–1.06)
Neusticosaurus edwardsii	*x*	1.23 (1.18–1.28)	1.54 (1.24–1.69)	1.84 (1.70–1.96)	4.8 (4.1–5.3)	0.66 (0.62–0.69)	0.19 (0.17–0.21)	0.78 (0.71–0.96)
	y	1.32 (1.20–1.39)	1.71 (1.49–1.84)	1.94 (1.81–2.12)	4.9 (4.3–5.5)	0.67 (0.63–0.69)	0.18 (0.16–0.21)	0.74 (0.65–0.83)

[a] Ratios of both sexes combined.

Variation in relative humerus length (table 9) can be attributed mainly to sexual dimorphism and is discussed in detail below. Only in *Neusticosaurus edwardsii* is humerus length not sexually dimorphic. The relative humerus length is about the same in sex *y* of the other three species and sex *x* of the other three species. Relative femur length (table 9) is especially noteworthy in *Neusticosaurus edwardsii* (Carroll & Gaskill 1985), which has a much shorter femur than all other pachypleurosaurs that show little variation in this characteristic. Some sexual dimorphism is observed in the other three species. The great size difference of humerus and femur so characteristic of *N. edwardsii* can clearly be attributed to a strong phylogenetic decrease in femur size.

Enough complete necks were available for all four species to investigate relative neck length (table 9). The length of the neck relative to snout–vent length is about the same in all three *Neusticosaurus* species, although their cervical counts differ considerably, as does the relative skull size between the two small *Neusticosaurus* species and *N. edwardsii*. No sexual dimorphism is apparent in neck length. The neck of *Serpianosaurus* appears to be slightly shorter than in *Neusticosaurus pusillus* and clearly shorter than in *N. peyeri* and *N. edwardsii*. This short neck is correlated with the large skull.

A look at the relative length of the tail (table 9) reveals that it is about the same in all species of *Neusticosaurus* although the number of caudal vertebrae varies considerably, from 42 to 58. The similarity of relative neck and tail lengths in all species supports the hypothesis that it is largely the number of vertebrae (i.e. segments) and not the segment size that changed through phylogeny. For *N. edwardsii* only three tails could be measured, and only six were available for *Serpionosaurus*. This sample was large enough to demonstrate that the tail in *Serpionosaurus* is clearly longer than in any of the *Neusticosaurus*.

12. Sexual dimorphism

Sexual dimorphism is common in modern reptiles, and there is no conceivable reason why this should not apply to extinct forms as well. In fossils, however, we are restricted to osteological characters whereas in modern reptiles the sexually dimorphic characters are not commonly expressed in the skeleton, only in the soft parts. This may reflect our incomplete knowledge of skeletal sexual dimorphism in modern forms. This lack of modern analogues and the often small samples of fossil reptiles commonly preclude recognition of sexual dimorphism in the fossil record. It is very difficult to distinguish between the two species and two sexes of one species if only a few specimens are available. On the other hand, the possibility of sexual dimorphism has not been seriously considered in many cases. Sex differences have been suspected in some taxa (in pelycosaurs, Romer & Price (1940); in many dinosaurs, Dodson (1987)), but only in few cases could they actually be documented (*Protoceratops*, Dodson (1976); *Chasmosaurus*, Lehman (1989); and *Pteranodon*, Bennet (1987)). Two criteria suggest sexual dimorphism in a fossil reptile: (i) a large sample (more than ten specimens) from one stratigraphic horizon contains two morphs that differ in some characters but are very close in others; (ii) these morphs are present in roughly equal numbers.

The Monte San Giorgio pachypleurosaurs are all known from large samples (more than 30 specimens) and in all of these a sexual dimorphism involving the forelimb can be documented. The existence of sexual dimorphism had been suspected by Arthaber (1924) and Kuhn-Schnyder (1959) who failed to document it. In addition to describing morphological

and morphometric sex differences of the four species, I discuss size differences between the sexes, sex ratios, and the problem of differentiating between male and female.

(*a*) *Morphology and morphometry*

Morphology of the two sexes of the small *Neusticosaurus* was already described in the descriptive sections. All relevant morphometric data for the four species can be found in table 9. Only data from adult specimens were used. Some measurements and ratios for *Serpianosaurus*, i.e. of the forelimb bones, the femur, and body length were taken from Rieppel (1989*a*). For *Neusticosaurus edwardsii* these values were taken from Carroll & Gaskill (1985).

Enough adults were available for morphometric comparison from the two small species of *Neusticosaurus* as well as from *Serpianosaurus*. The sample of *Serpianosaurus* is relatively homogeneous in size (figure 4*a*), except for one juvenile specimen (T 132). *N. edwardsii*, on the other hand, shows a great size range (figure 4*d*), and only the largest 11 specimens (standard length <40 mm) show clear morphological sex differences.

The one major dimorphism common to all four species is the morphological differentiation of the humerus. This bone has a rounded proximal end and a dorsoventrally flattened distal end. This is, however, all that the humeri of the two sexes have in common. It is interesting to note that a much greater difference exists between the humeri of different sexes of the same small species of *Neusticosaurus* than between humeri of the same sex of different species.

One sex, designated sex *x*, shows poor differentiation, i.e. little constriction of the shaft, a relatively narrow distal end with a poorly developed ectepicondylar ridge and no supinator ridge, no development of an anterior proximal trochanter, and restriction of the articular surfaces to the ends of the bone (figures 15*a*, *d* and 21*b*, *c*; Carroll & Gaskill 1985, fig. 3b). Humerus morphology of sex *x* is close to the juvenile condition (figure 35*d*).

The other sex, termed sex *y*, shows a well-differentiated humerus with a narrow shaft, a slightly expanded proximal end, and a greatly expanded distal end (figures 7*a*, 15*c*, 21*d* and 35*e*; Carroll & Gaskill 1985, fig. 3a). The distal end is subdivided by a well-developed ectepicondylar ridge and a supinator ridge and commonly has a posterodistal process. An anterior proximal trochanter is prominent, and is accompanied by an elongated groove in some species. Lobes of the proximal and distal articular surfaces extend onto the dorsal and ventral sides of the bone, and the distal articular surface is subdivided into a large anterior and a small posterior portion. The ectepicondylar foramen is located considerably more proximally than in sex *x*.

These qualitative observations can be quantified (tables 4 and 9). The ratio that best differentiates between the sexes is distal width : minimal diameter of the humerus shaft. All four pachypleurosaurs show a clear separation of the two sexual morphs in this ratio (figure 30). Only *Neusticosaurus pusillus* shows some overlap in ranges of the sexes. In *Neusticosaurus peyeri*, the ratio length : distal width also clearly quantifies the morphological dimorphism in the humerus (table 4).

Additional quantitative observations can also separate the sexes in particular taxa. In both small species of *Neusticosaurus*, the humerus is dimorphic in length relative to the femur; the humerus of sex *y* is up to 30% longer than of sex *x* (figure 31*b*, *c*). The same dimorphism is present but less well developed in *Serpianosaurus* and *N. edwardsii* (figure 31*a*, *d*). All four species exhibit dimorphism in the humerus length relative to body length (table 9), expressed as the humerus : trunk ratio (to facilitate direct comparison between species) and as the

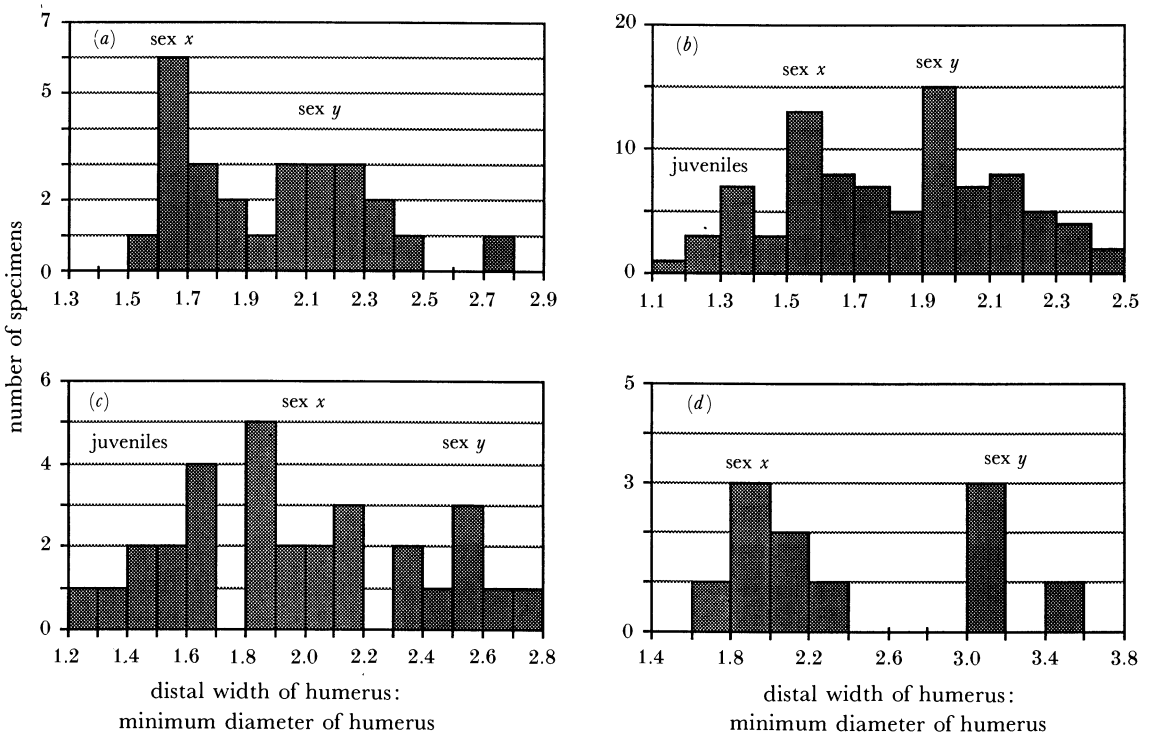

FIGURE 30. Histograms of the sexually dimorphic ratio distal width of humerus:minimal diameter of humerus in all four Monte San Giorgio pachypleurosaurids. Low values are characteristic of sex *x* and juveniles, high values indicate sex *y*; (*a*) *Serpianosaurus mirigiolensis*. Note bimodal distribution, only one juvenile is included in this sample; (*b*) *Neusticosaurus pusillus*. Note bimodal distribution; a few juveniles are included in this sample; (*c*) *Neusticosaurus peyeri*. Note trimodal distribution due to the many juveniles in this sample (see figure 6c); (*d*) *Neusticosaurus edwardsii*. Note bimodal distribution; only adult specimens were used.

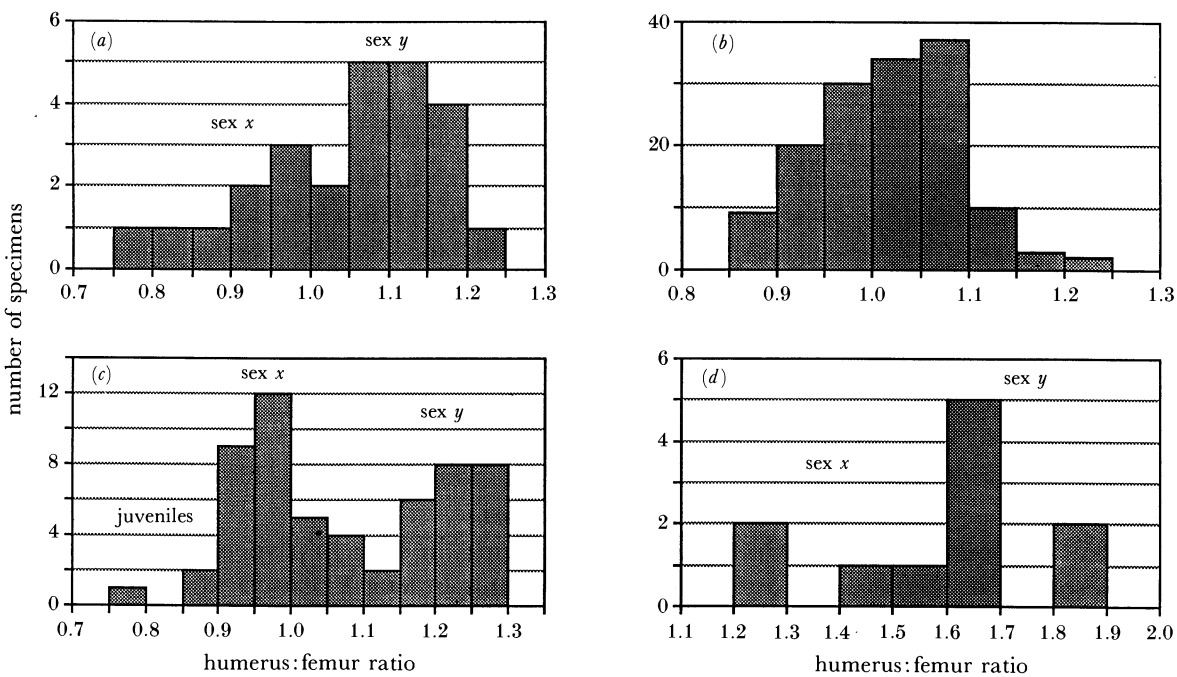

FIGURE 31. Histograms of the sexually dimorphic ratio humerus:femur in all four Monte San Giorgio pachypleurosaurids. (*a*) *Serpianosaurus mirigiolensis*, note bimodal distribution; (*b*) *Neusticosaurus pusillus*, a unimodal distribution, but see table 9; (*c*) *Neusticosaurus peyeri*, note bimodal distribution; (*d*) *Neusticosaurus edwardsii*.

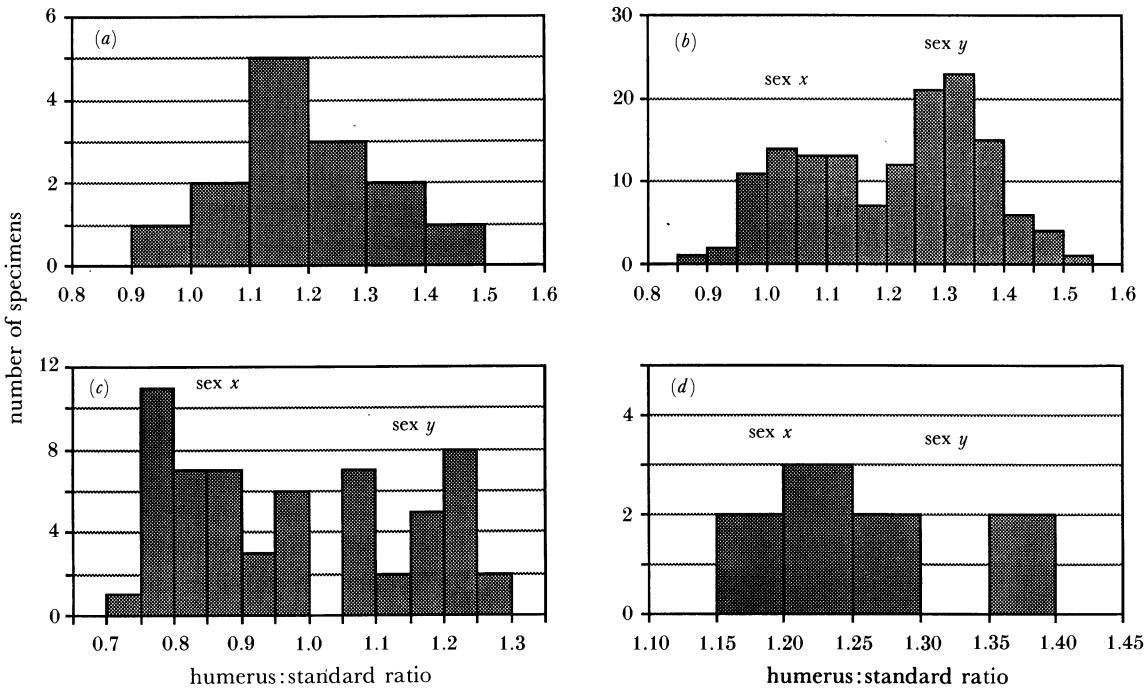

FIGURE 32. Histograms of the sexually dimorphic ratio humerus:standard in all four Monte San Giorgio pachypleurosaurids. Low values are characteristic of sex *x* and juveniles, high values indicate sex *y*; (*a*) *Serpianosaurus mirigiolensis*; (*b*) *Neusticosaurus pusillus*. Note bimodal distribution; (*c*) *Neusticosaurus peyeri*. Note bimodal distribution; (*d*) *Neusticosaurus edwardsii*.

humerus:standard length ratio (which is of greater accuracy, table 9; figure 32). Only in *Neusticosaurus peyeri* is the dimorphism of the humerus:trunk ratio well developed enough to be used for sexing, whereas the humerus:standard ratio allows sexing in both small species of *Neusticosaurus* (figure 32*b*,*c*) and *Serpianosaurus* (Rieppel 1989*a*).

A variation of the humerus:body length dimorphism can be observed in *Neusticosaurus pusillus*. Its femur shows a length dimorphism as well, unique among Monte San Giorgio pachypleurosaurs. It is sufficiently developed to allow clear sex differentiation (table 5). In this species, the two sexes differ in relative length of the limbs to the body, not only in humerus size and morphology.

Both small species of *Neusticosaurus* show no sex-related differences in the relative length of ulna and radius, to each other and to the humerus. However, relative to standard length, ulna and radius show a dimorphism. This is in accordance with the humerus length dimorphism. Interestingly, the hands of both small species of *Neusticosaurus* show no length dimorphism relative to body length, but well developed dimorphism relative to humerus length (table 4). Hand length, represented by the length of the third and longest metacarpal, is not sexually dimorphic. This phenomenon is less pronounced in *Serpianosaurus* (table 9) and could not be documented in *N. edwardsii* (table 9), possibly because of too small a sample size in both species.

Ulna and radius of *Serpianosaurus* show no detectable length dimorphism relative to standard length, but relative to humerus length (sex $x = 1.56$–1.8, sex $y = 1.6$–2.12; table 9). *Neusticosaurus edwardsii* exhibits only a weak humerus:radius dimorphism (sex $x = 1.7$–1.96, sex $y = 1.81$–2.02; table 9). The lack of radius:standard length dimorphism may be correlated with generally weaker dimorphism of humerus length in these two species.

Relative neck and tail length (table 9) of the small *Neusticosaurus* show no sexual dimorphism (even though it was suggested by Arthaber (1924) based on the very incomplete tails of Seeley's (1882) material) with the possible exception of relative tail length in *N. peyeri*. Size differences in the tail would have been valuable for sex identification (see below). The samples of sexed adult *Serpianosaurus* and *N. edwardsii* are too small to allow valid conclusions but strong dimorphism is clearly absent.

(*b*) *Size differences*

Most modern reptiles show sexual size differences. As documented in a detailed survey by Fitch (1981), females being larger than males is about as common in the group as a whole as is males being larger than females. The size differences are expressed by Fitch (1981) as female:male ratio (FMR), which is the snout-vent length (carapax length in turtles) of the female divided by that of the male, expressed as a percentage. Accordingly, if the FMR of a species is 100, females and males are, on the average, of equal size. If it is below 100, the male is larger and vice versa. Many factors (geographical variation, ecology, ontogenetic change) appear to be responsible for sexual size differences of both polarities. No clear hypothesis to predict FMRs has yet emerged, and the data set for modern reptiles is still very poor (Fitch 1981). In turtles, the females are commonly larger than the males whereas in crocodiles, the males are often considerably larger than the females. No clear trend can be seen in the squamates but sexual size differences appear to be less evident in this group anyway. In *Sphenodon* the male is larger (Moffat 1985).

For fossil examples, it has been recently suggested that in the small theropod dinosaur *Syntarsus* the females were larger than the males (Raath, in Dodson (1987)), as in modern birds of prey. Other fossil archosaurs show the entire range of FMRs. Dodson (1976) reported that, in the primitive ceratopsian dinosaur *Protoceratops*, the males are about the same size as the females, whereas Bennet (1987) found the males of the pterosaur *Pteranodon* to be larger than the females.

In fossil *Neusticosaurus*, trunk length (instead of snout–vent length) was used to calculate FMRs as the sample of specimens with measurable snout–vent lengths would have been too small. As mentioned previously, sexual dimorphism in the neck or skull length is not a factor, thus trunk length could be safely substituted for snout–vent length. In pachypleurosaurs it would be more appropriate to speak of the x:y ratio (XYR) or y:x ratio (YXR) because their sex cannot be ascertained and good evidence supporting either of the possibilities is lacking.

All three *Neusticosaurus* species show no great size differences between the sexes (table 10) when expressed by the FMR of mean trunk length (FMR_{mean}). The mean of the trunk length (table 10) in sex x of all three species is slightly higher than that in sex y. In both small *Neusticosaurus* species, where the data are best, and comparable to the best data for modern reptiles (Fitch 1981, p. 4), this is probably because the largest few specimens of each sample are all of sex x. This phenomenon is especially pronounced in *N. peyeri* and results in a very uneven FMR only when the largest specimens of each sex are compared (FMR_{max}). In the other two *Neusticosaurus*, the $FMR^{\bullet}_{max}$ is very similar to FMR_{mean}.

The FMR of *Serpianosaurus* differs greatly from that of *Neusticosaurus* however. First, the sexual size differences are much greater (table 10) and second, sex y is much larger than sex x in mean trunk length and has an even longer maximum length of each sex. This is exactly the opposite situation to that in all three *Neusticosaurus* species. Possible explanations are that *Serpianosaurus* is not sexually dimorphic but that we are instead observing different growth stages or two

TABLE 10. FEMALE:MALE RATIOS OF MONTE SAN GIORGIO PACHYPLEUROSAURS

(FMR_{mean}, female:male ratio of mean trunk length; FMR_{max}, female:male ratio of largest specimens; *n*, number of specimens.)

	hypothesis	FMR_{mean}	*n*	FMR_{max}	specimen	sex
Serpianosaurus mirigiolensis	*x* = female	82	20	55	T 97	*x*
	y = female	122	20	183	T 1045	*y*
Neusticosaurus pusillus	*x* = female	102	165	101	T 3484	*x*
	y = female	98	165	99	T 3934	*y*
Neusticosaurus peyeri	*x* = female	103	83	136	T 3445	*x*
	y = female	97	83	74	T 3397	*y*
Neusticosaurus edwardsii	*x* = female	110	11	113	T 3935	*x*
	y = female	91	11	88	T 3437	*y*

distinct species. Both are unlikely, discussed by Rieppel (1989*a*). Perhaps this discrepancy serves to illustrate the point of Fitch (1981) that 'sexual size differences are extremely labile within the class (Reptilia)'.

Because of the many possible causes of sexual size differences (Fitch 1981) and the conflicting pattern observed in the Monte San Giorgio pachypleurosaurs, their FMRs contribute little to differentiation into males and females.

(*c*) *Sex ratios*

The sex ratios in adult modern squamates and crocodilians is close to 1:1 (Turner 1977). However, the matter is somewhat more complicated, as discussed by Ferguson (1985) for crocodiles, and by several authors for turtles (Bull & Vogt 1979; Thompson 1988, and references therein). For example, in many chelonians, sex is determined by temperature during incubation (Thompson 1988), a mechanism that is considered primitive (Bull & Vogt 1979). These studies suggest that some variability in sex ratios is common but poorly understood.

Sex ratios in the sample of pachypleurosaurs from Monte San Giorgio indicate that sex ratios in living populations of these little nothosaurs were roughly 1:1 as in many modern reptiles. *Serpianosaurus* and *Neusticosaurus pusillus* show a 50–70% surplus of sex *y* whereas *Neusticosaurus peyeri* and *Neusticosaurus edwardsii* show a 40–70% surplus of sex *x*.

This disparity is not surprising for the small sample sizes of *Serpianosaurus* (30 specimens) and, particularly, of *N. edwardsii* (11 specimens). The surplus of sex *x* in *Neusticosaurus peyeri* is difficult to explain by an insufficient sample size (83 specimens). A better explanation may be that some sexually immature individuals are included in the sample of mature individuals of sex *x*. This view is supported by the fact that the sample for this species shows the highest proportions of juveniles (20.5%) of all four taxa. Only for the high number of sex *y* in *Neusticosaurus pusillus* is no explanation readily available. It may reflect a truly skewed sex ratio, taphonomic bias, errors in sexing, or probably a combination of the latter two.

The general correlation in mammals between strong sexual dimorphism and skewed sex ratios could also lend support to the view that sex ratios in living populations of pachypleurosaurs were close to 1:1, because they exhibit relatively few sex differences.

(*d*) *Sex identification*

It is, of course, very difficult to identify the sex of the two sexual morphs because direct anatomical indications of sex and primary sex characters are not preserved. Nevertheless, two tentative lines of evidence are presented here, the first one arguing for sex *y* being the female. The most definitely sexually dimorphic skeletal element in pachypleurosaurs is the forelimb, especially the humerus and radius. Both of these bones are much better differentiated in one sex (sex *y*) than in the other, and the muscle attachment and articular surfaces are much better developed in sex *y*. The bones are also relatively longer. This suggests that the forelimb musculature was much better developed in sex *y* and therefore more powerful. The animal must have used its forelimb in a sex-related function. The forelimb was probably not very important in swimming nor steering (Carroll & Gaskill 1985), especially in the small *Neusticosaurus* and *Serpianosaurus*. If pachypleurosaurs were oviparous, the females had to go ashore to lay eggs, whereas the males could remain in the water throughout their entire life. Locomotion on land must have largely consisted of dragging of the body with the forelimbs in a sea turtle-like fashion or phocid seal-like fashion. Thus the sex with the most strongly developed forelimbs (sex *y*) were females that used their forelimbs for crawling ashore to lay eggs. This is in accordance with Rieppel's (1989) suggestion that sex *x* in *Serpianosaurus* is the male.

The second, but considerably weaker line of evidence is the relative length of the tail. Fitch (1981, p. 3) remarked, without giving an explanation, that the tails of male reptiles are generally longer than those of females. In a sample of 22 sexed adult *Neusticosaurus pusillus* specimens, no statistically significant differences could be observed (table 9). In a sample of 18 sexed adult *Neusticosaurus peyeri*, however, the difference in tail length in the two sexes (table 9) was statistically significant at $p = 0.1$. This is not a high level of confidence, and the sample size is admittedly small, but this difference may hint at which sex is which, because sex *y* of *Neusticosaurus peyeri* appears to have a slightly longer tail. In analogy with modern reptiles (Fitch 1981, p. 3), sex *y* may represent the male sex. This is contrary to the first hypothesis. The same kind of test could not be performed in *Neusticosaurus edwardsii* nor in *Serpianosaurus* because of insufficient sample sizes.

13. Ontogenetic studies

The large samples of Monte San Giorgio pachypleurosaurs contain growth series. In particular, the small *Neusticosaurus peyeri* is represented by a growth series rare in fossil vertebrates, from embryo (Sander 1988) to large adult; this permitted detailed morphological and morphometric study of the ontogeny of this small nothosaur. Juvenile morphology of *Neusticosaurus pusillus* and its change during ontogeny could be compared to that of *N. peyeri*; few juvenile specimens are known for *Neusticosaurus edwardsii* or *Serpianosaurus*.

Comparison with modern reptiles was hampered by the poor state of knowledge of post-embryonic ontogeny and of ossification patterns. Embryologists studying modern vertebrates usually concentrate on chondrification of skeletal elements in the embryo but not their ossification (P. Alberch, personal communication), which usually occurs during the late embryonic stages and after hatching. The underlying but largely untested assumption is that ossification follows the pattern of chondrification. Rieppel (1989*b*) describes the case of a fossil

reptile (*Helveticosaurus*) that helps to cast doubt on this assumption. Chondrification studies are obviously of limited use to palaeontologists because we are restricted to bones; what is sorely needed is information on late-stage embryonic and post-hatching ossification.

Growth was studied quantitatively and comparatively in all four Monte San Giorgio pachypleurosaurs. One point of interest was allometric growth of the elements of the body and its implications for the evolution of the pachypleurosaurs. Other topics are growth in the adult and size distribution in the sexually mature population. Much evidence on these quantitative topics exists for modern reptiles. This invited comparisons and led to fruitful results. Recognition of the embryo of *Neusticosaurus peyeri* (Sander 1988) was possible only in comparison with growth data on modern reptiles.

These aspects of ontogeny contribute much detail to the understanding of the life history of *Neusticosaurus* that will be discussed later.

(*a*) *Growth and juvenile morphology of* Neusticosaurus peyeri

Although the anatomy of *N. pusillus* was described before that of *N. peyeri*, the juvenile morphology of the latter and its change through ontogeny will be described first because of the exceptional growth series of 24 juvenile and subadult specimens: T 3394 (F) (letters after specimen numbers indicate size class), T 3389 (E), T 3398 b (C), T 3403 (F), T 3408 (B; figure 34*b*), T 3433 (B), T 3443 (B), T 3444 (E), T 3461 (E), T 3537 (E), T 3586 (E), T 3589 (D), T 3607 (F), T 3615 (E), T 3704 (C), T 3705 (A; figures 33, 34*a*), T 3754 (F), T 3789 (B), T 3799 (F), T 3932 (D; figures 34*d*, 7*b* and 24*b*), T 4290 (D), T 4291 (B), T 4292 (C), and T 4299 (E). The smallest specimen is an embryo (Sander 1988) (figure 33), and the only one of class A; it is T 3705 (standard length 3.31 mm). Sexual maturity is reached in class F (12–14 mm standard length). The smallest adult is T 3582 (standard length 13.2 mm).

Sexual maturity is easily recognized by the development of sexual dimorphism. The proportions and morphology of sex *x* remain closer to the juvenile condition. Specimens of this sex fall into the range of subadults. Thus the smallest specimen that is clearly of sex *y* indicates the minimum size for sexual maturity in *Neusticosaurus peyeri*. It is reached in class F; the smallest sexually mature animal is T 3582 at a standard length of 13.2 mm (snout–vent length 118 mm), about two-fifths of maximum size (T 3445, 34.1 mm standard length, 275 mm smout–vent length). Trunk length at sexual maturity is about 55 mm, as observed in the next to smallest specimens (T 3403, T 3472, T 3715, T 3799). This is the same length (and same size class) at which *N. pusillus* reaches sexual maturity. Skull length in *N. peyeri* at sexual maturity is 21–25 mm, which is about two-thirds to three-quarters of maximum size.

After sexual maturity is reached, the humerus:femur ratio remains constant even if the animal continues to grow, but the allometric growth factor of the skull changes. Thus the onset of sexual maturity could have been detected without development of secondary sex characters.

The largest specimen of *Neusticosaurus peyeri* (T 3445) at a standard length of 34.1 mm (class Q) is ten times as large as the embryo (T 3705). T 3445, T 3481, and T 3484 are very large specimens, and the question regarding their classification as *N. peyeri* arose. In their morphology and proportions, they are similar to the smaller specimens. The large specimens fit into the right side of a normal distribution of body sizes (figure 4*c*). Remarkably, these three fossils are all of sex *x*. No justification except large size exists for separating the three largest *Neusticosaurus peyeri* specimens into a new species.

The embryo

The only fossils embryos described to date are those of ichthyosaurs, which are relatively common (Romer 1966; Carroll 1988), and dinosaurs (Currie 1987; Horner & Weishampel 1988). The smallest specimen of *Neusticosaurus* (T 3705; figure 33) is an embryo not yet ready to hatch (Sander 1988). The two independent lines of evidence supporting this conclusion are (i) the morphology of the specimen and (ii) its absolute and relative size (Sander 1988). The second argument will not be reiterated here, but the morphology merits a more detailed description than what was given previously (Sander 1988) and can serve as the basis for the 'monitoring' of morphological change through ontogeny in pachypleurosaurs.

Neusticosaurus peyeri skeletons are always preserved in dorsoventral view, with two exceptions, which lie laterally. One is the embryo and the other is the adult T 3396 (figure 27*a*). T 3705 (figure 33) is curled up with the head close to the tail, a unique pose for *Neusticosaurus* but a typical position for vertebrate embryos. The skull is of relatively enormous size, 76% of the trunk length (adults 40–50%). It is poorly ossified and has very large orbits with clearly visible

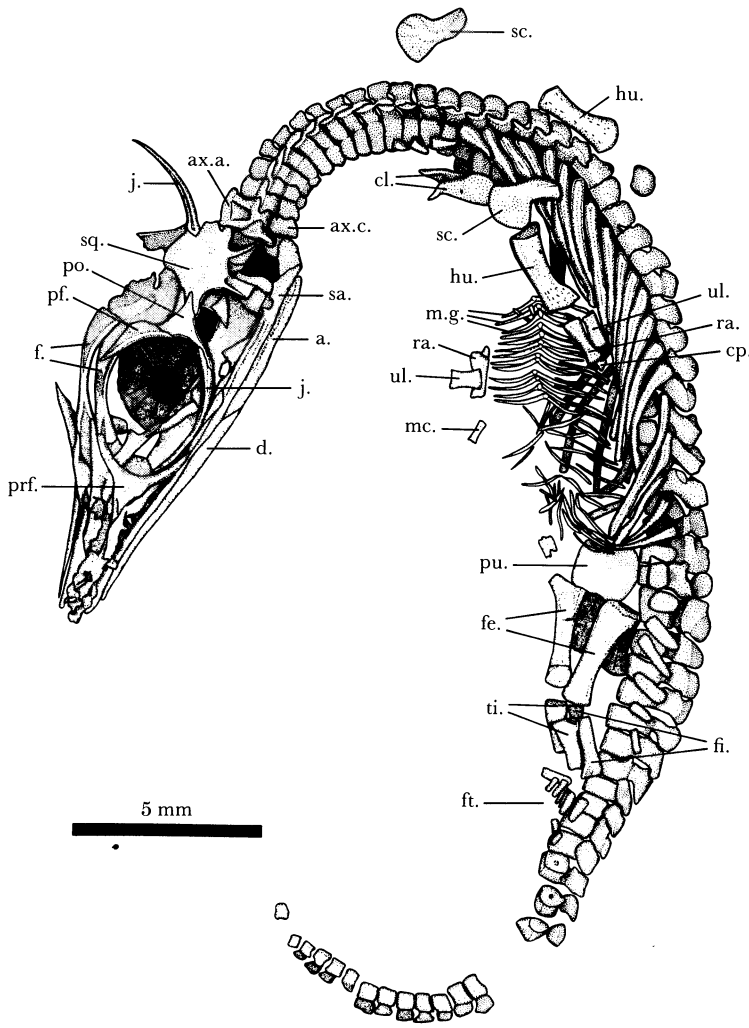

FIGURE 33. Embryo of *Neusticosaurus peyeri* (T 3705); lateral view. For discussion, see text.

sclerotic plates. The frontal bones are unfused and disarticulated. In all other specimens they are articulated, and they are at least partially fused in the adult. The other bones surrounding the orbit (prefrontal, jugal, postorbital, and postfrontal; figure 33) all appear very slender with relatively much thinner processes than in the adult (figures 17, 18, 19). The squamosal is relatively much larger and occupies most of the skull table. The ridge indicating the posterior limit of the skull table is not yet developed. The parietals cannot be discerned clearly because of poor ossification. The snout appears constricted relative to the orbits, and only a few teeth are present. The lower jaw is similar to the adult except for incomplete ossification of the symphyseal area and the retroarticular process.

The entire vertebral column but especially the neck is compressed anteroposteriorly with very short but high vertebrae. The axis arch especially is of relatively enormous size (figure 33). No cervical ribs are present. Only 26 caudal vertebrae, less than two-thirds of the adult number, and five (of eight) caudal ribs were counted. The tail reaches only 170% of trunk length, whereas the tail in juveniles reaches about 190% and that of adults 200–220% of trunk length (table 9; figure 34).

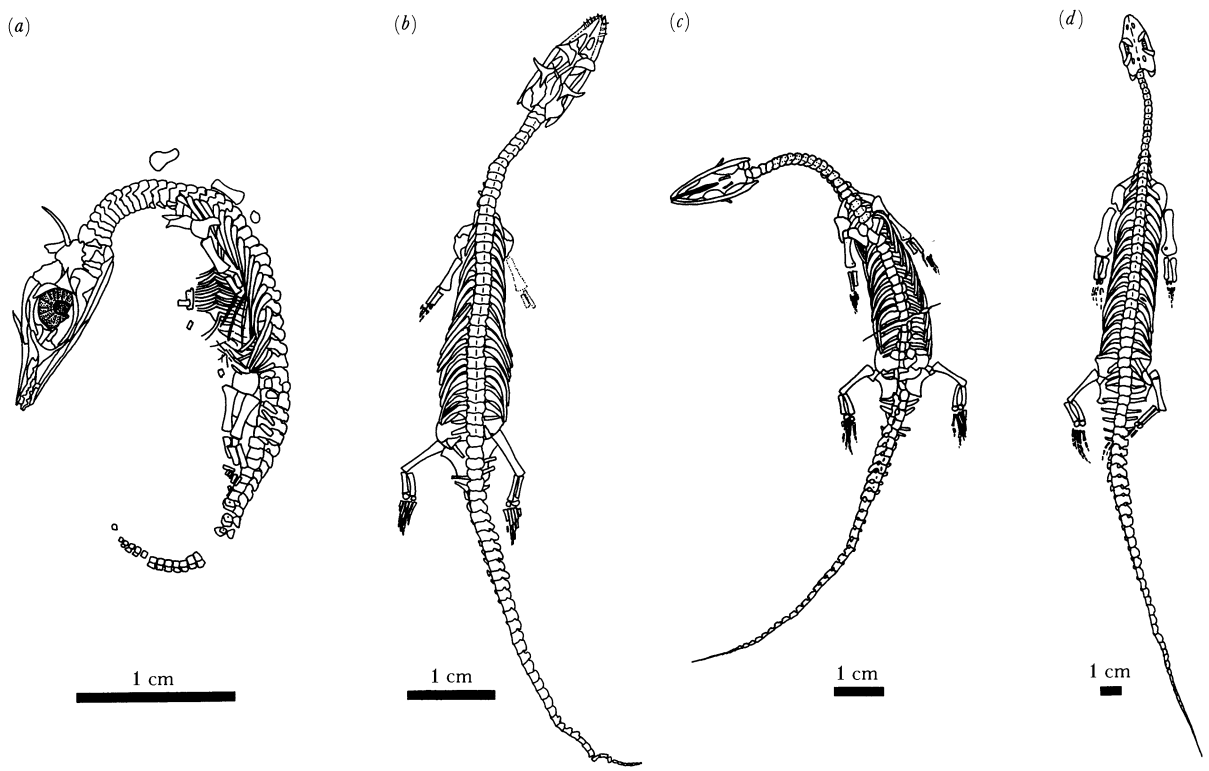

FIGURE 34. Growth series of *Neusticosaurus peyeri* illustrating overall proportional change during ontogeny. All specimens are drawn to approximately the same body length; (*a*) T 3705, size class A; (*b*) T 3408, size class B; (*c*) T 3932, size class D; (*d*) T 3393, size class I. Relative size of the skull decreases continuously whereas the forelimbs show positive allometry.

The interclavicle was probably not ossified, and clavicle and scapula differ greatly in shape from the adult. The scapular blade is relatively much larger than in the adult and the ventral portion is less elongated. It also lacks the anteroposterior ridge observed in older juveniles and adults (figures 33 and 35). In the pelvis, only the pubis is well exposed. It is almost round and

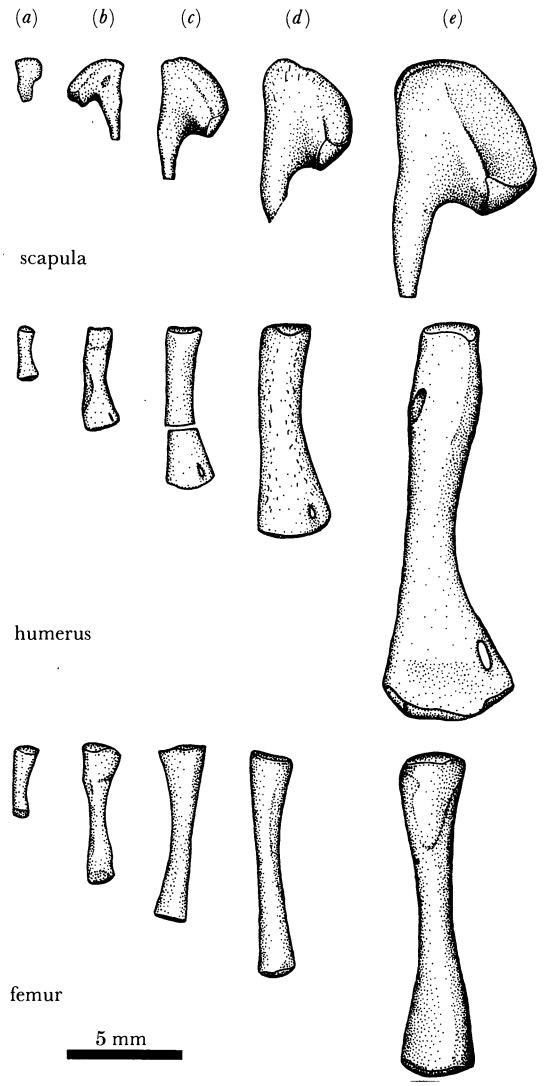

FIGURE 35. Growth series of scapula, humerus, and femur of *Neusticosaurus peyeri* in ventral view illustrating morphological and proportional change during ontogeny. All the bones are from the right side of the body, except the scapula in (*b*) and the femur in (*c*). Note shape differences in the scapulae and proportional differences between humeri and femora; (*a*) T 3705 is an embryo of size class A; (*b*) T 3789 is a small juvenile of size class B; (*c*) T 4290 is a juvenile of size class D; (*d*) T 3389 is a subadult of size class E; (*e*) T 3403 is a small adult of sex *y* and size class F.

lacks the obturator foramen. Humerus and femur are simple rods with slightly expanded, poorly ossified terminations. The humerus, which lacks the entepicondylar foramen, is much shorter than the femur (75% of the femur instead of 110% or 130% in adults, depending on sex; figure 35). Radius and ulna show little differentiation and unfinished terminations as well. The hand was unossified except for one carpal and one metacarpal bone.

It is difficult to identify this single carpal element. If ossification were to follow chondrification, the element would be an ulnare that chondrifies first in tetrapods (Burke & Alberch 1985; Shubin & Alberch 1986). In the foot no tarsals but some metatarsals and possibly the first phalanges are ossified. A similar condition is observed in a hatchling (T 3433) that shows an almost complete phalangeal count but no carpal bones. Chondrification of the

tarsal bones occurs before that of the metatarsals and phalanges in recent tetrapods (Burke & Alberch 1985; Shubin & Alberch 1986). This suggests that ossification does not follow chondrification in *Neusticosaurus*. The identity of the single carpal element must therefore remain uncertain. Surprisingly for the poor ossification of the skeleton, the gastral rib apparatus is completely developed.

The two types of dinosaur embryos described by Horner & Weishampel (1988) show different degrees of ossification. The hypsilophodontid embryo is ossified almost to an adult level whereas the hadrosaurid embryo shows poorly ossified long bone epiphyses suggesting differences in growth patterns and hatchling behaviour (Horner & Weishampel 1988). A condition similar to that in the hypsilophid dinosaur could be documented for *Neusticosaurus peyeri*. The second smallest specimen, T 3789, is 94 mm long, a factor of 2.6 smaller than the smallest sexually mature individual. T 3789 is only slightly larger than predicted hatchling size (Sander 1988), and reptiles of this size generally double their body size during the first year of their life (Currie 1978; Currie & Carroll 1984). This indicates that the animal died within the first few months of its life. Nevertheless, T 3789 is nearly ossified to an adult level; only the proportions are juvenile. This is also the condition observed in modern reptile hatchlings (Gans *et al.* 1985).

The second argument for T 3705 being an embryo relies mainly on extrapolation of hatchling:adult size ratios in modern reptiles. Depending on which group of modern reptiles was used, the embryo reached between one-half and two-thirds of hatchling size (Sander 1988); this explains the poor ossification relative to the hatchling T 3789.

Morphological change during ontogeny

Juvenile specimens of *Neusticosaurus peyeri* are characterized by concave, unfinished ends of the long bones and a rough bone surface with pits and deep grooves. Most bones are crushed, even the large long bones like the humerus and femur that are always intact in adults (figure 25*g*, *h*, *k*). In many cases the proximal and distal terminations withstand crushing so that the ends of the bones appear raised. These regions of good ossification are marked off by light bands. The bone terminations look remarkably similar to those of recent chelonians and crocodiles illustrated by Bellairs (1970, fig. 138*b*) that have no epiphyses. *Neusticosaurus* apparently lacked epiphyses as well. Pachyostosis is rarely developed in juveniles; its absence is most conspicuous in the ribs.

The juvenile skull is characterized by relatively large orbits and poor sutural connections. The orbits always contain a black, amorphous, organic-like matter, possibly remains of the sclera. Some adults show it as well, possibly because of the varying quality of preparation. In this black matter, the sclerotic ring is commonly delineated. The skull table is incompletely ossified at first, the parietals appearing almost completely separated by the pineal foramen. The same imperfect ossification is seen in the large external nares. The midline of the skull appears unossified in the smallest specimen (T 3705) and even the frontals are disarticulated from each other. The frontals of T 3408 (class B) are still unfused although articulated, whereas the suture is only faintly visible in T 4299 (class D) and is interrupted in the centre in adults (figure 17). The ventrolateral process of the postorbital is narrow in juveniles resulting in a large lower temporal embayment. In ventral view again the poor ossification along the skull midline is noteworthy. The anterior parts of the pterygoids do not touch one another until class F. The

palatine is hardly discernible at all whereas the vomers are present from early on. In juvenile skulls the teeth are relatively large.

The entire vertebral column, but especially the neck, appears anteroposteriorly compressed in the smallest specimens (figure 34*a*, *b*) (similar to that of adult *N. pusillus*). The individual vertebrae show different proportions as they are wider and shorter than in adults. This can be observed especially well in the neural arches, which are almost rectangular in outline instead of chevron-shaped. Ontogenetic lengthening of the cervicals is observable, and the adult shape is reached by class D. The neurocentral suture was weak, indicated by the commonly disarticulated neural arches. Collapse of the neural arch because of sediment compaction led to displacement of the centrum into the neural canal between the bases of the arches. In ventral view, this produced a characteristic double row of raised bumps, up to class E (T 3586).

The embryo has no cervical ribs and in class B (T 3789) the cervical ribs are just small nubbins without anterior or posterior processes. The anterior process is distinctly shorter than the posterior in class C (T 4292). The cervical ribs assume adult morphology in class E (T 3389). As mentioned before, only five caudal ribs and 26 caudals were counted in the embryo. In class B, a wide range of counts can be observed. T 3443 has four caudal ribs and 32 caudal vertebrae, whereas T 3789 has 41 caudals. An adult count of 43 caudals is exhibited by T 3408 (class B). The gastral apparatus is completely developed even in the smallest specimens.

The shoulder girdle elements show some change in shape during ontogeny, especially the scapula (figure 35). The scapular blade is very large in the youngest specimen and continuously decreases in size relative to the ventral part. The coracoids are less waisted than in the adult. A peculiar observation was made on the clavicles of T 3389 (class D) that appear to ossify from two centres, evidenced by a distinct suture separating the stem from the blade. A faint suture suggesting the same process was found in the clavicles of T 3932 and T 4290 (also class D). In adults this suture is not visible, and juveniles smaller than class D have undivided clavicles without a suture (figure 35). Judging by the class D specimens, the clavicle of *Neusticosaurus* appears to consist of one deep, posterior and one superficial, anterior part that are fused in the adult. A bipartite clavicle was recently described by Schmidt (1987) for another sauropterygian, the plesiosaur *Cryptocleidus*.

The pubis is less waisted than in the adult. The obturator foramen is slit-like in juveniles but may be closed as early as class E (T 3444). This indicates the usefulness of this character for separation of adults of the two small *Neusticosaurus* species. The ischium of juveniles has a very narrow lateral part.

Humerus and femur as well as radius, ulna, tibia, and fibula show little differentiation before adulthood (figures 34 and 35). The entepicondylar foramen in the humerus appears late in class B (T 3408), and the ends of humerus and femur are incompletely ossified in classes A–C. As mentioned above, sexual differentiation of the humerus begins with class F. Humerus and femur of large specimens (larger than class L) of sex *x* show strong pachyostosis.

Development of the ossification of manus and pes proved to be interesting (table 11). T 3705 (A) shows no carpals and tarsals, only metacarpals and metatarsals. The tarsal and carpal bones do not ossify before late in class B. One specimen of class B (T 3789) already has a complete manus (phalangeal formula 1–2–3–3–2). This is exceptional, however, as all other specimens up to class E show an incomplete hand (table 11). The fifth terminal phalanx was especially slow to ossify whereas the fourth terminal phalanx is almost always present. Terminal phalanges one to three are inconsistently ossified (table 11). Unfortunately, in two of three

TABLE 11. DEVELOPMENT OF THE PHALANGEAL FORMULA OF *NEUSTICOSAURUS PEYERI*

size class	specimen	manus	pes
A	T 3705	metacarpals, one carpal	metatarsals, no tarsals
B	T 3433	1–2–3–3–1, no carpals	—
B	T 3443	—	unknown, tarsals
B	T 3408	1–2–2–3–1	2–3–3–3–1
B	T 3789	1–2–3–3–2	2–3–3–4–3
B	T 3398b	0–1–2–3–1	2–3–3–3–2
C	T 3704	—	1–2–3–3–2
C	T 4292	1–2–2–2–1	2–3–3–4–2
D	T 3932	0–2–3–3–1	2–3–4–4–3
D	T 4290	1–1–2–3–2	—
E	T 3444	1–2–3–3–1	2–3–4–4–3
E	T 3615	—	1–3–4–4–3
E	T 3389	—	1–?–4–4–2
F	T 3394	—	2–3–4–4–3
F	T 3607	—	2–3–4–4–?
H	T 3755	1–2–3–3–2	2–3–4–4–3
H	T 3801	—	2–3–4–5–3
Ideal formula		1–2–3–3–2	2–3–4–4/5–3

specimens of class E and in all specimens of class F no phalangeal formula at all can be determined. This is because of an ontogenetic change of forelimb death pose. Juveniles show the forelimbs spread away from the body at angles from 20 to 30° (pose L; figure 29*a*). The 'adult' position (pose J; figure 29*a*) with the arms closely appressed to the thorax frequently obscures the hand; it is reached by class E. Another ontogenetic change in death pose is the common occurrence of lateral views of the skull (T 3705, T 3789, T 4292) in small juveniles (classes A–C). This is probably because of the relatively high and narrow skull in juveniles.

Complete ossification of the pes seems to be delayed until adulthood (class F; table 11). The second terminal phalanx is present in all juveniles except one, T 3704. This specimen is unusual because it shows the lowest phalangeal count of this species. Terminal phalanx three appears consistently in class D, whereas terminal phalanx four (the fourth of this toe) seems to appear somewhat earlier. Only by class H does the fifth (optional) phalanx of the fourth toe appear. Terminal phalanges two and five do not ossify consistently before adulthood (class F).

In *N. peyeri* the manus is faster to ossify than the pes, just the reverse of *Neusticosaurus pusillus*. This may be best explained by the reduced phalangeal count of this species, a neotenous character. In other words, the distal set of terminal phalanges never ossifies.

(*b*) *Growth and juvenile morphology of* Neusticosaurus pusillus

A growth series of ten juvenile (T 3387 (E) (letters behind specimens number indicate size class), T 3409 (B), T 3432 (E), T 3571 (E), T 3714 (D), X-ray of T 3748 (C), X-ray of T 3965 (E), T 3649c (E), T 4293 (D), and X-ray of T 4296 (C)) and 12 subadult specimens (class F; T 3558, T 3562, T 3569, T 3595, T 3603, T 3653, T 3657, T 3738, T 3757, T 3767, X-ray of T 3775, and T 3975) document growth in *Neusticosaurus pusillus*. The smallest specimen (T 3409; figure 27*c*) is a hatchling with a standard length of 4.7 mm. The smallest *Neusticosaurus pusillus* that is sexually mature is T 3562 with a standard length of 11.3 mm (class F). The trunk length at sexual maturity is about 55 mm, as seen in the next to smallest specimens (T 3558, T 3653, T 3657). Interestingly, this is the same length as in *Neusticosaurus peyeri*. Skull length

at sexual maturity is close to final size. The largest specimen (T 3451) is twice as large as the smallest adult with a standard length of 21.2 mm (class L). It is exceptionally large, however (figure 4*b*). The next largest specimens (T 3468, T 3484, T 3528, T 3639, and T 3750; all of sex *x*) show a standard length of about 18 mm (class J).

Morphological change during ontogeny is better documented in *Neusticosaurus peyeri*. Development in *N. pusillus* seems to proceed along the same lines. In small juveniles (T 3748, T 4296), the neural arches are commonly separated from the centra, and the crushing of the centra into the neural canals persists up to class D (T 3714). T 3409 (B) already has 41 caudal vertebrae and the adult count is reached by class D (T 3714 with 57 caudals).

The pattern of phalanx ossification of manus and pes is comparable in all digits and toes (table 12). The manus appears to have ossified slower than the pes. However, the sample for the manus is too small to document its ontogeny comprehensively. The smallest specimen (T 3409 (B)) already shows a fairly high phalangeal count. In fingers one to four, it is just one short of the full number; finger five is missing. The complete count for fingers one, two, and five is reached by class F (table 12). The terminal phalanges of the third and fourth fingers seem to be the last to appear. They were not observed in specimens smaller than class H.

TABLE 12. DEVELOPMENT OF THE PHALANGEAL FORMULA OF *NEUSTICOSAURUS PUSILLUS*

size class	specimen	manus	pes
B	T 3409	1–2–3–4–?	2–3–3–3–2
C	T 4296	—	2–3–3–4–2
D	T 4293	1–?–?–?–2	2–3–4–4–2
D	T 3714	—	2–3–4–4–2
E	T 3571	—	?–?–3–4–2
F	T 3387	2–3–3–3–?	2–3–4–4–2
F	T 3775	2–2–3–4–3	2–3–4–4–2
F	T 3738	—	2–3–4–5–3
F	T 3603	2–2–3–4–2	2–3–4–4–3
H	T 3637	2–3–4–5–?	2–3–4–4–3
J	T 3528	2–3–4–5–3	2–3–4–5–3
Ideal formula		2–3–4–5–3	2–3–4–5–3

In the pes (table 12), toes one and two show the full phalangeal count already in class B (T 3409), and toe three reaches it by class D. Toes four and five are not complete until sexual maturity (class F). Toe four shows three phalanges by class B, four by class D, and the optional fifth as early as class F. Thus this optional fifth phalanx appears considerably earlier than in *Neusticosaurus peyeri*.

(*c*) *Growth and allometry*

Both small species of *Neusticosaurus* exhibit complete growth series, and growth can be easily quantified. The same holds true to a lesser extent for *Serpianosaurus* and *Neusticosaurus edwardsii* that also show a large size range though no small juveniles. These species have a larger size range than the small *Neusticosaurus* solely because of their larger absolute size. The lack of small juveniles and the smaller sample sizes make the quantitative analysis for these species somewhat less reliable. Nevertheless, the data are sufficient for comparison with the small species of *Neusticosaurus*.

Growth was analysed by using reduced major axis regressions. This is the standard procedure for allometric studies because this type of regression takes the variability of both

variables, i.e. skeletal elements, into account (Imbrie 1956). The coefficient of regression or slope of the regression line, a, is called the growth ratio. A value of a greater than 1 indicates positive allometry; a value of a less than 1 indicates negative allometry, and if $a = 1$, growth is isometric. The y-intercept, B of the regression line is called the initial growth index (Imbrie 1956). To test for isometric growth and differences between growth ratios, the z-test according to Imbrie (1956) was used. Only in one case, in the comparison between skull:standard length growth ratios of *Serpianosaurus* and *Neusticosaurus edwardsii* (table 14), was the sample size too small to determine probability levels accurately. In this instance the values of a (table 13) are so different that little doubt remains that the valves are significantly different.

TABLE 13. ALLOMETRIC PARAMETERS AND TESTS FOR ISOMETRY OF MONTE SAN GIORGIO PACHYPLEUROSAURS

(Key: a, growth ratio; B, initial growth index; H_0 ($a = 1$), null hypothesis of test for isometry; fe., femur length; hu., humerus length; rej., rejected; skull, skull length; std., standard length; S_a, standard error of a.)

	a	n	S_a	$H_0(a = 1)$	B
Serpianosaurus					
skull:std.	0.825	11	0.056	rej., $p > 0.01$	0.593
hu.:std.	1.331	15	0.094	rej., $p > 0.01$	−0.374
fe.:std.	1.088	17	0.057	not rejected	−0.063
Hu.:fe.	1.272	25	0.063	rej., $p > 0.01$	−0.358
Neusticosaurus pusillus					
skull:std.	0.638	101	0.024	rej., $p > 0.01$	0.706
sex x only					
hu.:std.	1.076	64	0.033	rej., $p > 0.05$	0.063
fe.:std.	0.929	56	0.025	rej., $p > 0.01$	0.129
hu.:fe.	1.155	64	0.023	rej., $p > 0.01$	−0.214
sex y only					
hu.:std.	1.300	96	0.037	rej., $p > 0.01$	−0.234
fe.:std.	1.053	91	0.027	rej., $p > 0.05$	0.028
hu.:fe.	1.260	95	0.028	rej., $p > 0.01$	−0.296
Neusticosaurus peyeri					
skull:std.	0.627	49	0.023	rej., $p > 0.01$	0.668
sex x only					
hu.:std.	1.075	45	0.029	rej., $p > 0.01$	−0.166
fe.:std.	0.922	48	0.021	rej., $p > 0.01$	0.041
hu.:fe.	1.166	48	0.021	rej., $p > 0.01$	−0.215
sex y only					
hu.:std.	1.374	36	0.045	rej., $p > 0.01$	−0.414
fe.:std.	0.984	34	0.030	not rejected	−0.012
hu.:fe.	1.400	37	0.030	rej., $p > 0.01$	−0.403
Neusticosaurus edwardsii					
skull:std.	0.548	12	0.024	rej., $p > 0.01$	0.818
hu.:std.	1.016	22	0.048	not rejected	0.149
fe.:std.	0.960	22	0.051	not rejected	−0.055
hu.:fe.	1.095	28	0.049	not rejected	−0.134

Growth analysis focused on four elements: the skull, humerus, femur, and standard length. The growth of the first three was studied in relation to standard length. Humerus:femur length was also analysed. The three elements were chosen because of their prominence in the skeleton and because they exhibited allometric growth, albeit upon superficial inspection. No allometric growth can be observed within the limbs.

As discussed previously, the neck exhibits positive allometry due to differential lengthening

of the neck vertebrae during ontogeny. Growth of the tail is difficult to study, mainly because of insufficient sample numbers. It appears to grow with a positive allometry as well, partially because of the addition of segments in classes A and B, but also because of the lengthening of the caudal vertebrae.

In the following section, allometric growth is first described in each species separately. After the growth index, a, and the y-intercept, B, were calculated, a was tested for isometry (table 13). In the cases of the sexually dimorphic allometries, the data for the juveniles were used in both calculations. Next, growth of the skull, humerus, and femur are compared between species and sexes (figures 36–39) and their growth ratios were tested for similarity (table 14).

Allometric growth by species

The sample for *Serpianosaurus* is relatively small, between 11 and 25 specimens depending on the element studied, and it includes a four-fold increase in size from the smallest juvenile (T 132) to the largest adult (T 1045). The skull of *Serpianosaurus* shows negative allometry ($a = 0.825$; table 13). Because sexual dimorphism in the humerus is not expressed in the humerus:femur or humerus:standard length ratios in this species (Rieppel 1989*a*), the sexes were not differentiated in the allometric analysis. The humerus shows strong allometric growth relative to standard length ($a = 1.331$) and relative to femur length ($a = 1.272$), whereas the femur shows isometry ($a = 1.088$; table 13).

The sample size for *N. pusillus* ranges from 56 to 101 depending on sex and element studied (table 13). Growth of the skull exhibits strong negative allometry ($a = 0.638$) that is not sexually dimorphic. Clear sexual dimorphism is evident in humerus and femur growth. The humerus of sex x shows weak positive allometry relative to standard length ($a = 1.076$) and relative to the femur ($a = 1.155$). Allometry of the femur is weakly negative ($a = 0.929$). The humerus of sex y shows strong positive allometry relative to standard length ($a = 1.3$) and relative to the femur ($a = 1.26$), whereas the femur shows only very weak positive allometric growth ($a = 1.053$).

From 34 to 49 specimens, depending on sex and element, could be used in the growth analysis of *Neusticosaurus peyeri* (table 13). The skull allometry is also strongly negative ($a = 0.627$) in this species. The other three allometries were sorted by sex as in *Neusticosaurus pusillus*. The humerus of sex x shows weak positive allometry relative to standard length ($a = 1.075$) and relative to femur ($a = 1.166$). The femur exhibits weak negative allometric growth ($a = 0.922$). In sex y, the humerus shows strong positive allometry relative to standard length ($a = 1.374$) and relative to the femur ($a = 1.4$), whereas the femur exhibits isometric growth ($a = 0.984$; table 13).

In *Neusticosaurus edwardsii*, the situation is similar to that in *Serpianosaurus*. The sample size is small, from 12 to 28 depending on element. Because no sex differences could be observed in the humerus:femur, humerus:standard length, and femur:standard length ratios (table 9), the sexes were not treated separately (table 13). The size range of *N. edwardsii* includes an almost six-fold size increase from the smallest juvenile (T 3447) to the largest adult (T 3935). Except for the skull, which shows the strongest negative allometry of all pachypleurosaurs ($a = 0.548$), all elements grow isometrically. The growth ratio of humerus:standard length is 1.016, of humerus:femur 0.96, and of femur:standard length 1.095 (table 13).

Comparison of species and sexes

The skull of all four species shows strongly negative allometry (figure 36), as is the rule in most tetrapods. The growth ratio *a* is lowest for *Neusticosaurus edwardsii* ($a = 0.548$), which is not surprising given the very small skull of the adult. *Serpianosaurus* exhibits the least negative allometric growth ($a = 0.825$), which is correlated with the large skull of the adult animal. The two small *Neusticosaurus* species have almost identical *a*-values of 0.638 (*N. pusillus*) and 0.627 (*N. peyeri*) as expressed by the parallel regression lines in figure 36.

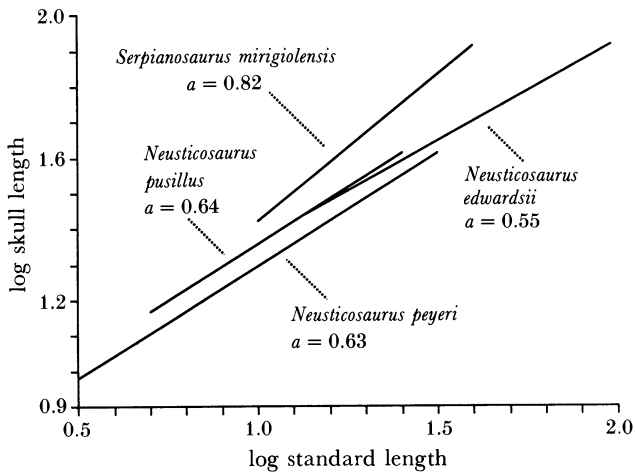

FIGURE 36. Graph of skull allometry of the four Monte San Giorgio pachypleurosaurids; *a* is the growth index. Note the decrease of *a* from the most primitive to the most advanced species.

The growth ratio of the humerus:standard length show the most interesting sex- and species-dependent differences. The *a*-value of *Serpianosaurus* is 1.331, which could not be discriminated from *a* of sex *y* of both small *Neusticosaurus* species (figure 37; table 14). Conversely, the growth ratio of sex *x* of both small *Neusticosaurus* could not be discriminated from that of *N. edwardsii* (figure 37; table 14). The positive allometry of the humerus in sex *y* in the small neusticosaurs produces the sexual dimorphism in relative humerus length (table 4).

The same pattern of similarity between *Serpianosaurus* and sex *y* of the small *Neusticosaurus* species and between *N. edwardsii* and sex *x* of the small *Neusticosaurus* species can be observed in femur growth (table 14; figure 39). The femur of *Serpianosaurus* tested positive for isometric growth with an *a* of 1.088 (table 13). The femur of sex *x* in both small species of *Neusticosaurus* shows weak negative allometry (*N. pusillus*, $a = 0.929$; *N. peyeri*, $a = 0.922$; figure 38) with no significant difference in *a*. Sex *y* of *N. pusillus* shows weak positive allometry ($a = 1.053$) that is not significantly different from that for *Serpianosaurus*. In contrast, sex *y* of *Neusticosaurus peyeri* and *N. edwardsii* both show isometry ($a = 0.984$ and 0.960, respectively). Femur growth ratios of the sexes of both small species of *Neusticosaurus* exhibit sexual dimorphism (figure 38; table 14).

The growth pattern of the humerus relative to femur (figure 39) is very similar to the other two growth ratios involving these bones. Humerus growth is strongly positive in *Serpianosaurus* ($a = 1.272$), in sex *y* of *Neusticosaurus pusillus* ($a = 1.260$) and in sex *y* of *N. peyeri* ($a = 1.400$). The growth ratio of the first two is statistically the same, whereas *a* for *N. peyeri* differs

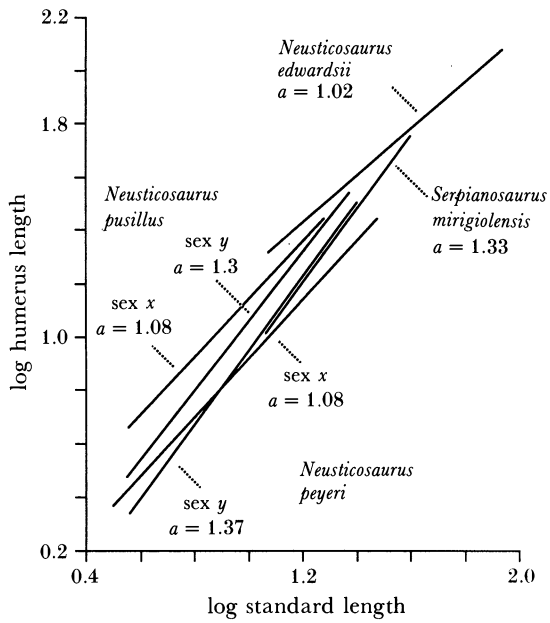

FIGURE 37. Graph of humerus allometry of the four Monte San Giorgio pachypleurosaurids; *a* is the growth index. Note that the lines for sex *x* of *Neusticosaurus pusillus* and *Neusticosaurus peyeri* are almost parallel to the line for both sexes of *Neusticosaurus edwardsii*, and that the lines for sex *y* of *Neusticosaurus pusillus* and *Neusticosaurus peyeri* are almost parallel to the line for both sexes of *Serpianosaurus mirigiolensis*.

TABLE 14. STATISTICAL DISCRIMINATION OF GROWTH RATIOS *a* OF MONTE SAN GIORGIO PACHYPLEUROSAURS

(The *z*-test was employed for statistical discrimination; +, rejected at $p > 0.01$ if not specified otherwise; ×, not rejected; fe., femur; hu., humerus; *N. ed.*, *Neusticosaurus edwardsii*; *N. pey.*, *Neusticosaurus peyeri*; *N. pus.*, *Neusticosaurus pusillus*; *Serpia.*, *Serpionosaurus mirigiolensis*; std., standard length (in millimetres).)

skull:std.	*N. ed.*	*N. pey.*	*N. pus.*		
Serpia.	+	+	+		
N. pusillus	+	×	—		
N. peyeri	+	—	—		
hu.:std.	*N. ed.*	*N. pey. y*	*N. pey. x*	*N. pus. y*	*N. pus. x*
Serpia.	+	×	+	×	+
N. pus. x	×	+	×	+	—
N. pus. y	+	+	+	—	—
N. pey. x	×	+	—	—	—
N. pey. y	+	—	—	—	—
fe.:std.					
Serpia.	+	>0.05	+	×	+
N. pus. x	×	+	×	+	—
N. pus. y	>0.05	+	+	—	—
N. pey. x	+	+	—	—	—
N. pey. y	×	—	—	—	—
hu.:fe.					
Serpia.	+	>0.05	×	×	>0.05
N. pus. x	×	+	×	+	—
N. pus. y	+	+	+	—	—
N. pey. x	×	+	—	—	—
N. pey. y	+	—	—	—	—

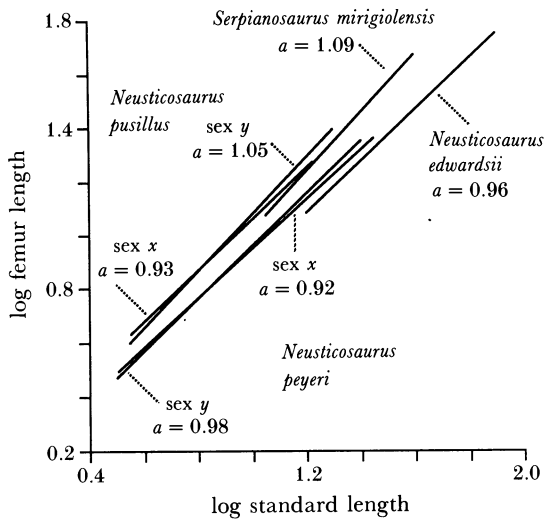

FIGURE 38. Graph of femur allometry of the four Monte San Giorgio pachypleurosaurids; *a* is the growth index. The same phenomenon as observed in the humerus allometry (figure 37) can be observed in the femur allometry.

significantly from *Serpianosaurus* at $p > 0.05$, and even more so from *N. pusillus* ($p > 0.01$; table 14). The humerus of sex *y* of *N. peyeri* thus shows a marked increase in positive allometric growth over *N. pusillus*. In sex *x* of both small *Neusticosaurus* species, the humerus shows weak positive allometry (figure 39). The two growth ratios are not statistically different from each other, but they can clearly be discriminated from sex *y* of the same species. These sex *x* growth ratios are also not significantly different from those of *N. edwardsii* that show isometric growth (table 14).

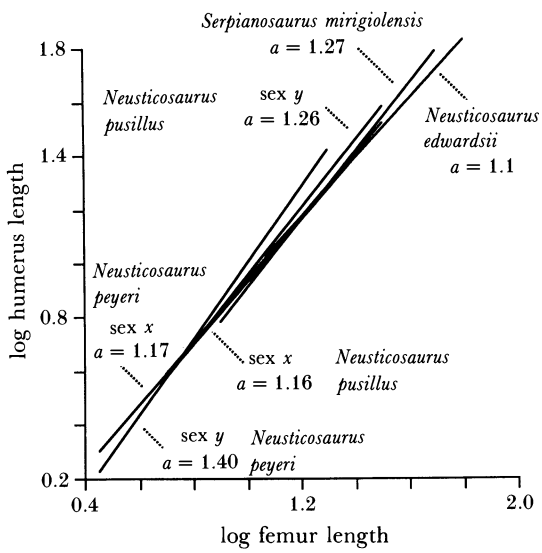

FIGURE 39. Graph of humerus to femur allometry of the four Monte San Giorgio pachypleurosaurids; *a* is the growth index. Again, *a* of sex *y* in both small *Neusticosaurus* is close to the value for *Serpianosaurus mirigiolensis*, and *a* of sex *x* is close to the value for *Neusticosaurus edwardsii*.

Discussion

The four pachypleurosaurs from Monte San Giorgio form a monophyletic taxon with *Serpianosaurus* as the most primitive and *Neusticosaurus edwardsii* as the most advanced member (figure 41). Evolution probably proceeded from *Serpianosaurus* via *Neusticosaurus pusillus* and *Neusticosaurus peyeri* to *Neusticosaurus edwardsii*.

A phylogenetic trend can be observed towards increasingly negative allometric growth of the skull, independent of absolute size. The pattern of the three allometries involving the limbs is most interesting. Sex *y* of *Neusticosaurus pusillus* and *N. peyeri* retains the ancestral (*Serpianosaurus*) pattern of strongly positive allometry of the humerus, whereas sex *x* of *N. pusillus* and *N. peyeri* initiate the descendant (*Neusticosaurus edwardsii*) pattern of isometric growth of the humerus. Sex *y* of *N. peyeri* slightly contradicts the trend with a small increase in *a* from 1.3 to 1.374. Thus in the small *Neusticosaurus* species, sex *x* shows a synapomorphy not seen in sex *y*, i.e. sex *x* is evolutionarily more advanced in terms of allometric growth than sex *y*.

(*d*) *Adult growth and maximum size*

Most reptiles continue to grow considerably after they reach sexual maturity (Porter 1972). No data have been available for fossil reptiles, but the Monte San Giorgio pachypleurosaurs suggest that these little nothosaurus were no exception. This fact becomes obvious with the inclusion of the very large specimens in *Neusticosaurus peyeri*. A detailed analysis of adult growth was only possible in *Neusticosaurus peyeri* and *Neusticosaurus pusillus* that have a sufficient sample size.

An empirical relation was established in modern reptiles between size at sexual maturity, mean adult size, and maximum size (Andrews 1982). In all cases snout–vent length was used as measure of size. The larger mean adult size, the relatively larger is maximum size, and the relatively smaller is size at sexual maturity (Andrews 1982). For example, in a small species with a mean adult snout–vent length of 40 mm, the largest individual reaches 113% of this length, whereas in a large species with 2000 mm mean adult length, the maximum size is 135%. The regressions for males and females differ slightly in modern reptiles. For *Neusticosaurus*, the mean values between males and females were used because the sexes in the fossil reptiles could not be identified with certainty. Hatchling size, size at sexual maturity, mean adult size, and maximum size for both small *Neusticosaurus* species are listed in table 15.

TABLE 15. HATCHLING SIZE, SIZE AT SEXUAL MATURITY, MEAN ADULT SIZE, AND MAXIMUM SIZE OF THE SMALL *NEUSTICOSAURUS*

(HL, hatchling size; SML, size at sexual maturity; ML, mean adult size; MAXL, maximum size. The first value in each column is standard length in mm, second is trunk length in mm; they are not necessarily from the same specimen. HL and SML are the same for both sexes because juveniles can not be sexed and the sexual maturity in sex *x* is not easily established. HL of *Neusticosaurus pusillus* is smaller than smallest specimen whose values are given. HL of *Neusticosaurus peyeri* is interpolated between T 3705 and T 3789.)

	sex	HL	SML	ML	MAXL
Neusticosaurus pusillus	*x*	<4.7–17.8	11.3–54.0	14.5–66.8	18.6–83.2
	y	<4.7–17.8	11.3–54.0	14.1–65.6	21.2–112.0
Neusticosaurus peyeri	*x*	*ca.* 4.0–16.0	13.2–53.0	18.3–70.1	34.1–126.7
	y	*ca.* 4.0–16.0	13.2–53.0	17.2–68.1	20.7–88.4

Mean adult size of *Neusticosaurus peyeri* is 155 mm (69 mm trunk length, 17.5 mm standard length) whereas *N. pusillus* is slightly smaller at 150 mm ML (66 mm trunk length, 14.3 mm standard length). Maximum size of *N. peyeri* is 186% of size at sexual maturity and the maximum size of *N. pusillus* is 146% of size at sexual maturity. The predicted value for the body size of both species would be only about 118% (180 mm snout–vent length). The predicted size at sexual maturity in *Neusticosaurus peyeri* is 77% of mean adult size, which is close to the observed value of 72%. The correspondence is even better for *N. pusillus*, where predicted (about 80%) and observed values (78%) are very close.

Assuming that mean adult size is not taphonomically skewed, the question regarding the origin of the large adults in *Neusticosaurus* arises. If the sample represented more than one population (in time or space), size differences of the observed magnitude would not be unusual (Andrews 1982). On the other hand, pachypleurosaurids could have been characterized by the ability to grow throughout their lives and the very large individuals could simply be the oldest. This is commonly assumed in modern reptiles as well (Bellairs 1970). Unfortunately, none of the large fossil specimens could be prepared for skeletochronology to test this hypothesis. Indeterminate growth in *Neusticosaurus* was certainly possible because of the lack of epiphyses.

14. Life cycle and mode of life

The life cycle of *Neusticosaurus peyeri* is best understood, and the following description is based mainly on this species. The life cycle of *N. pusillus* was probably very similar, whereas that of the larger pachypleurosaurs differed mainly in the absolute ages because *Neusticosaurus edwardsii* grew considerably older than the small *Neusticosaurus* species.

After hatching from the egg or live-birth at a snout–vent length of 50–60 mm (trunk length 16 mm; Sander 1988), the juvenile *Neusticosaurus* probably soon left the site of birth. Ossification proceeded rapidly (tables 11 and 12), enabling the hatchling to pursue an essentially adult lifestyle. It lived in the coastal surface waters preying on small nektonic invertebrates and fish. This is indicated by the many juveniles found together with adults in an autochthonous taphocoenosis produced by attritional mortality. Growth during the first year of life was rapid and continued at a high rate through a second year (table 6). As in modern reptiles, sexual maturation was triggered by a threshold body size and not by age (Castanet *et al.* 1988). Thus *Neusticosaurus* reached adult size and 'came of age' in its third year (figure 40, table 6) at a snout–vent length of 120 mm (55 mm trunk length; table 15). Under less favourable conditions maturation may have been delayed until age four years (table 6).

The females (sex *y*) developed strong and large forelimbs (table 4) that would have enabled them to crawl ashore on the coast or an island to deposit their eggs (the scenario for the females is, of course, very speculative). Sex *x* (male?) morphology changed little after the onset of sexual maturity. Certainly, the sexually dimorphic characters were useful in mate recognition as well. Both sexes were present in roughly equal numbers and were of about equal size (table 10). Growth continued after sexual maturation. The average snout–vent length in adults of the Monte San Giorgio population was about 150 mm (69 mm trunk length), and the average age five years. Some animals lived to an age of six and then died of disease or old age. The average life span of *Neusticosaurus* included three breeding seasons. There probably was a distinct breeding season like in most modern reptiles, although some extant tropical reptile species reproduce throughout the year (Bellairs 1970). Reproductive cycles may be one explanation

of the annuli observed in *Neusticosaurus* bones. Reproductively induced annuli are in better accordance with the presumed tropical climate during Ladinian times than seasonally induced growth interruptions.

Many of the little pachypleurosaurs undoubtedly fell victim to one of the many larger carnivores such as the nothosaur *Ceresiosaurus*. All that remains of them are the numerous coprolites that consist mainly of neusticosaur bones. Only very few individuals, mostly sex *x*, continued to grow to a large size (over 200 mm snout–vent length; table 15) and a 'ripe old age' of eight or nine years.

Neusticosaurus clearly was an aquatic animal (Zangerl 1935; Carroll & Gaskill 1985), as evidenced by its many aquatic adaptations such as the flattening of fore and hindlimbs, the loss of carpal and tarsal elements, the ventral expansion of the girdles, the laterally expanded tail region, and pachyostosis, to name a few (figure 40). It probably inhabited warm, shallow coastal, lagoonal, and estuarine waters (figure 40). In Germany, isolated *Neusticosaurus* bones are found together with indicators of fresh or at least brackish water such as aquatic amphibians (e.g. *Plagiosuchus*, personal observation at SMNS), lungfish (*Ceratodus*) teeth, and labyrinthodont remains (O. Fraas 1881). Because of its terrestrial middle ear, *Neusticosaurus* was unable to dive very deeply (Rieppel 1989*a*). This restricted it to the top of the water column. It probably was still able to venture on land, pushing itself along with fore- and hindlimbs.

The diet of these animals must have consisted of small, soft-bodied invertebrates (cephalopods) or small and juvenile fishes (Mateer 1976; Sanz 1980), the only food it could have caught and ingested in great numbers with its small, sharp teeth and small head on a long,

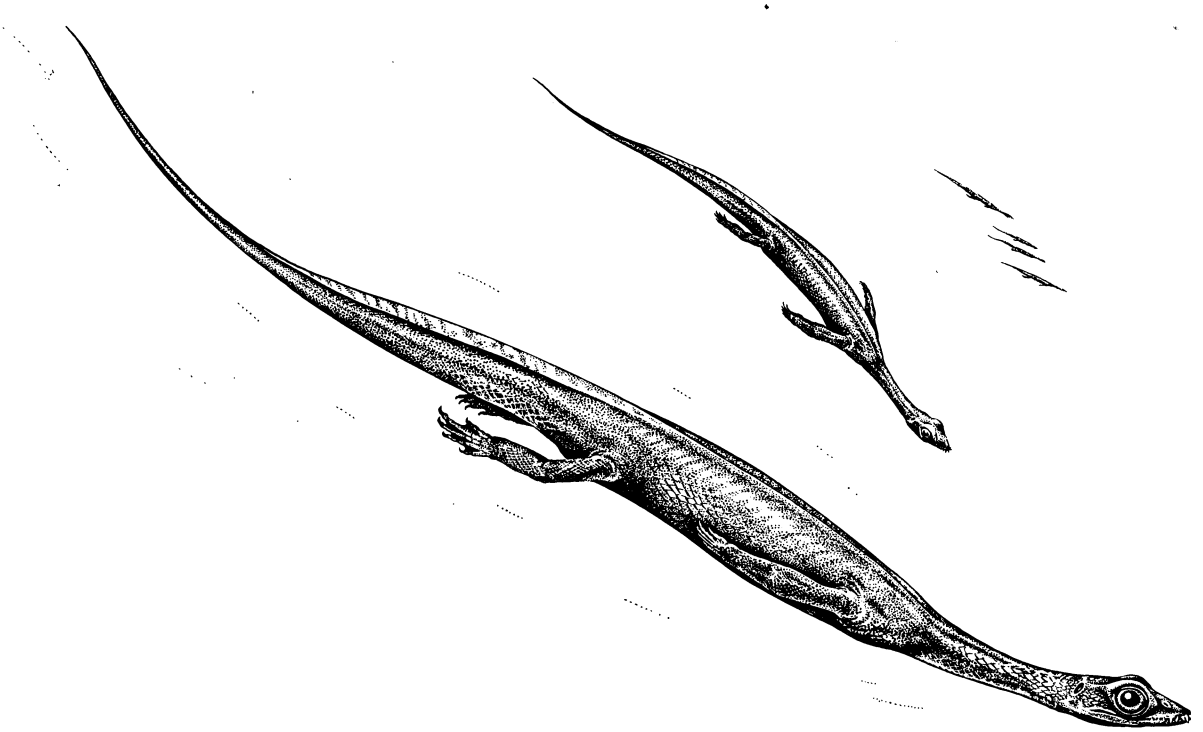

FIGURE 40. Life restoration of adult *Neusticosaurus peyeri* (overall length 25–30 cm). Note the swimming by lateral undulation. The front legs are closely appressed to the body, and the hind legs aid in steering. The squamation is based on T 3410. Drawing by B. Scheffold.

flexible neck. Very small subholosteans like *Habroichthys*, with an adult length of 25 mm (Brough 1939; T. Bürgin, personal communication), are known from the Cava Inferiore horizon (table 7) and the juveniles of *Luganoia* were certainly small enough to be preyed upon by *Neusticosaurus*. Contrary to Zangerl's (1935) belief, it is unlikely that juvenile *Neusticosaurus* were part of the diet of the adults for the simple reason that even the hatchlings are too large to be ingested as a whole.

The adaptive function of the pachyostosis in *Neusticosaurus* is unclear. It commonly occurs in slow-moving, sluggish aquatic vertebrates such as sirenians in which it functions to achieve neutral buoyancy (Schmidt 1985, 1986). In this way they need little effort to move up and down in the water column. Accordingly, it was suggested by Schmidt (1985, 1986) that walking along the seafloor ('bottom walk') was an important means of locomotion in *Neusticosaurus*. However, the inability to dive deeply and the anoxic bottom waters make this behaviour unlikely for the Monte San Giorgio neusticosaurs (figure 40). The animal would have been able to profit from its ability to walk along the seafloor only at the nearby reefs (Zorn 1971), if those were still in existence by early Ladinian times.

15. Relationships and phylogeny

(*a*) *Cladistic analysis*

Cladistic analysis is the established method of classification today and was therefore employed in this study. Fifteen characters (table 16) were selected for use in a cladistic analysis of the four species of pachypleurosaurs from Monte San Giorgio. Data for both small species of *Neusticosaurus* are derived from my own work, some data for *Serpianosaurus* were taken from Rieppel (1989*a*) and for *Neusticosaurus edwardsii* from Carroll & Gaskill (1985). Some data for these two taxa were also collected by myself. It is worth discussing the characters in detail to illustrate the problems of a cladistic analysis among very closely related forms.

Serpianosaurus was selected as the outgroup. *Dactylosaurus* was considered as well, but many characters used in this analysis cannot be ascertained in this animal (Gürich 1884; Nopcsa 1928; Sues & Carroll 1985). The monophyly of *Serpianosaurus* with *Neusticosaurus* can be established by the impedance matching middle ear (Rieppel 1989*a*) and the bone ornamentation. However, it cannot be shown that *Serpianosaurus* is the sister group of *Neusticosaurus*, because the other pachypleurosaurids are too poorly known (Rieppel 1989*a*). *Neusticosaurus* is a monophyletic taxon with one good synapomorphy, the tripartite gastralia. As far as is known, all other pachypleurosaurids have five elements per gastral rib (Rieppel 1987).

Character 1, the width of the skull table, is easily observed and correlated to the visibility of the cheek emargination from dorsal, the character used by Carroll & Gaskill (1985) to separate their *Pachypleurosaurus edwardsii* from *Neusticosaurus*. It appears to be independent of size. The primitive condition is clearly a narrow skull table, as observed in *Dactylosaurus* (Sues & Carroll 1985) and *Anarosaurus* (Carroll 1981). Character 2, the impedance matching middle ear is well developed in all four forms and is described in detail by Rieppel (1989*a*).

The relative length of the skull (character 3) shows a clear phylogenetic decrease within the four species (table 9). However, if *Dactylosaurus* or other pachypleurosaurids were chosen as outgroup, a skull : trunk ratio of about 0.4 would be primitive, indicating that *Serpianosaurus* has an unusually large skull within the Pachypleurosauridae. Character 4, the number of presacral vertebrae, is of great systematic value at the species level but of limited value on higher levels

because it appears to be phylogenetically unstable and reverses easily during evolution (figures 3 and 42). The primitive (*Serpianosaurus*) count is 36 for the Monte San Giorgio pachypleurosaurs.

In character 5, the height of the neural spines in the posterior trunk and anterior tail region, a high spine is the primitive condition if *Serpianosaurus* is selected as the outgroup. However, for pachypleurosaurids in general, a low spine appears to be primitive, as in *Dactylosaurus* (Sues & Carroll 1985). Neural spine height is of limited phylogenetic value because it is clearly correlated to body size and determined by functional constraints. The largest pachypleurosaurs (*Serpianosaurus*, *N. edwardsii*) show the relatively highest spines, whereas the small forms (*N. pusillus*, *N. peyeri*, *Dactylosaurus*) show low spines. High spines function to increase the swimming efficiency of the tail by increasing its lateral surface. The large pachypleurosaurs possibly needed a relatively more powerful swimming organ.

Character 6, the rib pachyostosis, appears to be relatively useful and easy to understand. Primitively, ribs are not pachyostotic (*Serpianosaurus*), but there too a correlation with size and mode of swimming, or both, could exist. The largest pachypleurosaur, *N. edwardsii* that, judging from its tail was a better swimmer than the small forms, exhibits no pachyostosis. It may have been lost secondarily. This may apply to *Serpianosaurus* as well. *Dactylosaurus* is polymorphic in this character.

Characters 7 (shape of anterior clavicle margin) and 8 (size of pectoral fenestra) are possibly correlated. The primitive pachypleurosaurid shoulder girdle (*Dactylosaurus*, *Serpianosaurus*) has angular clavicles and a large pectoral fenestra. It is smaller in advanced forms, and the anterior margin of the shoulder girdle acquires a rounded outline.

Character 9, the humerus:femur ratio, is primitively 1.0–1.2 as observed in *Serpianosaurus* (table 9). In both small species of *Neusticosaurus* it is clearly sexually dimorphic, with sex *x* showing the primitive condition and sex *y* the advanced. This contrasts with character 10 (allometric versus isometric growth of the humerus), in which sex *x* shows the advanced condition and sex *y* the primitive condition. The explanation is that the advanced state of character twelve, a relatively long humerus, is the result of a relatively much shorter femur in *N. edwardsii*, and not of positive allometric growth of the humerus. The humerus:trunk ratio has not changed much from the most primitive to the most advanced pachypleurosaurs (table 9). The femur:trunk ratio (character 11) is about 0.26 in *Serpianosaurus* (table 9). A lower ratio, i.e. a reduction of femur length is the advanced condition.

The reduction of the phalangeal count of manus and pes (characters 12 and 13) are useful characters for the cladistic analysis because the primitive condition is clearly established (2–3–4–5–3; Romer 1956), and the state of the characters is easily ascertained.

Character 14, the number of elements per gastral rib, is very useful because it shows no variation or gradual change. Only five elements, as in *Serpianosaurus* and *Dactylosaurus*, or three elements, as in *Neusticosaurus*, are possible. A high number is primitive (Romer 1956). Nothing more needs to be said about the bone ornamentation (character 15).

The matrix of character states (table 17) was analysed by using MacClade version 2.1 (by W. Maddison & D. Maddison) and yields a simple cladogram (figure 41). The most inclusive taxon is an unnamed subgroup of the Pachypleurosauridae; its synapomorphies are the impedance-matching middle ear and the bone ornamentation. The next subordinate taxon is the genus *Neusticosaurus*. It consists of three species, *N. pusillus*, *N. peyeri*, and *N. edwardsii*. All three are included in one genus. *N. pusillus* has no autapomorphy but forms a monophyletic

TABLE 16. CHARACTERS AND THEIR POSSIBLE STATES USED IN THE CLADISTIC ANALYSIS OF THE MONTE SAN GIORGIO PACHYPLEUROSAURS

(0 is primitive, 1 and 2 are advanced. *Serpianosaurus* (Rieppel 1989*a*) was selected as outgroup.)

character	state		
1. skull table	narrow (0)	wide (1)	—
2. impedance matching middle ear	present (1)	absent (0)	—
3. skull/trunk ratio	0.52 (0)	0.42 (1)	0.25 (2)
4. number of presacral vertebrae	36 (0)	less than 36 (1)	more than 36 (2)
5. neural spine height	high (0)	low (1)	—
6. ribs pachyostotic	absent (0)	present (1)	—
7. anterior margin of clavicle	angular (0)	rounded (1)	—
8. pectoral fenestra	large (0)	small (1)	—
9. humerus/femur ratio	1.0 (0)	1.25 (1)	1.6 (2)
10. humerus growth	allometric (0)	isometric (1)	—
11. femur/trunk ratio	>0.2 (0)	<0.2 (1)	—
12. phalangeal reduction in manus	absent (0)	present (1)	—
13. phalangeal reduction in pes	absent (0)	present (1)	—
14. number of elements in gastralia	5 (0)	3 (1)	—
15. bone ornamentation	absent (0)	present (1)	—

TABLE 17. DATA MATRIX USED FOR CLADISTIC ANALYSIS OF MONTE SAN GIORGIO PACHYPLEUROSAURS

(0 is primitive, 1 and 2 are advanced; *Serpianosaurus mirigiolensis* (Rieppel 1989*a*) was selected as outgroup; *N.*, *Neusticosaurus*.)

character number	1				5					10					15
Serpianosaurus	0	1	0	0	0	0	0	0	0/1	0	0	0	0	0	1
N. pusillus	0	1	1	2	1	1	0	0	0/1	0/1	0	0	0	1	1
N. peyeri	1	1	1	1	0	1	1	1	0/1	0/1	0	1	0	1	1
N. edwardsii	1	1	2	2	0	0	1	1	2	1	1	1	1	1	1

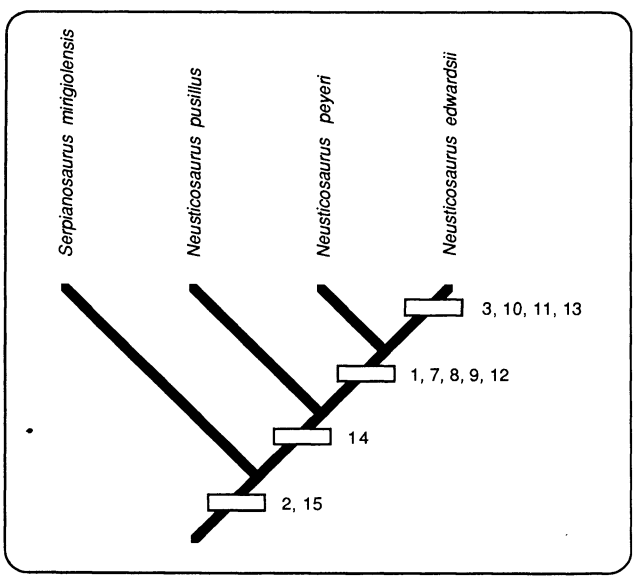

FIGURE 41. Cladogram of Monte San Giorgio pachypleurosaurids. Character numbers are explained in table 16. Not the congruency between the cladogram and the stratigraphic occurrence of the fossils.

taxon with *N. peyeri* and *N. edwardsii*. As discussed above, the correct name for this genus is *Neusticosaurus* because *Neusticosaurus* Seeley, 1882, has priority over *Pachypleurosaurus* Broili, 1927. The species *Neusticosaurus pusillus* is diagnosed by the absence of characters 1, 7, 13 and 14.

The genus *Neusticosaurus* possesses only one good synapomorphy, the three elements in the gastralia (character 12). Another is sex-dependent, the isometric growth of the humerus. *N. peyeri* and *N. edwardsii* are the next subordinate taxon. They share the following synapomorphies: wide skull table (1), round anterior margin of clavicle (7), small pectoral fenestra (8), and reduction of the phalangeal count in the hand (13). Autapomorphies of *N. edwardsii* are: the small skull (3), the short femur (9, 11), and reduction of the phalangeal count in the foot (13).

(*b*) *Heterochrony in the evolution of* Neusticosaurus

Heterochrony plays an important role in evolution (Gould 1977), and can produce considerable evolutionary change in combination with allometric growth. Since allometric growth is so prominent in the Monte San Giorgio pachypleurosaurs, heterochronic processes were evaluated as mechanisms of evolutionary transformation between the four species.

Two allometries of *Neusticosaurus* are of particular interest in this regard. One is the positive allometry of the humerus relative to the femur. In the presumed ancestor *Neusticosaurus pusillus* the humerus:femur ratio increases ontogenetically from 0.75 to a maximum of 1.15 (sex *y*). This trend is accentuated in *Neusticosaurus peyeri* with an ontogenetic increase of the humerus:femur ratio from 0.75 to 1.3 (sex *y*). Body size and age at sexual maturity are the same in the closely related species. Thus somatic development was accelerated in *Neusticosaurus peyeri* resulting in recapitulation.

The descendant of *N. peyeri* is *N. edwardsii*, which is three times as large and has a humerus:femur ratio of up to 1.8. This increase is mainly because of the much shorter femur and derives very little from relative size increase of the humerus (table 9). A possible explanation for the short femur could be the weak negative allometry of the femur ($a = 0.922$) in sex *x* of the ancestral *Neusticosaurus peyeri*. Sex *x* of *Neusticosaurus peyeri* is more advanced in certain characters, for example isometric growth of the humerus, which is also observed in *N. edwardsii*. However, the femur of *N. edwardsii* grows isometrically as well.

A heterochronic model of evolution from *N. peyeri* to *N. edwardsii* would call for retardation of maturation in a hypothetical intermediate between *N. peyeri* and *N. edwardsii*. This resulted in a larger overall size of the intermediate with a relatively smaller femur because of its negative allometry. The phylogenetic size increase continued from the hypothetical intermediate to *N. edwardsii*. To counteract further relative size decrease of the femur that may have been inadaptive, the femur of *N. edwardsii* evolved isometric growth. However, the shortened femur could be an entirely new character, and isometric growth of the humeri of sex *x* of *N. peyeri* and *N. edwardsii* could be pure coincidence.

(*c*) *A subpopulation of* Neusticosaurus pusillus

The mode of evolutionary transformation between the two small species of *Neusticosaurus* is illustrated by a subpopulation of *Neusticosaurus pusillus* that is slightly younger than its ancestor, *N. pusillus*, and somewhat older than its descendant, *N. peyeri*.

At Val Serrata (Cava Don Luigi; locality 13 in figure 1), four beds in the Cava Inferiore

horizon, labelled beds A–D, from oldest to youngst, contain specimens of *Neusticosaurus* (figure 6). Twenty specimens are known from beds C and D, but only seven (T 3400, T 3478, T 3561, T 3624, T 3625, T 3626, and T 3627) are prepared. All others were X-rayed to obtain vertebral counts and length measurements. The majority (16 prepared, 20 unprepared) of all specimens from this locality came from bed B, also known as *livello buono* ('good bed'). A look at the presacral counts for the four beds (figure 42) shows a marked decrease from bed B to bed C, from 40 to 42 presacrals to 37 to 39 presacrals. The usual presacral counts for *N. pusillus* is 40–42 presacrals (figure 3).

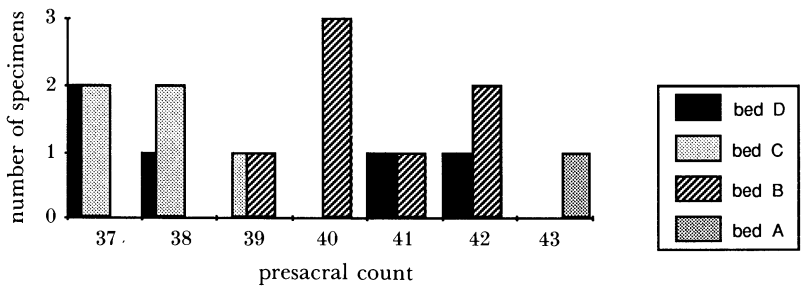

FIGURE 42. Histogram of presacral vertebral counts of *Neusticosaurus pusillus* from the four fossiliferous beds of the Cava Inferiore horizon (see figure 6).

No morphological differences between these individuals and those of the main population could be observed except for a less 'densely packed' cervical column in the subpopulation, which, of course, is a direct consequence of the lower number of vertebrae. The lower vertebral count of this population is also expressed in the trunk:standard length ratio that is below 4.5 (figure 43*a*) for most bed C specimens, whereas the majority of all *Neusticosaurus pusillus* specimens range from 4.5 to 4.9 (figure 43*a*).

More interesting is the observation that the humerus is relatively longer in sex *y* of the subpopulation (humerus:femur ratio averages 1.1–1.15; figure 43*b*) than in sex *y* of the main population (humerus:femur ratio averages 1.0–1.1; figure 43*b*). To find out whether an absolute size increase of the humerus or an absolute size decrease of the femur is responsible for this phenomenon, the humerus:trunk length and femur:trunk length ratios were computed. From figure 43*c*, *d* it is evident that mainly size increase in the humerus, and only to a lesser extent size decrease of the femur, has occurred because the humerus:trunk ratio of the subpopulation is higher than that of the main population but the femur:trunk ratio is the same in both populations.

No differences between the two populations could be observed in the relative length of the skull as both groups show a clear maximum of 4.0–4.25 in a histogram of the skull:trunk ratio (figure 43*e*).

Thus in two characters, the subpopulation shows changes towards the condition in the descendant *Neusticosaurus peyeri*: (i) decrease of the number of presacral vertebrae, and (ii) relative size increase of the humerus in sex *y*. In all other morphological aspects, it clearly belongs to *Neusticosaurus pusillus*, and the specimens of *Neusticosaurus* from beds C and D from Val Serrata (Cava Don Luigi) are a geologically younger population or subspecies of the species *Neusticosaurus pusillus* that shows greater similarity to the descendant *Neusticosaurus peyeri* than the main population. This is a case where gradual evolution is suggested by a

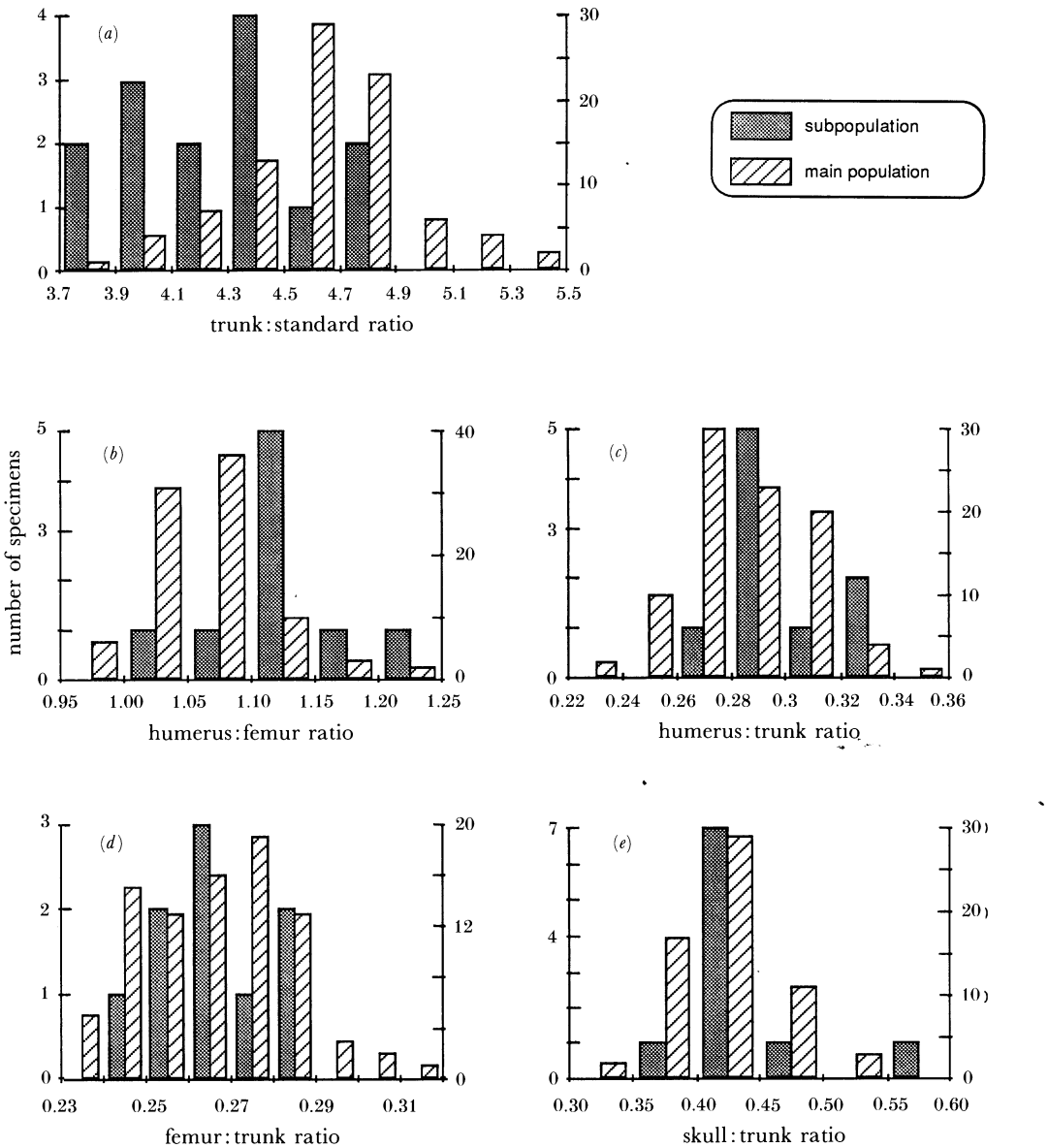

FIGURE 43. Comparison of the subpopulation and main population of *Neusticosaurus pusillus*. Left vertical axis refers to the number of specimens from the subpopulation, right vertical axis to the number of specimens from the main population; (*a*) distribution of trunk:standard ratios. The lower ratios of the subpopulation reflect its lower vertebral count; (*b*) distribution of humerus:femur ratios. Note higher ratios of the subpopulation; (*c*) distribution of humerus:trunk ratios. Note higher ratios of the subpopulation; (*d*) distribution of femur:trunk ratios. Little difference can be observed; (*e*) distribution of skull:trunk ratios. Again, little difference can be observed.

sufficiently complete fossil record. It is interesting to note that the amount of similarity of the subpopulation with its ancestor and descendant is correlated with the amount of stratigraphic separation. This suggests not only continuous but also continual evolution (*sensu* Gingerich 1984) from *N. pusillus* to *N. peyeri*.

This subpopulation also serves to illustrate that the binomial nomenclature is a

methodological problem in the recognition of gradual evolution (Sheldon 1987) because it cannot accommodate gradual change and intermediate populations between two species. For reasons of nomenclature, one is forced to divide a continuum by arbitrary cut-offs.

(*d*) *Phylogeny*

As was established above, the four Monte San Giorgio pachypleurosaurs form a monophyletic taxon (figure 41), and thus the possibility exists that they also form an evolutionary line of descent. This is probably the case for the genus *Neusticosaurus* with phylogeny proceeding from *N. pusillus* via *N. peyeri* to *N. edwardsii*. *Serpianosaurus* is probably not in the direct ancestry of *N. pusillus* but shares a common ancestor with it.

Incongruent with this phylogeny are the high neural spines in *Serpianosaurus* and *N. edwardsii* and possibly the loss of pachyostotic ribs. Both characters can be easily explained by convergence. The evolution of the presacral count is the largest incongruency encountered in this evolutionary line. Primitive appears to be a count of about 36, *N. pusillus* shows a strong increase to 41, next evolved *N. peyeri* with a decrease to 35, whereas *N. edwardsii* shows a slight increase to 36 and 37. However, segment number (i.e. vertebral number) varies easily in pachypleurosaurs and has little influence on body proportions. A peculiar primitive feature in *N. edwardsii* is the third element in the carpus that was probably present in cartilage in all the other forms. It only ossified in *N. edwardsii* because of its large size. This view is supported by the fact that only fully grown *N. edwardsii* individuals show this third element. The occasionally closed obturator foramen (which is always closed in *Dactylosaurus*) could be a primitive feature of the anatomy of *N. peyeri*.

The relations (figure 41) and phylogeny of the Monte San Giorgio pachypleurosaurs are compatible with their stratigraphic distribution. The 'primitive' *Serpianosaurus* occurs in the oldest bed of very early Ladinian age. The evolutionary line of *Neusticosaurus pusillus*, *N. peyeri*, and *N. edwardsii* occurs in a series of increasingly younger early to Middle Ladinian beds (Cava Inferiore horizon, Cava Superiore horizon, and Alla Cascina horizon; figure 5).

(*e*) *Speed of evolution*

Absolute speed of evolution is difficult to assess because of the poor resolution of radiometric dating of the Middle Triassic rocks at Monte San Giorgio (Hellman & Lippolt 1981). The relative speed of evolution could only be estimated by correlating morphological change to stratigraphic separation. The underlying assumption is that sedimentation rate remained roughly constant. Morphological change is difficult to measure and is only inadequately expressed in terms of synapomorphies. One approach was to count the number of changes in character state. In this case, morphological change appears to be evenly distributed. From *Serpianosaurus* to *N. pusillus*, six or seven steps occurred depending on sex. From *N. pusillus* to *N. peyeri*, six steps are again counted. From *N. peyeri* to *N. edwardsii* it took another seven steps.

Other factors like overall size are important for assessment of morphological change. The sum of synapomorphies, size, and proportions that could be called 'overall similarity' may be a good, but very subjective approach. Overall similarity appears to correlate fairly well with stratigraphic separation. *Serpianosaurus* is characterized by its large skull, wide body, and medium size, making it distinctive from all the other pachypleurosaurs, a fact that was acknowledged by the informal referral to '*Phygosaurus*' (see §1). Both species of *Neusticosaurus* look very similar. They are both small, with a small head, narrow body, and show the same

sexual dimorphism. For these reasons they probably would be included in one genus in traditional systematics whereas *N. edwardsii* would retain its own genus *Pachypleurosaurus*.

If morphometry is used to measure morphological change, both small *Neusticosaurus* species again exhibit great similarity. Very little change has occurred in absolute values and proportions (table 9). The same holds true for the allometry factors of these two species (table 13). However, the morphometric differences between *Serpianosaurus* and the small *Neusticosaurus* cannot be correlated with their stratigraphic separation. Dimensional change is largely restricted to skull size and overall body size. Proportions not involving the skull are close to the small *Neusticosaurus* species (table 9). *N. edwardsii*, on the other hand, shows a great increase in size, a proportionally very small skull and very short femur (table 9). More morphometric change has happened than suggested by the close stratigraphic proximity of *N. edwardsii* and *N. peyeri*.

Thus the speed of evolution was not constant from Grenzbitumenzone time to Alla Cascina time, and only in the small *Neusticosaurus* species is stratigraphic separation in accord with morphological change.

I thank my supervisor, Dr O. Rieppel, for continued help and encouragement. He, Dr C. T. Gee, Dr H. Rieber and Dr D. Bernoulli read the manuscript critically and improved it considerably. The fossils were skilfully prepared by Ms B. Balzarini, Ms A. Ceola, Mr F. Fassnacht, and Mr H. Lanz, who did most of the photographic work as well. Thanks go to Dr R. L. Carroll for providing me in 1985 with a then unpublished manuscript. Dr R. Wild (SMNS), Dr F. Westphal (GPIT), and Dr A. Milner (BMNH) graciously gave access to the respective collections in their care.

The Georges und Antoine Claraz-Schenckung (Zurich, Switzerland) provided financial support for fieldwork by myself and for previous excavations at Monte San Giorgio. Early stages of my project were funded by the Studienstiftung des deutschen Volkes (Bonn, F.R.G.).

References

Andrews, R. M. 1982 Patterns of growth in reptiles. In *Biology of the Reptilia*, vol. 13 (*Physiology D*) (ed. C. Gans & F. H. Pough), pp. 273–320. London: Academic Press.

Arthaber, G. v. 1924 Die Phylogenie der Nothosaurier. *Acta Zool.* **5**, 439–516.

Auffenberg, W. 1980 *The behavioral ecology of the Komodo Monitor*. Gainesville: University Presses of Florida.

Bartholomew, G. A., Bennett, A. F. & Dawson, W. R. 1976 Swimming, diving and lactate production of the marine iguana *Amblyrhynchus cristatus*. *Copeia*, pp. 709–720.

Bellairs, A. 1970 *The life of reptiles* vol. 2. New York: Universe Books.

Bennett, S. C. 1987 Sexual dimorphism in the pterosaur *Pteranodon*. *J. Vert. Paleont.* **7**, 11A.

Bernoulli, D. 1964 Zur Geologie des Monte Generoso (Lombardische Alpen). *Beitr. geol. Karte Schweiz*, N.F. **118**, 1–134.

Bernoulli, D., Govi, M., Graeter, P., Lehner, P., Reinhard, M. & Spicher, A. 1976 *Geologischer Atlas der Schweiz 1:25000, 1353 Lugano*. Schweiz. Geol. Kommission, map.

Boulenger, G. A. 1898 On a nothosaurian reptile from the Trias of Lombardy, apparently referrable to *Lariosaurus*. *Trans. zool. Soc. Lond.* **14**, 1–10.

Broili, F. 1927 Ein Sauropterygier aus den Arlbergschichten. *Sber. bayer. Akad. Wiss. math.-nat. Abt*, 205–228.

Brinkmann, R. 1986 *Brickmanns Abriß der Geologie. Zweiter Band. Historische Geologie, Erd- und Lebensgeschichte*, 12th/13th edn. Stuttgart: Enke.

Brough, J. 1939 *The Triassic fishes of Besano, Lombardy*. London: The Trustees of the British Museum (Nat. Hist.).

Bull, J. J. & Vogt, R. C. 1979 Temperature-dependent sex determination in turtles. *Science, Wash.* **206**, 1186–1188.

Burke, A. C. & Alberch, P. 1985 The development and homology of the chelonian carpus and tarsus. *J. Morph.* **186**, 119–131.

Carroll, R. L. 1981 Plesiosaur ancestors from the Upper Permian of Madagascar. *Phil. Trans. R. Soc. Lond.* B**293**, 315–383.

Carroll, R. L. 1984 The emergence of marine reptiles in the Late Paleozoic and Early Mesozoic. In *Third symposium on Mesozoic terrestrial ecosystems, short papers* (ed. W.-E. Reif & F. Westphal), pp. 41–46. Tübingen: Attempto Verlag.

Carroll, R. L. 1988 *Vertebrate paleontology and evolution.* New York: W. H. Freeman.

Carroll, R. L. & Gaskill, P. 1985 The nothosaur *Pachypleurosaurus* and the origin of plesiosaurs. *Phil. Trans. R. Soc. Lond.* B**309**, 343–393.

Castanet, J. 1987 La squelettochronologie chez les Reptiles. III – Application. *Ann. Sci. nat. Zool., Paris*, 13 série, **8**, 157–172.

Castanet, J. & Cheylan, M. 1979 Les marque de croissance des os et des écailles comme indicateur de l'âge chez *Testudo hermanni* et *Testudo graeca* (Reptilia, Chelonia, Testudinidae). *Can. J. Zool.* **57**, 1649–1665.

Castanet, J., Newman, D. G. & Saint Girons, H. 1988 Skeletochronological data on the growth, age, and population structure of the tuatara, *Sphenodon punctatus*, on Stephens and Lady Alice Islands, New Zealand. *Herpetologica* **44**, 25–37.

Colbert, E. H. 1983 *Dinosaurs. An illustrated history.* Maplewood: Hammond Inc.

Cornalia, E. 1854 Notizie zoologiche sul *Pachypleura edwardsii* Cor. Nuovo sauro acrodonte degli strati triassici di Lombardia. *Gior. Ist. lombardo Sci. Lett.* **6**, 1–46.

Curioni, G. 1863 Sui giacimenti metalliferi e butuminosi nei terreni triasici di Besano. *Mem. R. Ist. Lombardo di Scienze, Let. ed Art.* **9**, 241–268.

Currie, P. J. 1978 The orthometric linear unit. *J. Paleont.* **52**, 964–971.

Currie, P. J. 1981 *Hovasaurus boulei*, an aquatic eosuchian from the Upper Permian of Madagascar. *Palaeont. afr.* **24**, 99–168.

Currie, P. J. 1987 Discovery of nests of dinosaur eggs with embryos in the Two Medicine Formation of southern Alberta. *J. Vert. Paleont.* **7**, 15A.

Currie, P. J. & Carroll, R. L. 1984 Ontogenetic changes in the eosuchian reptile *Thadeosaurus. J. Vert. Paleont.* **4**, 68–84.

Dames, W. 1890 *Anarosaurus pumilio* nov.gen. nov.sp. *Z. dt. geol. Ges.* **42**, 74–85.

Darby, D. G. & Okajangas, R. W. 1981 Gastrolith from an Upper Cretaceous plesiosaur. *J. Paleont.* **54**, 548–556.

De Beer, G. R. 1937 *The development of the vertebrate skull.* Oxford University Press.

Deecke, W. 1886 Über *Lariosaurus* und einige andere Saurier der lombardischen Trias. *Z. dt. geol. Ges.* **38**, 170–197.

De Buffrenil, V., Farlow, J. O. & De Ricqules, A. 1986 Growth and function of *Stegosaurus* plates. *Paleobiology* **12**, 459–473.

De Ricqles, A. 1980 Tissue stucture of dinorsaur bone. Functional significance and possible relation to dinosaur physiology. In *A cold look at the warm-blooded dinosaurs*, AAAS Selected Symposium 28 (ed. R. D. K. Thomas & E. C. Olson), pp. 103–139. Colorado: West View Press.

De Ricqles, A. 1983 Cyclical growth in the long limb bones of a sauropod dinosaur. *Acta palaeont. pol.* **28**, 225–232.

Dodson, P. 1976 Quantitative aspects of relative growth and sexual dimorphism in *Protoceratops. J. Paleont.* **50**, 929–940.

Dodson, P. 1987 Review: Dinosaur Systematics Symposium, Tyrell Museum of Paleontology, Drumheller, Alberta, June 2–5, 1986. *J. Vert. Paleont.* **7**, 106–108.

Evans, S. 1980 The skull of a new eosuchian reptile from the Lower Jurassic of South Wales. *Zool. J. Linn. Soc.* **70**, 203–264.

Ferguson, M. W. J. 1985 Reproductive biology and embryology of the crocodilians. In *Biology of the Reptilia*, vol. 14. (*Development A*) (ed. C. Gans, F. Billett & P. F. A. Maderson), pp. 329–491. New York: John Wiley.

Fitch, H. S. 1981 Sexual size differences in reptiles. *Misc. Publ. Mus. nat. Hist. Univ. Kansas* **70**, 1–72.

Fraas, E. 1896 *Die schwäbischen Trias-Saurier.* Festgabe d. Königl. Nat.-Cab. Stuttgart. Stuttgart: E. Schweizerbart'sche Verlagshandlung.

Fraas, O. 1881 *Simosaurus pusillus* aus der Lettenhohle von Hoheneck. *Jh. Ver. vaterl. Naturk. Württ.* **37**, 319–324.

Frauenfelder, A. 1916 Beiträge zur Geologie der Tessiner Kalkalpen. *Eclog. geol. Helv.* **14**, 247–371.

Gans, C., Billett, F. & Maderson, P. F. A. (editors) 1985 *Biology of the Reptilia*, vol. 14. New York: John Wiley.

Gilmore, C. W. 1946 Notes on recently mounted reptile fossil skeletons in the United States National Museum. *Proc. U.S. natn. Mus.* **96**, 293–310.

Gingerich, P. D. 1984 Punctuated equilibria – where is the evidence? *Syst. Zool.* **33**, 335–338.

Gould, S. J. 1977 *Ontogeny and phylogeny.* Massachusetts: Harvard University Press.

Gürich, G. J. E. 1884 Über einige Saurier des oberschlesischen Muschelkalkes. *Z. dtsch. geol. Ges.* **36**, 125–144.

Hellman, K. N. & Lippolt, H. J. 1981 Calibration of the Middle Triassic time scale by conventional K–Ar and $^{40}Ar/^{39}Ar$ dating of alkali feldspars. *J. Geophys.* **50**, 73–88.

Hoffman, J. 1958 Einbettung und Zerfall der Ichthyosaurier im Lias von Holzmaden. *Meyniana* **6**, 10–55.

Hoffstetter, R. & Gasc, J. P. 1969 Vertebrae and ribs of modern reptiles. In *Biology of the Reptilia*, vol. 1. (*Morphology A*) (ed. C. Gans, A. d'A. Bellairs & T. S. Parsons), pp. 201–310. New York & London: Academic Press.

Horner, J. R. & Weishampel, D. B. 1988 A comparative embryological study of two ornithischian dinosaurs. *Nature, Lond.* **332**, 256–257.

Huene, F. v. 1956 *Paläontologie und Phylogenie der niederen Terapoden.* Jena: VEB Gustav Fischer.

Imbrie, J. 1956 Biometrical methods in the study of invertebrate fossils. *Bull. Am. Mus. nat. Hist.* **108**, 211–252.

Jeannet, A. 1933 Die Triasfauna der Tessiner Kalkalpen. 6. Note sur un *Miocidaris* nouveau. *Abh. Schweiz. Palaeont. Ges.* **53**, 1–7.

Lehman, T. M. 1989 Chasmosaurus mariscalensis, sp. nov., a new ceratopsicen dinosaur from Texas. *J. vert. Paleont.* **9**, 137–162.

Lull, R. S. & Wright, N. E. 1942 Hadrosaurian dinosaurs of North America. *Bull. geol. Soc. Am. Spec. Paper* **40**, 1–242.

Lydekker, R. 1889 *Catalogue of the fossil Reptilia and Amphibia in the British Museum (Natural History), part II.* London: The Trustees of the British Museum (Natural History).

Kuhn-Schnyder, E. 1959 Ein neuer Pachypleurosaurier von der Stulseralp bei Bergün (Kt. Graubünden, Schweiz). *Eclog. geol. Helv.* **52**, 639–658.

Kuhn-Schnyder, E. 1963 I Sauri del monte San Giorgio. *Arch. Stor. ticinese* **16**, 811–854.

Kuhn-Schnyder, E. 1964 Die Wirbeltierfauna der Tessiner Kalkalpen. *Geol. Rdsch.* **53**, 393–412.

Kuhn-Schnyder, E. 1974 Die Triasfauna der Tessiner Kalkalpen. *Neujahrsbl. Naturf. Ges. Zürich* **176**, 1–119.

Kuhn-Schnyder, E. 1987 Die Triasfauna der Tessiner Kalkalpen. 26. *Lariosaurus lavizzarii* n.sp. (Reptilia, Sauropterygia). *Schweiz, Paläont. Abh.* **110**, 1–24.

Manter, J. T. 1940 The mechanics of swimming in the alligator. *J. exp. Zool.* **83**, 345–358.

Mateer, N. J. 1976 On two new specimens of *Pachypleurosaurus* (Reptilia: Nothosauria). *Bull. geol. Inst. Upsala*, N.S. **6**, 107–123.

Martill, D. 1987 A taphonomic and diagenetic case study of a partially articulated ichthyosaur. *Paleontology* **30**, 543–555.

Moffat, L. A. 1985 Embryonic development and aspects of reproductive biology in the Tuatara *Sphenodon punctatus*. In *Biology of the Reptilia*, vol. 14, *Development A* (ed. C. Gans, F. Billett & P. F. A. Maderson), pp. 493–521. New York: John Wiley.

Müller, W. 1969 *Beitrag zur Sedimentologie der Grenzbitumenzone vom Monte San Giorgio (Kt. Tessin) mit Rücksicht auf die Beziehung Fossil – Sediment.* Kurzfassung der Dissertation. Riehen: Schudel.

Müller, W., Schmid, R. & Vogt, P. 1964 Vulkanogene Lagen aus der Grenzbitumenzone (Mittlere Trias) des Monte San Giorgio in den Tessiner Kalkalpen. *Eclog. geol. Helv.* **57**, 431–450.

Nopcsa, F. 1928 Paleontological notes on reptiles. *Geologica hung.* (ser. paleont.) **1**, 1–84.

Oelrich, T. M. 1956 The anatomy of the head of *Ctenosaura pectinata* (Iguanidae). *Misc. Publs. Mus. Zool. Univ. Mich.* **94**, 1–122.

Peabody, F. E. 1961 Annual growth zones in living and fossil vertebrates. *J. Morph.* **108**, 11–62.

Peyer, B. 1928 Über *Pachypleurosaurus edwardsi* Corn. aus der Trias der Tessiner Kalkalpen. *Act. Soc. Helv. Sci. Nat.* 109e session, 219.

Peyer, B. 1931 Die Triasfauna der Tessiner Kalkalpen. 4. *Ceresiosaurus calcagnii* nov.gen. nov.spec. *Abh. Schweiz. Paläont. Ges.* **51**, 1–68.

Peyer, B. 1932 Die Triasfauna der Tessiner Kalkalpen. 5. *Pachypleurosaurus edwardsii* Corn. spec. *Abh. Schweiz. Paläont. Ges.* **52**, 1–18.

Peyer, B. 1934 Die Triasfauna der Tessiner Kalkalpen. 7. Neubeschreibung der Saurier von Perledo. *Abh. Schweiz. Paläont. Ges.* **53**, 1–58.

Pinna, G. 1967 La collezione di rettili triassici di Besano (Varese) del Museo Di Storia Naturale di Milano. *Natura, Milano* **58**, 177–192.

Porter, K. R. 1972 *Herpetology.* Philadelphia: W. B. Saunders.

Reid, R. E. H. 1981 Lamellar-zonal bone with zones and annuli in the pelvis of a sauropod dinosaur. *Nature, Lond.* **292**, 49–51.

Reid, R. E. H. 1987 Bone and dinosaurian 'endothermy'. *Mod. Geol.* **11**, 133–154.

Rieber, H. 1973*a* Ergebnisse paläontologisch-stratigraphischer Untersuchungen in der Grenzibitumenzone (Mittlere Trias) des Monte San Giorgio (Kanton Tessin, Schweiz). *Eclog. geol. Helv.* **66**, 667–685.

Rieber, H. 1973*b* Cephalopoden aus der Grenzbitumenzone (Mittlere Trias) des Monte San Giorgio (Kanton Tessin, Schweiz). *Schweiz. Paläont. Abh.* **93**, 1–96.

Rieber, H. 1975 Die Posidonienschiefer (oberer Lias) von Holzmaden und die Grenzbitumenzone (Mittlere Trias) des Monte San Giorgio (Kt. Tessin, Schweiz). Ein Vergleich zweier Lagerstätten. *Jh. Ges. Naturk. Württ.* **130**, 163–190.

Rieber, H. & Sorbini, L. 1983 Middle Triassic bituminous shales of Monte San Giorgio (Tessin, Switzerland). *First Int. Congr. Paleoecol. Excursion* **11**A, 1–40.

Rieppel, O. 1985 Die Triasfauna der Tessiner Kalkalpen 25. Die Gattung *Saurichthys* (Pisces, Actinopterygii) aus der mittleren Trias des Monte San Giorgio, Kanton Tessin. *Schweiz. Paläont. Abh.* **108**, 1–85.

Rieppel, O. 1987 The pachypleurosauridae: an annotated bibliography. With comments on some lariosaurs. *Eclog. geol. Helv.* **80**, 1105–1118.

Rieppel, O. 1989*a* A new pachypleurosaur (Reptilia: Sauropterygia) from the Middle Triassic of Monte San Giorgio, Switzerland. *Phil. Trans. R. Soc. Lond.* B**323**, 1–73.

Rieppel, O. 1989*b* *Helveticosaurus zollingeri* Peyer (Reptilia, Diapsida). Skeletal paeodomorphosis, functional anatomy and systematic affinities. *Palaeontographica.* **208**, 123–152.

Romer, A. S. 1956 *Osteology of the Reptiles.* University of Chicago Press.

Romer, A. S. 1966 *Vertebrate Paleontology*, 3rd edn. University of Chicago Press.

Romer, A. S. & Price, L. I. 1940 Review of the Pelycosauria. *Geol. Soc. Am. Spec. Pap.* **28**, 1–538.

Rusconi, C. 1948 Plesiosaurios del Jurásico de Mendoza. *An. Soc. Cien. Argent.* **146**, 327–351.

Sander, P. M. 1987 Taphonomy of the Lower Permian Geraldine Bonebed in Archer County, Texas. *Palaeogeogr., Palaeoclim., Palaeoeco.* **61**, 221–236.

Sander, P. M. 1988 A fossil reptile embryo from the Middle Triassic of the Alps. *Science, Wash.* **239**, 780–783.

Sander, P. M. 1989 *Stratigraphic position of the vertebrate localities at Monte San Giorgio, Switzerland.* Zürich: Paläont. Inst. u. Museum. (Open file report.)

Sanz, J. L. 1980 Algunas precisiones morfofuncionales en Nothosauria y Pachypleurosauria (Sauropterygia, Reptilia). *Estudios geol.* **36**, 421–426.

Schäfer, W. 1972 *Ecology and paleoecology of marine environments.* University of Chicago Press.

Scheuring, B. W. 1978 Mikrofloren aus den Meridekalken des Monte San Giorgio (Kt. Tessin). *Schweiz. Paläont. Abh.* **100**, 1–100.

Schmidt, M. 1928 *Die Lebewelt unserer Trias.* Öhringen: Hohenlohe'sche Buchhandlung.

Schmidt, S. 1985 Paleoecology of nothosaurs. In *Third symposium on Mesozoic terrestrial ecosystems, short papers* (ed. W.-E. Reif & F. Westphal), pp. 215–218. Tübingen: Attempto–Verlag.

Schmidt, S. 1986 Lokomotion und Lebensweise der Nothosaurier (Diapsida, Sauropterygia; Trias). Ph.D. thesis, University of Tübingen.

Schmidt, S. 1987 Phylogenie der Sauropterygier (Diapsida; Trias – Kreide). *Neues Jb. Geol. Paläont. Abh.* **173**, 339–375.

Seeley, H. G. 1882 On *Neusticosaurus pusillus* (Fraas), an amphibious reptile having affinities with terrestrial Nothosauria and with marine Plesiosauria. *Q. Jl geol. Soc. Lond.* **38**, 350–366.

Sheldon, P. A. 1987 Parallel gradualistic evolution of Ordovician trilobites. *Nature, Lond.* **330**, 561–563.

Shubin, N. H. & Alberch, P. 1986 A morphogenetic approach to the origin and basic organization of the tetrapod limb. In *Evolutionary biology*, vol. 20 (ed. M. K. Hecht, B. Wallace & G. T. Prance), pp. 319–387. New York: Plenum Press.

Storrs, G. W. 1981 A review of occurrences of Plesiosauria (Reptilia: Sauropterygia) in Texas with description of new material. M.A. thesis, University of Texas.

Sues, H.-D. & Carroll, R. L. 1985 The pachypleurosaurid *Dactylosaurus schroederi* (Diapsida: Sauropterygia). *Can. J. Earth Sci.* **22**, 1602–1608.

Taylor, M. A. 1981 Plesiosaurs – rigging and ballasting. *Nature, Lond.* **290**, 628–629.

Thompson, M. B. 1988 Influence of incubation temperature and water potential on the sex determination in *Emydura macquarii* (Testudines: Pleurodira). *Herpetologica* **44**, 86–90.

Tschanz, K. 1989 *Lariosaurus buzzii* n.sp. from the Middle Triassic of Monte San Giorgio (Switzerland) with comments on the classification of nothosaurus. *Palaeontographica.* (In the press.)

Turner, F. B. 1977 The dynamics of populations of squamates, crocodilians and rhynchocephalians. In *Biology of the Reptilia*, vol. 7, (*Ecology and Behaviour A*) (ed. C. Gans & D. W. Tinkle), pp. 157–264. New York & London: Academic Press.

Vialli, V. 1941 Su tre esemplari di *Pachypleurosaurus edwardsi* (CORN.) del Museo del Milano. *Riv. di Sci. Nat 'Natura'* **32**, 34–42.

Voorhies, M. R. 1969 Taphonomy and population dynamics of an Early Pliocene vertebrate fauna, Knox County, Nebraska. *Univ. Wyoming Contrib. Geol. Spec. Pap.* **1**, 1–69.

Wagner, G. 1950 *Einführung in die Erd- und Landschaftsgeschichte.* Öhringen: Hohenlohe'sche Buchhandlung.

Wasmund, E. 1935 Die Bildung von anabituminösem Leichenwachs unter Wasser. *Schriften Brennstoffgeol.* **10**, 1–70.

Weigelt, J. 1927 *Rezente Wirbeltierleichen und ihre paläontologische Bedeutung.* Leipzig: Verlag von Max Weg.

Willems, H. & Wuttke, M. 1987 Lithogenese lakustriner Dolomite und mikrobiell induzierte 'Weichteil-Erhaltung' bei Tetrapoden des Unter-Rotliegenden (Perm, Saar-Nahe-Becken, SW-Deutschland). *N. Jb. Geol. Paläont. Abh.* **174**, 213–238.

Wirz, A. 1945 Die Triasfauna der Tessiner Kalkalpen. 15. Beiträge zur Kenntnis des Ladinikum im Gebiete des Monte San Giorgio. *Schweiz. Paläont. Abh.* **65**, 1–84.

Wuttke, M. 1983 Aktuopaläontologische Studien über den Zerfall von Wirbeltieren. Teil I: Anura. *Senckenbergiana lethaea* **64**, 529–560.

Young, C. C. 1958 On the new Pachypleurosauroidea from Keichou, South-west China. *Vert. palasiatica* **2**, 69–82.

Zangerl, R. 1935 Die Triasfauna der Tessine Kalkalpen. 9. *Pachypleurosaurus edwardsi*, Cornalia sp. Osteologie – Variationsbreite – Biologie. *Abh. Schweiz. Paläont. Ges.* **56**, 1–80.

Ziegler, B. 1980 *Einführung in die Paläobiology. Teil 1. Allgemeine Paläontologie*, 3rd edn. Stuttgart: E. Schweizerbart'sche Verlagsbuchhandlung.

Zittel, K. v. 1887–1890 *Handbuch der Paläontologie*, vol. III. München: E. Oldenbourg.
Zorn, H. 1971 Paläontologische, stratigraphische und sedimentologische Untersuchungen des Salvatoredolomits (Mitteltrias) der Tessiner Kalkalpen. *Schweiz. Paläont. Abh.* **91**, 1–90.

KEY TO ABBREVIATIONS USED IN FIGURES

a.	angular
a.a.	atlas arch
a.c.	atlas centrum
ac.a.	accessory articulation
ar	articular
a.r.	altas rib
as	astragalus
ax.a.	axis arch
ax.c.	axis centrum
ax.i.c.	axis intercentrum
ax.r.	axis rib
bo.	basioccipital
ca.	calcaneum
ca.r.	caudal rib
cb.1	first ceratobranchial
cl.	clavicle
cn.	coronoid
co.	coracoid
co.f.	coracoid foramen
cp.	carpal
c.r.	cervical rib
c.t.f.	chorda tympani foramen
d.	dentary
d.a.	dorsal arch
d.c.	dorsal centrum
d.r.	dorsal rib
ent.f.	entepicondylar foramen
eo.	exoccipital
f.	frontal
fe.	femur
fi.	fibula
ft	foot
g.	gastral element
hu.	humerus
icl.	interclavicle
il.	ilium
im	intermedium
is.	ischium
j.	jugal
l.g.	lateral element of gastral rib
m.	maxillary
mc.1	metacarpal 1
mc.5	metacarpal 5
m.g.	medial element of gastral rib
mt.1	metatarsal 1
mt.5	metatarsal 5
n.	nasal
o.f.	obturator foramen
pa.	parietal
p.ar	prearticular
pf.	postfrontal
pl.	palatine
pm.	premaxillary
po.	postorbital
poz.	postzygapophysis
prf.	prefrontal
prz.	prezygapophysis
pt.	pterygoid
pu.	pubis
q.	quadrate
qj.	quadratojugal
r.	rib
ra.	radius
ri.a.	rib articulation
sa.	surangular
se.	scale
sc.	scapula
so.	supraoccipital
sp.	splenial
sc.p.	sclerotic plates
sq.	squamosal
s.r.	sacral rib
ti.	tibia
ul.	ulna
uln.	ulnare
v.	vomer
3.a.	third neural arch
3.c.	third centrum
3.r.	third rib

Italicized abbreviations refer to lengths (in millimetres).

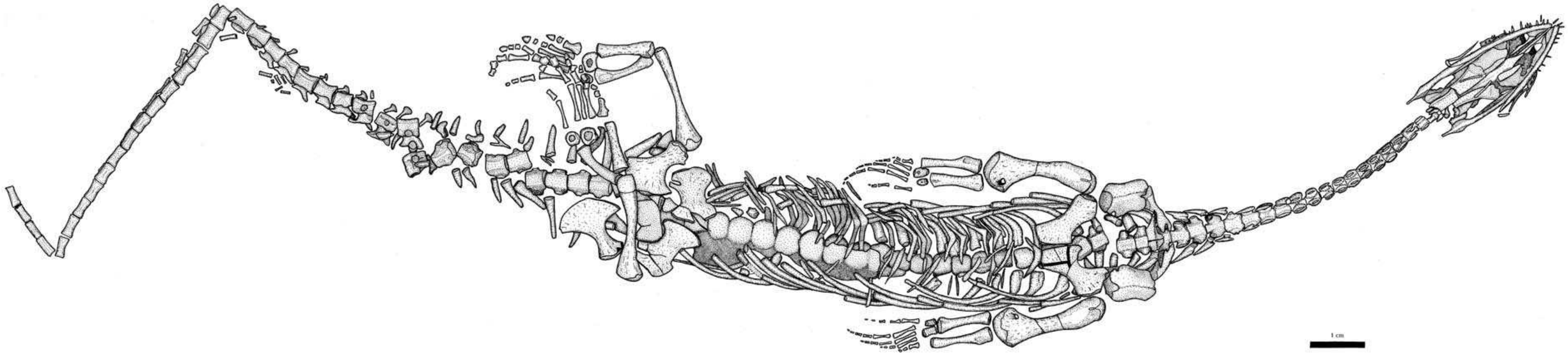

FIGURE 7*a*. Large adult specimen (T 3934) of *Neusticosaurus pusillus* from Monte San Giorgio; ventral view.

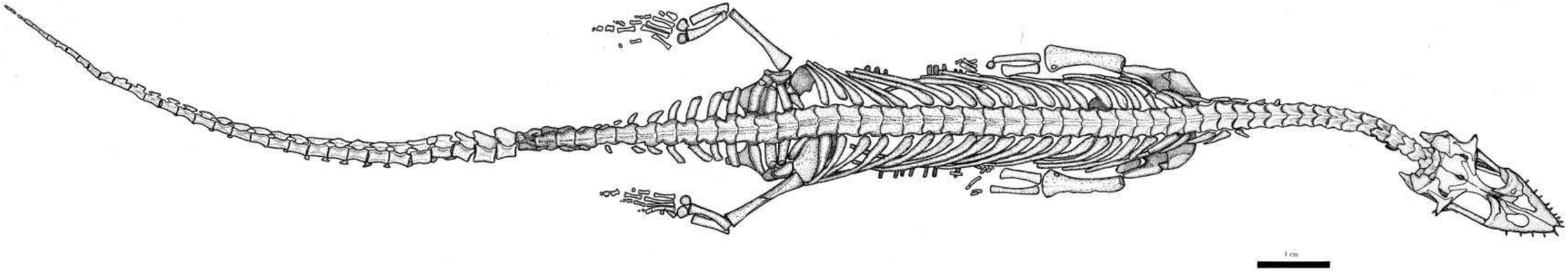

FIGURE 7*b*. The type specimen of *Neusticosaurus peyeri* (T 3615); dorsal view.

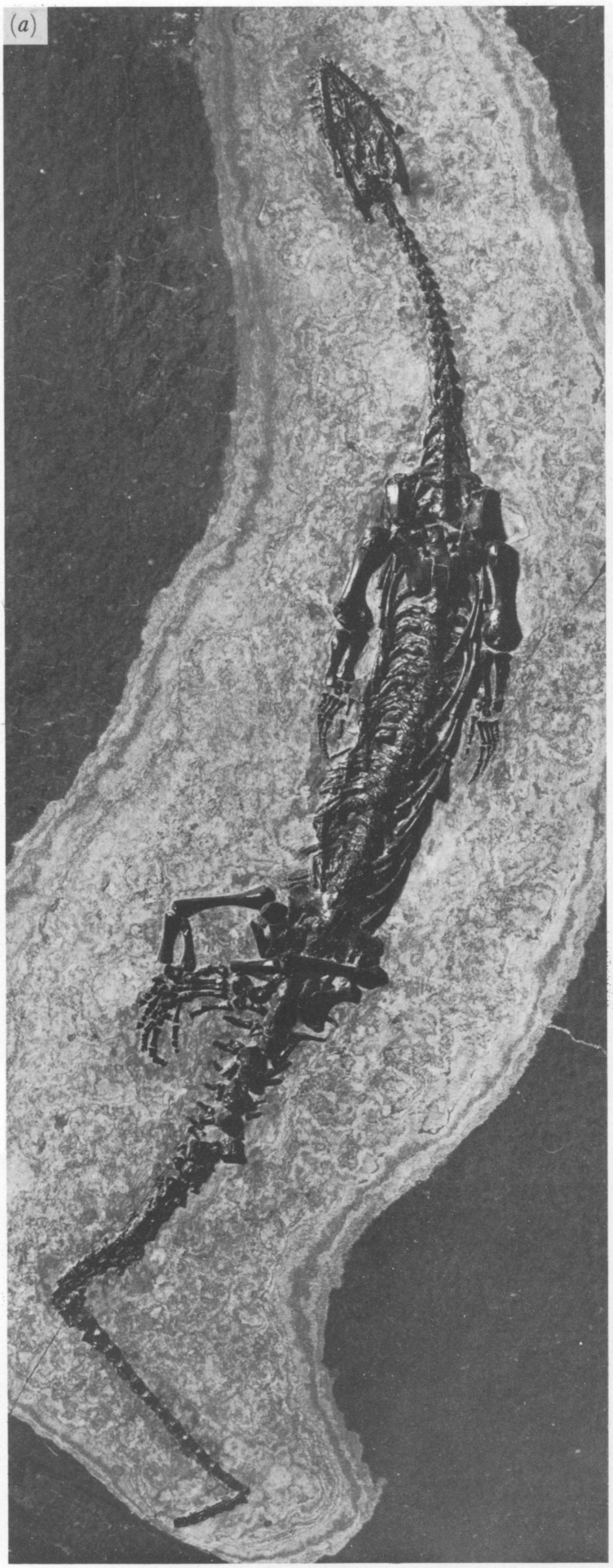

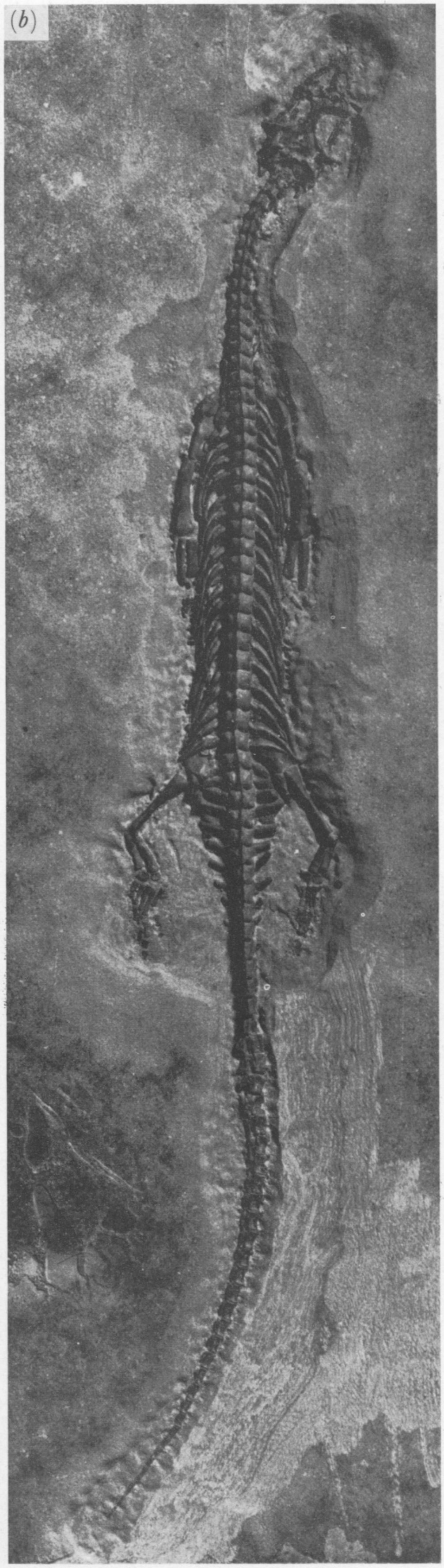

FIGURE 24. For description see opposite.

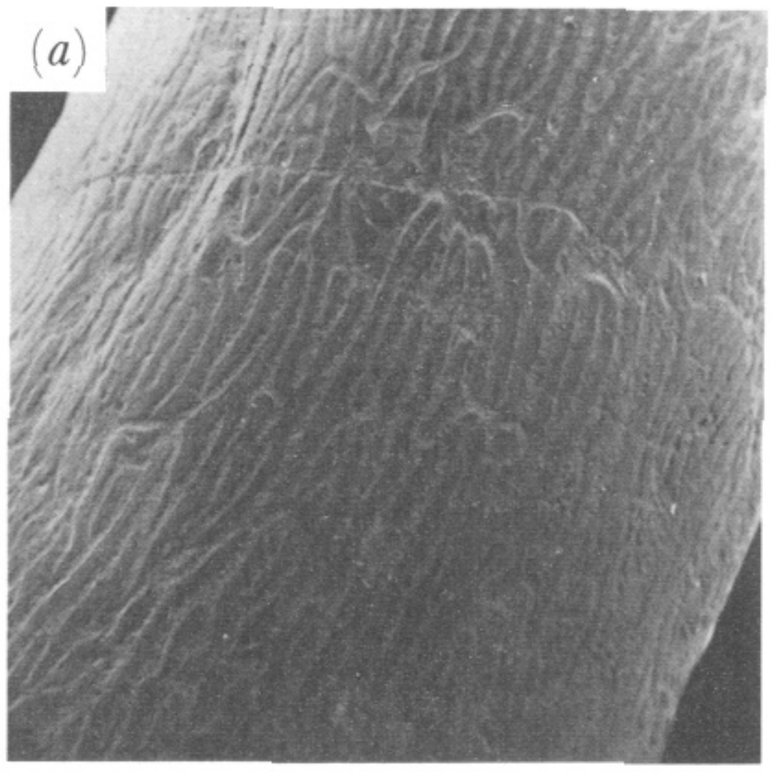

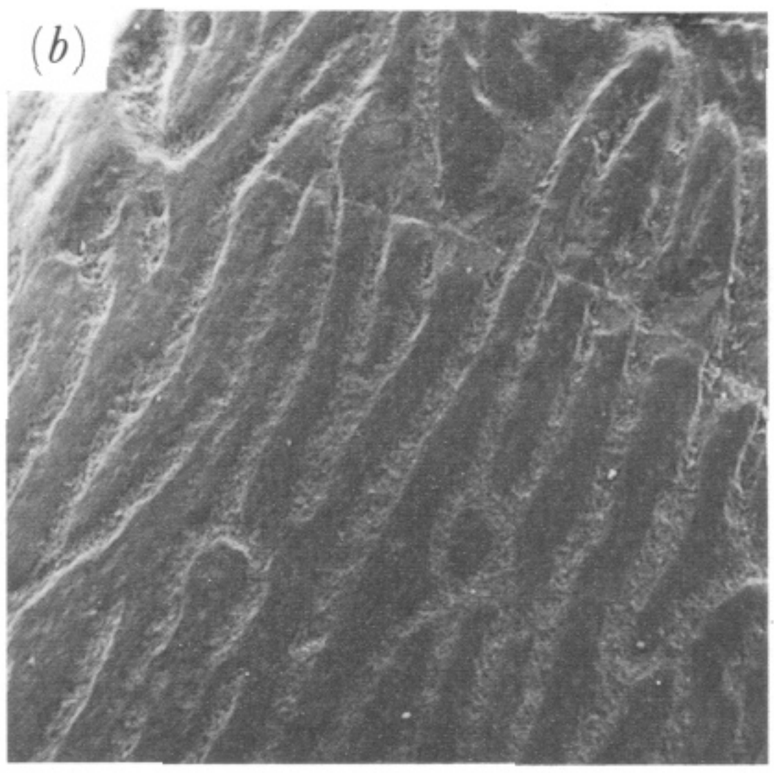

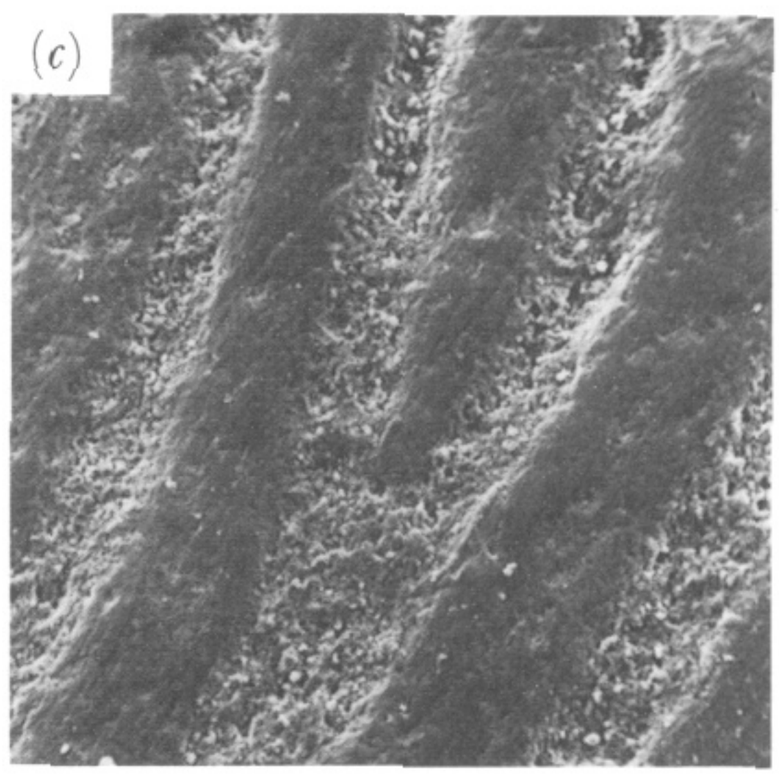

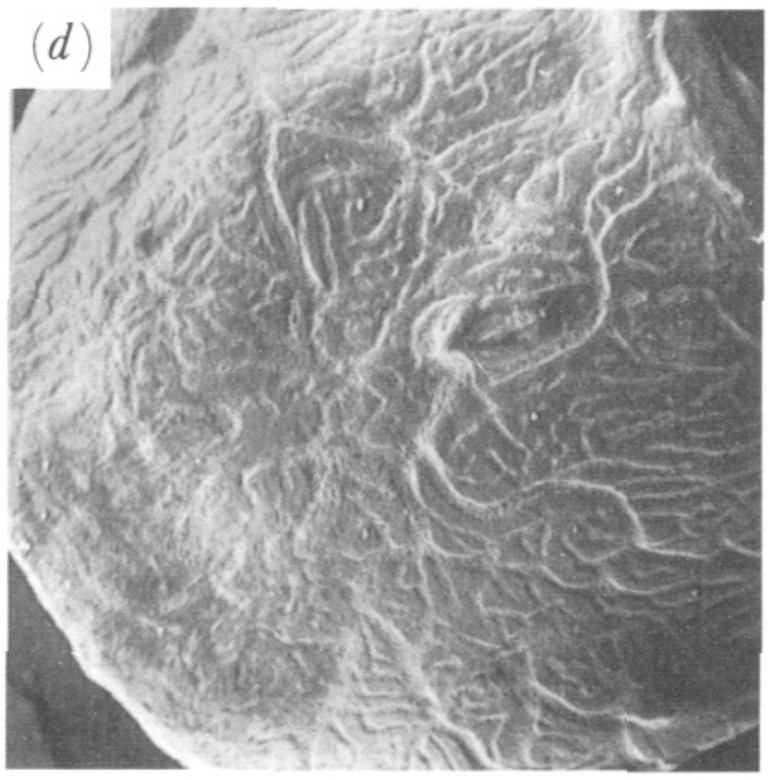

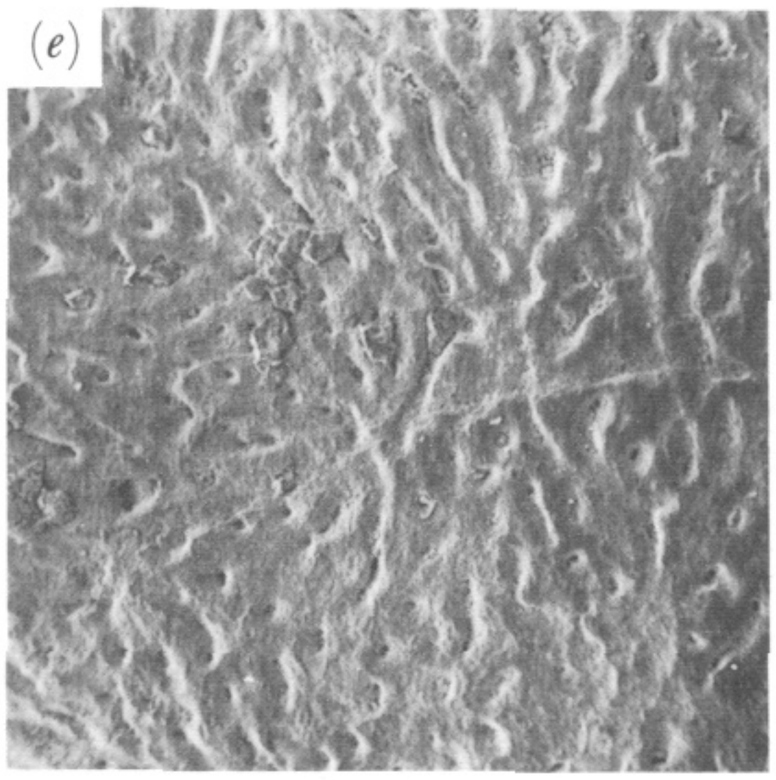

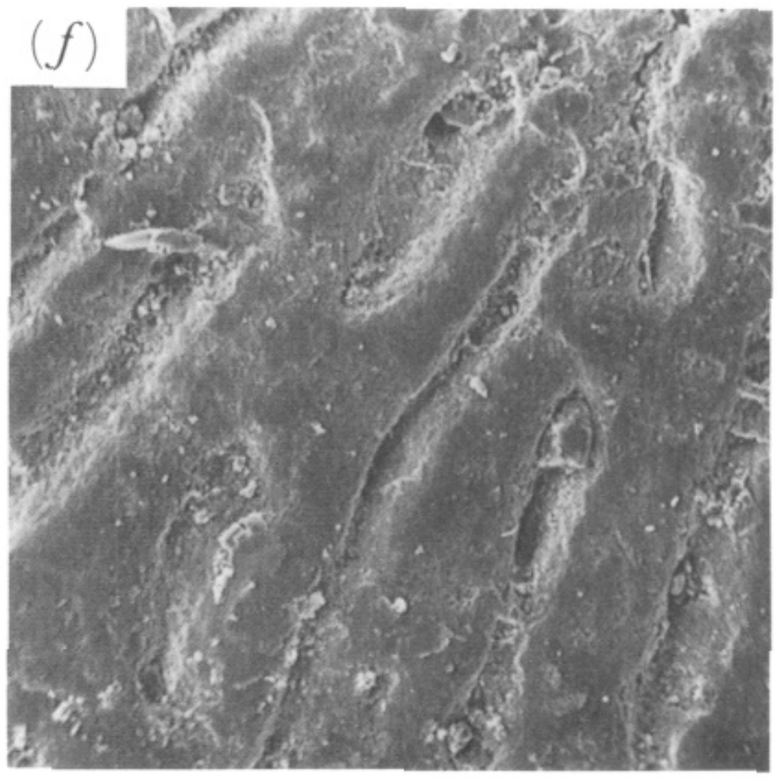

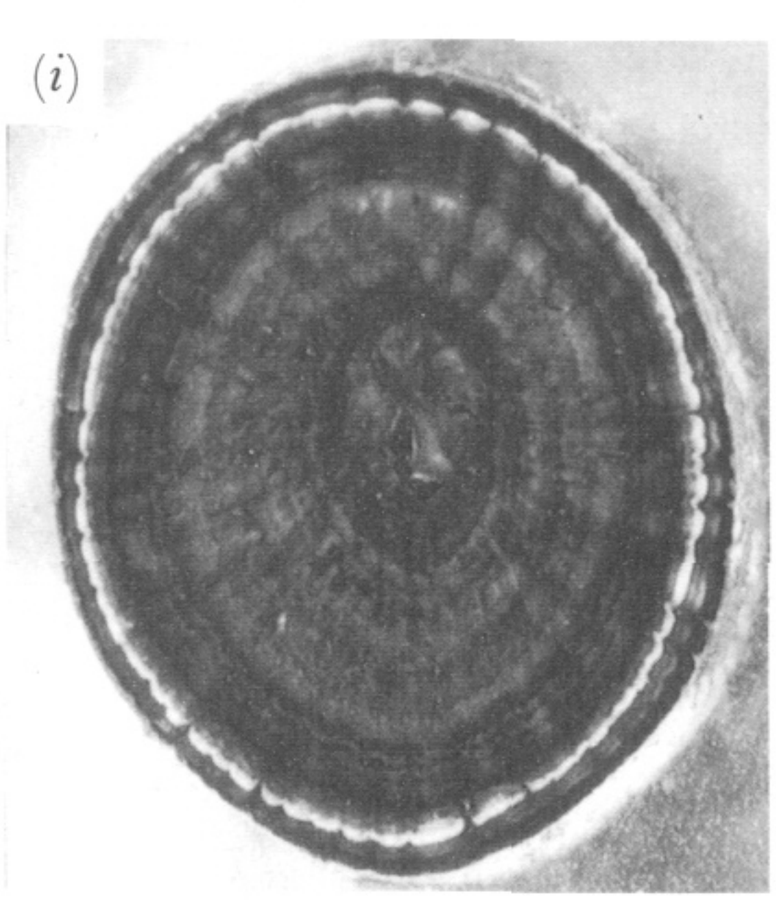

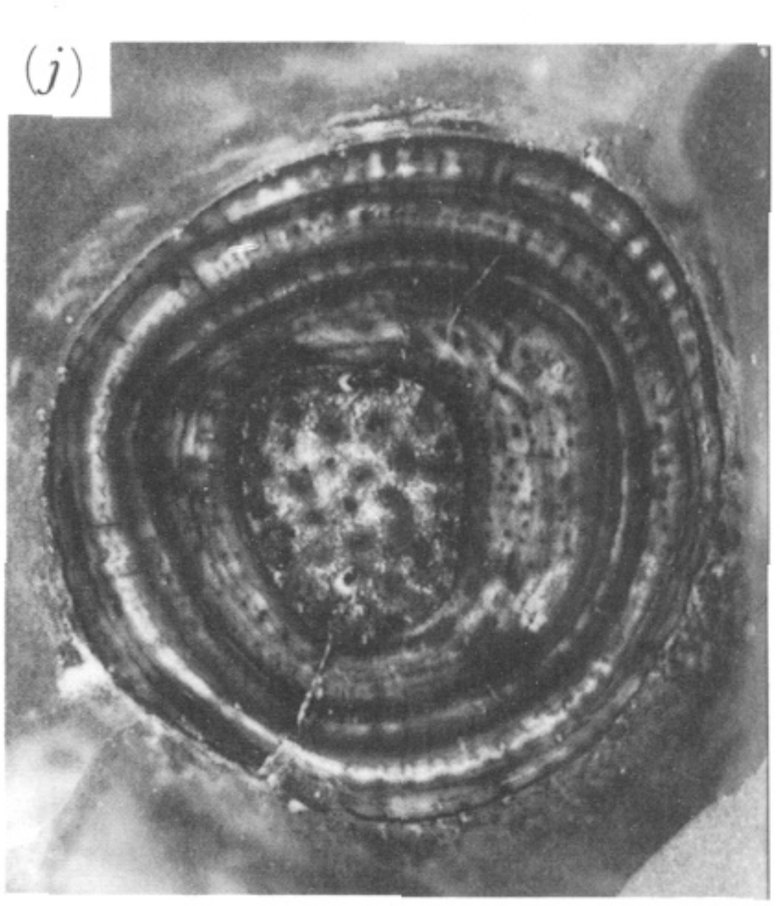

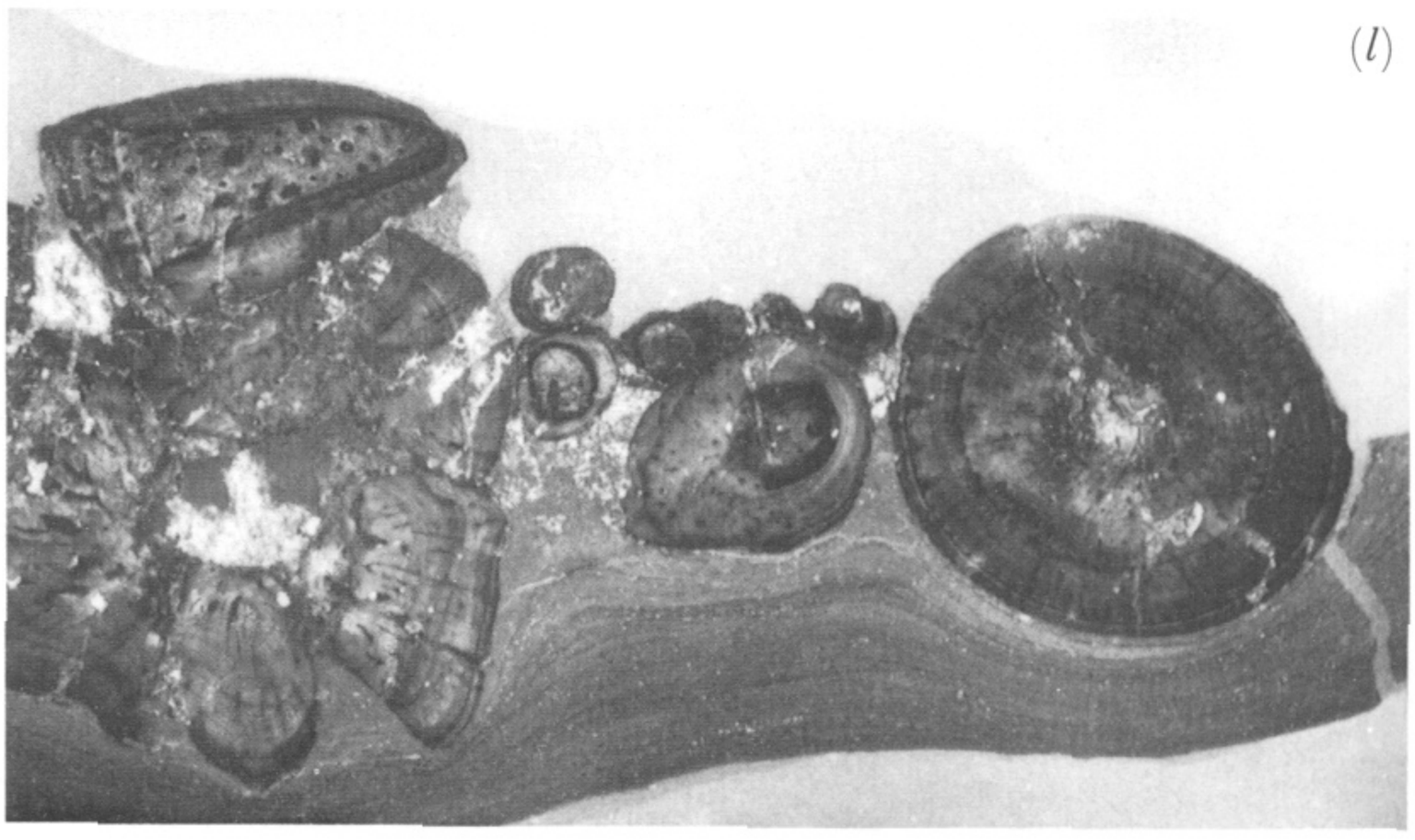

FIGURE 25. For description see page 620.

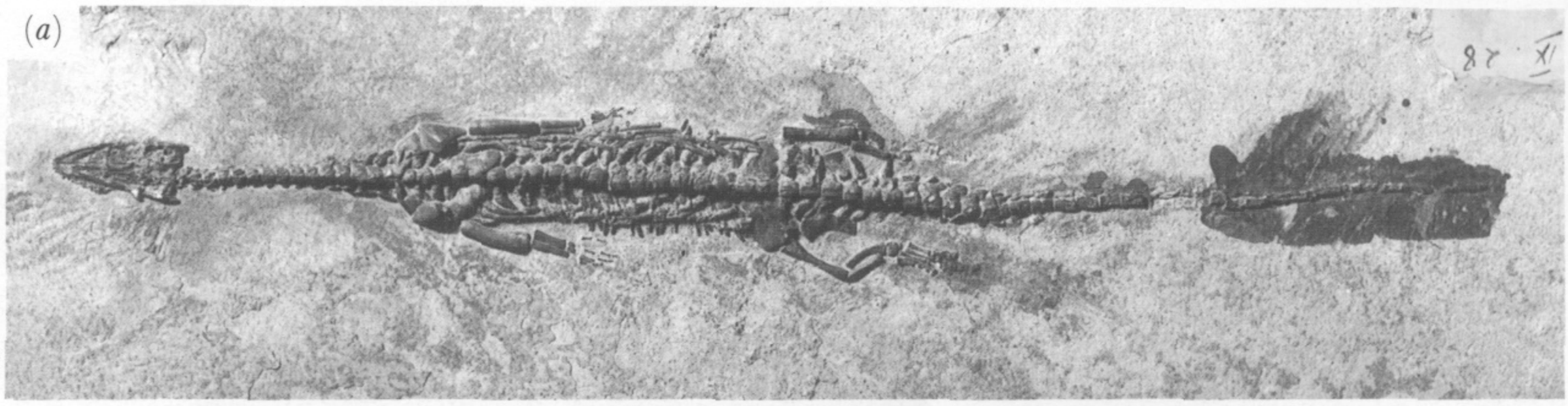

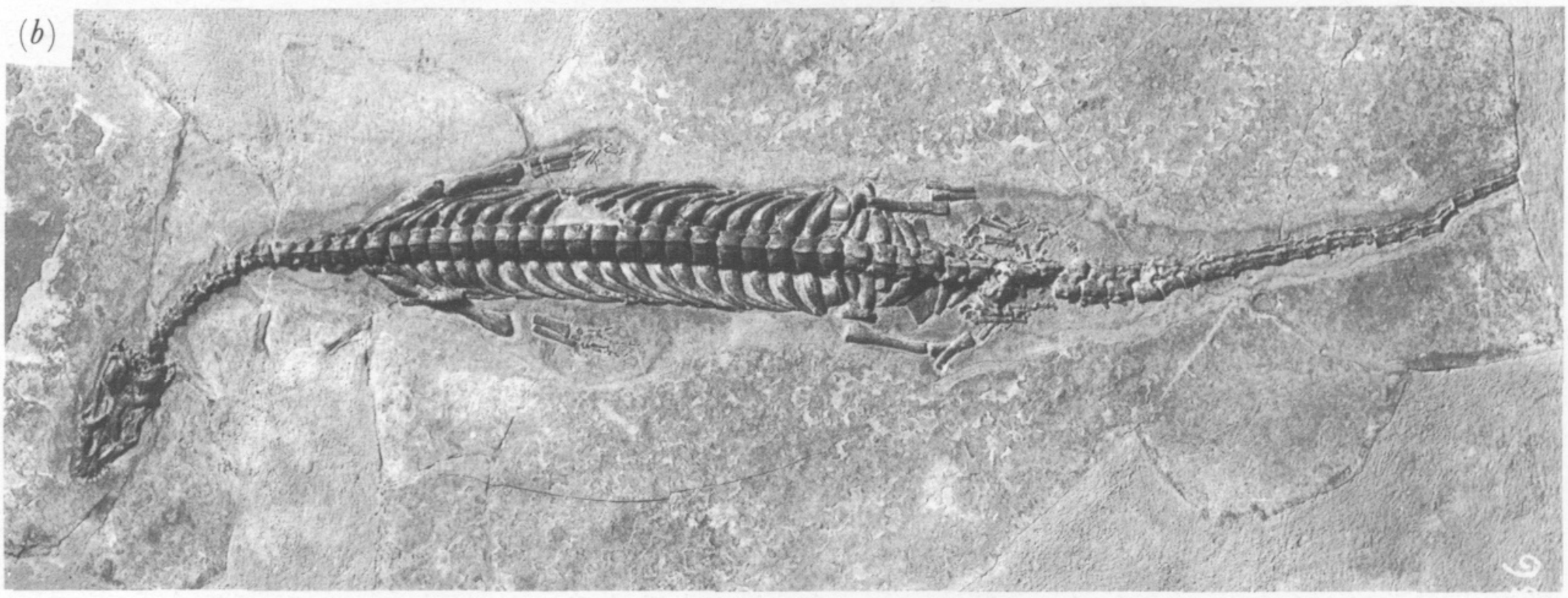

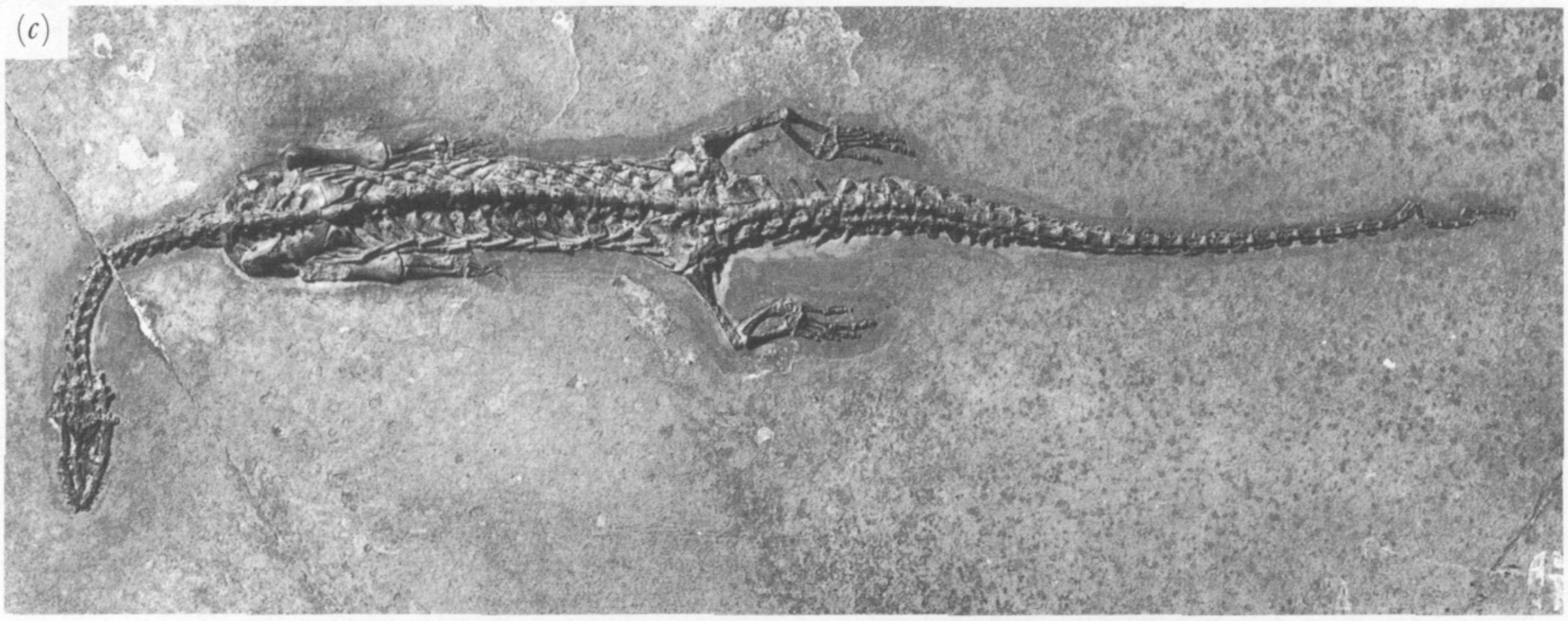

FIGURE 26. For description see page 621.

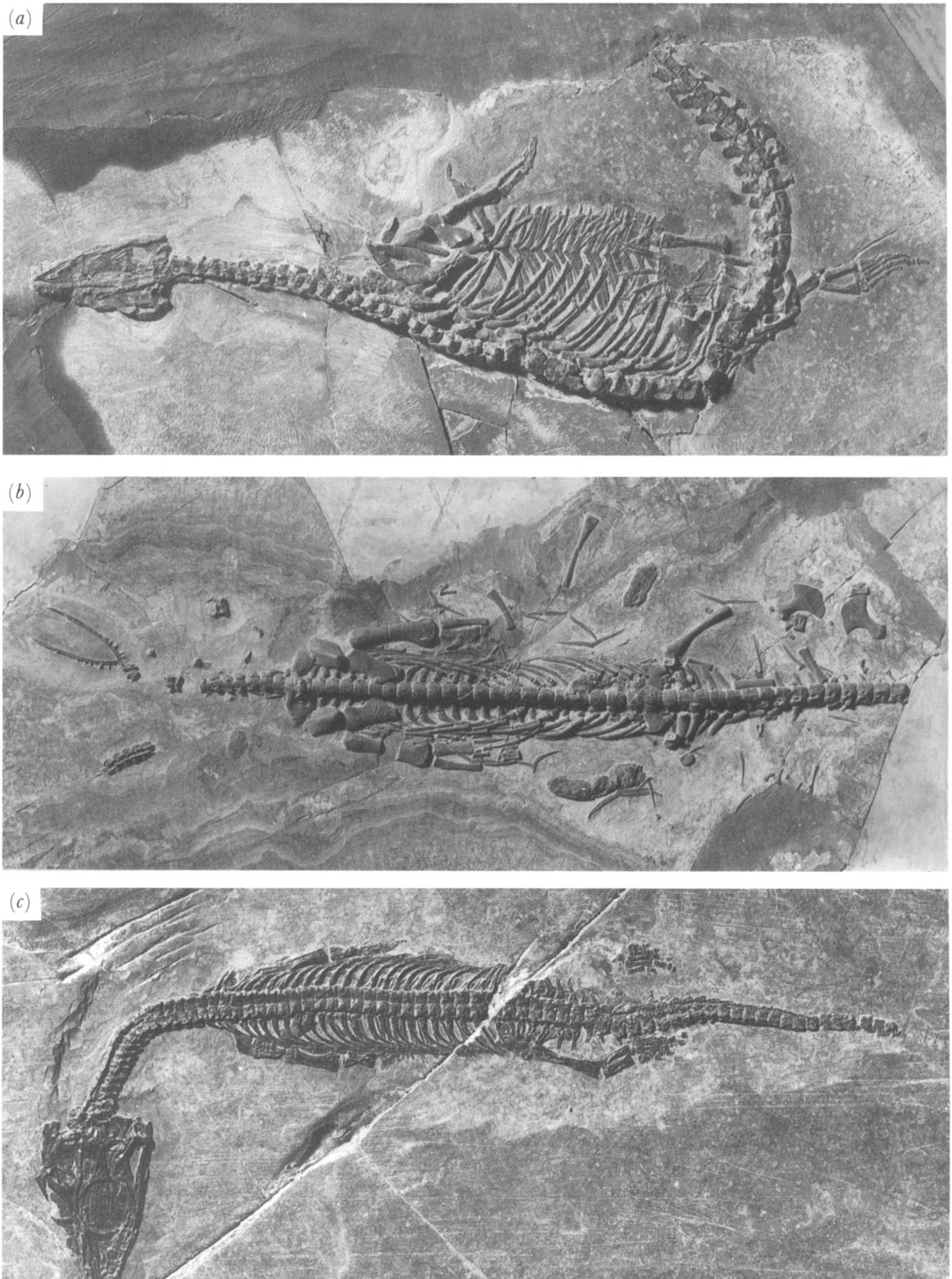

FIGURE 27. For description see opposite.